

**WestminsterResearch**

<http://www.westminster.ac.uk/research/westminsterresearch>

**Molecular and cellular insights into iron regulation**

**Kosha Mehta**

School of Life Sciences

This is an electronic version of a PhD thesis awarded by the University of Westminster. © The Author, 2012.

This is an exact reproduction of the paper copy held by the University of Westminster library.

---

The WestminsterResearch online digital archive at the University of Westminster aims to make the research output of the University available to a wider audience. Copyright and Moral Rights remain with the authors and/or copyright owners.

Users are permitted to download and/or print one copy for non-commercial private study or research. Further distribution and any use of material from within this archive for profit-making enterprises or for commercial gain is strictly forbidden.

---

Whilst further distribution of specific materials from within this archive is forbidden, you may freely distribute the URL of WestminsterResearch:  
(<http://westminsterresearch.wmin.ac.uk/>).

In case of abuse or copyright appearing without permission e-mail [repository@westminster.ac.uk](mailto:repository@westminster.ac.uk)

**Molecular and cellular  
insights into iron regulation**

Kosha Mehta

School of Life Sciences

University of Westminster

May 2012

A thesis submitted in partial fulfilment of the requirements of the  
University of Westminster for the degree of Doctor of Philosophy  
May 2012

## Abstract

The iron hormone hepcidin is regarded as the main iron homeostatic regulator in the human body. It is predominantly produced by hepatocytes in response to systemic iron excess. However, since the cellular and molecular mechanisms involved in hepcidin expression are not fully understood, this project involved studying hepcidin expression and the role of the pro-region of the hepcidin pro-hormone in regulation of iron homeostasis.

Iron overdose in Chinese hamster ovary-transferrin receptor variant (CHO TRVb1) cells resulted in increased hepcidin peptide secretion after 30 min and 2 hours ( $p < 0.03$ ) as well as 24 and 48 hours ( $p < 0.01$ ). Also, partial characterisation of the previously unknown CHO-gene sequences of *Hfe*, *Slc40-a1* and *Irp2*, was achieved. To determine the effect of intracellular iron overload on hepcidin expression, recombinant transferrin receptor 1 (rec-TfR1) HepG2 cells were created which express modified *TfR1* to maximise iron uptake. Upon holotransferrin (5 g/L) treatment these cells showed significantly increased iron uptake which was in contrast to the response by Wt HepG2 cells. Also, it was shown for the first time that hepcidin peptide secretion increased upon iron overdose to HepG2 cells after 30 min, 2,4,24 and 48 hours ( $p < 0.05$ ). Also, holotransferrin treatment (5 g/L) increased *hepcidin* mRNA levels; in Wt HepG2 cells by 0.6 fold (on average) after 30 min, 2,4,6 and 24 hours and in rec-TfR1 HepG2 cells by 0.5 fold after 2 h ( $p < 0.02$ ). Gene expression studies of *TfR1*, *SLC40-A1*, and *HFE* upon iron overdose showed opposing functionalities of *TfR1* and *SLC40-A1* in maintaining intracellular iron homeostasis and emphasised the significance of HFE in hepcidin induction. Additionally, localisation studies with the pre-pro derivative of preprohepcidin identified its presence in the nucleus, suggesting its involvement in the gene regulation process and thus possible participation in maintaining iron homeostasis.

In conclusion, rec-TfR1 HepG2 cells partially resemble haemochromatotic cells and the findings indicate that hepcidin regulation involves the interaction between several iron-related genes and the extracellular and intracellular iron levels.



2.2.14	Pre iron supplementation optimisations	45
2.2.15	Iron supplementations	47
2.2.16	Viability assay	48
2.2.17	Determination of cellular iron and protein content	49
2.2.17.1	Determination of cellular iron content by the ferrozine assay	50
2.2.17.2	Determination of cellular protein content by the Bradford assay	50
2.2.18	RNA extraction and complementary DNA (cDNA) synthesis	51
2.2.19	Real time PCR using SYBR green as detector	53
2.2.19.1	Standard dilution series	54
2.2.19.2	Analysis of real time PCR data	55
2.2.20	Detection of transferrin receptor on cell-surface	55
2.2.21	Detection of human TfR1 in CHO TRVb1 cells	57
2.2.22	Determination of hepcidin peptide concentrations	60
2.2.23	Restriction digest	60
2.2.24	Localisation studies of preprohepcidin derivatives	61
2.2.25	Statistical analysis	62

**Chapter 3 Effect of iron supplementation on hepcidin expression in recombinant Chinese hamster ovary cells**

3.1	<b>Introduction</b>	63
3.1.1	Aims and objectives	64
3.2	<b>Approach and optimisations</b>	65
3.2.1	Concept behind primer design and sequence acquisition	65
3.2.2	PCR optimisations	69
3.3	<b>Results</b>	70
3.3.1	Characterisation of CHO gene sequences	70
3.3.2	Functional analysis of characterised gene sequences	72
3.3.3	CHO specific primers and preliminary real time PCR	76
3.3.4	Hepcidin gene sequencing in CHO cells	80
3.3.4.1	Magnesium chloride gradient PCR	81
3.3.4.2	Amplification of amplicon to increase product yield	82
3.3.4.3	Cloning of DNA fragment	83
3.3.4.4	Reverse primers with unique hepcidin specificity	84
3.3.4.5	Primer specificity	85

3.3.4.6	Hepcidin primers for other species	86
3.3.4.7	cDNA usage for sequencing	88
3.3.4.8	Cloning of cDNA fragment	89
3.3.5	TfR1 transcript status in CHO TRVb1 cells	90
3.3.6	TfR1 protein status in CHO TRVb1 cells	91
3.3.7	Iron overdose and CHO TRVb1 cells	92
<b>3.4</b>	<b>Discussion</b>	<b>96</b>
3.4.1	Summary of ferroportin, HFE and IRP2 gene sequencing in CHO cells	99
3.4.2	Hepcidin gene sequencing in CHO cells	100
3.4.3	Effect of iron supplementation on CHO TRVb1 cells	103

## **Chapter 4 Effect of iron overload on TfR1-recombinant HepG2 cells**

<b>4.1</b>	<b>Introduction</b>	<b>107</b>
4.1.1	Aims and objectives	108
<b>4.2</b>	<b>Results</b>	<b>109</b>
4.2.1	Cell-surface expression of TfR1 in HepG2 cells	109
4.2.2	Iron related genes in rec-TfR1 HepG2 cells	112
4.2.3	HepG2 cells under steady state conditions: 48 h study	112
4.2.4	Iron overdose and Wt HepG2 cells : 48 h study	115
4.2.5	Iron overdose and rec-TfR1 HepG2 cells : 48 h study	118
4.2.6	HepG2 cells under steady state condition : 4 h study	122
4.2.7	Effect of iron overdose on HepG2 cells : 4 h study	124
4.2.8	Iron overdose and hepcidin secretion by HepG2 cells	130
<b>4.3</b>	<b>Discussion</b>	<b>132</b>
4.3.1	Regulation of iron uptake by TfR1	134
4.3.2	Effect of intracellular iron overload on hepcidin expression	136
4.3.3	Influence of holotransferrin concentration and exposure-time on Hepcidin	139
4.3.4	Relationship between HFE and hepcidin	142
4.3.5	Effect of intracellular and extracellular iron levels on HFE	144
4.3.6	HepG2 cells have an iron holding threshold	147

## **Chapter 5 Significance of preprohepcidin derivatives**

<b>5.1 Introduction</b>	148
5.1.1 Aims and objectives	149
<b>5.2 Results</b>	150
5.2.1 Identification of hydrophilic regions in preprohepcidin	150
5.2.2 Putative binding of preprohepcidin derivatives to HFE	150
5.2.3 Conservation of regions of potential interaction	152
5.2.4 Nuclear localisation signals in preprohepcidin	153
5.2.5 Localisation studies of pro-peptide of preprohepcidin	155
5.2.5.1 Screening of plasmid constructs	156
5.2.5.2 Location of hepcidin pro-peptide in Wt HepG2 cells	158
<b>5.3 Discussion</b>	160

## **Chapter 6 Overall summary and future work**

<b>6.1 Overall summary</b>	165
<b>6.2 Future Work</b>	168

<b>References</b>	172
-------------------	-----

### **Appendix**

I. Creation of rec-TfR1 HepG2 cells
II. Urea gel buffers
III. Detection of iron in BSA
IV. Viability studies in BSA
V. Confirmation of HepG2 gene sequence identity
VI. Pilot temperature gradient RT PCR
VII. Amplification efficiencies of genes
VIII. Accession numbers of genes and proteins
IX. CHO- <i>FPN</i> gene sequencing
X. CHO- <i>HFE</i> gene sequencing
XI. CHO- <i>IRP2</i> gene sequencing
XII. CHO- <i>hepcidin</i> gene sequencing
XIII. CHO-temperature gradient PCRs
XIV. CHO reference genes
XV. Primers for human and CHO- <i>TfR1</i>
XVI. HepG2 reference genes

## List of Figures

<u>Chapter 1</u>		Page No
Figure 1.1	Pathways of iron absorption and utilisation	2
Figure 1.2	Cell types involved in iron absorption and circulation	4
Figure 1.3	Proposed model of haem iron uptake by an enterocyte	7
Figure 1.4A	Significant sites of cleavage in preprohepcidin (84-mer)	10
Figure 1.4B	Structure of bioactive hepcidin-25	10
Figure 1.5	Systemic regulation of iron by hepcidin	13
Figure 1.6	Factors affecting hepcidin production	15
Figure 1.7A	Pathways leading to transcriptional up-regulation of hepcidin	17
Figure 1.7B	Pathways leading to transcriptional down-regulation of hepcidin	17
Figure 1.8	Cellular regulation of iron by iron regulatory proteins (IRPs)	18
<u>Chapter 2</u>		
Figure 2.1	Alignment of human TfR1 mRNA and protein	28
Figure 2.2	Schematic of the cloning vector, pCEP4 plasmid	31
Figure 2.3	A typical DNA	41
Figure 2.4	A 6 M urea gel assay	45
Figure 2.5	Effect of hygromycin B on HepG2 cells	47
Figure 2.6	A typical iron standard curve	50
Figure 2.7	A typical protein standard curve	51
Figure 2.8	Analysis of TfR1 standard curve	54
Figure 2.9	Analysis of cell-surface TfR1 in Wt HepG2 cells by flow cytometry	57
Figure 2.10	Cloning vector pEGFP-N1 plasmid	61
<u>Chapter 3</u>		
Figure 3.1	Concept of "PCR walking" used for CHO gene sequencing	66
Figure 3.2	Partial alignment of ferroportin mRNA sequences	67
Figure 3.3	Temperature gradient PCR for 1st round of CHO ferroportin gene sequencing with primers ferroportin (F) and (R)	70
Figure 3.4	Amplicons of generated for 1st round of CHO gene sequencing	71
Figure 3.5	Functional significance of the characterised CHO-ferroportin Sequence	73
Figure 3.6	Functional significance of the characterised CHO-Hfe sequence	74
Figure 3.7	Functional significance of the characterised CHO-Irp2 sequence	75
Figure 3.8	Preliminary real time PCR with CHO-specific primers	78
Figure 3.9	Standard dilution curves of HFE and beta actin genes in CHO cells	79
Figure 3.10	Amplicons of CHO genome obtained with hepcidin primers (F) and (R1a)	80
Figure 3.11	Amplicons of CHO DNA under MgCl <sub>2</sub> gradient using hepcidin primers (F1) and (R1a)	81

Figure 3.12	Amplification of amplicon to increase product yield	82
Figure 3.13	Amplification of cloned plasmids	83
Figure 3.14A	Amplification of CHO DNA with only the forward primer F1	85
Figure 3.14B	Probable position of binding of forward primer F1, to function as a reverse primer	85
Figure 3.15	Amplification of CHO genome with hepcidin primers used for other species	86
Figure 3.16	Amplification of CHO genome with hepcidin primers designed on human transcript	87
Figure 3.17	Amplicon of Wt CHO cDNA obtained with hepcidin primers F2 and R2a	88
Figure 3.18	Amplification of cloned Wt CHO cDNA	89
Figure 3.19	Amplicons of TfR1 transcript in CHO cells	90
Figure 3.20	TfR1 protein expression in CHO TRVb1 cells	91
Figure 3.21	TfR1 response of CHO TRVb1 cells on iron overload	93
Figure 3.22	Holotransferrin overdose and hepcidin peptide production by CHO TRVb1 cells	94
Figure 3.23	Iron content in CHO TRVb1 treatment media	94
Figure 3.24	Viability studies in CHO TRVb1 cells	95
Figure 3.25	Intracellular iron levels in CHO TRVb1 cells upon iron supplementation	95
Figure3.26	Hepcidin peptide secretion by CHO TRVb1 cells upon iron supplementation	96

#### **Chapter 4**

Figure 4.1	Effect of holotransferrin overdose on cell-surface expression of TfR1	110
Figure 4.2	Effect of iron overdose on TfR1 cell-surface expression in HepG2 cells	111
Figure 4.3	Amplicons of transcripts iron-related genes in rec-TfR1 HepG2 cells	112
Figure 4.4	Viability studies and iron content in HepG2 cells under steady state conditions	113
Figure 4.5	Basal mRNA expression of iron-related genes in HepG2 cells	114
Figure 4.6	Viability studies and intracellular iron levels in Wt HepG2 cells under holotransferrin treatments	116
Figure 4.7	mRNA expression of iron related genes in Wt HepG2 cells upon holotransferrin treatments	117
Figure 4.8	Viability studies and intracellular iron levels in rec-TfR1 HepG2 cells under holotransferrin treatments	119
Figure 4.9	mRNA expression of iron related genes in rec-TfR1 HepG2 cells upon holotransferrin treatments	120
Figure 4.11	Viability and iron uptake in HepG2 cells under steady state conditions : 4 h study	122
Figure 4.12	Basal mRNA expression of iron-related genes in HepG2 cells : 4 h study	123
Figure 4.13	Iron levels in treatment media for HepG2 cells	124
Figure 4.14	Viability studies and iron uptake in HepG2 cells under holotransferrin treatment : 4 h study	125

Figure 4.15	Effect of holotransferrin treatment on gene expression in Wt HepG2 cells	127
Figure 4.16	Effect of holotransferrin treatment on gene expression in HepG2 (p) cells	128
Figure 4.17	Effect of holotransferrin treatment on gene expression in rec-TfR1 HepG2 cells	129
Figure 4.18	Gene expression in HepG2 cells under holotransferrin overdose over time	130
Figure 4.19	Effect of prolonged iron overdose on hepcidin peptide secretion by HepG2 cells	131
Figure 4.20	Effect of iron overdose on hepcidin peptide secretion by HepG2 cells	132
Figure 4.21	Hepcidin secretion by HepG2 cells under iron deprivation	138
Figure 4.22	Hepcidin induction by holotransferrin and maintenance medium	139
Figure 4.23	Hepcidin mRNA response towards increasing holotransferrin Concentrations	140
Figure 4.24	Hepcidin peptide release under holotransferrin overdose over time	141
Figure 4.25	HFE sense iron levels	144
Figure 4.26	Iron sensing by HFE in rec-TfR1 HepG2 cells under increasing holotransferrin concentrations	146

## **Chapter 5**

Figure 5.1	Crystal structure of cytoplasmic region of HFE protein	148
Figure 5.2	Hydrophilicity scale for human preprohepcidin	150
Figure 5.3	Graphical representation of binding scores of HLA to different combinations of preprohepcidin nonamers	151
Figure 5.4	Conservation of alpha regions in the HFE protein in various species	152
Figure 5.5	Conservation of amino acids within the pro-region of preprohepcidin	153
Figure 5.6	Nuclear localisation signal in preprohepcidin	154
Figure 5.7	Similarity between KRAB and pro-region of preprohepcidin	155
Figure 5.8	Restriction digests of pEGFPN1 plasmid constructs	156
Figure 5.9	Amplicons of pEGFPN1-preprohepcidin constructs with designed vector primers	157
Figure 5.10	Transfection of HepG2 cells with pEGFPN1 plasmids	159
Figure 5.11	Localisation of prepro-region in HepG2 cells	160

## List of Tables

<b><u>Chapter 1</u></b>		<b>Page No</b>
Table 1.1	Overview of important proteins involved in iron metabolism	8
<b><u>Chapter 2</u></b>		
Table 2.1	Primers for CHO gene sequencing and real time PCR	37
Table 2.2	Primers used for hepcidin gene sequencing in CHO cells	38
Table 2.3	Primers for PCR optimisations and real time PCR with HepG2 cells	38
Table 2.4	PCR protocol and cycles	39
Table 2.5	SYBR real time PCR protocol and cycles	53
<b><u>Chapter 3</u></b>		
Table 3.1	Similarities between hamster, human, mouse and rat genomes	65
Table 3.2	Percentage identity between characterised CHO gene sequences and other species	72
Table 3.4	Sequence similarities between characterised CHO sequence and other species	89
<b><u>Chapter 5</u></b>		
Table 5.1	Identification of plasmid pEGFPN1-preprohepcidin constructs	158



## Acknowledgements



I am grateful to my Director of studies, Dr. Vinood Patel for giving his time, valuable advice and the necessary support to accomplish this PhD.



Thanks to Dr. Sebastien Farnaud for conceiving such an interesting project and for his advice and help.



My heartfelt thanks to Dr. Pamela Greenwell for supporting me selflessly throughout this project. Your generosity has been admirable.

Also thanks to:

Dr. Paul Brown and Dr. Mitla Gracia for creation of recombinant HepG2 cells.

Dr. Mark Busbridge for measuring hepcidin peptide levels.

Dr. Guglielmo Rosignoli for flow cytometry.

My gratitude towards my family.

Thank you life for being kind and beautiful, always.

## **Authors Declaration**

I declare that the present work was carried out according to the guidelines and regulations of the University of Westminster. The work is original except where indicated by special reference in the text.

The submission as a whole or part is not substantially the same as any that I previously or am currently making, whether in published or unpublished form, for a degree, diploma or similar qualification at any university or similar institution.

Until the outcome of the current application to the University of Westminster is known, the work will not be submitted for any such qualification at another university or similar institution.

Any views expressed in this work are those of the author and in no way represent those of the University of Westminster.

Signed: Kosha. J. Mehta

Date: July 2012

### **List of abbreviations**

Bp	Base pairs
BSA	Bovine serum albumin
CHO	Chinese hamster ovary
DMSO	Dimethyl sulphoxide
Ds	Double stranded
FCS	Foetal calf serum
GFP	Green fluorescent protein
H (h)	Hour
HLA	Human leukocyte antigen
IRE	Iron responsive elements
IRP	Iron regulatory proteins
LB	Luria-Bertani
MHC	Major Histocompatibility complex
Min	Minutes
MTT	3-(4,5-Dimethylthiazol-2-yl)-2,5-diphenyltetrazolium bromide
NCBI	National centre for biotechnology information
NTBI	Non-transferrin bound iron
PBS	Phosphate buffered saline
PCR	Polymerase chain reaction
Rec	Recombinant
RPM	Rotations per minute
RT	Room temperature
RT PCR	Real time polymerase chain reaction
SDS	Sodium dodecyl sulphate
Sec	Seconds
TBI	Transferrin bound iron
TfR	Transferrin receptor
UTR	Untranslated region
Wt	Wild type

# Chapter 1

## Introduction

Iron is an essential element required by human beings for their survival and development. Although 13-18 mg of iron is obtained through diet per day, only 1-2 mg is absorbed into the circulation. This dietary iron may be in two forms; the haem iron as present in meat and the non-haem iron which is mostly ferric ( $\text{Fe}^{3+}$ ) iron, as found in nuts, fruits and vegetables. Irrespective of the form of iron consumed the process of iron absorption occurs predominantly in the duodenum, from where it enters the circulation and is distributed to different parts of the body to be used for various metabolic purposes, as seen in Fig.1.1 (reviewed in Andrews, 2000 and Miret et al., 2003).

The amount of iron absorbed by the duodenum is governed by various factors. For example, during iron deficiency iron absorption increases to 2-4 mg per day and during iron overload the absorption can reduce to 0.5 mg per day. Secondly, the process of iron absorption may be enhanced or inhibited by the presence of certain substances. For example, vitamin C creates an acidic environment in the lumen and enhances non-haem iron absorption by reducing ferric iron ( $\text{Fe}^{3+}$ ) to ferrous iron ( $\text{Fe}^{2+}$ ) making it more soluble and thus bioavailable. On the other hand, tannins present in tea and fruit juices, phytates present in cereals and polyphenolic compounds found in all plant products inhibit the absorption of dietary non-haem iron, as reviewed in Dzikaite et al., 2006 and Sharp and Srai, 2007.

Figure not included due to copyrights.

**Fig. 1.1 Pathways of iron absorption and utilisation**  
Adapted from Andrews (2000).

Iron is absorbed into the circulation and utilised for various cellular processes, primarily for the production of red blood cells (Fig. 1.1). The high requirement of iron for erythropoiesis is reflected in the fact that the total amount of iron in the body is 3-4 g, out of which about 2.5 g is bound to haemoglobin. Approximately two million red blood cells are synthesised every second in the bone marrow which requires 25-30 mg of iron per day for haem synthesis. Apart from erythropoiesis, iron is also used in the synthesis of myoglobin which is an oxygen binding protein found in muscle tissues of vertebrates, aconitase, which converts citrate to

isocitrate in the citric acid cycle and the membrane bound cytochromes, that are involved in electron transport chain in mitochondria. Also, iron acts as a cofactor for ribonucleotide reductase which converts ribonucleotides to deoxyribonucleotides, eventually used in DNA synthesis (reviewed in Andrews and Schmidt, 2007 and Muckenthaler et al., 2008).

### **1.1 Iron absorption and distribution**

The three main cell types involved in iron metabolism are the iron-absorbing duodenal enterocytes, the iron-recycling reticuloendothelial macrophages and the iron-storing liver hepatocytes. Fig. 1.2 shows the cellular events in the absorption of iron. It begins when a ferric reductase duodenal cytochrome b (Dcytb) located on the apical surface of enterocytes reduces the poorly bioavailable  $\text{Fe}^{3+}$  iron to  $\text{Fe}^{2+}$  iron. The low pH of proximal duodenum along with an acidic climate of the brush border membrane maintains iron in the  $\text{Fe}^{2+}$  state. This  $\text{Fe}^{2+}$  iron can then be transported across the brush border membrane into the enterocyte via the protein, divalent metal transporter-1(DMT1). The process of haem iron uptake also occurs at the surface of enterocytes but through a different mechanism, briefly explained in section 1.2.1. Once inside the cell, iron enters the proposed labile iron pool (LIP) which may act as an iron reservoir for various cellular activities. Within the cell, excess iron is stored in the protein ferritin, where each ferritin molecule can hold up to 4500 iron atoms (reviewed in Andrews and Schmidt, 2007 and Miret et al., 2003).

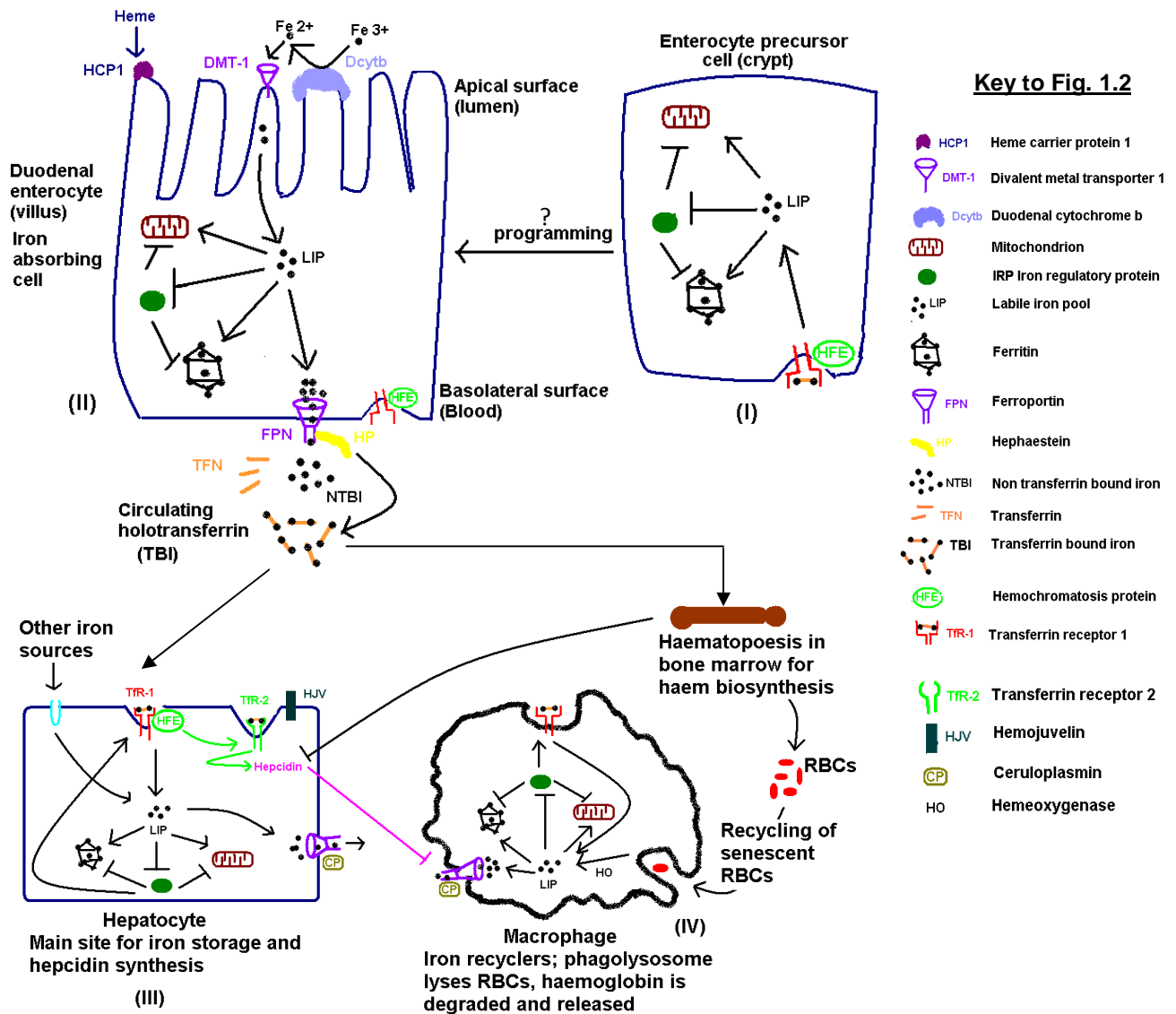


**Fig. 1.2 Cell types involved in iron absorption and circulation**

The mechanism of iron absorption and circulation, along with the roles of participating proteins are briefly shown in the figure.

- (I) Proposed programming of crypt cells to absorb iron.
- (II) Mature villus duodenal enterocytes absorb non-haem iron.
- (III) Hepatocytes store iron as well as produce hepcidin. Here, both TBI and NTBI uptake of iron occurs.
- (IV) Macrophages engulf senescent erythrocytes, particularly in the spleen, and recycle iron back into circulation through ferroportin.

Processes in (III) and (IV) are common to both haem and non-haem iron transport and utilisation. Adapted from Muckenthaler et al., (2008).

Iron can be translocated outside the enterocytes into the circulation through the sole known mammalian transmembrane iron-exporter, ferroportin. Ferroportin is a unidirectional ferrous exporter and is expressed on the basolateral surface of the enterocyte which is in access with the circulation. It is present on all cell types involved in iron transport (Nemeth et al., 2004). During the exit of iron from the enterocyte, ferroportin is assisted by the ferroxidase hephaestin which converts  $\text{Fe}^{2+}$  to  $\text{Fe}^{3+}$  whereas the ferroxidase ceruloplasmin assists in the loading of  $\text{Fe}^{3+}$  onto transferrin. Transferrin is the iron carrier protein in circulation which can hold up to two atoms of iron in the form of  $\text{Fe}^{3+}$  per protein molecule and this transferrin is referred to as diferric transferrin or holotransferrin. It transports iron throughout the body via the circulation and binds to the transferrin receptor-1 (TfR1) present on cell surfaces to form a complex of diferric transferrin-TfR1. This complex is then internalised into a vesicle. The low pH of vesicle and intracellular DMT1 assist in the release of iron from this complex into the cell cytoplasm (Miret et al., 2003, Muckenthaler et al., 2008).

Once the iron is released into the cytoplasm, the complex without iron is then recycled back to the cell surface for further iron uptake. Each TfR1 can undertake approximately 100 such recycling processes in its lifetime. Thus TfR1 functions to bring iron into the cells and the cells maintain intracellular iron levels by changing the expression levels of TfR1 on the cell surface (Aisen, 2004, Huebers and Finch, 1987). Hence, while maintaining normal intracellular iron levels, the more iron the cells require, the higher is the expression level of TfR1.

Although TfR1 is present on the surface of all cells involved in iron transport, another type of transferrin receptor, TfR-2, is expressed mainly on hepatocytes. It has been proposed that TfR-2 binds to HFE, the haemochromatosis protein, and induces hepcidin synthesis and may act as a sensor of diferric transferrin in the circulation (Gao et al., 2009). HFE has also been shown to interact with TfR1 to regulate transferrin-bound iron uptake, as shown in Fig. 1.2 (Kroot et al., 2011).

Along with the transferrin-bound iron, non-transferrin bound iron (NTBI) is also found in the systemic circulation. Although its chemical nature has not been confirmed yet, it is predicted to be in the form of iron bound to citrate or acetate. Iron in circulation could also be associated with albumin and other low molecular weight species. The uptake of such NTBI by cells is predominantly mediated by calcium channels and metal iron transporters (Andrews and Schmidt, 2007, Crichton et al., 2002).

### **1.1.1 Haem iron absorption**

Haem iron absorption is yet to be fully understood. It has been proposed that in the lumen, the haem moiety in food is processed to separate the globin fraction. The protoporphyrin ring enters the enterocyte in an intact form with the help of the haem carrier protein-1 (HCP1) (Shayeghi et al., 2005), which is highly expressed in the duodenal cells. Once inside the enterocyte, haem oxygenase excises the iron present in the protoporphyrin ring and this iron ( $\text{Fe}^{2+}$ ) joins the labile iron pool (Fig. 1.3). From here, iron could either be stored in ferritin molecules for future use or could be exported outside the cell into the circulation via a pathway common to

non-haem iron export, seen in Fig. 1.2 parts (III) and (IV). The degradation of haem iron via haem oxygenase leads to the formation of biliverdin, which is further reduced to bilirubin by biliverdin reductase. Bilirubin is then transported to the liver and excreted into bile (Andrews and Schmidt, 2007, Miret et al., 2003, Raffin et al., 1974, Sharp and Srai, 2007).

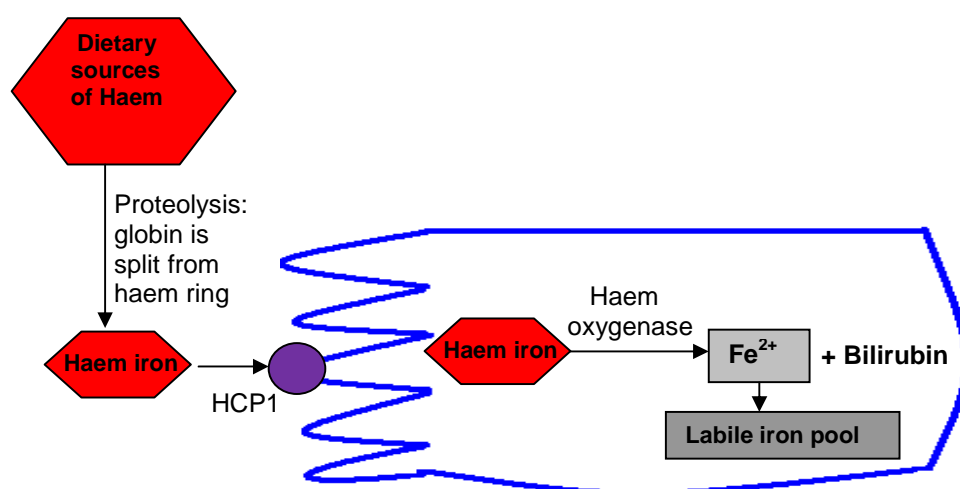


Fig. 1.3 Proposed model of haem iron uptake by an enterocyte

Iron absorbed through haem or non-haem pathways is partly retained in the intracellular ferritin of enterocytes. After 2-3 days, when enterocytes slough from the gut into the lumen, iron present in these cells is also lost via faeces (Andrews and Schmidt, 2007).

## 1.2 Overview of proteins involved in iron absorption and iron circulation

An overview of the functions of some of the significant proteins involved in iron absorption and circulation are shown in table 1.1.

Protein and chromosome location in humans	Cell/tissue in which normally expressed	Known or postulated function	Result of mutation	Named disorder	Clinical manifestations
HFE 348-mer <i>HFE</i> 6p21.3	All tissues except brain. Predominantly in hepatocytes.	Regulates cellular iron absorption by binding to TfR1 on cell surface and reducing its affinity for holotransferrin.  Regulates hepcidin production.	Increased iron influx in cells leads to tissue iron overload and organ damage.  Progressive increase in plasma iron.	Haemochromatosis type 1 (HFE 1), most common form of iron overload,	Intestinal iron hyperabsorption.  Reduced hepcidin levels despite of iron overload, which normally induces hepcidin expression  Cardiac disease, hypogonadism bronze skin pigmentation, hepatic cirrhosis, arthropathy and diabetes.
Hemojuvelin 426-mer <i>HJV</i> 1p21	Adult and foetal liver, heart, and skeletal muscle.	Membrane protein which exists in membrane bound and soluble forms.  It functions as co-receptor for bone morphogenetic proteins (BMP) signalling.  Regulates hepcidin production.	Increased iron influx in cells.  No hepcidin produced.	Juvenile haemochromatosis or Haemochromatosis type 2A (HFE2A)	
Hepcidin 25-mer <i>HAMP</i> 19q13.1	Predominantly in liver.	Maintains systemic iron levels by regulating both intestinal iron absorption and iron release from macrophages.	Lack of hepcidin leads to uncontrolled release of iron from macrophages. Iron overload in cells and tissues.	Haemochromatosis type 2B (HFE2B)	
Transferrin receptor 2 801-mer <i>TfR2</i> 7q22	Homologue of TfR1. Mainly in liver	Competes with TfR1 for binding with HFE. Acts as a sensor of holotransferrin in circulation.  Regulates hepcidin production.	Increased iron influx. High liver iron content.	Haemochromatosis type 3 (HFE3)	

Table 1.1 continued overleaf.

Protein and chromosome location in humans	Cell/tissue in which normally expressed	Known or postulated function	Result of mutation	Clinical manifestations
Ferroportin 571-mer <i>SLC40A1</i> 2q32	Macrophages, basolateral side of intestinal enterocytes, placenta, muscle and spleen.	Exports iron from enterocytes, macrophages and placenta.	Loss of function leads to decreased iron efflux by intestinal enterocytes and macrophages resulting in tissue iron overload of, particularly the reticuloendothelial cells.  Hepcidin resistance	Increased levels of hepcidin and anaemia.
Transferrin 698-mer <i>Tf</i> 3q21	Synthesised in liver and circulates in blood.	Iron carrier protein that transports iron from sites of absorption and haem degradation to those of storage and utilisation.	Increased iron influx in cells.	Increased retention of iron in the reticuloendothelial system and anaemia.
Ceruloplasmin 1065-mer <i>CP</i> 3q23-q25	Expressed by liver and secreted in circulation.	Multicopper oxidase. Assists in transporting iron outside the cells. Possesses ferroxidase activity oxidizing Fe <sup>2+</sup> to Fe <sup>3+</sup> without releasing radical oxygen species.	Decreased iron efflux from cells.	Iron accumulation in the brain as well as visceral organs, retinal degeneration and diabetes mellitus.  Neurological manifestations seen unlike all other genetic haemochromatosis.
Divalent metal transporter 1 568-mer <i>NRAMP2</i>	Ubiquitously expressed in transmembrane regions and also present intracellularly.	Involved in apical iron uptake into duodenal enterocytes. Involved in iron transport from acidified endosomes into the cytoplasm.	Unregulated iron uptake.	Abnormal haemoglobin content in the erythrocytes which are reduced in size. Progressive liver iron overload.

**Table 1.1 Overview of important proteins involved in iron metabolism**

Information on proteins and clinical manifestations adapted from Andrews and Schmidt, (2007), Dzikaite et al., (2006), Gehrke et al., (2003) Jacolot et al., (2008) and Pieterangelo, (2006).

### 1.3 The iron hormone hepcidin

The iron hormone hepcidin, also referred to as LEAP-1 (liver associated antimicrobial peptide), plays a significant role in maintaining iron homeostasis (Pigeon et al., 2001). In humans, hepcidin is encoded by the *HAMP* gene which contains 3 exons, located on chromosome 19q13.1. As explained in Fig. 1.4A, hepcidin is initially synthesised as an 84-mer preprohormone called preprohepcidin.

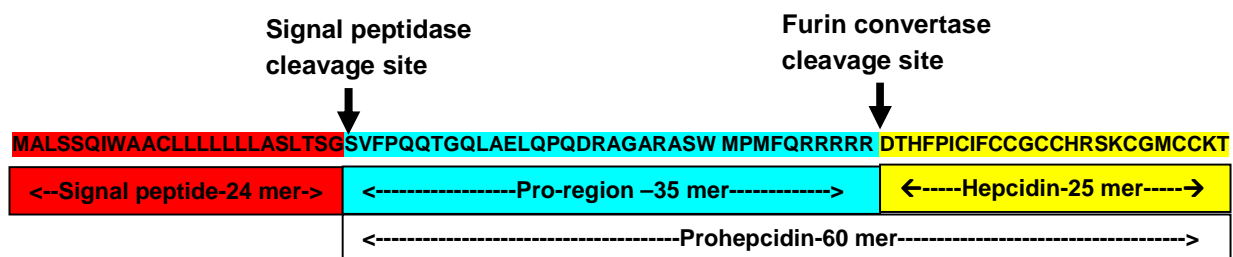


**Fig. 1.4A Significant sites of cleavage in preprohepcidin (84-mer)**

Sites of action of signal peptidase and furin convertase are shown in the figure. Cleavages eventually lead to the bioactive hepcidin-25.

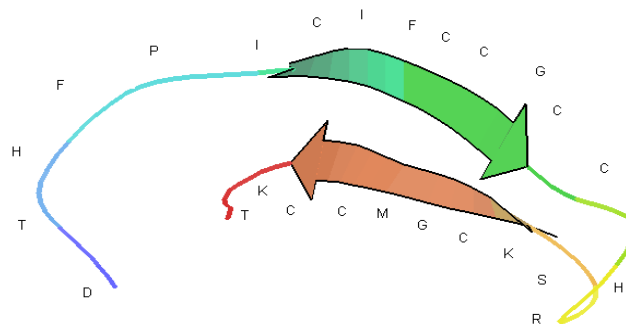


**Fig. 1.4B Structure of bioactive hepcidin-25**

Hepcidin forms a hairpin-like structure (Hunter et al., 2002); figure adapted from protein databank (PDB), PDB ID 1M4F, available at <http://www.rcsb.org/pdb/>

This preprohepcidin is cleaved by a signal peptidase to remove the N-terminal 24-mer signal peptide. The remaining 60-mer peptide, referred to as prohepcidin is post-translationally cleaved by a furin like convertase to secrete the 25-mer mature bioactive hepcidin (2.7 kDa) which circulates in blood (Krause et al., 2000) at a concentration of 1.1-55 ng/mL (Ashby et al., 2009).

The small size of hepcidin-25 helps its excretion through urine where it offers antibacterial protection to the host (Ashby et al., 2009, Park et al., 2001). Although the most predominant form in circulation is hepcidin-25, other truncated forms like hepcidin-22 and hepcidin-20 have also been identified in human urine. These are either absent or present in low concentrations in the circulation (Park et al., 2001) which suggests that they are biologically less significant than hepcidin-25 in regulating iron levels. This has been supported by studies which showed that the N-terminal region is important for hepcidin-25 to exhibit its bioactivity and thus the other isoforms display much reduced iron regulatory activity as compared to hepcidin-25 (Nemeth and Ganz, 2006). It is not yet known if there are any other biological functions of these isoforms of hepcidin.

Although hepcidin is predominantly produced by the liver hepatocytes, it has been detected in low levels in the heart, brain, lung, tonsils, trachea, prostate gland, adipose tissue, adrenal gland, thyroid gland and bone marrow (Bekri et al., 2006, Krause et al., 2000, Park et al., 2001, Pigeon et al., 2001). Hepcidin exhibits antifungal and antibacterial properties and structurally resembles other known peptide antibiotics such as the defensins (Krause et al., 2000, Pigeon et al., 2001).

So far, apart from humans, hepcidin has been found in mice, rats, dogs and fish (Nemeth et al., 2003). The furin cleavage site as well as the function and structure of hepcidin-25 are well conserved between fish and mammals. In particular, the 8 cysteine residues in hepcidin-25, as seen in Fig .4B, are highly conserved amongst

species and the cysteines involved in the vicinal bond are believed to have structural and functional significance (Jordan et al., 2009).

Along with similarities, there are some genomic differences between species with regards to hepcidin. Unlike the human genome which contains only one copy of the *HAMP* gene, mice possess two copies, *Hamp-1* and *Hamp-2*, possibly due to a gene duplication event (Pigeon et al., 2001). Various studies were conducted to understand the functional significance of these two genes encoding hepcidin. It was earlier shown by Ilyin et.al (2003) that iron excess in the liver of mice upregulated both genes at the transcriptional level. Later, Lou (2009) showed that although *Hamp-1* transgenic mice developed severe anaemia, *Hamp-2* transgenic mice developed like the non-transgenic mice. This erased the possibility of functionality of *Hamp-2* gene in mice. Hence, although the two genes encoding hepcidin are independently transcribed and bear high sequence similarity, *Hamp-1* is believed to be the bioactive molecule which regulates iron levels. Apart from mice, the fish *Paralichthys olivaceus* has also been shown to possess two genes encoding hepcidin (Kim et al., 2005).

### **1.3.1 Function of hepcidin in systemic iron homeostasis**

Under normal physiological conditions regulation of iron takes place at both the systemic and cellular level. The systemic regulation of iron is mediated by hepcidin and the mechanism of its action is explained as follows.

The receptor of hepcidin is the transmembrane iron exporter ferroportin, located at the basolateral surface of duodenal enterocytes and on macrophages. As explained in Fig. 1.5, an increase in systemic iron levels lead to an increase in hepcidin expression (Nemeth and Ganz, 2006, Andrews and Schmidt, 2007).

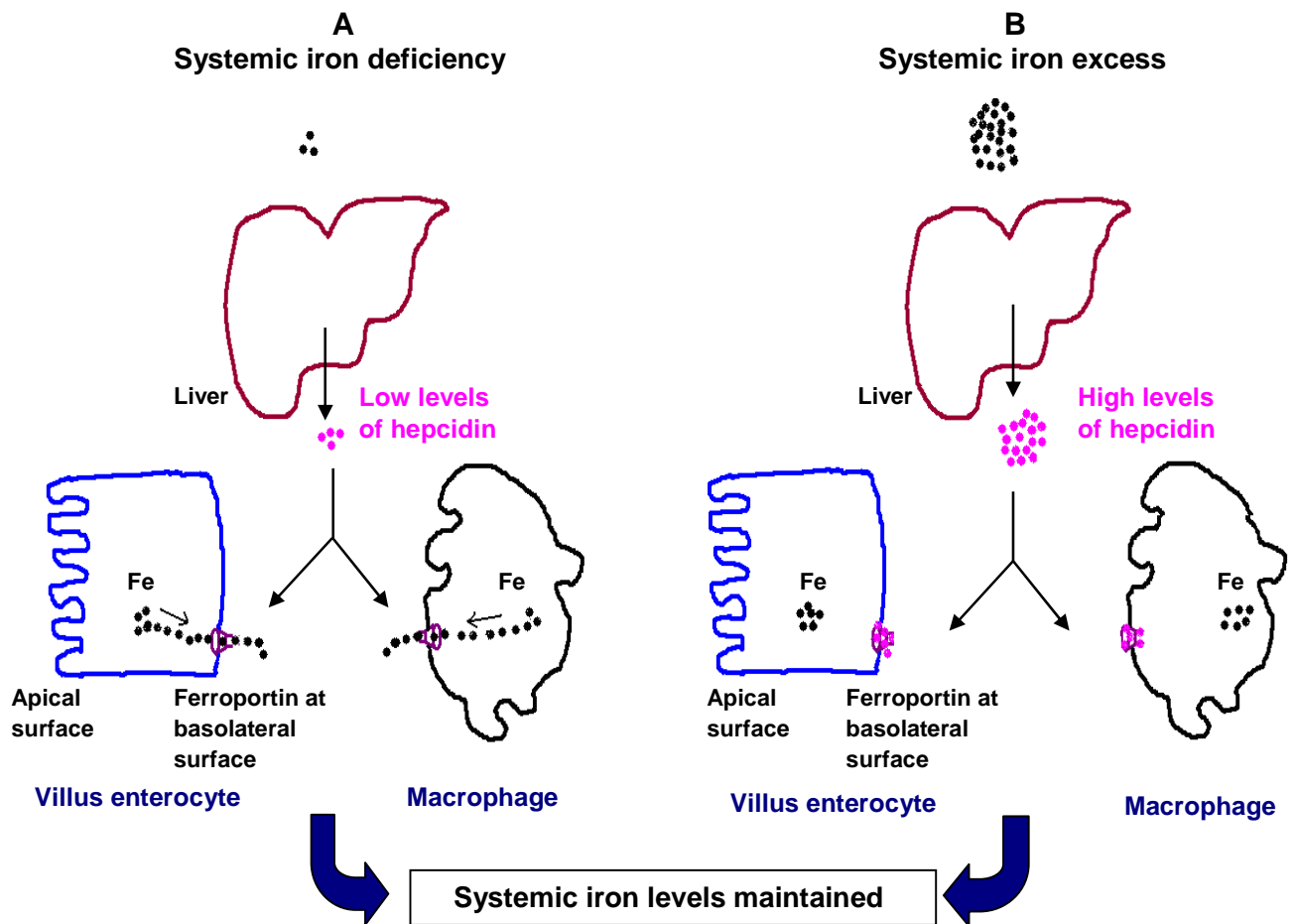


**Fig. 1.5 Systemic regulation of iron by hepcidin**

**A:** Under systemic iron deficiency, less hepcidin is produced. Low levels of hepcidin are unable to degrade all ferroportin. Undegraded ferroportin export iron outside the cells into circulation to raise systemic iron levels.

**B:** Under systemic iron excess, hepcidin levels rise. High levels of hepcidin degrade ferroportin which is now unable to export iron outside the cells. This results in iron retention within the cells and iron is not exported into the circulation. Systemic iron levels are thus not further elevated.

Once the hepatocytes secrete hepcidin into the circulation, hepcidin interacts with ferroportin present on cell surfaces. The complex is then internalised via endocytosis and ferroportin is degraded in the lysosomes through proteolysis (Nemeth et al., 2004). Since ferroportin functions as an iron exporter, this degradation of ferroportin inhibits iron release from enterocytes, macrophages and placental cells into the circulation, thus preventing further systemic iron elevation. In contrast, systemic iron deficiency leads to a decrease in hepcidin production (Pigeon et al., 2001) and a resultant increase in iron efflux from cells, thus raising systemic iron levels.

The significance of hepcidin in regulating iron levels has been understood through knockout and over-expression studies. Mice that over-express *Hamp-1* die of severe anaemia due to over-degradation of ferroportin, intracellular iron retention and unavailability of iron in the circulation for erythropoiesis (Nicolas et al., 2002). Conversely, constitutive hepcidin expression in a mouse model of iron overload haemochromatosis prevented iron overload (Nicolas et al., 2003). This evidence indicates that hepcidin plays a crucial role in regulating systemic iron levels in the body by inhibiting duodenal iron absorption and controls the release and recycling of iron by macrophages and iron mobilisation from the hepatocytes.

### **1.3.2 Overview of hepcidin regulation**

Apart from iron overload, conditions like inflammation and infection also lead to an increase in hepcidin production. In contrast, iron deficiency, increased erythropoiesis and hypoxia lead to a decrease in hepcidin production. Also, as

explained in table 1.1, the presence of functional genes *HFE*, *TfR2*, *HAMP* and *HJV* are required to execute a normal hepcidin response and mutations in these genes lead to reduction or abolishment of hepcidin production. Regulators of hepcidin expression have been summarised in Fig. 1.6.

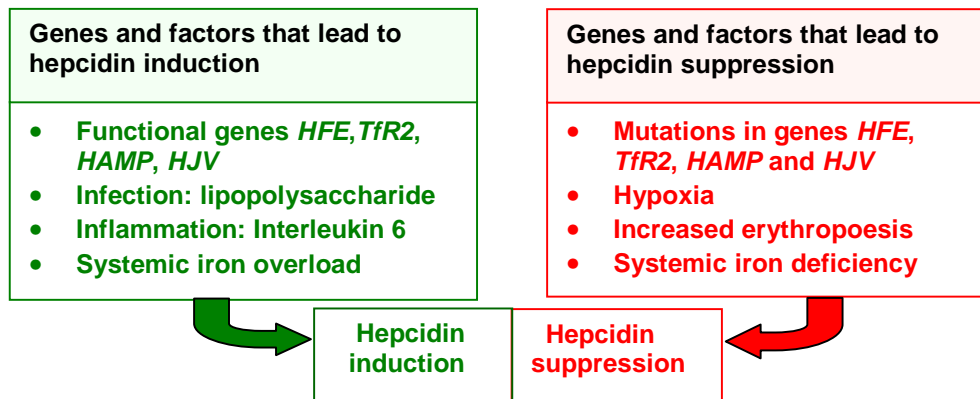


**Fig. 1.6 Factors affecting hepcidin production**  
Important genes and factors that lead to an increase and decrease in hepcidin expression.

The purpose of modulation of hepcidin production during infections and inflammation is to support host defence mechanisms. For example, localised high doses of hepcidin have been found in phagosomes in macrophages infected with tuberculosis bacteria (Sow et al., 2007). This can be explained by the fact that these organisms require iron for survival. An increase in hepcidin production leads to more sequestration of iron within the cells thus reducing the bioavailability of iron for the invading pathogens. Also, the increase in hepcidin causes a lowered iron absorption in the duodenum (Nicolas *et al.*, 2002). However, in the host this response also limits the bioavailability of iron for erythroid precursors and often contributes to the anaemia associated with infections and inflammation. Consequently, hepcidin acts as a marker of anaemia of inflammation (AI) (Ganz,

2011). Although several mechanisms for regulation of hepcidin have been proposed, there has been no evidence to date of any other type of control, except at transcriptional levels (Truksa et al., 2007). An overview of signal transduction pathways, in particular the bone morphogenetic proteins (BMP)-SMAD, janus kinase/signal transducer and activator of transcription-3 (JAK-STAT) and HIF pathways which appear to regulate *hepcidin* transcription, are shown in Fig. 1.7.

Briefly, intracellular iron stores influence the binding of BMPs to their receptors on the cell surface (Fig. 1.7A and 1.7B). As shown in Fig. 1.7A, membrane-bound HJV (mHJV) acts as a BMP co-receptor and assists in this process. This leads to phosphorylation and activation of the intracellular SMAD proteins which transmit a signal to the nucleus to increase *HAMP* transcription in the cells (Babitt et al., 2006). During inflammation, IL6 induces *HAMP* transcription via the JAK/STAT pathway (Babitt et al., 2006, Wang et al., 2005). As shown in Fig. 1.7B, when iron stores are low, mHJV is cleaved by furin and/or matrilysin 2 (a transmembrane protease encoded by the gene *TMPRSS6*, expressed predominantly in liver) to form soluble HJV (sHJV). The sHJV disrupts the BMP-mediated activation and instead leads to down-regulation of *HAMP* transcription (Finberg et al., 2010).

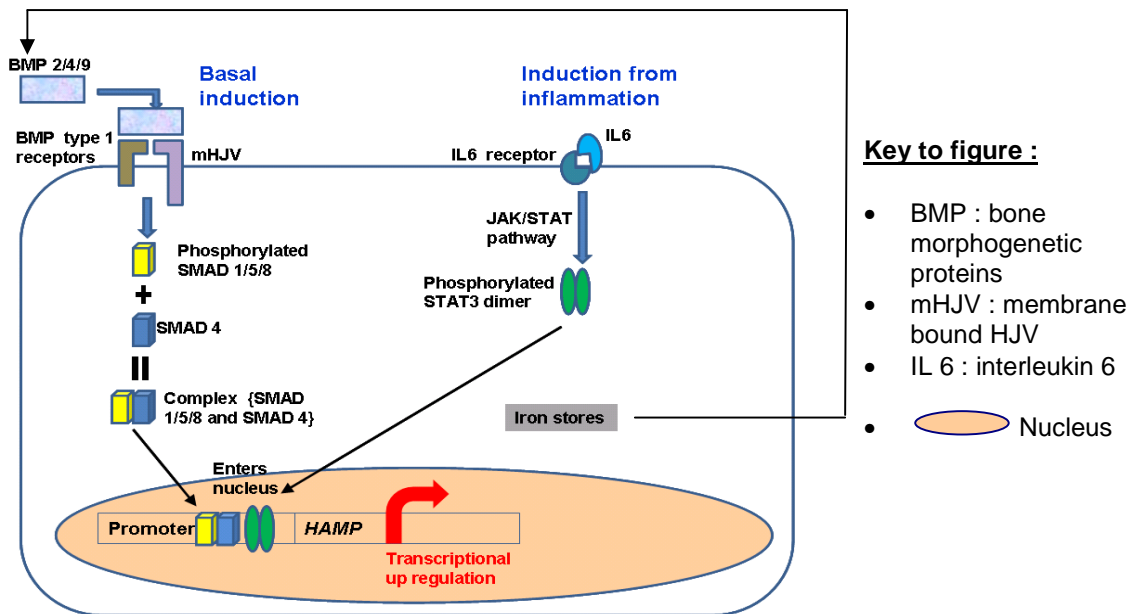


**Fig. 1.7A Pathways leading to transcriptional up-regulation of hepcidin**

The complex of SMAD proteins enter the nucleus, bind to the promoter region of hepcidin gene and stimulate *HAMP* transcription. Also, the STAT3 dimer formed as a result of IL6 binding to its receptor leads to upregulation of hepcidin. High liver iron stores promote hepcidin synthesis via the BMP pathway.

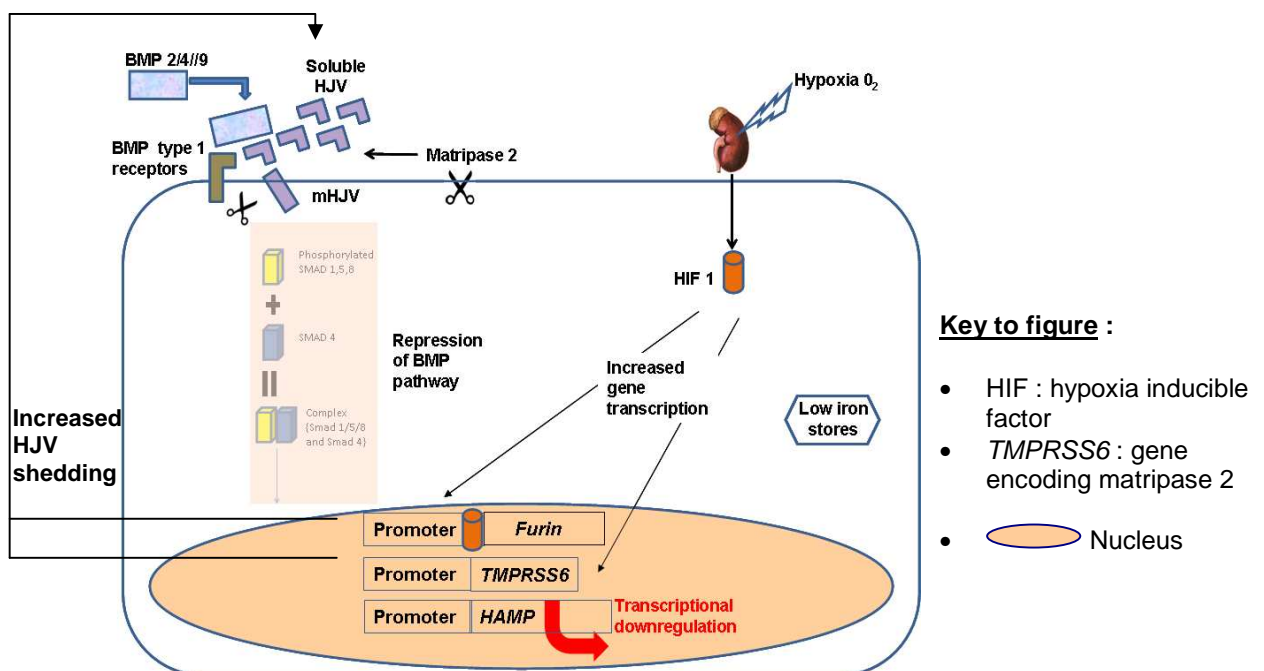


**Fig. 1.7B Pathways leading to transcriptional down-regulation of hepcidin**

Both furin and matrilase 2 are able to cleave mHJV to soluble HJV. The soluble HJV does not allow a stable complex to be formed between BMP ligands and receptors, thus inhibiting *HAMP* transcription via the BMP pathway. Hypoxia inducible factor increases the transcription of genes that would cleave the mHJV to soluble HJV. Adapted from Andrews (2007).

## 1.4 Regulation of cellular iron levels

Cellular iron homeostasis is mediated by binding of the two iron regulatory proteins (IRP), IRP1 and IRP2, to iron responsive elements (IREs) on the mRNA of some iron-regulated genes. Binding of IRP1 to IRE in 5' untranslated regions (UTRs) of transcripts prevent protein synthesis whereas binding of IRP1 to IREs in the 3' region provides stability to mRNA and allows translation into proteins. The binding of the IRPs to the IREs is in turn regulated by the presence of iron (Fig. 1.8).

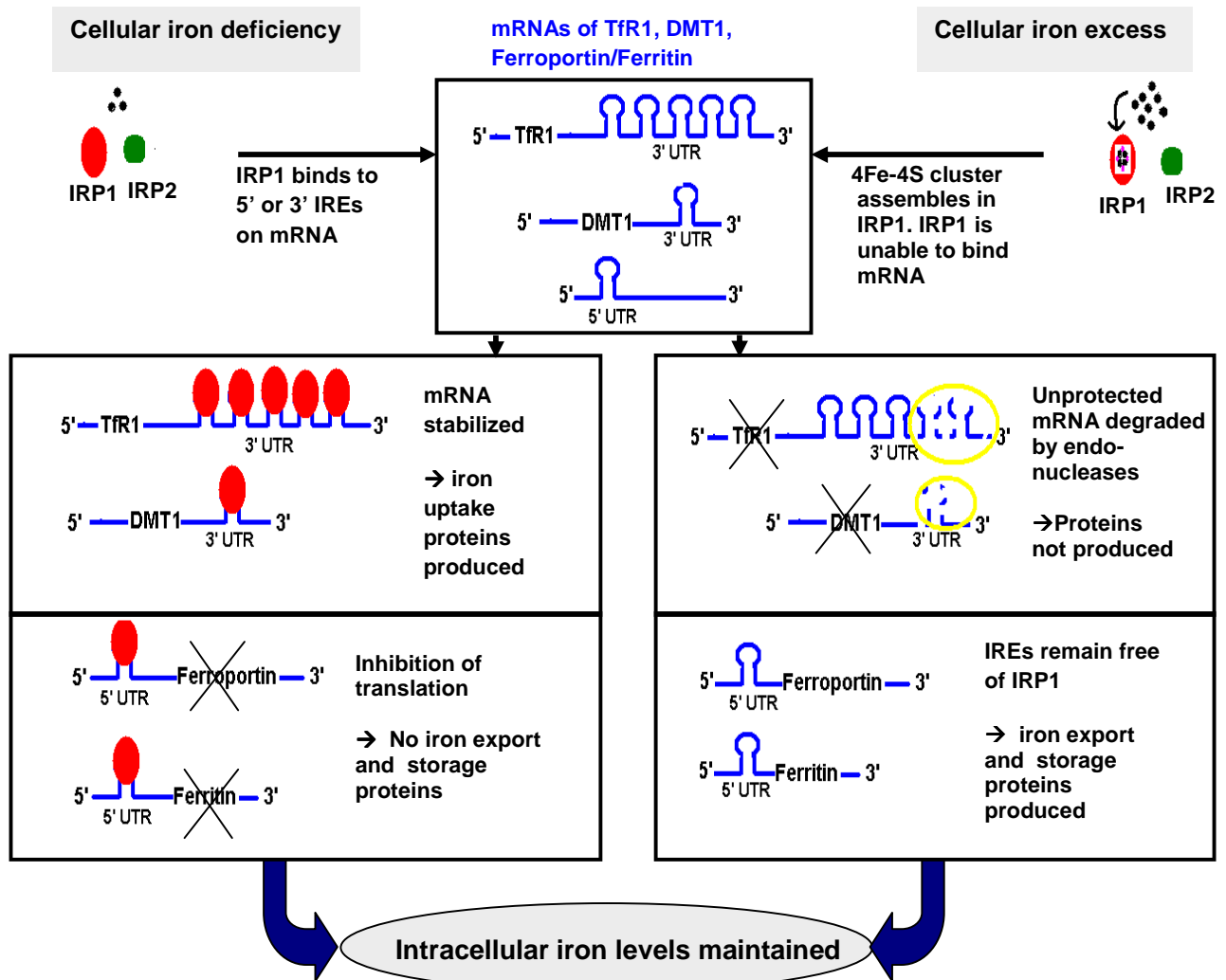


**Fig. 1.8 Cellular regulation of iron by iron regulatory proteins (IRPs)**

Binding of IRPs to IREs in 5' UTR and 3' UTR lead to different effects. IRP binding to 5' IREs result in inhibition of protein production whereas binding to 3' IREs favour protein production.

As shown in Fig. 1.8, when cellular iron levels are sufficient or in excess, an iron-sulphur cubane (4Fe-4S) is formed which prevents the binding of IRP1 to the IRE in 5' UTR of mRNA of genes encoding ferroportin and ferritin. This permits translation of the mRNA into proteins to favour more iron storage within cells and more iron efflux. Thus cellular iron overload is prevented. In contrast, under cellular iron depletion, IRP1 is iron-free and can therefore bind to the IREs in 3' UTR on transcripts of genes encoding TfR1 and intestinal DMT1. In doing so it stabilises the mRNAs and therefore increases the expression of both proteins, hence facilitating increased iron uptake by cells to eliminate cellular iron deprivation. Thus the IRP-IRE network maintains cellular iron levels (Muckenthaler et al., 2008).

### **1.5 Iron homeostasis and disorders**

Iron is essential for survival and growth but free iron can be toxic. Since iron has the ability to accept and donate electrons, it can catalyse the Fenton reaction that leads to the generation of hydroxyl radicals. These radicals can cause severe damage to cells and tissues and thus high levels of iron can be deleterious. Additionally, there is no physiological pathway for iron excretion except by blood loss and the natural means of iron loss from the body occurring as a result of sloughing of mucosal cells and/or menstruation is minimal (Miret et al., 2003, Nemeth and Ganz, 2006). Hence maintaining iron homeostasis is crucial.

The significance of body iron homeostasis can be realised by reflecting on the diseases and conditions in which iron homeostasis is disturbed. Considering iron

deficiencies, broadly, there are two types: absolute iron deficiency and functional iron deficiency. Absolute iron deficiency is characterised by depleted iron stores. This can be due to excessive blood loss or pregnancy when there is increased demand for iron or malnutrition when there is decreased supply of iron. This is also referred to as iron deficiency anaemia and could have one of the many observable effects such as developmental retardation in children. Surprisingly, a large proportion of the world population, approximately one third, is believed to be suffering from iron deficiency anaemia. On the other hand, functional iron deficiency, as seen in cancer and inflammation is referred to as anaemia of inflammation or anaemia of chronic disease. These are characterised by low serum iron levels despite replete iron stores due to iron-restricted erythropoiesis (Munoz et al., 2011, Muckenthaler et al., 2008).

Current treatments to alleviate iron deficiency anaemia involve increasing iron levels in the body by using ferrous salts. Although approximately 200 mg of inorganic iron per day is given to the patients, low doses have been found to be effective. Also, when the dose of iron is more than required, the unabsorbed iron salts cause nausea, abdominal pain and constipation. Thus low doses of iron salts between 50-100 mg of iron should be recommended (Munoz et al., 2011).

On the other extreme of iron deficiency is iron overload, which could be acquired or functional. Examples of acquired iron overload are the iron overdose in children which is the commonest poisoning in children, iron overload as a result of repeated blood transfusions and/or alcohol consumption and Bantu siderosis (Munoz et al., 2011).

Functional iron overload, referred to as hereditary haemochromatosis, is the most frequent genetic disorder in Caucasians and results from defects in some of the genes involved in iron metabolism described in table 1.1. Under haemochromatosis, intestinal iron absorption can exceed iron loss by ~ 3 mg/day (Pietrangelo, 2006), the effect of which can be tissue specific. For instance the liver possesses high levels of antioxidants and cytoprotective enzymes. This suggests that a substantially high level of liver iron overload would be required to observe the toxic effects of iron. On the other hand, in the reticuloendothelial cells e.g. macrophages, only about a 2-3 fold increase in cellular iron would lead to changes in normal cell functions (Crichton et al., 2002, Munoz et al., 2011).

Presently, phlebotomy is offered as the commonest therapy to remove excess iron from the body of haemochromatosis patients. The rationale behind this is to reduce the potential of iron-mediated tissue injury. However, since this strategy has its own complications, other therapeutic measures like using iron chelating drugs are also being used. This involves the use of iron chelators like deferoxamine, deferriprone and deferasirox which have their respective advantages. For example, deferriprone has a better half life than deferoxamine and is excreted in urine. Hence it is preferred over the use of deferoxamine. However, the use of these chelators has some limitations such as inadequate and/or variable chelation. Also, the lowest safety limit of iron overload with chelating therapies is yet to be determined (Munoz et al., 2011, Smith et al., 2011).

## **1.6 Heparin as a biomarker in diseases**

Since hepcidin is regarded as the main iron homeostasis regulator, involvement of hepcidin in any iron-associated disease is expected. For instance the levels of hepcidin-25 are high in the serum of patients suffering from anaemia of chronic disease. Also, increased hepcidin concentrations mark infections and inflammatory diseases like malaria and chronic kidney disease (Kroot et al., 2011). Not surprisingly, hepcidin has been identified as a type 2 acute phase protein (Nemeth et al., 2003). Levels of hepcidin are high in cases of obesity, acute myocardial infarction and acquired forms of non-haemochromatotic iron-overload resulting from excessive alcohol consumption, whereas iron deficiency anaemia shows inhibition of hepcidin synthesis and thus very low serum hepcidin concentrations (Kroot et al., 2011).

Since hepcidin has been associated with such a wide range of conditions, its significance lies not only in maintaining iron homeostasis but also as a marker for diagnosing various disorders. One of the most recent applications of hepcidin as a biomarker is a study which proposed that measuring hepcidin concentrations can be a way to assess the requirement for iron supplementation in young athletes (Borrione et al., 2011). Additionally, a close relationship between iron and glucose metabolism has been previously shown. Increased iron stores were found to predict the development of type 2 diabetes while iron depletion was found to be protective (Fernandez-Real *et al.*, 2002). Also, accumulation of iron in specific regions of the brain is associated with neurodegenerative diseases such Alzheimer's disease and Parkinson's disease (Crichton et al., 2002).

Hence studies related to iron regulation and hepcidin would lead to a better understanding of several aspects of human metabolomics and also find various diagnostic and therapeutic applications.

### **1.7 Background and overall aims of the project**

In humans and in animal models, increased systemic iron levels lead to increased hepcidin levels and increased urinary hepcidin excretion (Lin et al., 2007, Nemeth et al., 2003, Pigeon et al., 2001). In humans, a 4-5 fold increase in hepcidin levels within 24 hours of iron dosage has been reported (Lin et al., 2007). Likewise, a high iron-supplemented diet given to mice resulted in a 10-fold higher iron concentration in the liver and a 4-fold increase in *Hamp* mRNA in the livers of these mice (Muckenthaler et al., 2003, Pigeon et al., 2001).

However, these findings could not be replicated *in vitro*. High iron dosage to cells either increased or decreased or had no effect on *hepcidin* mRNA expression. For instance, holotransferrin treatment of HepG2 cells led to either a decrease (Jacolot et al., 2008) or have no effect (Gehrke et al., 2003) on *hepcidin* mRNA. In primary hepatocytes it led to an increase (Lin et al., 2007, Rapisarda et al., 2010) or decrease (Nemeth et al., 2003) in *hepcidin* mRNA. Treatment of HepG2 cells using inorganic iron sources showed a dose-dependent *hepcidin* mRNA response (Fein et al., 2007) or a decrease in *hepcidin* mRNA (Jacolot et al., 2008). On the other hand in hepatocytes, such sources either showed no change (Lin et al., 2007, Pigeon et al., 2001), or a decrease in *hepcidin* mRNA expression (Dzikaite et al., 2006, Nemeth et al., 2003). Other studies showed that *hepcidin* expression was

influenced by the plating and culturing time of hepatocytes (Lin et al., 2007) and by the presence and absence of serum in the medium (Pigeon et al., 2001, Nemeth et al., 2003). The presence of macrophages along with the HepG2 cells was also crucial to observe a rise in *hepcidin* mRNA expression in HepG2 cells (Jacolot et al., 2008) whereas another group showed that the presence of other cell types was not necessary (Montosi et al., 2005).

These varied and inconclusive findings require clarification and further investigation as it would aid in a better understanding of how iron regulates hepcidin, which is not yet known, or whether they both regulate each other via a feedback mechanism.

One reason for the decrease in *hepcidin* transcription, as observed by some groups, could be due to the cells' inability to uptake the supplemented iron. Most of these iron overdose experiments have been performed using inorganic sources of iron like ferrous sulphate, ferric ammonium citrate, ferric citrate or ferric nitrilotriacetic acid. Since the predominant physiologically relevant form of iron is the iron bound to transferrin, these inorganic iron sources may not be preferred by the cells as much as transferrin-bound iron. Secondly, iron uptake mechanisms of the inorganic iron sources are not fully defined yet. It is likely that such iron forms may enter the cells and be quickly sequestered, consequently leading to a decrease in *hepcidin* mRNA expression as the cells may not have recognised the high intracellular iron content.

Also, TfR1 on the cell surface controls the amount of iron intake by cells (Muckenthaler et al., 2008). If the cell is iron deficient it will express more TfR1 on its cell surface to encourage iron uptake until cellular iron sufficiency is reached. After this stage the cells would stop further TfR1 synthesis or decrease TfR1 expression to prevent further iron uptake and thus intracellular iron overload. In this situation *hepcidin* mRNA expression may not increase because of the lack of intracellular iron overload. This may keep *hepcidin* levels stable rather than lead to an increase (Gehrke et al., 2003). In addition, commercially available holotransferrin is only between 5 % and 20 % diferric (Farnaud, personal communication). Transferrin containing such a low proportion of holotransferrin would not create an iron-rich environment for the cells to uptake high levels of iron. This would result in stable intracellular iron content and not an intracellular iron overload. These issues were addressed in this study in reference to hepcidin expression, where TfR1 on the cell surface of different cell lines and their responses under different conditions was also analysed. Whilst defining the nature of the supplemented iron source, cellular iron overload on iron supplementation was investigated.

### **Overall aims**

1. To study the effect of iron supplementation on the regulation of hepcidin and other iron homeostasis regulators in the Chinese hamster ovarian cell lines and human liver carcinoma cell lines.
2. To investigate the role of the pro-peptide region of the prohormone of hepcidin.

## Chapter 2

### Materials and Methods

#### 2.1 Materials

Primers for polymerase chain reaction (PCR), Hams' F12 medium, Dulbecco's Phosphate Buffered Saline (PBS) 1X and hygromycin B were purchased from Invitrogen (Loughborough, UK). Foetal calf serum (FCS) was purchased from Biosera (Ringmer, UK). PCR reagents, proteinase K, cDNA preparation, gel extraction and PCR product purification kits were purchased from Qiagen (Crawley, UK). The pGEM-T easy vector system was bought from Promega (Southampton, UK). All other reagents and labware were purchased from Sigma-Aldrich (Poole, UK) and VWR (East Grinstead, UK) respectively, unless otherwise stated.

#### 2.2 Methods

##### 2.2.1 Cell culture

All cell lines were grown and maintained in their respective maintenance medium in tissue culture flasks at 37 °C in a humidified atmosphere of 95 % air and 5 % CO<sub>2</sub>. The maintenance medium was changed every 2-3 days and cells were passaged by trypsinisation (0.025 % trypsin EDTA for 5 minutes) on reaching 70-80 % confluence. To neutralise the trypsin, maintenance medium was added and centrifugation was performed at 1000 rotations per minute (rpm) (89 x g) for 5 min. The supernatant was removed, fresh maintenance medium was added to the cell pellet and the cells were plated at the required density for iron-related studies.

## **2.2.2 Chinese hamster ovary (CHO) cell lines**

Wild type CHO AA8 (Wt CHO) was a kind gift from Professor Keith Caldecott (University of Sussex, Falmer, East Sussex, UK). The CHO transferrin receptor variant cell line (CHO TRVb1 clone B6), constitutively expressing the human transferrin receptor-1 was kindly donated by Dr. Heinz Zoller (University of Innsbruck, Austria). These two CHO cell lines were maintained in Ham's F12 nutrient mixture (1X) containing 2 mM glutamax supplemented with 10 % FCS and 1 % antibiotic/antimycotic solution (100X) (Fisher Scientific International Inc., UK).

## **2.2.3 HepG2 cell lines**

### **2.2.3.1 Wild type HepG2 cells**

Wild type HepG2 (Wt HepG2), a hepatocarcinoma cell line, was bought from the Health Protection Agency (Colindale, London UK). These cells were maintained in Eagle's Minimum Essential Medium (EMEM), 1 % non-essential amino acids, 2 mM glutamax, 1 % antibiotic/antimycotic solution and 10 % FCS.

### **2.2.3.2 Creation of recombinant HepG2 cells**

Recombinant HepG2 (rec-TfR1 HepG2), a HepG2 cell line that constitutively expresses human TfR1 receptor, was created in collaboration with Dr. Paul Brown (King's College, London, UK). Details on the creation of this cell line are in appendix I.

**Principle:** The coding region of human *TfR1* gene, devoid of its IRE was cloned into the plasmid vector pCEP4 (Invitrogen-Life technologies, UK). This recombinant plasmid was transfected into Wt HepG2 cells, resultantly giving rise to the

recombinant HepG2 cells. Since the IRE of *TfR1* has been removed, on iron supplementation the cells should take up iron continuously regardless of their intracellular iron content, permitting intracellular iron overload. The human *TfR1* mRNA and the protein sequence alignment below shows the region of interest cloned into the vector pCEP4. It also shows the primers designed for cloning and real time PCR.

```

ggcggctcgggacggaggacgcgctagtgtagtgaggcttctagaactacaccgaccctc 62
  R L G T E D A L V - V R A S R T T P T L
Gtgcctccctcatcctcgggggctggctggagcggccgctccggctggtccagcagc 122
  V S S L H P A G L A G A A A P V L S S S
Catagggagccgcacggggagcgggaaagcggctcgggcccaggcggggcggcgggat 182
  H R E P H G E R E S G R G P R R G G R D
Ggagcggggcgcgagcctgtgggaaagggctgtggcggcgcctcggagcggctgcaggt 242
  G A G P R A C G E G A V A A P R A A A G

```

forward primer for cloning

**Tgatatatgcccgcgaccatggatcaagctagatcagcattctc >>**

```

Tcttctgtgtggcagttcagaatgatggatcaagctagatcagcattctcctaactgttt 302
  S S V W Q F R M M D Q A R S A F S N L F
Ggtggagaaccattgtcatatacccggttcagcctggctcggcaagtagatggcgataac 362
  G G E P L S Y T R F S L A R Q V D G D N
Agtcatgtggagatgaaacttgctgtagatgaagaagaaaatgctgacaataacacaaaag 422
  S H V E M K L A V D E E E N A D N N T K
Gcfaatgtcacaacacaaaagggtgtagtggaagtatctgctatgggactattgctgtg 482
  A N V T K P K R C S G S I C Y G T I A V
Atcgtcttttcttgattggatttatgattggctacttgggctattgtaaggggtagaa 542
  I V F F L I G F M I G Y L G Y C K G V E
Ccaaaaactgagtgtagagactggcaggaaccgagctcctcagtgagggaggaccagga 602
  P K T E C E R I A G T E S P V R E E P G
Gaggacttccctgcagcagctcgcttatattgggatgacctgaagagaaagtgtcggag 662
  E D F P A A R R L Y W D D L K R K L S E
Aaactggacagcagacttaccagcaccatcaagctgctgaatgaaaatcatatgtc 722
  K L D S T D F T S T I K L L N E N S Y V
Cctcgtgaggctggatctcaaaaagatgaaaatcttgcggtgtatgttgaatcaattt 782
  P R E A G S Q K D E N L A L Y V E N Q F
Cgtgaatttaactcagcaagctcggcgtgatcaacatttggtaagattcaggtcaaa 842
  R E F K L S K V W R D Q H F V K I Q V K
Gacagcgtcaaaaactcggatgatcatagttgataagaacggtagacttgtttacctggg 902
  D S A Q N S V I I V D K N G R L V Y L V
Gagaactcctgggggttatgtggcgtatagtaaggctgcaacagttactgtaactgggtc 962
  E N P G G Y V A Y S K A A T V T G K L V
Catgctaattttggactaaaaagattttgaggatttatacactcctgtgaatggatct 1022
  H A N F G T K K D F E D L Y T P V N G S
Atagtgtgtcagagcagggaaaatcacctttgcagaaaagggtgcaaatgctgaaagc 1082
  I V I V R A G K I T F A E K V A N A E S
Ttaaatgcaattgggtgtgttgatatacatggaccagactaaatttccattgttaacgca 1142
  L N A I G V L I Y M D Q T K F P I V N A
Gaatcttcaattcttggacatgctcatctggggacaggtgacccttacacacactggatc 1202
  E L S F F G H A H L G T G D P Y T P G F
Cctccttcaatcacactcagtttccaccatctcggatcaggtgctcctaatatacct 1262
  P S F N H T Q F P S R S S G L P N I P
Gtcagacaactccagagctgctgcagaaaagctgtttgggaatggaagggagactgt 1322
  V Q T I S R A A A E K L F G N M E G D C
Ccctctgactggaaaacagactctacatgtaggatggttaacctcagaaaagcaaatgtg 1382
  P S D W K T D S T C R M V T S E S K N V
Aagctcactgtgagcaatgtgctgaaagagataaaaattcttaacatctttggagtatt 1442

```

### Key to *TfR1* mRNA and protein alignment

- Region of the primers used for cloning the insert into the vector
- Coding sequence and the 760-mer protein, including the cytoplasmic and transmembrane region. This is the region cloned into the vector.
- Cytoplasmic region that regulates internalization of TfR1.
- Transmembrane region
- Extracellular region
- Trypsin cleavage site between R and L to produce soluble serum TfR1

```

K L T V S N V L K E I K I L N I F G V I
Aaaggctttagaaccagatcactatggttagttggggcccagagagatgcatggggc 1502
K G F V E P D H Y V V V G A Q R D A W G
      Forward primer for TfR1 >>>
Cctggagctgcaaaatccgggtgtaggcacagctctcctattgaaactgcccagatgttc 1562
P G A A A K S G V G T A L L L K L A Q M F
Tcagatagtgcttaaaagatgggttcagcccagcagaagcattatctttgccagttgg 1622
S D M V L K D G F Q P S R S I I F A S W

<<<
Agtgctggagactttggatcggttggtgccactgaatggctagagggatacctttcgtcc 1682
S A G D F G S V G A T E W L E G Y L S S
<<< Reverse primer for TfR1
Ctgcatttaaggctttcacttatattaatctggataaagcggttcttggtagcagcaac 1742
L H L K A F T Y I N L D K A V L G T S N
Ttcaaggcttctgccagcccactggtgtatagccttattgaaaaaatgcaaaatgtg 1802
F K V S A S P L L Y T L I E K T M Q N V
Aagcatccggttactgggcaatttctatcaggacagcaactgggcccagcaaagttgag 1862
K H P V T G Q F L Y Q D S N W A S K V E
Aaactcactttagacaatgctgctttcccttcccttgcataattctggaatcccagcagtt 1922
K L T L D N A A F P F L A Y S G I P A V
Tctttctggttttggcaggacacagattatccttatttgggtaccaccatggacacctat 1982
S F C F C E D T D Y P Y L G T T M D T Y
Aaggaactgattgagagctcctgagttgaacaaagtgccagcagcagctgcagaggtc 2042
K E L I E R I P E L N K V A R A A A E V
Gctggtcagttcgtgattaaactaacccatgatgttgaattgaactggactatgagagg 2102
A G Q F V I K L T H D V E L N L D Y E R
Tacaacagccaatgctttcatttggaggatctgaaccaatcacagagcagacataaag 2162
Y N S Q L L S F V R D L N Q Y R A D I K
Gaaatggcctgagtttcaagtggtgtattctgctcgtggagacttctcctggtact 2222
E M G L S L Q W L Y S A G G F F R A T
Tccagactaacaacagatcttcgggaatgctgagaaaacagacagatcttgcataagaaa 2282
S R L T T D F G N A E K T D R F V M K K
Ctcaatgatcgtgcatgagagtgaggatataccttctcctcctacgtatctccaaaa 2342
L N D R V M R V E Y H F L S P Y V S P K
Gagtctcctttcgcagacttctcctggtcctcggctcctcagcagcagcagcagcagc 2402
E S P F R H V F W G S G S H T L P A L L
Gagaacttgaaactgcgtaaaacaaaataaacggtgcttttaatgaaacgctgttcagaaa 2462
E N L K L R K Q N N G A F N E T L F R N

<<< ctgcaa
Cagttggctctagctacttggactattcagggagctgcaaatgcctctctggtgacgtt 2522
Q L A L A T W T I Q G A A N A L S G D V

<<< Reverse primer for cloning
Accctgtaactgttactcaaaattatccttagggcgcg
Tgggacattgacaatgagttttaaagtgtgatacccatagcttccatgagaacagcagggt 2582
W D I D N E F - M - Y P - L P - E Q Q G

Agtctggtttctagacttctgctgatcgtgctaaatctttagtagggctacaaaacctga 2642
S L V S R L V L I V L N F Q - G Y K T -
Tgttaaaattccatcccacatcttggtagctactagatgtctttaggcagcagcttttaa 2702
C - N S I P S S W Y Y - M S L G S S F -
Taccgggtagataacctgtacttcaagttaaagtgaataaccacttaaaaaatgtccatg 2762
Y R V D N L Y F K L K - I T T - K M S M
Atggaatattccctatctctagaattttaaagtgctttgtaagtgggaactgcctctttcc 2822
M E Y S P I S R I L S A L - W E L P L S
Tgttgttgttaattgaaaatgcaaaaccagttatgtgaatgctctcctgaaatcctaag 2882
C C C - - K C Q K P V M - M I S L N P K
Ggctggctctctgctgaaggttgtaagtgggttcgcttactttgagtgatcctccaacttca 2942
G W S L L K V V S G S L T L S D P P T S
Tttgatgctaaatagagataaccaggttgaagacctctcctcaaatgagatcctaagccttt 3002
F D A K - E I P G - K T S P N E I - A F
Ccataaggaatgtagcaggtttcctcattcctgaaagaaacagttaactttcagaagaga 3062
P - G M - Q V S S F L K E T V N F Q K R
Tgggcttgttttcttctgcaatgaggtctgaaatggaggtcctcttctgctggataaaatgag 3122
W A C F L A N E V - N G G P S A G - N E
Gttcaactgttgattgacggaataaggccttaatatgttaacctcagtgatcatttatgaa 3182
V Q L I R P - Y V N L S V I Y E
Aagaggggaccagaagccttagctatattttcttctcctctgctccttcccccat 3242
K R G P E A K D L V Y F L F L C P F P H

```

### Key to *TfR1* mRNA and protein alignment

- Extracellular coding region
- The c-terminal region that binds to transferrin
- Cell attachment site and required for binding to transferrin
- Region of the primers used for cloning the insert into the vector

```

Aagcctccatttagtcttttggattttttgtttcttccaaagcacattgaagagaacca 3302
K P P F S S L L F L F L P K H I E R E P
Gtttcaggtgttagttgcagactcagtttgcagactttaagaataatagctgcaa 3362
V S G V - L Q T Q F V R L - R I I C C Q
Attttggccaaagtgttaactcttaggggagagctttctgtccttttggcactgagatatt 3422
I L A K V L I L G E S F L S F W H - D I
Tattgtttatattatcagtgacagagttcactataaatgggtttttttaatagaatataa 3482
Y C L F I S D R V H Y K W C F F N R I -
Ttattggaagcagtgccctccataaattatgacagttatactgtcgggtttttttaaataa 3542
L S E A V P S I I M T V I L S V F F K -
Aagcagcatctgctaataaaacccaacagataactggaagttttgcatattatggtcaaac 3602
K Q H L L A I K P N R Y W K F C I Y G Q H
Ttaagggttttagaaaacccgctcagcccaatgtaattgaataaagttgaagctaagat 3662
L R V L E N S R Q P N V I E - S - S - D

```

TfR1-IRE forward primer >>>

```

Ttagagatgaattaaatttaattaggggtttagtaaaagccagcaatgaccagataagaa 3722
L E M N - I - L G V A K K R A L T R - E
Tgctgggttttccataaattgcagtgaaattgtgaccaagttataaatcaatgtcacttaaagg 3782
C W F S - M Q - I V T K L - I N V T - R
Ctgggtagctactcctgcaaaattttatagctcagtttataccaaggtgtaactctaattc 3842
L W - Y S C K I L - L S L S K V - L - F

```

<<< TfR1 reverse primer

```

Ccatttgcataaatttccagtagctttgtcacaatgtaaacacattatcgggagcagtggtc 3902
P F A K F P V P L S Q S - H I I G S S V
Ttccataatgtataaaagcaaggtagtttttaccctaccacagtgctctgtatcggagaca 3962
F H N V - R T R - F L P T T V S V S E T
Gtgatctccatagtttactactaagggtgtaagtaattatcgggaacagtggtttccataa 4022
V I S I C Y T K G V S N Y R E Q C F P -
Ttttcttcagcaatgacatcttcaaagcttgaagatcgtagtatcacaatgtagtccc 4082
F S S C N D I F K A - R S L V S N M Y P
Aactcctataatccctatcttttagtttttagttgcagaaacattttgtggtcattaagc 4142
N S Y N S L S F S F S C R N I L W S L S
Attgggtgggtaaatcaaccactgtaaaatgaaattactacaaaatttgaatttagct 4202
I G W V N S T T V K - N Y Y K I - N L A
Tgggtttttgttacctttatgggttttccaggtcctctacttaatgagatagcagcatac 4262
W V F V T F M V S P G P L L N E I A A Y
Attataatggttctgtatgacaagtcatttttaattatcacattatgtcatgtttac 4322
I Y N V C Y - Q V I L I Y H I I C M L P
Cctataaacttagtgccgacaagtttataatccagaattgaccttttgactaaagcagag 4382
P I N L A V R T T S F N P E L T F - L K A E
Ggactttgtatagagttttggggctgtgggaaggagagtcctcctgaaggtctgacac 4442
G L C I E G L G A V G K E S P L K V - H
Gtctgcctaccattcgtgggtgatcaatgtaagtgtaggtatgaataagttcgaagctccg 4502
V C L P I R G D Q L N V G M N K F E A P
Tgagtgaaccatcatataaacgtgtagtagctgtttgtcatagggcagttggaacgg 4562
- V N H H I N V - Y S C L S - G S W K R
Cctcctagggaaaagttcatagggctctctcagggtcttagtgctactacctagatatta 4622
P P R E K F I G S L Q V L S V T Y L D L
Cagcctcacttgaatgtgtcactactcacagtcctcttaattctcagttttatctttaat 4682
Q P H L N V S L L T V S L I F S F I F N
Ctctctttttatcttggactgacatttagcgtagctaaagtgaaggtcatagctgagat 4742
L L F Y L G L T F S V A K - K G H S - D
Tcctgggttcgggtgttacgcacacgtacttaaatgaaagcatgtggcatgttcatcgtat 4802
S W F G C Y A H V L K - K H V A C S S Y
Aacacaatatgaatacagggcatgcattttgcagcagtgagctcttccagaaaacccttt 4862
N T I - I Q G M H F A A V S L F R K P F
Tctacagtttaggttgagttacttctatcaagccagtagctaacaggtcctaatatt 4922
S T V R V E L L P I K P V R A N R L N I
Cctgaatgaaatatcagactagtgacaagctcctgggtcctgagatgtcttctcgttaagg 4982
P E - N I R L V T S S W S - D V F S L R
Agtagggccttttggaggttaaaggtata 5010
S R A F W R - R Y

```

### Key to *TfR1* mRNA and protein alignment

- 3' IRE region on the mRNA of *TfR1*
- The actual endonuclease site on the mRNA within the IRE region

**Fig. 2.1 Alignment of human *TfR1* mRNA and protein**

The alignment shows the coding region of *TfR1* cDNA that was cloned into vector pCEP4. It also shows the IRE located in the 3' region (Casey et al., 1988) as well as the actual endonuclease site within the IRE region (Binder et al., 1994). Information on *TfR1* obtained from Proteinknowledgebase UniProtKB at [www.uniprot.org/uniprot/P02786](http://www.uniprot.org/uniprot/P02786).

Fig. 2.2 is a representation of the plasmid pCEP4 into which the TfR1 segment of interest was cloned. Since the plasmid pCEP4 contains a hygromycin B resistance gene, the rec-TfR1 HepG2 cells were maintained in the same medium as the Wt HepG2 cells, with the addition of 200 µg/mL hygromycin B as a selection for exclusive growth of recombinant HepG2 cells.

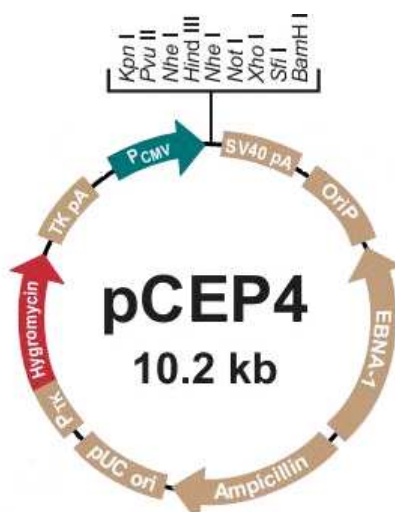


**Fig. 2.2 Schematic of the cloning vector pCEP4 plasmid**

Image adapted from life technologies at <http://products.invitrogen.com/ivgn/product/V04450>

### 2.2.3.3 Creation of HepG2 cells containing empty plasmid: HepG2 (p) cells

HepG2 (p) cells were created to be used as a control in iron supplementation experiments. The cells were created by transfection of the Wt HepG2 cells with the empty pCEP4 plasmid. The method of creation was as per X-tremeGENE-9 DNA transfection reagent protocol (Roche, West Sussex, UK) and is briefly described as follows.

**Pre- transfection cell culture conditions:** Wt HepG2 cells were seeded at a density of  $8 \times 10^4$  cells per well in 6 wells of a 24 well plate. Cells were allowed to

grow for 48 hours until they reached approximately 60 % to 70 % confluence, ready to be transfected.

**Preparation of transfection medium:** On the day of transfection, the transfection medium was prepared. This was composed of X-9 (transfection reagent) and serum-free EMEM. These two were mixed in 3 different ratios, each ratio in duplicate. The ratios were 3:100, 4:100 and 6:100, i.e. 3  $\mu$ L of X-9 and 100  $\mu$ L of serum free medium, 4  $\mu$ L of X-9 and 100  $\mu$ L of serum-free EMEM, and 6  $\mu$ L of X-9 and 100  $\mu$ L of serum-free EMEM. These 6 tubes containing the transfection medium were divided into 2 sets; one set was for the test (plasmid) and the other for the control (no plasmid). The test set of tubes were supplemented with 1  $\mu$ g of the plasmid pCEP4. To the control set, instead of the plasmid, serum-free and antibiotic-free medium was added. All preparations were mixed gently and incubated at room temperature (RT) for 20 min.

**Transfection:** For transfection, Wt HepG2 cells growing in the maintenance medium, as described above, were washed once with PBS to remove any cell-bound antibiotics. To each of the 6 wells, 1 mL of EMEM (with 10 % FCS and without antibiotics) was added. 50  $\mu$ L from each of the transfection preparations was added to each of the respective wells, the plate was mixed gently and the cells were incubated at 37 °C in an incubator for 48 hours. Following this, the transfection medium was removed and replaced with maintenance medium containing 500  $\mu$ g/mL of hygromycin B. The medium was replaced after 3 days, and the cells were maintained in a medium containing 500  $\mu$ g/mL hygromycin B.

After 3 weeks, the cells were maintained in a maintenance medium containing 200 µg/mL of hygromycin B and passaged in the same way as the other HepG2 cell lines.

#### **2.2.4 Liquid nitrogen storage and cell revival**

All cell lines were stored in NUNC vials in 90 % FCS and 10 % dimethyl sulphoxide (DMSO) in the Cryo 1°C freezing container, (Nalgene ), at -80 °C for 24 hours and then transferred to liquid nitrogen for long term storage. When reviving the cells from liquid nitrogen, frozen vials were quickly defrosted in an incubator at 37 °C. To wash away the DMSO, contents were transferred to a 15 mL centrifuge tube, followed by addition of warm maintenance medium and centrifugation at 1000 rpm (89 x g) for 4 min. The supernatant was discarded and the cell pellet was resuspended in maintenance medium and seeded in a 25 cm<sup>2</sup> flask containing warm maintenance medium to initiate cell growth.

#### **2.2.5 DNA extraction from cell lines and rodent liver tissues**

DNA was extracted from cells in order to perform PCRs to confirm the presence of a gene of interest and/or to confirm its sequence identity by subsequent sequencing. DNA was also extracted from rodent tissues which served as a positive control in PCRs since the expected product size with respective primers was known.

**Principle:** Addition of lysis buffer makes cells permeable and lyses the cells. Sodium dodecyl sulphate (SDS) present in the lysis buffer removes membrane lipids and thus assists the lysis buffer. Proteinase K added later inactivates

nucleases that degrade DNA; its action is enhanced by SDS. It also removes the cellular and histone proteins bound to DNA, making the DNA more “accessible”. Finally, isopropanol precipitates the DNA.

**Methodology:** DNA extraction from tissues and cell lines was performed using the isopropanol-ethanol precipitation method (Maniatis *et al.*, 1982). To extract DNA from cell lines, cells were grown in a 75 cm<sup>2</sup> tissue culture flask. On reaching 80-90 % confluence, cells were trypsinised and transferred to a 15 mL centrifuge tube. After centrifugation at 800 x *g* for 5 minutes, the supernatant was removed. To the cell pellet or rodent liver tissues, 3 mL of lysis buffer [100 mM Tris (pH 8), 50 mM NaCl, 10 mM EDTA, 0.2 % SDS] and 10 µL of proteinase K (20 mg/mL) was added, mixed and incubated overnight in a water bath maintained at 65 °C. After overnight incubation, contents were transferred to a 1.5 mL eppendorf tube and centrifuged at 13,000 rpm (16,060 x *g*) for 20 min. The supernatant was transferred to a fresh eppendorf tube and 600 µL of cold isopropanol was added, the tubes were vortexed and again centrifuged at 13,000 rpm (16,060 x *g*) for 15 min. The supernatant was discarded and 2 µL of 5 M sodium chloride, 100 µL of distilled water and 200 µL of cold absolute ethanol (BDH, East Grinstead, UK) were added, mixed and incubated at -20 °C for 1 hour. The tubes were then centrifuged at 13,000 rpm (16,060 x *g*) for 10 min, the supernatant was discarded and the pellet was dried in a speed vacuum. The DNA pellet was suspended in 50 µL of nuclease-free, diethylpyrocarbonate (DEPC)-treated water (Ambion, Warrington, UK) and stored at -20 °C.

### 2.2.6 DNA purification and concentration

The extracted DNA was purified and concentrated to improve its quality for PCRs and subsequent sequencing.

**Methodology:** To the DNA to be purified, 10 M ammonium acetate was added (at 1/10<sup>th</sup> of DNA solution to be purified). Following this, an equal volume of 100 % isopropanol was added and the mixture was then incubated at RT for 20 min. Centrifugation was performed at 13,000 rpm (16,060 x *g*) for 10 min at RT. The supernatant was removed, 100 µL of 70 % ethanol was added, the tubes were vortexed and centrifuged at 13,000 rpm (16,060 x *g*) for 10 min at RT. The supernatant was removed and the precipitated DNA was suspended in 50 µL of nuclease-free water. The DNA was stored at -20 °C and only the DNA preparations with a 260/280 ratio >1.8 were used in PCRs.

### 2.2.7 Primer design and gene annotation

The following databases, software programmes, algorithms and tools were used to design primers.

- a. National Center for Biotechnology Information (NCBI) for accession of gene sequences and software *blastn* to match the characterised sequence of a gene with existing gene sequences in the database.
- b. Genome Net for *Clustal-W* alignment, a multiple sequence alignment tool to align gene sequences from different species, aiming to identify most conserved regions to design primers.
- c. Software *Primer 3* (available at <http://frodo.wi.mit.edu/>) to design gene-specific primers.

All primers were designed to have similar properties such as GC content close to 60 %, melting temperature (T<sub>m</sub>) close as 60 °C and product size less than 200 base pairs (bp) to facilitate their use in real time PCR. Once the primers were designed, each primer was checked for its gene specificity at the NCBI database with *blastn*.

Tables 2.1, 2.2 and 2.3 shows all the primers used for PCRs and real time PCRs.

- Table 2.1 lists the primers designed based on conserved nucleotides between human, mouse and rat. These were the primers used for the 1<sup>st</sup> and 2<sup>nd</sup> rounds of CHO gene sequencing.
- Table 2.1 also shows the CHO-specific primers, referred as “CHO for x forward” and “CHO for x reverse”, where is x the gene of interest. These were designed exclusively on the characterised CHO gene sequence and were used in real time PCR optimisations with the CHO cells.
- Table 2.2 shows the hepcidin primers used for rat, mouse and human genomes, published by other research groups.
- Table 2.3 shows the primers used for PCR optimisations and real time PCR with HepG2 cells.

The genes have been annotated in the text as follows:

<b>Protein</b>	<b>Gene encoding the protein in humans</b>	<b>Gene annotation in text</b>
Hepcidin	<i>HAMP</i> ( <i>Hamp</i> in rodents)	<i>Hepcidin</i> gene
Ferroportin	<i>SLC40A1</i>	<i>Ferroportin</i> gene
TfR1	<i>TfRC</i>	<i>TfR1</i> gene
HFE	<i>HFE</i>	<i>HFE</i> gene

Genes	Forward (F) primers 5' to 3'	Reverse (R) primers 5' to 3'
<b>Primers designed based on multiple sequence alignments of different species</b>		
<i>Hfe</i>	(F) CTCTTCATGGGTGCCTCA	(R) CACCCTTTCAGNCTCTGACT
	(F1) CAATNGCTNNAGGGTGACTTC	(R1) AAGAGTTGGTCATCCACGTAG
	(F2) ATAATCATGAGAATCGCCGTG	(R2) TTCACCAAAGNAGGCACTTG
<i>Ferroportin</i>	(F) ATCGGATGTGGCACTTTGC	(R) GCCACTTTAAGTCTNGCATTCT
	(F1a) CTTTCCAACCTCAGCTACAGTGTT	(R1) CGTAGACAGCTGTCAAGAGGA
	(F1b) TCCAACCTCAGCTACAGTGTT	
	(F2) TAGCAGGCTCTGTTCTGG	(R2a) CCATTATTCCAGTTATNGCTGATGC
	(R2b) ATTATTCCAGTTATNGCTGATGC	
<i>Irp2</i>	(F) AATGCACCAAATCCTGGAG	(R) AGGCACTGGTTGCAAATG
	(F1) TAATATGGTCTCCGGCGATG	(R1) TCCTCGGCAGGTAGTCTGG
	(F2) CCAGACTACCTGCCGAGGA	(R2) CATTTAAGCAAGCCTGGAAATC
<i>Hepcidin</i>	(F) GCTGCCTGTCTCCTGCTTC	(R) ATGGGGAAGTTGRTGTCTC
	(F1) CTGCCTGTCTCCTGCTTC	(R1a) ATGGGGAAGTTGNTGTCTC
		(R1b) AGGNCAGGAATNAATANTGGGG
	(F2) NCTCCTGCTNCTCCTCCT	(R2a) AGAANNNGCANATGGGGAAG
		(R2b) ATGGGGAAGTNGTGTCTC
<b>Genes and source of primers</b>	<b>Primers designed for Real time PCR on the basis of characterised CHO sequence</b>	
<i>Hfe</i>	Hfe for CHO (F) AACCACAGTAAGGGCAGTAAGC	Hfe for CHO (Rx) GAGGCACTTGCTGCTTCAG
		Hfe for CHO (Ry) GCTCTCCATTCCAGTGTCGT
<i>Ferroportin</i>	FPN for CHO (F) ATGGGTGCTCACTGTCTGCTA	FPN for CHO (R) GCATTCATATCTGCTAATCTGCTTC
<i>Irp2</i>	Irp2 for CHO (F) ATTCTTGGGTGGGGAGTTG	Irp2 for CHO (R) CCTACTTGCCTGAGGTGCTT
<i>Beta actin</i> (Bahr et al., 2009)	(F) GCTCTTTTCCAGCCTTCCTT	(R) GAGCCAGAGCAGTGATCTCC
<i>Pabpn1</i> (Bahr et al., 2009)	(F) GTGGCCATCCTAAAGGGTTT	(R) CGGGAGCTGTTGTAATTGGT
<b>CHO endogenous TfR1</b>	(F) CCCAGCAGAAGCATTATCTTT	(R) TTCCCATCAATTGGATGTCTT

Table 2.1 Primers for CHO gene sequencing and real time PCR

	Forward (F) primers 5' to 3'	Reverse (R) primers 5' to 3'
<b>Source of Primers</b>	<b>Hepcidin primers published by other research groups</b>	
(Fein et al., 2007)	(FF) CTGCAACCCCAGGACAGAG	(RR) GGAATAAATAAGGAAGGGAGGGG
(Lin et al., 2007)	Mouse hepcidin -1 (F) TTGCGATACCAATGCAGAAGA	Mouse hepcidin -1 (R) GATGTGGCTCTAGGCTATGTT
(Dzikaite et al., 2006)	Rat hepcidin (F)-x TGACAGTGCCTGCTGATG	Rat hepcidin (R)-x GGAATTCTTACAGCATTACAGCAGA
(Zhang et al., 2004)	Rat hepcidin F-y CGAGACACCAACTTCCCATAT	Rat hepcidin R-y GCTCTTGGCTCTCTATGTTATGCA
pGEM-T easy vector primers (Greenwell., P.)	(F) GCGGCCGCGGAATTTCG	(R) GCGGCCGCGAATTCA

Table 2.2 Primers used for hepcidin gene sequencing in CHO cells

Genes and source of primers	Forward (F) primer 5' to 3'	Reverse (R) primer 5' to 3'
<b>Primers designed for HepG2 cells</b>		
<i>Hepcidin</i>	(F I) ACAGCCAGACAGACGGCACGA (F II) CCTGACCAGTGGCTCTGTTT	(R I) TTCGCCTCTGGAACATGGGCATC (R II) CACATCCCACACTTTGATCG
<i>TfR1</i>	(F) AAAATCCGGTGTAGGCACAG	(R) TTAATGCAGGGACGAAAGG
<i>TfR1-IRE</i>	(F Ia) AAGCGAGCACTGACCAGATAA (F Ib) GGTTGCTAAGAAGCGAGCAC F2 CTAACACATTATCGGGAGCA	(R I) TGCTCCCGATAATGTGTTAGG (R2) TTCAAGCTTTGAAGATGTCATTG
<i>GAPDH</i>	(F) GCCAAAAGGGTCATCATCTC	(R) GGTGCTAAGCAGTTGGTGGT
<b>Primers for HepG2 cells, as published by other research groups</b>		
<i>Hepcidin</i> (Jacolot et al., 2008)	(F III) CCTGACCAGTGGCTCTGTTT	(R III) CTCTGGAACATGGGCATCCA
<i>Hepcidin</i> (Wrighting and Andrews, 2006)	(F IV) CTGCAACCCCAGGACAGAG	(R IV) GGAATAAATAAGGAAGGGAGGGG
<i>HFE</i> (Jacolot et al., 2008)	(F I) TGATCTGGGAGCCCTCACC	(R I) GACGACAAAAACAGCAATTCC
<i>HFE</i> (Rapisarda et al., 2010)	(F II) AGAACAGGGCCTACCTGGAG	(R II) TGTGTCACCTTCACCAAAGG
<i>Ferroportin</i> (Jacolot et al., 2008)	(F I) TGTTTCTGGTAGAGCTCTAT	(R I) GATATAGCAGGAAGTGAGAA
<i>Ferroportin</i> (Recalcati et al., 2010)	(F II) GGGTCGCGTAGTGTCAT	(R II) CAGGTAGTCGGCCAAGGAT
<i>18s</i> (Provenzano et al., 2007)	(F) AACTTTCGATGGTAGTCGCCG	(R) CCTTGGATGTGGTAGCCGTT
<i>Actin</i> (Rapisada., personal communication)	(F) CCAACCGCGAGAAGATGA	(R) CCAGAGGCGTACAGGGATAG

Table 2.3 Primers for PCR optimisations and real time PCR with HepG2 cells

### 2.2.8 Polymerase chain reactions (PCRs)

PCRs were performed to confirm the presence of a gene of interest, followed by sequencing to confirm product identity.

**Principle:** Primers bind to DNA at complementary regions and Taq Polymerase, extends the primers by adding complementary bases to the free 3' OH end of the primers, until it reaches the end of a defined region. After the first cycle of PCR, two strands of DNA are produced, identical to the original strands. In the second cycle these form the template for synthesis of the correctly sized amplicons.

Subsequent cycles lead to a logarithmic increase in the number of copies of the region of DNA, defined by the primers.

**Methodology:** The PCR protocol adapted from Qiagen's Taq PCR master mix protocol (Qiagen) is shown in Table 2.4. The annealing and extensions times were chosen depending on the size of the product expected. For example, the annealing time of 1 min and final extension of 10 min were chosen for products more than 500 bp in length. Different annealing temperatures shown in table 2.4 represent the temperature gradient PCRs, as explained in the following section. All PCRs were performed on the Eppendorf® Mastercycler gradient.

Contents	Volume	PCR cycle steps
DEPC water	5.5 µL	1. Initial denaturation temperature: 94 °C for 3 min 2. Denaturation: 94 °C for 30 sec 3. Annealing: 55 °C , 58 °C or 60 °C for 45 sec or 1 min 4. Extension: 72 °C for 1 min 5. Repeat step 2 to 4, 29 times 6. Final extension: 72 °C for 5 or 10 min 7. Final hold: 4 °C
Qiagen Taq PCR master mix (2X)	12.5 µL	
5µM Forward primer	2.5 µL	
5µM Reverse primer	2.5 µL	
DNA template (200ng)	2 µL	
Total volume	25 µL	

**Table 2.4 PCR protocol and cycles**

The volume of contents is adapted from Qiagen's Taq PCR master mix kit protocol.

### **2.2.9 Temperature and magnesium chloride gradient PCR**

In order to identify the most appropriate annealing temperature for primer binding to the DNA template, multiple PCR tubes were set up for a sample and subjected to a gradient of annealing temperatures ranging from 51 °C to 61 °C. To avoid variability between PCR mixtures in different tubes, a single PCR master mix with the DNA was aliquoted in 25 µL volumes in each 0.2 mL PCR tube and then placed at desired temperatures on the PCR machine. The temperature which resulted in the highest product formation and a unique product was chosen as the most appropriate annealing temperature. A magnesium chloride (MgCl<sub>2</sub>) gradient PCR was set up in a range from 1.5 mM to 4 mM to facilitate more specific binding of primers. The annealing temperature chosen was as identified by the temperature gradient PCR.

### **2.2.10 Agarose gel electrophoresis**

The presence and size of a PCR product was determined by agarose gel electrophoresis.

**Principle:** During electrophoresis, porous agarose helps in migration of DNA from the negative electrode to the positive electrode. Ethidium bromide intercalates between the double strands of DNA and fluoresces when exposed to UV light. This detects the presence of product.

**Methodology:** After the PCR, 5 µL of 5X DNA loading buffer (Bioline, London, UK) was added per 25 µL of a PCR reaction. 18 µL of amplicon was run on 0.8 %, 1 %, 2 % or 3 % agarose gel (Web scientific, Cheshire, UK ) using 1X Tris-Borate-EDTA buffer (Fisher Scientific International Inc., Loughborough, UK). Alongside the

products to be analysed, 10 µL sample of a DNA ladder (Web scientific Cheshire, UK), as seen in Fig. 2.3, was loaded in one well. The gel was electrophoresed at 100 volts until the loading dye had run 2/3<sup>rd</sup> of the gel. The gel was then observed under a UV transilluminator to check the DNA products.

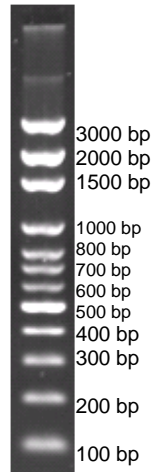


**Fig. 2.3 A typical DNA ladder**

### **2.2.11 Cloning and transformation**

Two PCR products of similar sizes on agarose gel are difficult to gel extract and sequence. Cloning of a dual product segment into a vector, followed by transformation and selection of clones aid in extraction and subsequent sequencing of each product.

**Principle:** The dual product segment was cut from the gel and ligated to a plasmid vector; the principle being that one plasmid would ligate to only one product. This created two kinds of recombinant plasmids, each one with one of the two products. These recombinant plasmids were then transformed into competent cells to obtain multiple copies of plasmids. These plasmids were then extracted from the competent cells and PCRs were performed to check sequence identity.

**Methodology:** The dual product segment was gel extracted and purified using Qiagen's gel extraction kit, according to manufacturer's instruction. The purified section was then ligated to the pGEM-T Easy Vector system I and the recombinant plasmids were transformed into competent *Escherichia coli* XL-1 Blue cells, according to the manufacturer's protocol. For transformation, Luria-Bertani (LB) agar and LB broth were prepared and autoclaved at 121 °C for 15 min. The LB agar was heated in a microwave oven and cooled to 40-50 °C. Since the plasmid pGEM-T contains ampicillin resistance gene, ampicillin solution (100 µg/mL) was filtered using 0.22 µm filter unit and added to the LB agar. Along with this, isopropyl β-D-1 thiogalactopyranoside solution (IPTG) (0.5 mM) and bromo-chloro-indolyl-galactopyranoside (X-gal) (80 µg/mL) were also filtered and added to the LB agar. X-gal as added to aid selection due to the presence of *lacZ* gene on the plasmid. The contents were mixed and plates poured. Agar was allowed to solidify and plates were surface spread with transformed *E. coli* cells. After overnight incubation at 37 °C, blue and white colonies were observed. White colonies, which represented successful ligation of product to the vector were selected and inoculated in LB broth with ampicillin (100 µg/mL) and incubated at 37 °C overnight on shaker. Recombinant plasmids from these cells were extracted and purified using Qiagen's Qiaprep spin Miniprep kit (Qiagen). PCRs were performed using the purified plasmid and the vector primers as well as the designed gene primers. Amplicons were electrophoresed at 100 volts on an agarose gel to confirm the presence of the expected product. The products were either gel extracted or purified using Qiagen's gel extraction kit or PCR product purification kit and sent for sequencing.

### 2.2.12 Sequencing PCR products

The identity of the obtained PCR product was confirmed by sequencing.

**Principle:** Single stranded primer binds to a strand of dsDNA to be sequenced and the primer is extended by addition of nucleotides complementary to the DNA strand. As a convention the top and the bottom strands of DNA are represented as 5' to 3' and 3' to 5', respectively. The forward primer binds to and thus reads the bottom strand of DNA and the reverse primer binds to and thus reads the top strand of DNA; both reads are given to the customer in 5' to 3' direction.

**Methodology:** PCR products for sequencing were purified either using Qiagen's gel extraction kit or Qiagen's PCR product purification kit, as per manufacturer's instructions. The concentration and purity of DNA was checked using a Nanodrop 3.1 (Thermo Scientific, UK) and sent to the Wolfson Institute for Biomedical Research (University College London) or GATC-Biotech (London, UK) for sequencing, as per their respective specifications. Forward and backward reads for a product were requested. Characterised sequences were accessed and analysed using Applied Bio systems sequence scanner v 1.0. The forward and backward reads were aligned using *blastn* at NCBI to obtain the most clearly sequenced section of the DNA. This section of sequence was then used to find its matches in the NCBI database.

### 2.2.13 Determination of iron saturation of holotransferrin

In order to check the iron saturation of holotransferrin used in iron supplementation experiments, a urea gel assay was performed.

**Principle:** Transferrin is a bi-lobed protein. The N-lobe corresponds to the amino terminus of the protein and the C-lobe corresponds to the carboxyl terminus of the protein. Each lobe can accommodate up to one  $\text{Fe}^{3+}$  ions. Transferrin can thus exist in 4 different forms : holotransferrin, when both the lobes of transferrin are occupied by  $\text{Fe}^{3+}$ ; monoferric transferrin, when only one of the two lobes of transferrin is occupied with  $\text{Fe}^{3+}$  and apotransferrin when no  $\text{Fe}^{3+}$  is bound to transferrin (Makey and Seal, 1976).

Since apotransferrin is iron-free, it is easily unfolded by 6 M urea and thus runs slowly on the gel. On the contrary, iron bound to transferrin does not allow urea to unfold the protein structure. Since the protein remains intact, iron bound transferrin runs at a comparatively faster rate than apotransferrin. Thus the 4 forms of transferrin have different mobilities on a 6 M urea gel and this allows identification of the different forms (Evans and Williams, 1978)(Makey and Seal, 1976).

**Methodology:** Solutions of holotransferrin (SCIPAC LTD, Kent, UK) 5 g/L and apotransferrin (SCIPAC LTD, Kent, UK) were prepared in 0.01 mM sodium bicarbonate. The concentrations and preparation of buffers and solutions are mentioned in appendix II. Briefly, two 400  $\text{cm}^2$  glass plates were prepared with 1 mm spacers between the two plates. Acrylamide gel solution was prepared and poured in between the glass plates and allowed to set with a comb of wells. The gel was then pre-equilibrated with stock buffer in the appropriate tank.

Samples for loading were prepared by adding 20  $\mu$ L of transferrin solutions to 30  $\mu$ L of sample buffer. From this, 40  $\mu$ L of sample was loaded into each well of the gel and 110 volts current was applied for 16 hours. Gels were then removed from the glass plates and stained overnight with coomassie blue solution with gentle agitation. This was followed by overnight destaining in 10 % acetic acid and 10 % methanol. The gel was placed on a scanner and a photograph was taken. As seen in Fig. 2.4 the vast majority of the protein was holotransferrin, as expected, with some proportions of monoferric transferrins.

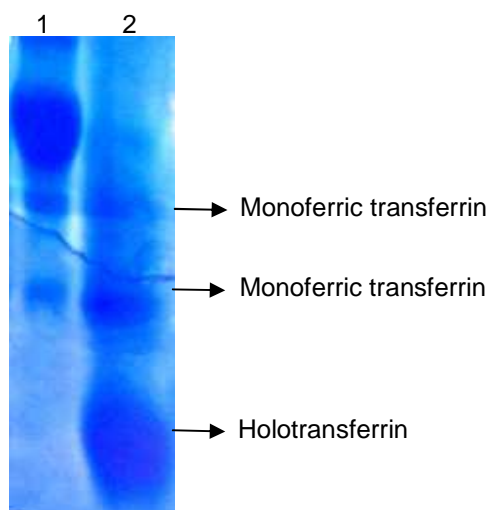


**Fig. 2.4 A 6 M urea gel assay**  
Lane 1: Apotransferrin  
Lane 2: Holotransferrin (SCIPAC)

#### **2.2.14 Pre-iron supplementation optimisations**

For the iron supplementation experiment it was important that the iron supplied to the cells was of a defined concentration, type, and the sole source of iron available to the cells. Since FCS, which is a component of normal maintenance medium, may contain inorganic iron as well as holotransferrin, it was necessary to ensure that the iron supplementation studies were performed in a serum-free medium.

However, the survival of cells without FCS for a long period of time would be difficult. Hence bovine serum albumin (BSA) was chosen as a substitute for FCS. Since iron can bind to albumin (Silva and Hider, 2009), BSA was checked for the presence of any bound iron through the ferrozine assay described in section 2.2.17.1. Results revealed that there was no detectable iron in 4 % BSA prepared in deionised water (appendix III). Thus it was concluded that the BSA was iron-free and the holotransferrin supplementation prepared in a medium containing BSA would be the only source of iron available to the cells.

Following this, cells were grown in different BSA concentrations (1 % BSA to 8 % BSA made in serum-free EMEM) to check the minimum concentration of BSA that would support cell survival in the absence of FCS throughout the duration of an iron supplementation experiment. The medium of choice was EMEM as it does not contain any inorganic iron. Cell viabilities were determined (section 2.2.16) after 6 hours, 24 hours and 48 hours and the results were compared to the cells growing in normal maintenance medium with FCS at that time point. Viability studies along with cell morphology observations suggested that the BSA-free and serum-free medium was the most suitable for the cells up to 48 hours (appendix IV).

Hence for the iron supplementation experiments, the cells were treated with the desired concentration of holotransferrin prepared in serum-free and BSA-free EMEM. Throughout the thesis, the term 'iron overdose' refers to the treatment of the cells whereas 'iron overload' refers to high intracellular iron content.

Also, before every experiment, the difference between the Wt HepG2 cells and rec-TfR1 HepG2 cells was established by growing the cells in 500 µg/mL hygromycin B in one well of a 6 well plate. The recombinant HepG2 cells survived in hygromycin B due to the presence of the hygromycin B resistance gene in the pCEP4 plasmid whereas the Wt HepG2 cells died after 5-7 days. This confirmed the cell type.

Images of HepG2 cells grown under different conditions are shown in Fig. 2.5.

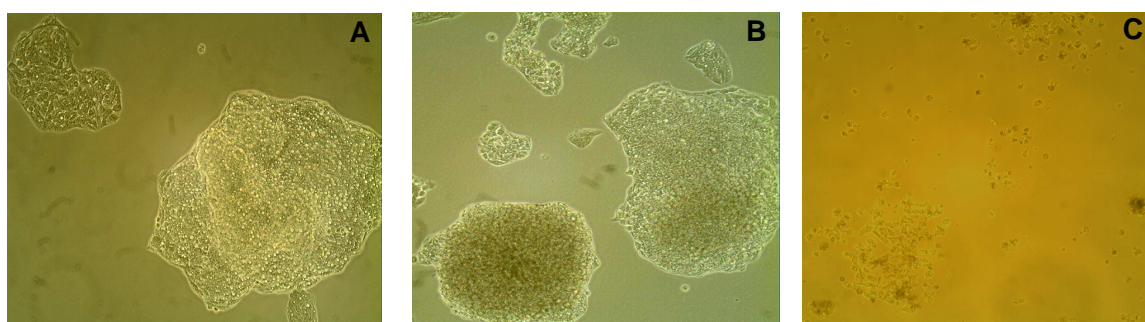


**Fig. 2.5 Effect of hygromycin B on HepG2 cells**

**A:** Wt HepG2 cells in maintenance medium without hygromycin B.

**B:** Rec-TfR1 HepG2 cells in maintenance medium with 500 µg/mL hygromycin B.

**C:** Wt HepG2 cells in maintenance medium with 500 µg/mL of hygromycin B.

### 2.2.15 Iron supplementations

For the iron supplementation experiments, cells were seeded at a density of  $3 \times 10^5$  per well in a 24 well plate or  $5 \times 10^5$  per well in a 6 well plate in maintenance medium with hygromycin B (for rec-TfR1 HepG2 and HepG2 (p) cells) and without hygromycin B (for Wt HepG2 and CHO TRVb1 cells). The medium was changed every 48 hours until the cells reached 60 % - 70 % confluence. For the next 24 hours all cells were incubated in fresh hygromycin-free maintenance medium.

Following the 24-hour hygromycin-free incubation the cells were washed twice with warm PBS to remove traces of FCS. This was followed by holotransferrin treatments (1 g/L to 5 g/L for 30 min, 2, 4, 6, 24 and 48 hours). These

holotransferrin treatment solutions were prepared in BSA-free, serum-free and hygromycin-free EMEM, denoted as 0 g/L. Alongside the holotransferrin treatments, cells were also treated with 0g/L which represented the untreated control, as well as the maintenance medium to enable comparisons between different conditions.

Cells were incubated for the required period of time and assessed for viability (as per section 2.2.16), intracellular iron concentration (as per section 2.2.17) and gene expression (as per sections 2.2.18 and 2.2.19).

### **2.2.16 Viability assay**

Following the experimental treatments, cell viability was assessed using the MTT assay (Mosmann, 1983).

**Principle:** Live cells possess active reductase enzymes. The enzymes convert MTT (3-(4,5-dimethylthiazol-2-yl)-2,5-diphenyl tetrazolium bromide), a yellow tetrazolium salt, into purple coloured insoluble formazan crystals. The formazan crystals are dissolved by DMSO and the solution is read spectrophotometrically. Since these enzymes are only found in active mitochondria, this conversion only occurs in live cells. Hence, the higher the absorbance, the higher the viability of cells, compared to the control.

**Methodology:** To compare the viability of cells in between different treatments,  $2.5 \times 10^4$  cells were seeded per well of a 96 well plate in maintenance medium. The plate was incubated overnight at 37 °C in a humidified atmosphere with 5 % CO<sub>2</sub>. The following day, the maintenance medium was removed and the cells were

washed twice with warm PBS to remove traces of the maintenance medium.

Treatment media were then added to each well and the plates were again incubated at 37 °C in a humidified atmosphere with 5 % CO<sub>2</sub>. On completion of the treatment exposure period, the old media were replaced with 200 µL of fresh media per well. This was followed by addition of 5 µL per well of 5 mg/mL of MTT prepared in PBS. The plates were incubated at 37 °C for 2 hours, the media were removed and 100 µL DMSO was added to each well. Plates were incubated at RT for 15 min, vortexed for 30 sec and absorbances were read at 550 nm using a spectrophotometer. The absorbance values of blanks (medium only) were subtracted from controls and treated samples.

#### **2.2.17 Determination of cellular iron and protein content**

In order to determine the intracellular iron level, cells were washed twice with ice cold PBS and the plates were frozen at -20 °C to induce cell lysis. After overnight incubation, to each well, 200 µl (in a 24 well plate) or 500 µl (in a 6 well plate) of 50 mM sodium hydroxide was added. Cells were detached by rocking on a plate shaker for 2 hours and collected in sterile 1.5 mL tubes. Cell lysis was further promoted by vortexing and one freeze-thaw cycle. The samples (i.e. cells) were dissolved in 50 mM NaOH, syringed using a 25 G needle and centrifuged for 10 min at 13,000 rpm (16,060 x *g*) at 4 °C. The supernatant was collected in a 1.5 mL tube, from which 100 µL was used in the ferrozine assay for iron determination and 5 µL was used in the Bradford assay for protein quantification. The iron content determined through the ferrozine assay was expressed as nmoles of iron per mg of protein.

### 2.2.17.1 Determination of cellular iron content by the ferrozine assay

**Principle:** In an acidic environment and reducing conditions, iron is detached from the proteins to which it is bound and converted from  $\text{Fe}^{3+}$  to  $\text{Fe}^{2+}$ . The iron detection reagent contains ferrozine, a chromophore with an aromatic ring structure, which binds to  $\text{Fe}^{2+}$  iron and gives a purple colour, which is measured spectrophotometrically.

**Methodology:** Iron standards were prepared (10  $\mu\text{M}$  to 150  $\mu\text{M}$  or 5  $\mu\text{M}$  to 20  $\mu\text{M}$ ) from an iron atomic absorption standard solution (Fig. 2.6). The ferrozine assay was modified from Riemer et al. (2004). The supernatant of the cell lysate was used for the ferrozine assay. Additionally, 45  $\mu\text{L}$  of iron detection reagent was added to the samples and the samples were incubated for 1 hour at RT in the dark. The intensity of the colour was measured spectrophotometrically at 550 nm.

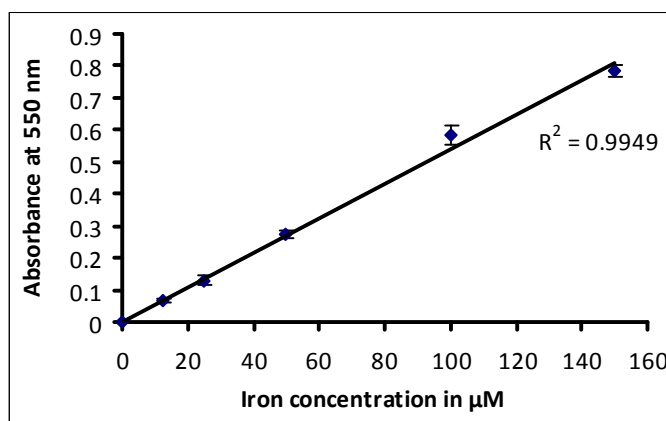


Fig. 2.6 A typical iron standard curve

### 2.2.17.2 Determination of cellular protein content by the Bradford assay

**Principle:** The dye Brilliant Blue G present in the Bradford reagent binds to the proteins in the solution to form blue coloured complexes. These complexes cause

a shift in the absorption maximum of the dye from 465 to 595 nm. The higher the absorbance, the more protein present in the sample.

**Methodology:** The Bradford assay was performed as per the manufacturer's guidelines (Sigma-Aldrich, Gillingham, UK) using the BSA protein standard liquid in the range from 0 -1.4 mg/mL.

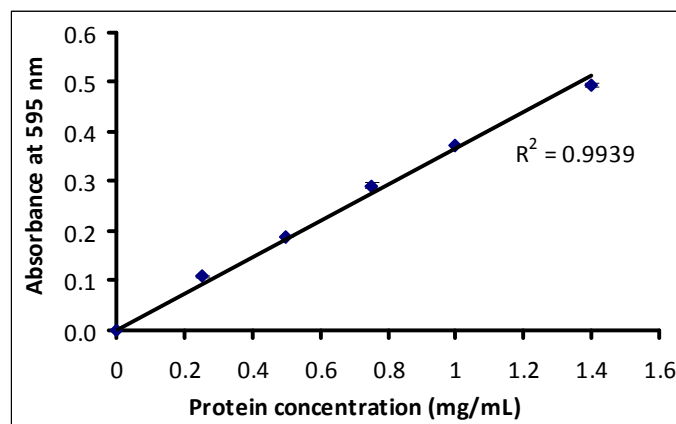


Fig. 2.7 A typical protein standard curve

### 2.2.18 RNA extraction and complementary DNA (cDNA) synthesis

In order to understand gene expression under treatment conditions, RNA was extracted from cells, converted to cDNA and used as a template in real time PCR.

**Principle:** TRI reagent lyses the cells and keeps the RNA stable to be processed.

Addition of 1-bromo-3-chloropropane facilitates phase separation, i.e. separation of RNA from DNA and proteins. The supernatant which contains RNA is treated with isopropanol to precipitate RNA.

**Methodology:** RNA was extracted from cells with TRI reagent using the manufacturer's protocol (Sigma-Aldrich, Gillingham, UK), which was modified as

described as follows. The entire process was performed on ice, except when indicated otherwise. Cells were washed with warm PBS. TRI reagent was directly added dropwise to the cells: 1 mL for 25 cm<sup>2</sup> flask, 200 µL for a well of a 24-well plate and 500 µL for a well of a 6-well plate. In the case of 24-well plates, TRI reagent-cell suspensions were pooled together to increase the RNA concentration. The cell suspensions were collected in 1.5 mL tubes and stored overnight at -80 °C to prevent RNA degradation. The next day, tubes were thawed on ice and incubated at RT for 15 min. 150 µL of 1-bromo-3-chloropropane was added per 500 µL of cell suspension in the TRI reagent, mixed by inverting the tubes and incubated at RT for 3 min. For phase separation, tubes were centrifuged at 4000 rpm (1,523 x g) for 15 min at 4 °C. The resultant top layer containing RNA was aliquoted into a separate tube. Isopropanol, at 1/4<sup>th</sup> this volume, was added and RNA was precipitated overnight at -20 °C. The following day, tubes were centrifuged at 13,000 rpm (16,060 x g) for 15 min at 4 °C. To the RNA pellet, 500 µL of 70 % ethanol was added and centrifuged at 10,000 rpm (9,520 x g) for 10 min at 4 °C. The supernatant was removed completely and tubes were allowed to dry on ice. The RNA was suspended in 30 µL of DEPC-treated nuclease-free water and stored at -80 °C. Reverse transcription and cDNA synthesis from this RNA was performed according to Qiagen's QuantiTect reverse transcription kit protocol. All RNA preparations used in cDNA conversions had a 260/280 ratio >1.7. Once the cDNA was prepared, it was immediately analysed through real time PCR to prevent any degradation.

### 2.2.19 Real time PCR using SYBR green as detector

**Principle:** Real time PCR (RT PCR) measures the amount of product formed during a PCR in real time. In the SYBR green real time PCR, the fluorescent dye SYBR green binds to the minor grooves of DNA and binds only to double stranded (ds) DNA. As the cycles progress, an increase in fluorescence is measured by the machine which provides a set of  $C_T$  (threshold cycle) values.  $C_T$  is a cycle at which there is a significant detectable increase in the amount of fluorescence. Hence, the higher the initial starting template cDNA, the earlier the fluorescence will reach a certain threshold and lower will be the  $C_T$  value. These  $C_T$  values are then mathematically processed further for biological interpretations.

**Methodology:** All real time PCRs were performed using Qiagen's Quantifast SYBR green kit, as per manufacturer's protocol (Table 2.5). cDNA equivalent to 100 ng RNA was used in each reaction, except when performing standard dilution curves as described in the following section. The reactions were carried out in the Rotor-gene Q machine (Qiagen, Crawley, UK) and results were analysed using Rotor-gene software series 1.7. Products were electrophoresed on 1 % agarose gel to ensure product formation of the expected size.

Contents	Volume	Real time PCR cycle steps
Nuclease free water	4 $\mu$ L	1. Initial denaturation temperature: 95 °C for 10 min 2. Denaturation: 94 °C for 10 sec 3. Annealing: 60 °C for 15 sec (or 12 sec) 4. Extension: 72 °C for 20 sec (or 15 sec) 5. Repeat step 2 to 4, 39 times or 34 times
SYBR green master mix	10 $\mu$ L	
5 $\mu$ M Forward primer	2 $\mu$ L	
5 $\mu$ M Reverse primer	2 $\mu$ L	
cDNA equivalent to 100 ng RNA.	2 $\mu$ L	
Total volume	20 $\mu$ L	

**Table 2.5 SYBR real time PCR protocol and cycles**

The table describes standard real time PCR protocol. The cycling steps described represent the default cycle, except when modified for optimisations as indicated in the brackets.

### 2.2.19.1 Standard dilution series

Firstly, a PCR was performed to confirm the presence of all genes of interest in the cell line of interest. Amplicons obtained were sent for sequencing to confirm the sequence identity of each gene (appendix V). This was followed by a pilot real time temperature gradient PCR to ensure that the default annealing temperature was the most appropriate for product formation (appendix VI).

Amplification efficiencies of all genes of interest were determined by setting up a 2-fold dilution series of the cDNA template with the respective primers. The starting amount of the template was cDNA equivalent to 100 ng RNA. As an example, the *TfR1* gene is analysed in Fig. 2.8. The standard curves showing the amplification efficiencies and analysis of all other genes of interest are in appendix VII.

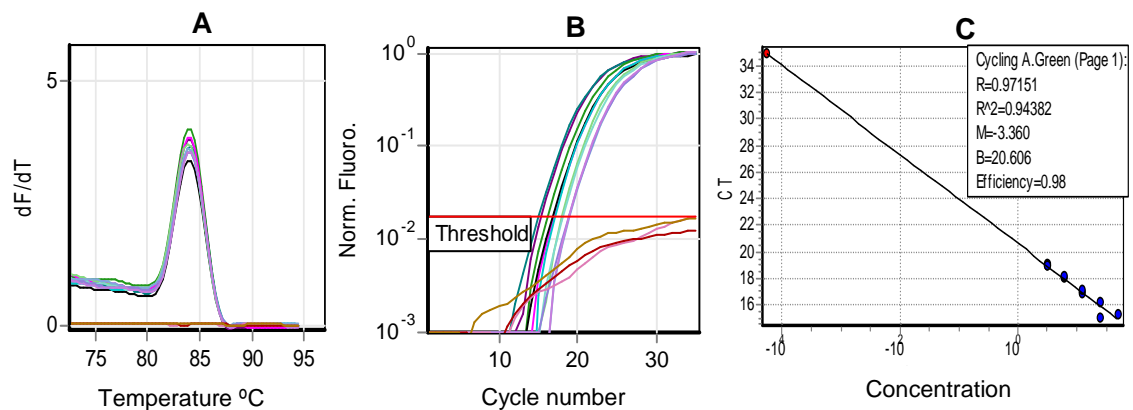


**Fig. 2.8 Analysis of TfR1 standard curve**

**A** : Melt curve: shows the presence of a single peak, indicating unique product formation without any detectable primer dimers.

**B** : Cycling curve: a sigmoidal curve of cycle number vs. fluorescence. The shape suggests that as the substrates are depleted over the course of cycles and thus the curve flattens towards the end. The line of threshold is placed above the negative controls (nuclease-free water). This displays a set of  $C_T$  values which are used by the software to plot the efficiency of the reaction, as seen in part C.

**C** : Efficiency curve: displays the efficiency of the reaction.

### 2.2.19.2 Analysis of real time PCR data

The  $C_T$  values obtained from a particular experiment were analysed by the comparative method, also referred to as the Delta-Delta  $C_T$  ( $\Delta\Delta C_T$ ) relative quantification. Essentially, the method is based on the following calculations:

- (I)  $\Delta C_T$  of sample =  $C_T$  of target gene -  $C_T$  of reference gene (in this study it was glyceraldehyde 3-phosphate dehydrogenase, *GAPDH*)
- (II)  $\Delta C_T$  of untreated =  $C_T$  of target gene -  $C_T$  of reference gene
- (III)  $\Delta\Delta C_T = \Delta C_T$  of sample -  $\Delta C_T$  of untreated
- (IV) Normalised target gene expression of sample =  $2^{-\Delta\Delta C_T}$

### 2.2.20 Detection of transferrin receptor on cell surface

The effect of holotransferrin treatments on the cell surface expression of TfR1 was studied using flow cytometry.

**Principle:** The human transferrin receptor, to be detected, binds to a complementary primary antibody. A fluorescein isothiocyanate (FITC)-labelled secondary antibody binds to the primary antibody and this label is detected by the flow cytometer. The higher the fluorescence detected, the higher would be the number of transferrin receptors present on the cell surface.

**Method:** Cells were seeded at a density of  $5 \times 10^5$  cells per well in a 6 well plate. After 24 hours, the cells were washed with PBS to remove traces of the maintenance medium. Following this, the cells were either serum deprived for 24 hours followed by addition of the treatment medium or the treatment medium was added immediately after washing the cells without any period of serum deprivation.

The cells were then incubated with the treatment medium for the desired period of time and harvested for flow cytometry. Cell harvesting was accomplished by dissociation of cells with 500  $\mu\text{L}$  of TrypLE Express (ThermoFisher Scientific, UK), per well of a 6 well plate for 7 min, followed by centrifugation for 4 min at 1000 rpm (89 x  $g$ ). Cells were suspended in PBC (PBS containing 0.15 % BSA and 1 mM calcium chloride) and  $200 \times 10^3$  cells from each well were transferred to a 96 well plate. Cells were washed 3 times with PBC by centrifugation at 3800 rpm ( $\sim 1,263$  x  $g$ ) for 30 sec, on slow acceleration and no brake. Then, to each well, 20  $\mu\text{L}$  of blocking IgG (i.e.  $\gamma$ -globulins from human blood) was added at the concentration of 16 mg/mL prepared in PBC.

The primary antibody, in this study the human transferrin receptor antibody (Abcam Cambridge, UK), was prepared at the optimised concentration of 5  $\mu\text{g}/\text{mL}$  in PBC. 20  $\mu\text{L}$  of this solution was added to each of the test wells whereas the control wells were supplemented with 20  $\mu\text{L}$  of PBC. The controls cells without the primary antibody and the treated cells with the primary antibody were incubated for 45 min on ice. The cells were then washed with PBC, as previously described, to remove any non-specifically bound primary antibody. A FITC-labelled secondary antibody STAR9B, rabbit F (ab')<sub>2</sub> anti-mouse IgG (ABD Serotec Kidlington,UK) was added, at a concentration of 10  $\mu\text{g}/\text{mL}$ ; 40  $\mu\text{L}$  was added to each well. The cells were incubated for 30 min on ice and washed twice with PBC and once with PBS, as previously described. The cell layer formed at the bottom of each well was resuspended in 200  $\mu\text{L}$  of PBS. At the time of analysis using the flow cytometer, this 200  $\mu\text{L}$  of cell suspension was transferred to a tube already containing 200  $\mu\text{L}$

of PBS. Thus for each sample 400  $\mu$ L of cell suspension was analysed. All samples were kept on ice during analysis. Fig. 2.9 shows a typical analysis of cell surface TfR1 via flow cytometry.

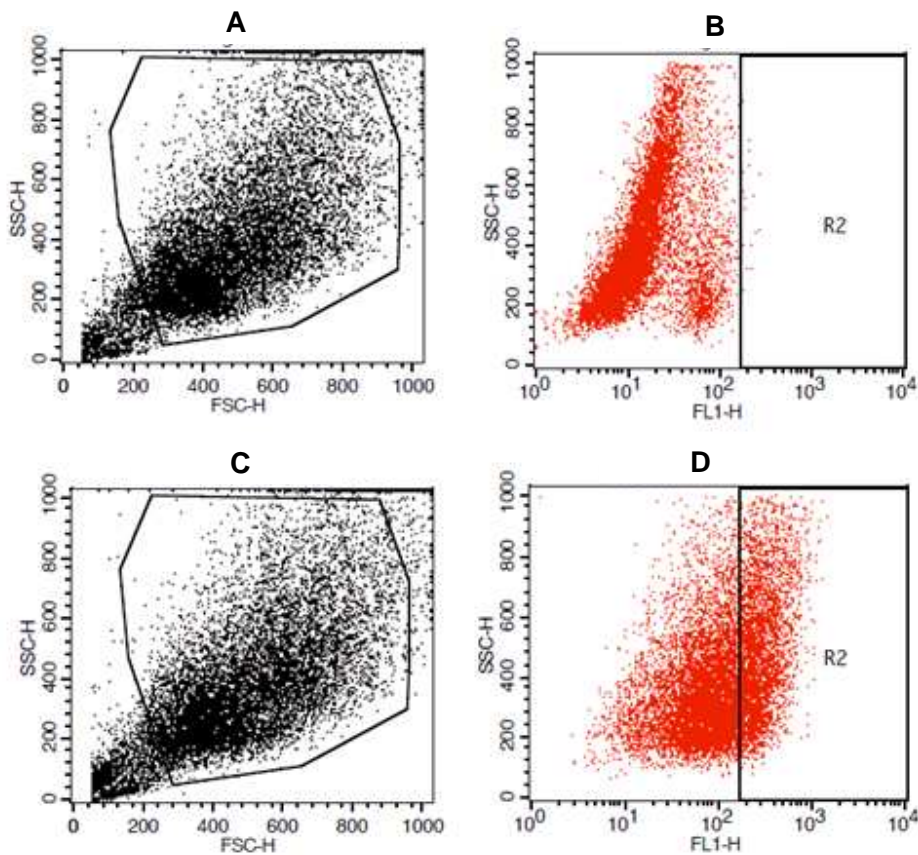


**Fig. 2.9 Analysis of cell-surface TfR1 in Wt HepG2 cells by flow cytometry**

**A and B** : Cells without the primary antibody (negative control)  
**C and D** : Cells treated with primary antibody (test)

### 2.2.21 Detection of human TfR1 in CHO TRVb1 cells

The presence of human TfR1 protein in the CHO TRVb1 cells was checked using dot blot chemiluminescence and Western blotting.

**Principle of chemiluminescence:** Anti-human TfR1 antibody binds to the TfR1 and a secondary antibody conjugated to horseradish peroxidase (HRP) binds to

the primary antibody. The HRP produces luminescence on exposure to chemiluminescent substrates, the proportion of luminescence being directly proportional to the amount of protein.

**Methodology:** Wt CHO and CHO TRVb1 cell lines were grown in a 25 cm<sup>2</sup> flask in the maintenance medium. On reaching 70 % confluence, cells were trypsinised as normal. The supernatant was removed and the cell pellet was resuspended in 100 µL of PBS. To this, 100 µL of 2X loading buffer (800 µl of milliQ water, 2 mL of 0.5 M tris pH 6.8, 1.6 mL glycerol, 3.2 mL of 10% SDS, 0.5 mL of 0.1 % bromophenol blue) was added. The mixture was vortexed for 5 sec and 5 µL of each cell extract was applied as a dot on a nitrocellulose membrane (Bio-Rad, UK) and allowed to dry for 5 min at RT. Following this, the nitrocellulose membrane was blocked overnight at 4 °C on a shaker, in 5 % milk prepared in PBST (0.05% Tween 20 in PBS).

On the following day, the milk was removed and the membrane was washed with distilled water. Then the membrane was placed in a clean tray prior to the addition of the antibody. The primary antibody, human TfR1 antibody (Cell science) (100 µg/mL), was diluted 1:2000 in PBS containing 1 % BSA. This antibody solution was added onto the membrane and incubated for 1 hour at 37 °C on a shaker. After incubation, the membrane was washed three times for 10 min each wash on a shaker with PBST followed by a final wash with PBS for 10 min.

A rabbit anti-mouse HRP-conjugated secondary antibody (Dako UK Ltd, UK) was diluted 1:1000 by using 1 % BSA in PBS. This was added onto the nitrocellulose membrane and the membrane was incubated at RT for 1 hour on a shaker. After incubation the membrane was washed with distilled water once, followed by two 10 min washes with PBST and one wash with distilled water for 10 min.

A mixture of 750  $\mu$ l of each of the ECL™ Western Blotting Detection Reagents (Amersham, GE healthcare, UK) was prepared in a tube and mixed thoroughly and added onto the membrane. Two Ryman films were placed on the nitrocellulose membrane like a “sandwich” such that the nitrocellulose membrane was in the middle and the two films were on either side. One X-ray film was placed on top of the sandwich and this assembly was put in a cassette and developed in the dark for 10 min. The luminescent signal was thus captured on the film.

SDS PAGE and blotting was performed using the MINI- Protean-3 cell system (Laemmli buffer system) and Bio-Rad's Ready Gel, precast gels (BIO-RAD, UK) as per manufacturer's recommendation. The samples for SDS PAGE were prepared by addition of dithiothreitol (DTT) at a final concentration of 10 mM to the previously prepared cell extract in loading buffer. The samples were boiled for 5 min at 100 °C and 20  $\mu$ L was loaded per well. The samples were subjected to electrophoresis and immunoblotting was performed with the antibodies used in the dot blot. The concentrations of the primary and secondary antibody as well as the detection system were the same as those used in the dot blot.

### **2.2.22 Determination of hepcidin peptide concentrations**

The concentration of hepcidin-25 in the medium was measured by radioimmunoassay in collaboration with Dr. Mark Busbridge, Imperial college, London UK (Busbridge et al., 2009).

### **2.2.23 Restriction digest**

pEGFPN1 plasmid constructs containing preprohepcidin derivatives were obtained from Dr. Sebastien Farnaud. In order to identify these plasmid constructs, each was digested with the restriction enzymes *Bam*HI (Promega, UK) and *Hind* III (Promega, UK), as per the manufacturer's restriction digest protocol. Prior to digestion, the yield of the plasmid was increased by transformation of each of the recombinant plasmid constructs into *E.Coli* XL1 blue cells as explained in section 2.2.11, except that here 50 µg/mL of kanamycin sulphate (Fisher BioReagents) was used as a selection antibiotic (since the plasmid possesses a kanamycin resistance gene) without the addition of X-gal and IPTG in the agar plates. Following this, the purified plasmids were subjected to single and double restriction digest. Essentially, 1.5 µg of plasmid per 20 µL of the digestion reaction was added and the reaction mix was incubated at 37 °C for 1 hour. An aliquot (2 µL) of loading buffer was added to 10 µL of the reaction mixture and electrophoresed on 2 % agarose gel at 100 V to check for post-digestion products. The host plasmid is shown in the Fig. 2.10.

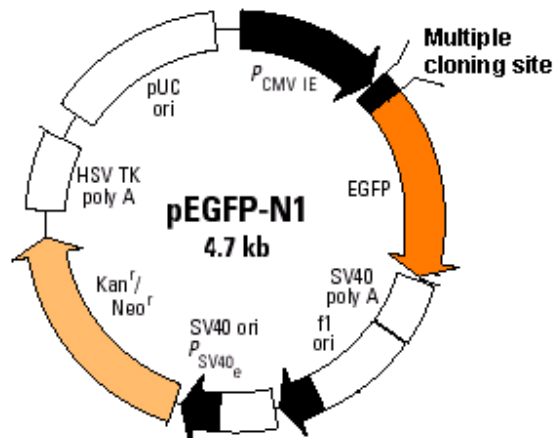


**Fig. 2.10 Cloning vector pEGFP-N1 plasmid**  
 Restriction sites for enzymes *HindIII* and *BamHI* are located within the multiple cloning site. The figure is adapted from Clontech available at <http://www.liv.ac.uk/physiology/ncs/catalogue/Cloning/pEGFP-N1.htm>

#### 2.2.24 Localisation studies of preprohepcidin derivatives

Localisation studies were performed by transfecting Wt HepG2 cells with the recombinant pEGFPN1 plasmid containing the 'pre-pro' construct of preprohepcidin. The transfection reagent used, Lipofectamine LTX and Plus reagent (Life technologies), is specially formulated to transfect the difficult-to-transfect HepG2 cells.

**Principle of transfection:** Lipid globules surround the plasmids. These lipid-coated globules fuse with the cell membranes and the lipid-coated plasmids are uptaken by the cells.

**Methodology:** HepG2 cells were seeded at a cell density  $2 \times 10^5$  cells per well of a 6 well plate and the transfection procedure was performed using the Lipofectamine LTX and PLUS reagent, adapted from the manufacturer's recommendation. Essentially, the Wt HepG2 cells growing in maintenance medium

were trypsinised and seeded into 6 well plates at a cell density of  $2 \times 10^5$  cells per well. After overnight incubation, the transfection procedure was initiated. A transfection mix containing 2.5  $\mu\text{g}$  of pEGFPN1 plasmid, 500  $\mu\text{L}$  of Optimum I medium and 2.5  $\mu\text{L}$  of PLUS reagent was prepared and incubated for 10 min at RT. Following this, 10  $\mu\text{L}$  lipofectamine LTX was added to this preparation and incubated for a further 25 min at RT. Once the transfection mix was ready, the maintenance medium from the cells was aspirated and replaced with 2.5 mL of maintenance medium without antibiotics and 100  $\mu\text{L}$  of transfection mix per well. The plate was gently rocked and incubated at  $37^\circ\text{C}$  for 24 hours. Cell fixation was performed by washing the cells with PBS followed by addition of 2 mL of ice cold paraformaldehyde (4%) and incubation at  $37^\circ\text{C}$  for 20 min. The paraformaldehyde was then removed and 2 mL PBS was added to each well, followed by wrapping the plates with foil and storing the plates at  $4^\circ\text{C}$ . Prior to analysis by confocal microscopy, the PBS was removed and the cells were washed 2 times with fresh PBS. The cells were permeabilised using Triton-X 100 (0.1% in PBS) for 10 min at RT and washed 3 times with PBS. This was followed by incubation with the nuclear staining dye TO-PRO-3 (1  $\mu\text{M}$  in PBS) for 20 min. After washing the cells with PBS, 2 mL of fresh PBS was added to the cells followed by observation by confocal microscopy.

### **2.2.25 Statistical analysis**

Statistical analysis of the data was carried out using one-way or two-way ANOVA, accompanied by post-hoc analysis using the software SPSS, version 19. The level of significance was set at  $p < 0.05$ .

## Chapter 3

### Effect of iron supplementation on hepcidin expression in recombinant Chinese hamster ovary cells

#### 3.1 Introduction

Although in humans and in animal models systemic iron excess leads to a rise in hepcidin production (Lin et al., 2007, Pigeon et al., 2001), these results have not been replicated in cell lines and primary hepatocytes. Iron overdose to cells resulted in variable *hepcidin* mRNA expression in different cell types as explained in chapter 1 section 1.7. This may partly be attributed to TfR1 on the cell surface which regulates iron uptake by the cells and thus limits the increase in intracellular iron levels. To overcome this limitation, in this study, modified Chinese hamster ovary (CHO) cells were used which are devoid of the endogenous TfR1 and instead over-express the human TfR1 (McGraw et al., 1987). Due to this specific property it was hypothesised that the cells would permit intracellular iron overload upon iron overdose and the resultant effect on gene expression could be studied. Also, the mechanisms involved in the transferrin cycle in CHO cells have been well described and have similar properties to other cell types (Yamashiro et al., 1984). Hence these cells were considered suitable for studies related to transferrin-bound iron uptake.

The gene sequence of *hepcidin* and other iron-related genes in the CHO cells have not yet been determined. Therefore, it was necessary to first characterise these gene sequences to enable expression analyses in real time and thus establish the

CHO cells as a model system to study *hepcidin* and iron regulation. The other iron-related genes in CHO cells chosen for this study were *ferroportin*, *Hfe* and *Irp2*.

### **3.1.1 Aims and objectives**

**Aim:** To characterise iron-related genes in CHO cells.

Since the hamster species is a rodent it was expected to have high genomic similarities with the mouse, rat and human genome. Hence, primers designed based on conserved nucleotides between these three species should also bind to the CHO genome. This would enable product formation and subsequent sequencing of the previously unknown gene sequences.

**Objectives:**

1. To identify conserved nucleotides between human, mouse and rat in the gene of interest and design primers based on these conserved regions.
2. To probe the CHO genome with the designed primers and optimise PCR conditions to facilitate maximum product formation.
3. To sequence CHO genes and analyse these using *blastn* at NCBI to confirm sequence identity and compare it to the pre-characterised sequences in the database.
4. To study the effect of iron overdose on hepcidin expression in CHO TRVb1 cells.

## 3.2 Approach and optimisations

### 3.2.1 Concept behind primer design and sequence acquisition

The aim of characterisation of previously unknown gene sequences in CHO cells was based on the hypothesis that there were genomic similarities between the hamster and human, mouse and rat. To confirm this, some pre-characterised hamster mRNA sequences were compared to corresponding transcripts in human, mouse and rat. As seen in table 3.1, the hamster genes showed high sequence similarity with the corresponding genes in the mentioned three species.

<b>Genes in <i>Cricetulus griseus</i> (hamster)</b>	<b>Human</b>	<b>Mouse</b>	<b>Rat</b>
<i>Transferrin receptor</i>	82% 99%	87% 100%	87% 100%
<i>Dihydrofolate reductase</i>	83% 65%	86% 75%	97% 28%
<i>Heat shock protein</i>	89% 96%	93% 90%	93% 90%
<i>Ferritin</i>	87% 88%	91% 99%	90% 99%
<i>Transferrin</i>	82% 99%	88% 100%	88% 100%
<i>Alpha tubulin</i>	93% 83%	95% 83%	94% 99%

**Table 3.1 Similarities between hamster, human, mouse and rat genomes**

The NCBI accession numbers of genes are in appendix VIII.

Key to table:

- **Sequence similarity with CHO genes**
- **Sequence coverage**

Using this principle, for a particular iron-related gene of interest, primers were designed based on conserved nucleotides between human, mouse and rat mRNA sequences. These primers were used to probe the CHO genome to obtain a partial sequence of that gene. This was the 1<sup>st</sup> round of sequencing. This partially characterised gene sequence was compared to corresponding pre-characterised gene sequences in the NCBI database and the identity of the CHO sequence was

confirmed. Following this, primers were designed again based on the partially characterised CHO sequence obtained from the 1<sup>st</sup> round of sequencing and conserved nucleotides between the mentioned three species. These primers, one CHO-specific and another based on conserved nucleotides, were used to probe the CHO genome to obtain a CHO gene product. This was the 2<sup>nd</sup> round of sequencing. Thus, as explained through Fig. 3.1, the concept of “PCR walking” was employed to characterise previously uncharacterised genes in the CHO cells.

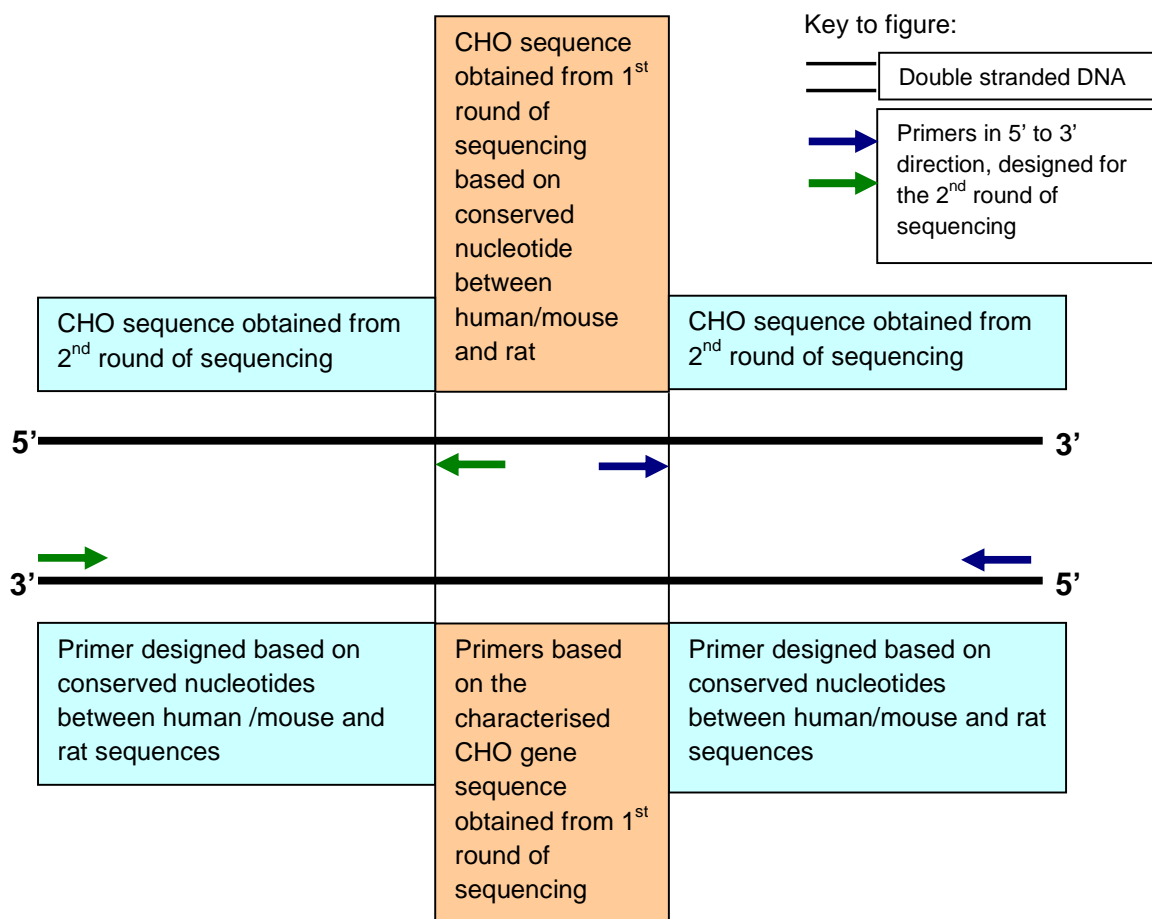


**Fig. 3.1 Concept of “PCR walking” used for CHO gene sequencing**

At every round of sequencing, the gene specificity of each designed primer was checked using *blastn* at NCBI. The characterised gene sequences of CHO cells

were further used to design CHO-specific and exon spanning primers for real time PCR. To identify conserved regions, mRNA and protein multiple sequence alignments were created using ClustalW2 (available at [www.ebi.ac.uk](http://www.ebi.ac.uk)). As an example, Fig. 3.2 demonstrates the approach used to design primers and the resultant gene sequence acquired for *ferroportin* gene in CHO cells.

```

HumanSLC40A1_      -----CTAGGCTCGGACGACCTGCTGAGCCTCCCAAACCGCTTCCATAAGGCTTTGGCCTT 120
MouseSlc40a1_     -----CTGCGGCCGG-----TGGATCCTCCAACCCGCTCCATAAAGGCTTTGGCCTT 99
RatSlc40a1_       -----CTGCGGCCGG-----TGGACCCTCCAACCCGCTTCCATAAAGGCTTTAGCCTT 61
-----** * *** ** * **** * **** * **** * **** * **** * **** *

5'TCCAACCTCAGCTACAGTGTT >>> 3' (Fla)
TCCAACCTCAGCTACAGTGTT >>> 3' (Flb)

HumanSLC40A1_     TCCAACCTCAGCTACAGTGTTAGCTAAGTTTGGAAAGAAGGAAAAAGAAAATCCCT-GG 179
MouseSlc40a1_     TCCAACCTCAGCTACAGTGTTAGCTAAGTTTGGAAAGAAGACAAAAAGAAGACCCCG-TG 158
RatSlc40a1_       TCCAACCTCAGCTACAGTGTTAGCTAAGTTTGGAAAGAAGACATAAAGAAGACCCCGGTG 121
***** * **** * **** * **** * **** * **** * **** * **** *

5'ATCGGATGTG >>>
-----TTCTTCTCTACCTTGGTCATCTCTCTCTACTTGGGGAGATCGGATGTG 476
-----TTCTTCTCTACCTTGGCCACTCTCTCTCCACTTGGGGGATCGGATGTG 456
-----TTCTTCTCTACCTTGGCCACTCTCTCTCCACTTGGGGGATCGGATGTG 416
-----***** * **** * **** * **** * **** * **** * **** * **** *

GCACCTTTC >>> 3' (F)
HumanSLC40A1_     GCACCTTTCGGTGTCTGTGTTTCTGGTAGAGCTCTATGGAAACAGCCTCCTTTTGACAGC 536
MouseSlc40a1_     GCACCTTTCAGTGTCTGTGTTTCTGGTGGAACTCTATGGAAACAGCCTTCTTTGACAGC 516
RatSlc40a1_       GCACCTTTCAGTGTCTGTGTTTCTGGTGGAACTCTACGGAAACAGCCTCCTTTGACAGC 476
***** * **** * **** * **** * **** * **** * **** * **** *

AGCCTCCTCTTGACAGC
(R1) 3'<<< AGGAGAACTGTGC

HumanSLC40A1_     AGTCTACGGGCTGGTGGTGGCAGGGTCTGTTCTGGTCTGGGAGCCATCATCGGTGACTG 596
MouseSlc40a1_     TGTCTATGGACTGGTGGTGGCAGGCTCTGTTCTGGTCTGGGAGCCATCATTTGGTACTG 576
RatSlc40a1_       TGTCTACGGGCTGGTGGTGGCAGGCTCTGTTCTGGTCTGGGAGCCATCATTTGGTACTG 536
***** * **** * **** * **** * **** * **** * **** * **** *

TGTCTACGGGCTGGTGGTAGCAGGCTCTGTTCT
<<< ACAGATGC 5' 5' TAGCAGGCTCTGTTCTGG >>>3' (F2)

3'<<< TCTTACGNTCTGAATTCACCG 5' (R)

HumanSLC40A1_     GGTGGACAAGAATGCTAGACTTAAAGTGGCCAGACCTCGCTGGTGGTACAGAATGTTTC 656
MouseSlc40a1_     GGTGGATAAGAATGCCAGACTTAAAGTGGCCAGACGTCAGTGGTGGTTCAGAATGTGTC 636
RatSlc40a1_       GGTGGATAAGAATGCCAGACTTAAAGTGGCCAGACGTCCTCGTGGTGGTTCAGAATGTATC 596
***** * **** * **** * **** * **** * **** * **** * **** *

AGTGGCCAGACTTCACTGGTGGTGCAGAACGCTCTC
HumanSLC40A1_     AGTCATCCTGTGTGGAATCATCCTGATGATGGTTTTCTTACATAAACATGAGCTTCTGAC 716
MouseSlc40a1_     CGTCATCCTCTGCGGAATCATCCTGATGATGGTTTTCTTACACAAGAATGAGCTCCTGAC 696
RatSlc40a1_       AGTCATCCTCTGCGGGATCATCCTGATGATGGTTTTCTTACACAAGAATGAGCTTCTGAA 656
***** * **** * **** * **** * **** * **** * **** * **** *

CGTCATTCTCTGCGGGATCATCCTGATGATGGTTTTCTTACAAAAACGAGCTTCTGAC
HumanSLC40A1_     CATGTACCATGGATGGGTTCTCTCTCTCTGCTATATCCTGATCATCACTATTGCAAATAT 776
MouseSlc40a1_     CATGTACCATGGATGGGTTCTCTCTCTGCTACATCCTGATCATCACTATTGCAAACAT 756
RatSlc40a1_       CATGTATCATGGATGGGTTCTCTCTCTGCTACATCCTGATCATCACTATTGCAAACAT 716
***** * **** * **** * **** * **** * **** * **** * **** *

CATGTATCATGGATGGGTTCTCTCTCTGCTACATCCTGATCATCAGGATTGCAAACAT
5' ATGGGTGCTCACTGTCTGCTA 3'>>> (FPN for CHO F)

HumanSLC40A1_     TGCAAATTTGGCCAGTACTGCTACTGCAATCACAATCCAAAGGGATTGGATTGTTGTTGT 836
MouseSlc40a1_     TGCAAATTTGGCCAGTACTGCCACTGCGATCACAATCCAAAGGGACTGGATTGTTGTTGT 816
RatSlc40a1_       TGCGAATTTGGCCAGTACTGCCACTGCAATTACAATCCAAAGGGACTGGATTGTTGTCGT 776
***** * **** * **** * **** * **** * **** * **** * **** *

TGCAAATCTGGCCAGTACTGCTACTGCAATCAGATCCAAAGGGACTGGATTGTTGTTGT

```



The NCBI accession numbers of all gene sequences used to design primers are listed in appendix VIII. Transcripts alignments and other information on sequencing of *ferroportin*, *Hfe* and *Irp2* genes are in appendices IX, X and XI, respectively.

### **3.2.2 PCR optimisations**

The CHO cells were maintained in cell culture as described in methods sections 2.2.1 and 2.2.2, whereas DNA was extracted as per methods section 2.2.5. In all PCRs, rat liver DNA and/or mouse kidney were used as positive controls as these would yield gene products of expected sizes with the respective primers. Nuclease-free water was used as a negative control and here no product was expected since there was no template in this reaction.

To identify the most appropriate annealing temperature which would facilitate unique product formation in high amounts, temperature gradient PCRs were performed as described in methods sections 2.2.8 and 2.2.9. This optimisation was performed with each primer pair designed for every gene for the 1<sup>st</sup> round of sequencing (table 2.1 and appendix XIII). An example of the temperature gradient PCR for *ferroportin* gene in the 1<sup>st</sup> round of sequencing is shown in Fig. 3.3. In this case, the appropriate annealing temperature that yielded a single product of the expected size was identified as 51 °C and multiple PCR reactions were set at 51 °C. The PCR products from these multiple tubes were pooled together, purified and sent for sequencing (section 2.2.12) to confirm sequence identity.

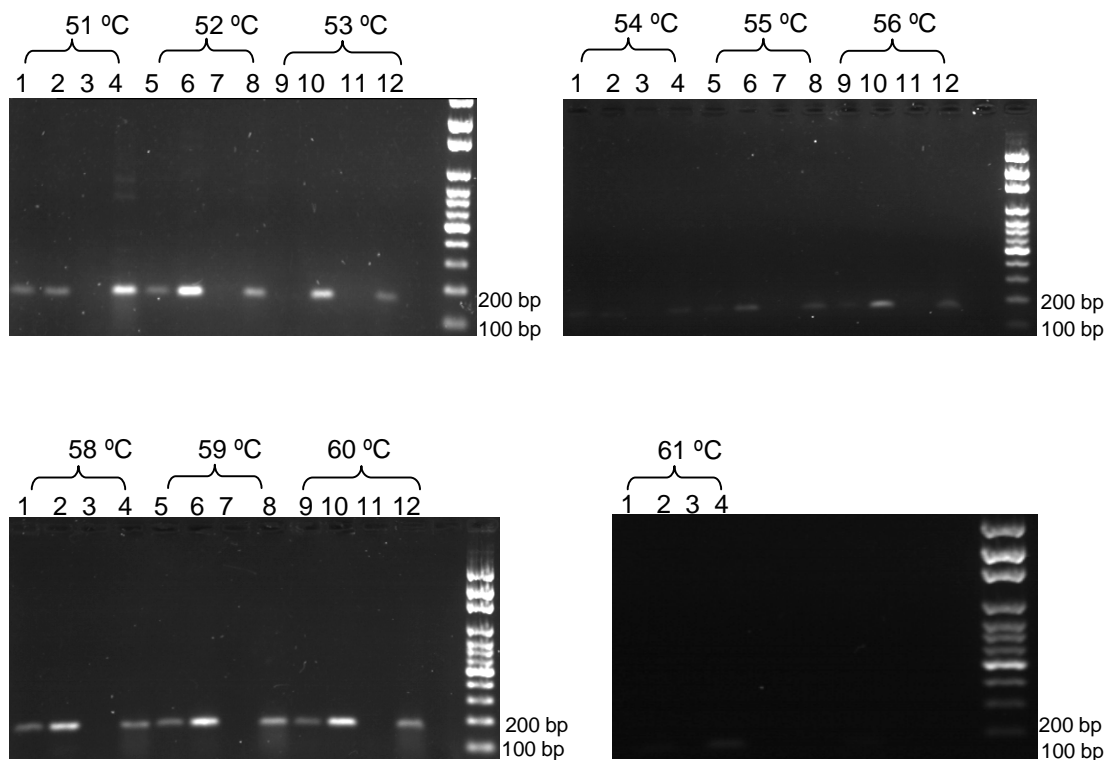


**Fig. 3.3 Temperature gradient PCR for 1<sup>st</sup> round of CHO *ferroportin* gene sequencing with primers ferroportin (F) and (R)**

DNA was extracted from the CHO TRVb1 cells (as per methods section 2.2.5) and amplified under different annealing temperatures (as described in sections 2.2.8 and 2.2.9). cDNA synthesis from mouse kidney was performed as described in section 2.2.18.

In all figures:

Lanes 1,5,9 = mouse kidney cDNA; expected product size=160 bp

Lanes 2,6,10 = rat liver DNA, expected product size=160 bp

Lanes 3,7,11 = negative control

Lanes 4,8,12 = CHOTRVb1 DNA

### 3.3 Results

#### 3.3.1 Characterisation of CHO gene sequences

Using the concept explained in section 3.2.1 and PCR optimisations described in section 3.2.2, previously unknown sequences of iron-related genes in CHO cells were characterised. As a representation, CHO gene products obtained from the 1<sup>st</sup> round of sequencing are shown in Fig. 3.4.

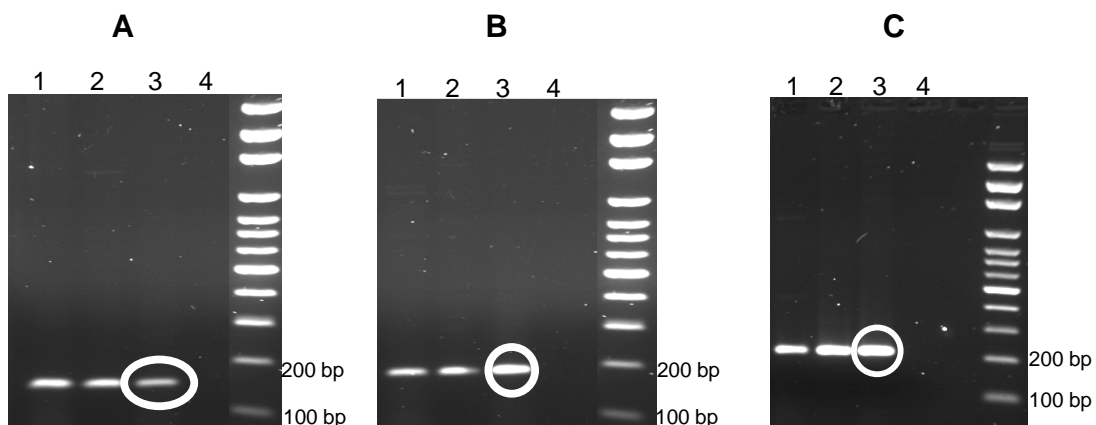


**Fig. 3.4 Amplicons generated for 1<sup>st</sup> round of CHO gene sequencing**

Encircled products were purified and their sequence identity was confirmed as described in methods section 2.2.12.

**A:** Amplicons of *ferroportin* gene in rodents and CHO cells with primers ferroportin (F) and (R); expected size of controls= 160 bp

**B:** Amplicons of *HFE* genes in rodents and CHO cells with primers HFE (F) and (R); expected size of controls= 185 bp

**C:** Amplicons of *IRP2* gene in rodents and CHO cell lines with primers IRP2 (F) and (R); expected size of controls= 215 bp

Lane 1= rat liver DNA (control)

Lane 2= mouse liver DNA (control)

Lane 3= CHO TRVb1 DNA

Lane 4= negative control

The characterised CHO gene sequences of products encircled in Fig. 3.4, were compared to the corresponding pre-characterised gene sequences in other species and their identities were studied. For example, the characterised CHO-*ferroportin* sequence shares 92 % identity with the human-*ferroportin* gene sequence, as shown below.

>ref|NG\_009027.1| Homo sapiens solute carrier family 40 (iron-regulated transporter), member 1 (SLC40A1),

Score = 78.8 bits (86), Expect = 2e-12  
 Identities = 49/53 (92%), Gaps = 0/53 (0%)  
 Strand=Plus/Plus

```

CHO Ferroportin      1 CAGCCTCCTCTTGACAGCTGTCTACGGGCTGGTGGTAGCAGGCTCTGTTCTGG 53
                    |||
Human Ferroportin  10548 CAGCCTCCTTTTGACAGCAGTCTACGGGCTGGTGGTGGCAGGGTCTGTTCTGG 10600
  
```

Following this, the 2<sup>nd</sup> round of CHO gene sequencing was initiated with primers listed in table 2.1. Coincidentally, for all genes of interest, the primers F1 & R1 showed minimal product formation, whereas primers F2 & R2 (R2a for *ferroportin* and *Irp2* genes) yielded a comparatively higher amount of product (appendix XIII). Hence these were used for subsequent sequencing reactions.

Percentage identities between the characterised CHO gene sequences and pre-existing gene sequences in the database were tabulated (Table 3.2). Data showed that the iron-related genes bore very high level of genomic similarities between the hamster and human, mouse and rat, as hypothesised.

Genes	CHO sequence characterised in 1 <sup>st</sup> round of sequencing			CHO sequence characterised in 2 <sup>nd</sup> round of sequencing		
	Human	Mouse	Rat	Human	Mouse	Rat
<i>Ferroportin</i>	92 %	92 %	96 %	89 %	93 %	92 %
<i>Hfe</i>	86 %	91 %	87 %	80 %	88 %	88 %
<i>Irp2</i>	95 %	94 %	96 %	92 %	97 %	96 %

**Table 3.2 Percentage identity between characterised CHO gene sequences and other species**

The table shows identities between the characterised CHO gene sequences and the pre-characterised gene sequences of other species in the NCBI database. Full details on the sequencing data on characterised CHO gene sequences for *ferroportin*, *HFE* and *IRP2* genes are in appendices IX, X and XI, respectively.

### 3.3.2 Functional analysis of characterised gene sequences

In order to understand the link between the genome and proteome and whether genomic similarities seen in table 3.1 inferred proteomic similarities, the characterised CHO gene sequences were translated to protein sequences and compared to corresponding protein sequences in other species. Fig. 3.5 shows functionally significant amino acids in ferroportin in different species.



ferroportin, reflecting the significance of this amino acid in ferroportin degradation and internalisation (De Domenico et al., 2008). This amino acid is also conserved in the CHO cells within the hepcidin binding domain. Binding of hepcidin to ferroportin leads to phosphorylation of either Y302 or Y303 followed by ferroportin internalisation (De Domenico et al., 2007) and degradation, involving K253 (De Domenico et al., 2006). Interestingly, these amino acids in the CHO proteome lie in the same position relative to other amino acids, as in human, mouse and rat proteomes. Additionally, in the CHO cells, the amino acids N144 and V162 are conserved, which if mutated, exhibit hepcidin insensitivity (Wallace et al., 2009). Also, the cysteines which form disulphide bonds and usually play a significant role in the folding and stability of proteins (Sevier and Kaiser, 2002), are well conserved in the characterised CHO-ferroportin sequence. Similarly, functional analysis of the characterised CHO-*Hfe* sequence was performed (Fig. 3.6).



**Fig. 3.6 Functional significance of the characterised CHO-*Hfe* sequence**  
 Translation of CHO-*Hfe* sequence was carried out as described in legend of Fig. 3.5.  
 Key to alignment:

- $\alpha 1$  and  $\alpha 2$  : domains of HFE protein involved in interaction with transferrin
- H63D : mutation that leads to haemochromatosis in humans
- \* represents conserved amino acid between species.

The alignment in Fig. 3.6 reveals high conservation of the alpha 1 and alpha 2 regions of Hfe protein. These regions are known to interact with the transferrin receptor and play a role in transferrin-bound iron uptake (reviewed in Fleming, 2009). Also, the characterised *Hfe* gene sequence in CHO cells showed the presence of histidine H63 at the same relative position as other species. A mutation (H63D) leads to the development of hereditary haemochromatosis in humans (reviewed in Pietrangelo, 2006).

The iron regulatory proteins IRP1 and IRP2 play a significant role in maintaining cellular iron levels by binding to IREs on transcripts of various genes (reviewed in Muckenthaler et al., 2008). It has been proposed that IRP2 acts as an iron sensor within cells (Kang et al., 2003). Functional analysis of the characterised CHO-*Irp2* revealed the presence of important amino acids proposed to be involved in iron binding (Kang et al., 2003), as shown in Fig. 3.7.

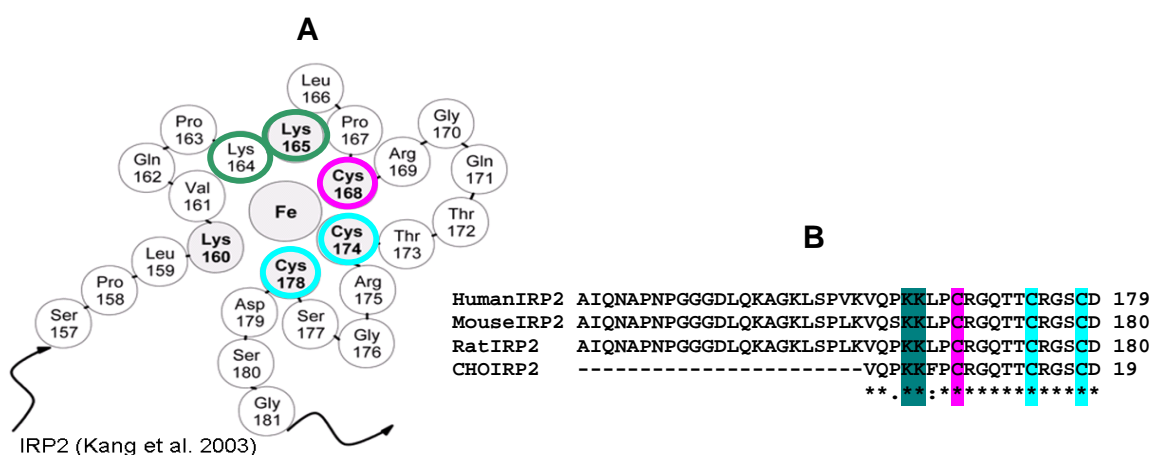


**Fig. 3.7 Functional significance of the characterised CHO-*Irp2* sequence**

Translation of CHO-*Irp2* gene sequence was carried out as described in legend of Fig. 3.5.

**A:** The encircled amino acids have been proposed to be involved in iron binding.

**B:** The proposed amino acids are conserved in the CHO proteome in the same relative position, as in other species. \* represents conserved amino acid between species.

### 3.3.3 CHO specific primers and preliminary real time PCR

The purpose of characterising gene sequences in the CHO cells was to enable gene expression analysis upon iron overdose and thus using the CHO cells as a model system to study iron regulation. To serve the purpose, CHO-specific primers were designed based on the characterised CHO gene sequences. While designing these primers the exon–exon boundaries in the human, mouse and rat genomes were taken into consideration; assuming that these boundaries would be similar in the hamster genome (appendices IX-XI). These CHO-specific primers were used to amplify the CHO cDNA to confirm their appropriateness for use in real time PCR (appendix XIII). The resultant CHO gene products obtained were sequenced to confirm sequence identity.

For the *Hfe* gene in CHO cells, three CHO-specific primers were designed, one forward and two reverse primers Hfe-for-CHO-Rx and Hfe-for-CHO-Ry. Both primer pairs yielded unique products of expected sizes (appendix X). The primer Hfe-for-CHO-Rx spans the exon-exon boundary in other species and therefore was initially considered appropriate for the real time PCR as it would eliminate the possibility of binding to DNA. However, the product size obtained with this primer (319 bp) was more than that recommended for an ideal real time PCR (<200 bp). Conversely, although the primer Hfe-for-CHO-Ry did not span exon-exon boundary, the product size formed (167 bp) is considered ideal for the real time PCR. Hence, despite formation of a single product of the expected size with both the reverse primers, the primer Hfe-for-CHO-Ry was used to amplify the CHO-*Hfe* gene.

On confirming gene identity, it was used in the subsequent standardisation of RT PCR (Fig. 3.8).

Selection of a reference gene is crucial for the analysis of real time PCR data. Ideally, the expression levels of the reference gene should stay relatively stable on exposure to different stimuli. However, many studies have observed fluctuations in the expression levels of these genes and also that this variability was species-, cell- and tissue-specific and at times was dependent on the experiment conditions (reviewed in Bahr et al., 2009).

In this context, Bahr et.al., (2009) validated the use of some reference genes for CHO cells. From this group, *beta actin*, that has been traditionally used as a reference gene and *pabpn1* gene were chosen for this study. The *pabpn1* gene encodes for a poly (A) binding protein which functions in the nucleus, unlike the actins which are found in the cytoplasm. The intention behind this selection was to normalise the genes of interest against two reference genes which function in different cell locations. This would improve the reliability of the real time PCR data.

On performing a PCR with the designed primers (Table 2.1) formation of unique products confirmed the appropriateness of the primers of reference genes (appendix XIV) and the designed CHO-specific primers for genes of interest (appendix XIII). Following this, a preliminary real time PCR was performed, as shown in Fig. 3.8, to confirm the uniqueness of products formed and the appropriateness of the designed primers.

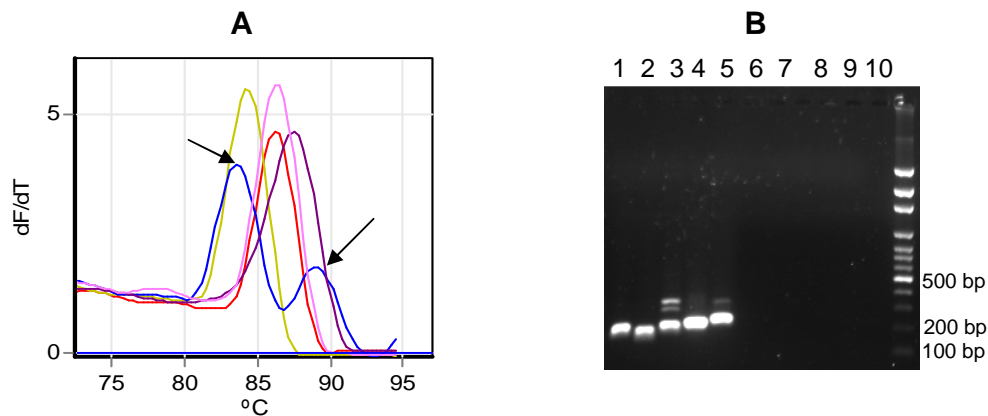


**Fig. 3.8 Preliminary real time PCR with CHO-specific primers**

CHO TRVb1 cDNA was probed with different primer pairs (Table. 2) in a real time PCR, as described in methods section 2.2.19.

**A:** Melt curve, shows formation of two peaks with the Irp2 primers Irp2-for CHO (F) and (R).

**B:** Amplicons from real time PCR, CHO TRVb1 cDNA and CHO specific primers electrophoresed on agarose gel.

Lane 1= Primers HFE for CHO (F) and (Ry); expected product size= 167 bp

Lane 2= Primers FPN for CHO (F) and (R); expected product size= 147 bp

Lane 3= Primers Irp2 for CHO (F) and (R); expected product size= 177 bp

Lane 4= Primers beta actin (F) and (R); expected product size= 187 bp

Lane 5= Primers pabpn1 (F) and (R); expected product size~200 bp

Lanes 6-10= negative controls with respective primers

As seen in Fig. 3.8, the melt curve (A) shows the presence of two peaks with the Irp2 primers. This suggested the formation of a non-specific product, as was confirmed by agarose gel electrophoresis of the real time PCR products ((B) lane 3). Thus the Irp2 primers required redesigning. Secondly, although the *pabpn1* primers showed single product formation in the melt cure (A), agarose gel electrophoresis revealed the presence of another product, as detected in (C) lane 5. Hence the *beta actin* gene product seen in (B) lane 4 was sequenced. On confirming its identity it was concluded that *beta actin* should be used as reference gene instead of *pabpn1* for further real PCR with CHO cells. The *Hfe* and *ferroportin* genes showed unique product formation, confirming their appropriateness for further real time PCRs.

Before performing gene expression analysis the amplification efficiencies of the genes are required to be determined to ensure that the efficiencies between the gene of interest and the reference gene closely match each other. Hence amplification efficiencies of *Hfe* and *beta actin* genes were determined, as shown in Fig. 3.9.

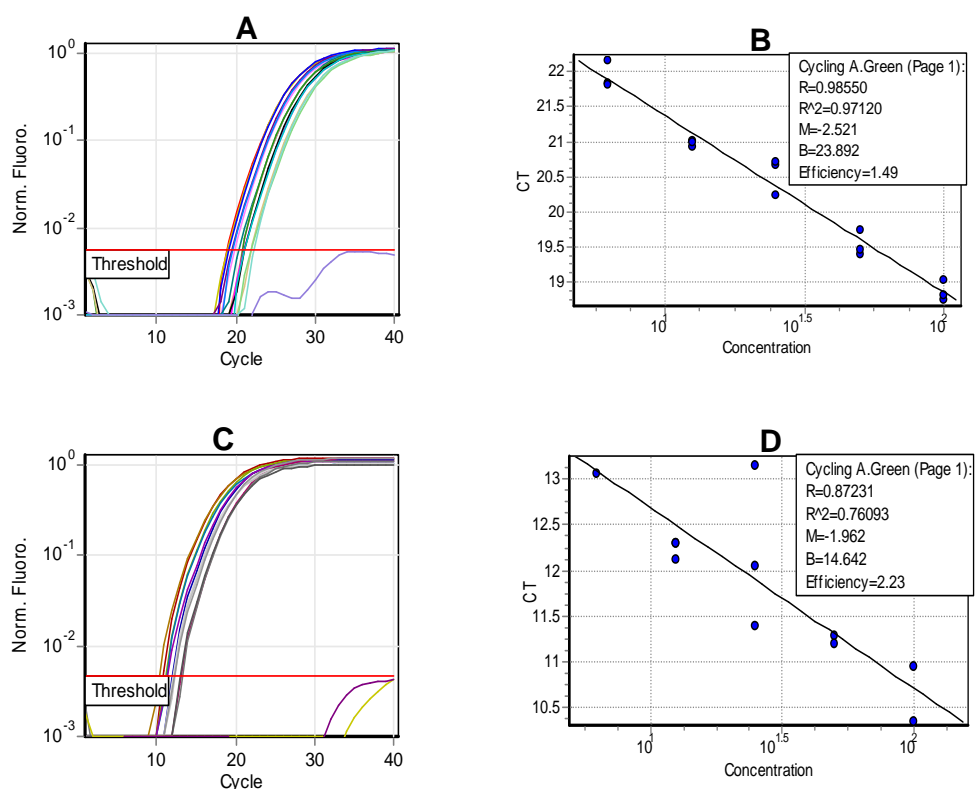


**Fig. 3.9 Standard dilution curves of *Hfe* and *beta actin* genes in CHO cells**

In order to check the amplification efficiencies of genes, serial dilution of CHO cDNA were prepared (1:2) and probed with respective primers of each gene, as described in methods section 2.2.19.

**A and C:** Fluorescence curves of *Hfe* and *beta actin* genes, respectively

**C and D:** Efficiency curves of *Hfe* and *beta actin* genes, respectively

### 3.3.4 *Hepcidin* gene sequencing in CHO cells

Partial sequencing of *ferroportin*, *Hfe* and *Irp2* genes in CHO cells was successful, as represented by Fig. 3.4. Comparisons between characterised CHO genes and corresponding genes in human, rat and mouse showed that there is high degree of genomic similarity between these species (Table 3.1). Using the same approach, attempts were made to obtain the *hepcidin* gene sequence in CHO cells.

Accordingly, conserved nucleotides on *hepcidin* mRNA alignment between mouse and rat (appendix XII), were identified and hepcidin primers (F) and (R) were designed. PCRs with these primers and CHO DNA could not yield a unique product at any of the annealing temperatures (appendix XIII). Hence, a new reverse primer R1a was designed which allowed more flexibility in binding the template than the previous reverse primer and a combination of hepcidin F and R1a was probed with the CHO DNA (Fig. 3.10). As previously observed, this combination of primers also resulted in multiple products.

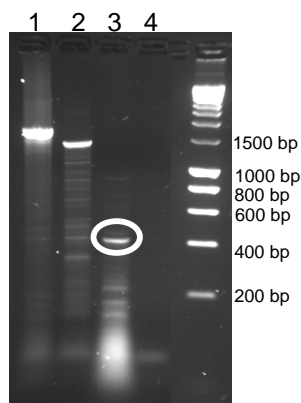


**Fig. 3.10 Amplicons of CHO genome obtained with hepcidin primers (F) and (R1a)**

DNA was extracted as described in methods section 2.2.5 and amplified with hepcidin primers, as listed in Table. 2. Lane 1 = rat liver DNA; lane 2 = mouse liver DNA, expected size of products for lanes 1 and 2 ~1500bp. Lane 3=CHO TRVb1 DNA, Lane 4 = negative control

The encircled predominant product of ~400 bp (lane 3) was gel purified and sent for sequencing. However the sequence of this product could not be obtained.

### 3.3.4.1 Magnesium chloride gradient PCR

To facilitate sequencing, a new forward primer hepcidin F1 was designed and used in combination with primer R1a. This combination showed the presence of two prominent products (Fig. 3.11, lane 1) of sizes ~1000 bp and 500 bp. In order to increase specificity of product formation and reduce non-specific binding of primers, a magnesium chloride gradient PCR was performed, ranging from 1.5 mM to 4 mM.

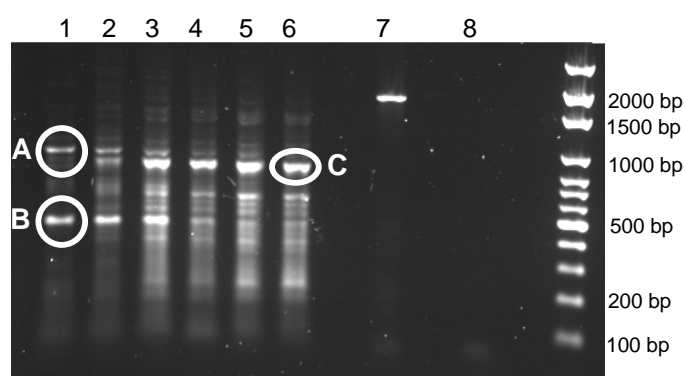


**Fig. 3.11 Amplicons of CHO DNA under  $MgCl_2$  gradient using hepcidin primers (F1) and (R1a)**

Increased specificity of product formation was obtained (as per methods section 2.2.9) when a series of PCR reactions were set up with increasing concentrations of  $MgCl_2$ . Encircled products were gel purified and sent for sequencing (as described in methods section 2.2.12). Lanes 1 to 6 = 1.5 mM, 2 mM, 2.5 mM, 3 mM, 3.5 mM and 4 mM  $MgCl_2$ , respectively. Lane 7 = rat liver DNA (1.5mM  $MgCl_2$ ), expected product size ~1500 bp. Lane 8 = negative control

It was observed that as the concentration of magnesium chloride increased, products A and B, seen in Fig. 3.11, lane 1, could not be formed and instead, two other products of sizes ~ 900 bp and 700 bp increased in intensity. Gel purification of these predominant products A, B and C followed by sequencing could not yield the sequence of any of these products. Thus increasing magnesium chloride concentration could not help the purpose of obtaining *hepcidin* gene sequence.

### 3.3.4.2 Amplification of amplicon to increase product yield

It was observed that one of the reasons for not acquiring the *hepcidin* gene sequence was the inability of primers to yield products in large amounts. Hence to increase product yield and facilitate sequencing, PCR products were reused as templates in subsequent PCRs. Thus products A and B observed in Fig. 3.11 were gel purified and used as templates in PCRs (Fig. 3.12-X).

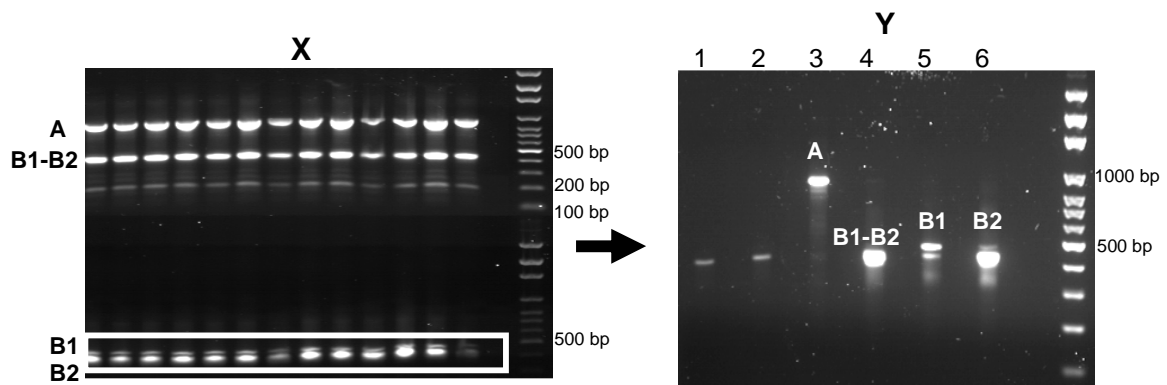


**Fig. 3.12 Amplification of amplicon to increase product yield**

The PCR products obtained from the 1<sup>st</sup> round of amplification were used as templates in the 2<sup>nd</sup> round of PCR to increase product yield. Purified products of each lane were sent for sequencing as described in methods section 2.2.12.

**X:** Amplicons of CHO TRVb1 DNA obtained using hepcidin primers F1 and R1a

Product A was obtained when gel extracted band A, seen in Fig 27, was used as template. Products B1-B2 were obtained when gel extracted band B, seen in Fig 27 was used as a template.

**Y:** Confirmation of presence of product before sequencing

Lane 1 = CHO TRVb1 DNA; lane 2= Wt CHO DNA;

lanes 3,4,5,6 = gel purified products of A, B1-B2, B1 and B2, respectively.

Gel electrophoresis of the products on 2 % agarose gel (Fig. 3.12X, boxed) identified the presence of a double band B1-B2. Products A, B1-B2, B1 and B2 were gel purified and electrophoresed (Fig. 3.12Y) before sequencing to confirm the presence of products. However, sequences of none of these products could be obtained. The reason for sequencing problems with the dual product segment B1-B2 could be attributed to multiple priming as these products had very similar sizes.

### 3.3.4.3 Cloning of DNA fragment

Since the size of the products B1 and B2 were similar to the size of the predominant product observed in Fig. 3.10 (lane 3) and Fig. 3.11 (lane 1), it was decided to sequence the products B1 and B2 first, followed later by sequencing the product A. The products B1 and B2 were closely spaced on the gel due to similarity in sizes. Hence to separate the products B1 and B2 and then sequence these, the product segment B1-B2 was gel purified and cloned into a pGEM-T easy vector system. This was followed by transformation into competent *E.coli* XL-1 Blue cells. The recombinant plasmids were extracted, purified and amplified using the designed hepcidin primers and vector primers.

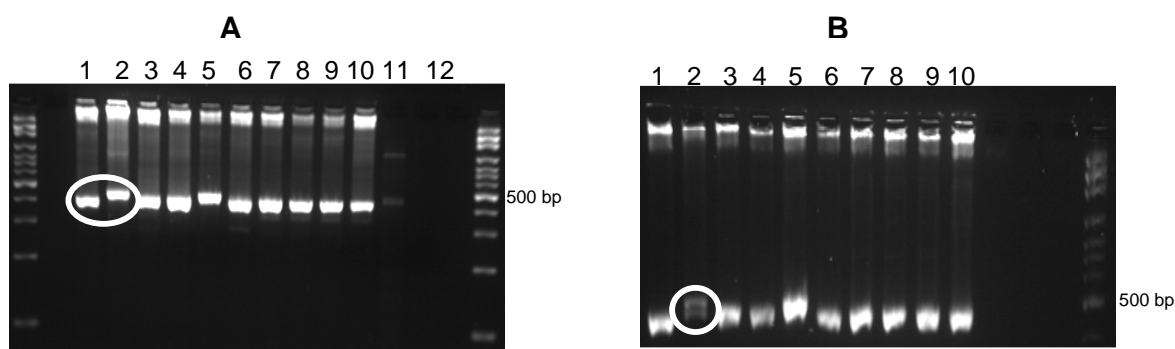


**Fig. 3.13 Amplification of cloned plasmids**

The dual segment product B1-B1 seen in Fig. 3.12 was gel purified and cloned into pGEM-T Easy vector system as described in methods section 2.2.11. The yield of plasmid was increased by transformation of the recombinant plasmid into *E.coli* XL-1 Blue cells. Plasmids were purified from selected colonies of recombinant cells and amplified with hepcidin and vector primers as shown in the figure. Encircled products were gel purified and sent for sequencing as described in methods section 2.2.12.

**A:** Amplicons of cloned plasmids obtained using hepcidin primers F1 and R1a  
Lanes 1 to 10 = Amplicons of 10 random recombinant plasmids obtained from 10 different recombinant colonies. Expected size of products = ~ 450 bp. Lane 11 = Wt CHO DNA.  
Lane 12 = negative control.

**B:** Amplicons of cloned plasmids obtained using pGEM-T easy vector primers pGEM-T easy forward and reverse. Expected size of products = ~ 450 bp including the vector sequence.

Fig. 3.13A shows that separation of the products B1 and B2 was successful via cloning, as indicated by the presence of two distinct bands of different sizes (encircled in Fig. 3.13A, lanes 1 and 2). Sequencing of the product in lane 1 was successful. Although the sequence did not match the *hepcidin* gene sequence, 5 % coverage of the characterised sequence matched a DNA binding protein in rat, as shown below.

```

CHO sequence characterised (5% coverage)      78 AATCACTAGTGAATTCGCGGCCG 400
                                             |||
[Rattus norvegicus]GENE_ID:64470 Ddb1       3769 AATCACTAGTGAATTCGCGGCCG 3791
Damage-specific DNA binding protein-1

```

This suggests a potential role of this sequence in entering the nucleus to bind DNA. The other product seen in Fig. 3.13A lane 2, could not be sequenced, possibly because it still comprised two products, as seen in Fig. 3.13B, lane 2.

#### 3.3.4.4 Reverse primers with unique *hepcidin* specificity

To improve the specificity of primer binding and encourage unique product formation, a new reverse primer, *hepcidin* R1b was designed, part of which indicated unique specificity for *hepcidin* gene at the NCBI-*blastn*. PCR conditions were optimised with *hepcidin* primer pairs F1 and R1b (appendix XIII). Results showed formation of diffused products in minimal amounts, which could be due to the degeneracy of the reverse primer. As this primer pair did not give a unique product, this combination of primers was not used any further.

### 3.3.4.5 Primer specificity

Since attempts made so far could not yield the *hepcidin* gene sequence and the primers F1 and R1a resulted in multiple products (Fig. 3.11 and Fig. 3.12), the specificity of the primers was checked by using only one of the primers of the primer pair in separate PCR reactions, i.e. using only the forward primer F1 and only the reverse primer R1a for amplification, as shown in Fig. 3.14A. This should not yield products.

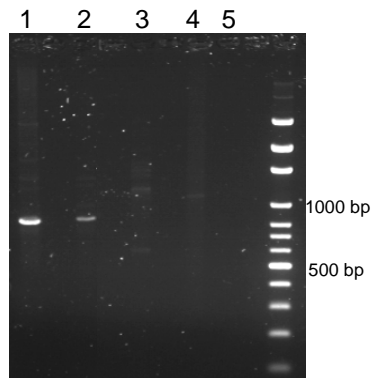


**Fig. 3.14 A Amplification of CHO DNA with only the forward primer F1**

Lane 1 = Wt CHO DNA  
Lane 2 = CHO TRVb1 DNA  
Lane 3 = rat liver DNA  
Lane 4 = mouse liver DNA  
Lane 5 = negative control

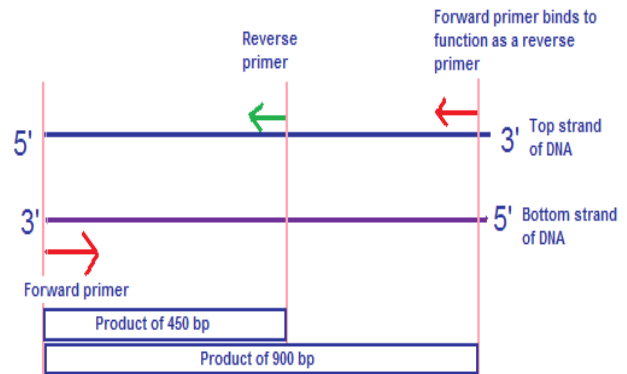


**Fig. 3.14 B Probable position of binding of forward primer F1, to function as a reverse primer**

Amplification of CHO DNA using only the forward primer resulted in a product of ~ 900 bp (Fig. 3.14A, lane 1). This suggested that the forward primer also functioned as a reverse primer by binding to a region in CHO DNA ~ 900 bp away from where it was originally designed to bind. This region could be within an intron and would be complementary and reverse of a section of the top DNA strand, as explained through Fig. 3.14B. Hence it was concluded that this was the product “A” seen in figures 3.11 and 3.12 and that this was a non-specific product and should

not be sequenced. Thus, the forward primer required to be redesigned. On using only the reverse primer, no product was observed (results not shown for brevity).

### 3.3.4.6 Hepcidin primers for other species

Previously it was seen that the hamster genomes bears high genomic similarities with the genomes of human, mouse and rat (Tables 3.1 and 3.2). Hence published hepcidin primers used for these species (Table 2.2) were used to amplify the unknown CHO-hepcidin gene (Fig. 3.15). The resultant PCR products were electrophoresed on 2 % agarose gels to facilitate the separation of any closely-sized products. It was observed that amplification of CHO DNA with mouse hepcidin-1 primers (A), rat hepcidin primers-x (A) and rat hepcidin primers-y (B), resulted in either no product or non-specific products. Also, human hepcidin primers (C) showed non-specific product formation with the CHO DNA.

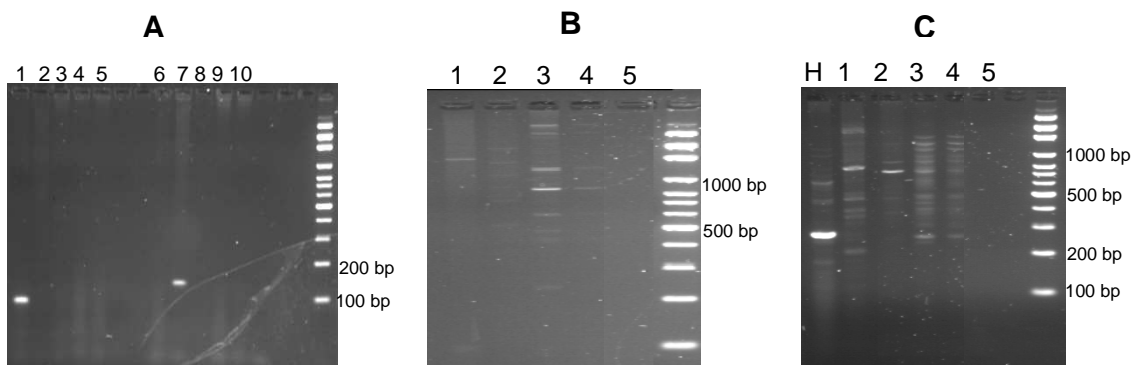


**Fig. 3.15 Amplification of CHO genome with hepcidin primers used for other species**  
**A:** Amplicons of CHO DNA obtained with rat hepcidin primers (x) and mouse hepcidin-1 primers  
 Lanes 1-5 = Products obtained with rat hepcidin primers (x)  
 Lanes 6-10 = Products obtained with mouse hepcidin-1 primers  
 Expected product size of lane 1 (rat Liver DNA) = 95 bp  
 Expected product size of lane 7 (mouse liver DNA) = 120 bp  
**B:** Amplicons obtained with rat hepcidin primers (y)  
 Expected product size of lane 1 (rat Liver DNA) = 95 bp  
**C:** Amplicons obtained with human hepcidin primers FF and RR  
 Lane H = HepG2 DNA, expected product size = 300 bp  
 In all figures:  
 Lanes 1,6 = rat liver DNA; Lanes 2,7 = mouse liver DNA; Lanes 3,8 = WT CHO DNA;  
 Lanes 4,9 = CHO TRVb1 DNA; Lanes 5,10= negative control.

Since the amplification of CHO DNA using mouse, rat and human hepcidin primers did not yield a specific product within the CHO genome (Fig. 3.15) and also due to the non-specificity of the forward hepcidin primer (Fig. 3.14), new hepcidin primers were designed based on conserved nucleotides between hepcidin transcripts of mouse, rat and human (appendix XII). One forward (F2) and two reverse primers (R2a and R2b) were designed and used to amplify CHO DNA. PCR products were electrophoresed on a 3 % agarose gel to enable separation of any closely sized products (Fig. 3.16).

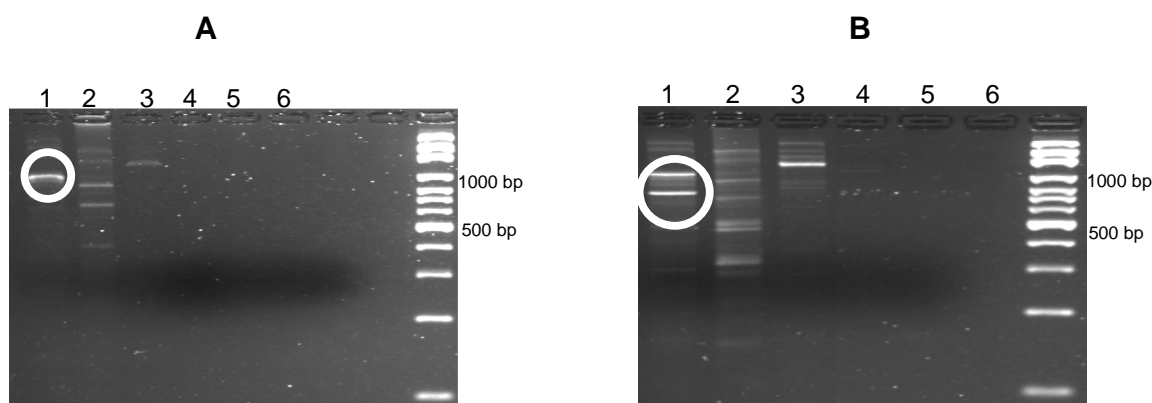


**Fig. 3.16 Amplification of CHO genome with hepcidin primers designed on human transcript**  
 Since primers designed based on conserved regions between mouse and rat *hepcidin* could not characterise CHO-*hepcidin*, primers were redesigned based on conserved regions between the human, mouse and rat *hepcidin* transcript alignment. The CHO genome was amplified with these primers.

**A:** Amplicons obtained using hepcidin primers F2 and R2a

**B:** Amplicons obtained using hepcidin primers F2 and R2b

Lane 1 = WT CHO DNA; Lane 2 = rat liver DNA; Lane 3 = HepG2 DNA;

Lane 4 = WT CHO DNA with only forward primer; Lane 5 = WT CHO DNA with only reverse primer;

Lane 6 = negative control. Expected sizes of products in lane 2 and 3 ~1400 bp

Here the reverse primer R2a yielded one prominent product (Fig. 3.16A, lane 1) whereas reverse primer R2b yielded two products (Fig. 3.16B, lane 1). Hence it was concluded that the hepcidin primer pair F2 and R2a was more specific and was used in subsequent PCRs.

### 3.3.4.7 cDNA usage for sequencing

So far in this study, sequencing the *hepcidin* gene using the DNA had presented various challenges. Thus, although the approach used to sequence *hepcidin* mRNA (cDNA) was more expensive, it was concluded that this would be more fruitful than sequencing *hepcidin* DNA. Accordingly, Wt CHO cDNA was amplified with hepcidin primers F2 and R2a.

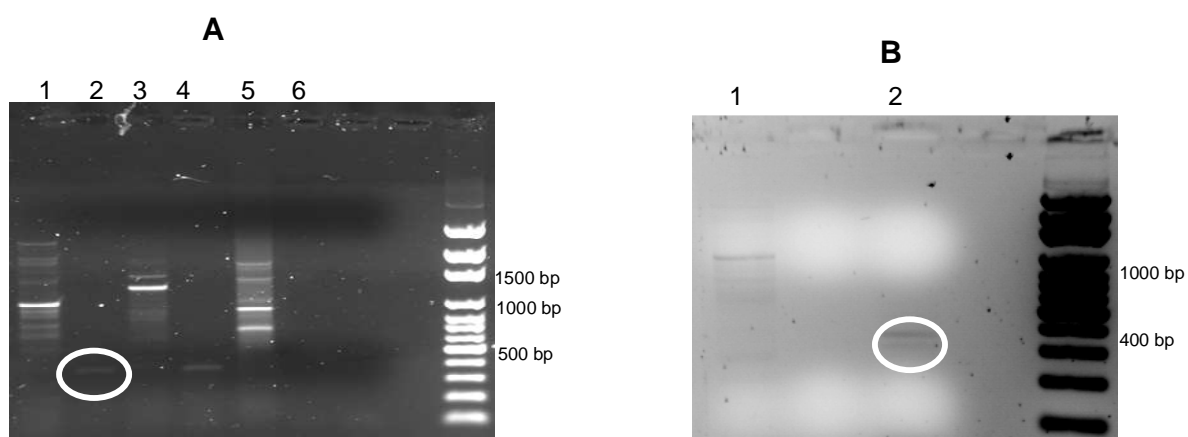


**Fig. 3.17 Amplicon of Wt CHO cDNA obtained with hepcidin primers F2 and R2a**

CHO cDNA amplified with selected hepcidin primer pair is shown in the figure. The encircled product was sent for sequencing as described in methods section 2.2.12.

**A:** Lane 1 = WT CHO DNA; lane 2 = WT CHO cDNA; lane 3 = HepG2 DNA;  
Lane 4= HepG2 cDNA; Lane 5= rat liver DNA (expected size ~1400 bp); lane 6= negative control  
**B:** Purified WT CHO cDNA before sequencing.  
Lane 1 = WT CHO DNA; lane 2 = WT CHO cDNA

As seen in the Fig. 3.17A, lane 2, the Wt CHO cDNA yielded a product of ~ 400 bp, similar to the product observed in figures 3.10-3.13. Hence multiple tubes of reaction in lane 2 were set up. Before sequencing, the presence of the product was confirmed (Fig. 3.17B, lane 2). However, sequence of the purified product could not be obtained, possibly because of two closely sized products (Fig. 3.17B, lane 2). This suggested that cloning the cDNA products and then sequencing would be an alternative strategy.

### 3.3.4.8 Cloning of cDNA fragment

The cDNA product (Fig. 3.17B, lane 2) was cloned into the pGEM-T easy vector system. The recombinant plasmids containing Wt CHO cDNA were amplified with vector primers and hepcidin primers (Fig. 3.18).

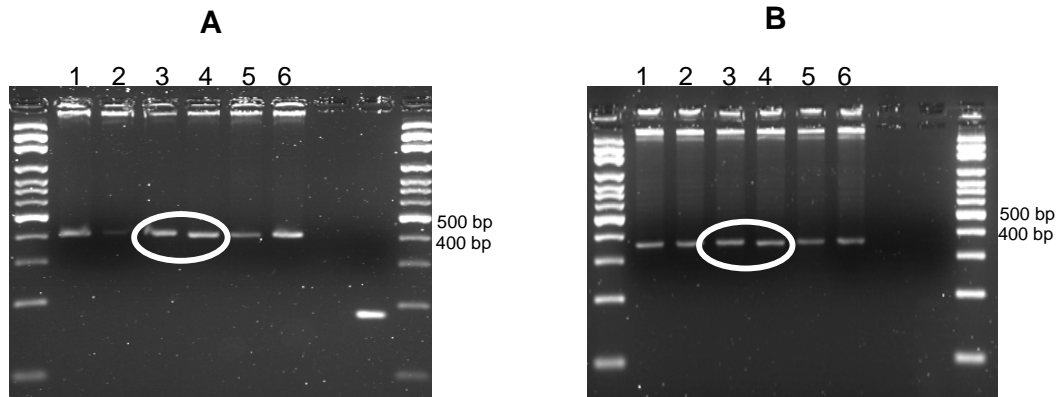


**Fig. 3.18 Amplification of cloned Wt CHO cDNA**

With the aim of sequencing *hepcidin* mRNA in the CHO cells, the cDNA from Wt CHO cells was synthesised as described in methods section 2.2.18 and amplified with vector and hepcidin primers, as shown in the above figure.

**A:** Amplicons of cloned plasmids obtained on using pGEM-T easy vector primers, pGEM- T easy forward and reverse.

**B:** Amplicons of cloned plasmids obtained on using hepcidin primers F2 and R2a.

Expected size of products ~ 450 bp, including the vector sequence

Lanes 1 to 6 = Amplicons of 6 different recombinant plasmids obtained from 6 different recombinant colonies.

Fig. 3.18A (lanes 3 and 4) showed products of different sizes indicating that the two products seen in Fig. 3.17B had been successfully separated via cloning. The encircled product in Fig. 3.18A was gel purified and sequenced with vector primers. However, instead of the expected *hepcidin* sequence, the characterised sequence matched a section of RNA splicing factor 3a, as shown in table 3.3.

NCBI Accession	Description	Query coverage	Max identity
XM_003502240.1	PREDICTED: <i>Cricetulus griseus</i> splicing factor 3a,	99%	100%
BC092058.1	<i>Mus musculus</i> splicing factor 3a, subunit 3	99%	95%
NM_001025698.1	<i>Rattus norvegicus</i> splicing factor 3a, subunit 3	97%	95%
BC011523.1	<i>Homo sapiens</i> splicing factor 3a, subunit 3	97%	89%

**Table 3.3 Sequence similarities between the characterised CHO sequence and other species**

Since the gene sequence of *hepcidin* in the CHO cells could not be characterised, gene expression analysis of *hepcidin* upon iron exposure was hampered. Hence studies apart from gene expression analysis were conducted which focussed on the iron uptake mechanisms and the consequent effect on hepcidin peptide production by the CHO TRVb1 cells. These studies included confirmation of human TfR1 at mRNA and protein levels under steady state conditions followed by analysis of cell surface TfR1, intracellular iron levels and finally measurements of hepcidin peptide levels upon iron overdose to cells.

### 3.3.5 TfR1 transcript status in CHO TRVb1 cells

The presence of human TfR1 at mRNA level in the CHO TRVb1 cells under steady state conditions was checked, as shown in Fig. 3.19.

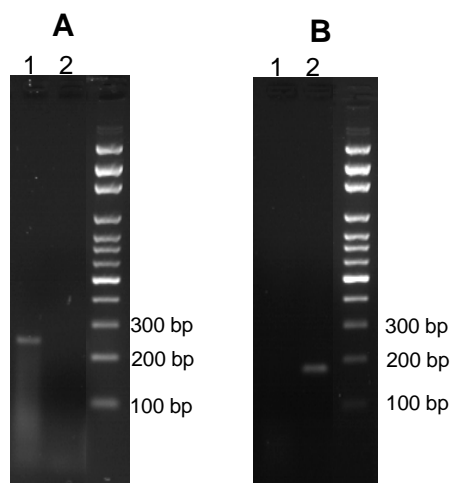


**Fig. 3.19 Amplicons of *TfR1* transcript in CHO cells**

cDNA from CHO TRVb1 and Wt CHO cells was extracted and amplified as described in methods sections 2.2.18 and 2.2.8, respectively, using the CHO-endogenous and human-TfR1 primers (Table 2.1).

**A:** Amplicons obtained on using CHO-endogenous TfR1 primers

Lane 1= Wt CHO cDNA; expected size of product= 230 bp (appendix XV)

Lane 2= CHO TRVb1 cDNA; no expected product

**B:** Amplicons obtained on using human TfR1 primers

Lane 1= Wt CHO cDNA; no expected product

Lane 2= CHO TRVb1 cDNA; expected product size= 179 bp (appendix XV)

As seen in Fig. 3.19A (lane 1), the CHO-endogenous *TfR1* transcript was amplified by CHO-specific TfR1 primers whereas CHO TRVb1 cDNA in lane 2 showed the absence of the CHO-endogenous *TfR1* transcript. Likewise, human TfR1 primers were unable to form a product with the Wt CHO cDNA, but successfully formed a product with CHO TRVb1 cDNA, as expected (Fig. 3.19B). Together this confirmed the presence of human *TfR1* mRNA and the absence of CHO-endogenous *TfR1* mRNA in the CHO TRVb1 cells.

### 3.3.6 TfR1 protein status in CHO TRVb1 cells

The status of TfR1 protein in the CHO TRVb1 cells under steady state conditions was checked, as shown in Fig. 3.20.

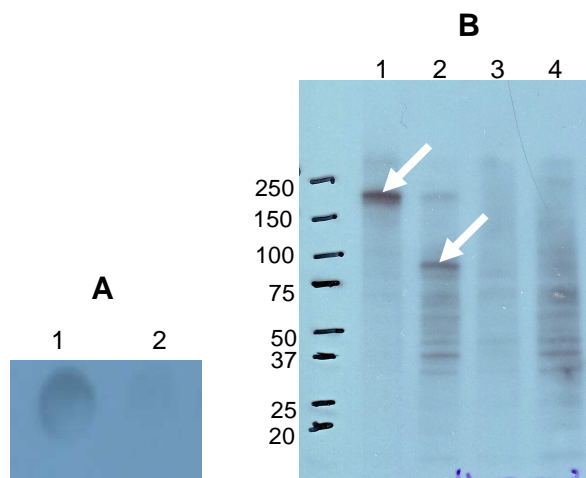


**Fig. 3.20 TfR1 protein expression in CHO TRVb1 cells**

CHO TRVb1 cells were grown in maintenance medium and the cell pellet was probed with human TfR1 antibody, as described in methods section 2.2.21.

**A** : Dot blot detected human TfR1 protein in CHO TRVb1 cells

Lane 1= Cell extract of CHO TRVb1 cells

Lane 2= Cell extract of Wt CHO cells

**B** : Western blot detected humanTfR1 protein in CHO TRVb1 cells

Lane 1= CHO TRVb1 cells under non reducing conditions

Lane 2= CHO TRVb1 cells under reducing conditions

Lane 3= Wt CHO cells under non reducing conditions

Lane 4= Wt CHO cells under reducing conditions

The marker is in kDa.

The CHO TRVb1 cells expressed human TfR1 protein, as seen by the dot blot in Fig. 3.20A (lane 1) and Western blot in Fig. 3.20B (lanes 1 and 2). Here, under non-reducing conditions human TfR1 protein showed a prominent band of approximately 180 kDa (Fig. 3.20B, lane 1), and under reducing conditions a band of smaller size, approximately 85-90 kDa was observed (Fig. 3.20B, lane 2), as previously shown by Turkewitz et al. (1988). No human TfR1 protein was detected in Wt CHO cells. This confirmed the suitability of CHO TRVb1 cells for iron-related experiments upon holotransferrin treatment as required to be conducted in this study.

### **3.3.7 Iron overdose and CHO TRVb1 cells**

The CHO TRVb1 cells were treated with holotransferrin (5 g/L) and the resultant effect of treatment on cell surface expression of TfR1 is shown in Fig. 3.21. Here, Wt HepG2 cells, which express the endogenous TfR1 of human origin, were also treated simultaneously and the effect on the two cell types were compared. Each treatment undergone by the CHO TRVB1 cells is represented by figures 3.21 (A), (B) and (C). It was observed that under steady state conditions i.e. in the maintenance medium, CHO TRVb1 cells express approximately twice the levels of TfR1 protein on the cell surface than the Wt HepG2 cells (Fig. 3.21D). Iron overdose for a period of 48 h caused a significant gradual decrease ( $p < 0.03$ ) in surface expression of TfR1 in the Wt HepG2 cells, whereas the CHO TRVb1 cells showed constant levels of cell-surface TfR1 (Fig. 3.21E). This implied that CHO TRVb1 cells not only displayed higher levels of TfR1 than the Wt HepG2 cells under basal conditions but also under iron overload.

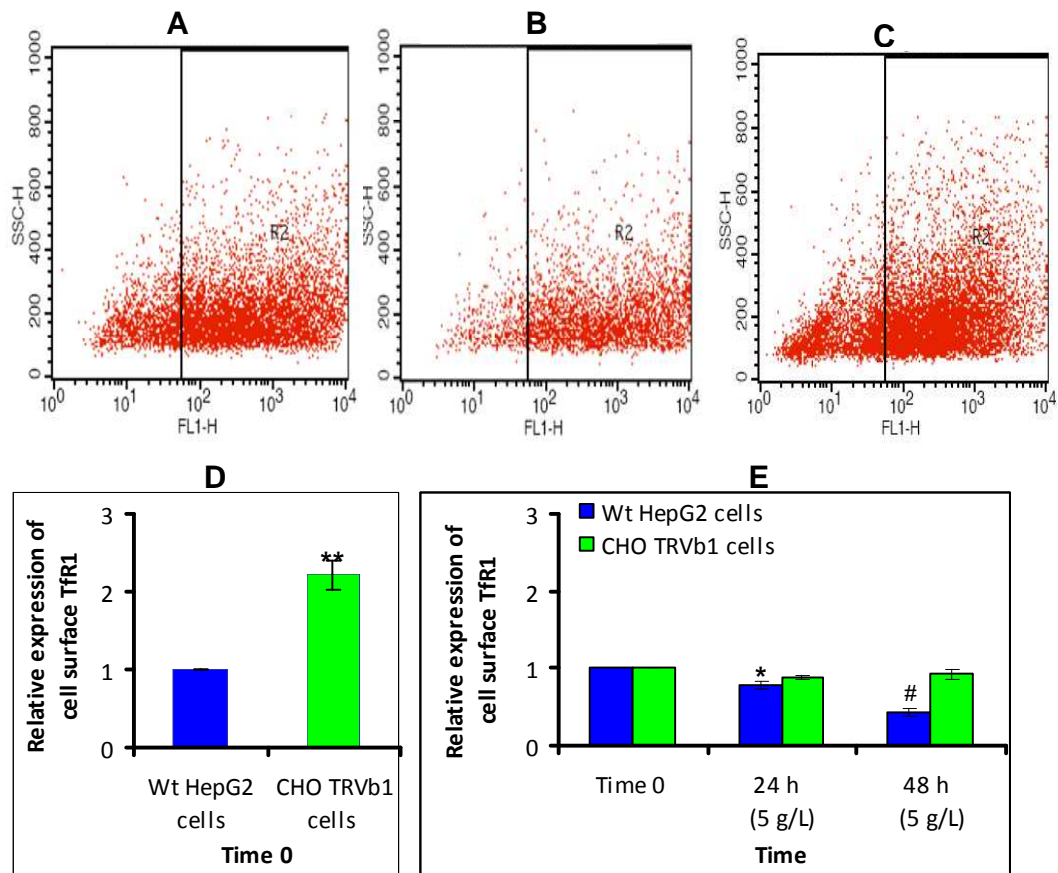


**Fig. 3.21 Tfr1 response of CHO TRVb1 cells on iron overload**

CHO TRVb1 and Wt HepG2 cells were treated with 5 g/L holotransferrin and analysed for cell-surface Tfr1 by flow cytometry as described in methods sections 2.2.15 and 2.2.20, respectively. Flow cytometry images of CHO TRVb1 cells before treatment i.e. time 0 (A) and after holotransferrin treatment for 24 h (B) and 48 h (C) are shown.

D : Cell-surface Tfr1 under steady state conditions (maintenance medium).

E : Cell-surface Tfr1 after 5 g/L holotransferrin treatment.

Time 0 represent cells under steady state conditions.

Data is presented as mean  $\pm$  SEM (n=3).

\*  $p < 0.03$  compared to time 0, \*\*  $p < 0.01$ , #  $p < 0.03$  compared to 24 h.

Under the same experimental conditions, hepcidin peptide levels in the treatment medium were measured. Data revealed that the CHO TRVb1 cells increased the production of hepcidin peptide with an increase in extracellular holotransferrin levels over time (Fig. 3.22). Iron overdose for 24 h significantly induced an approximately 4-fold increase in hepcidin peptide production and increased by approximately 7-fold after 48 h ( $p < 0.01$ ).

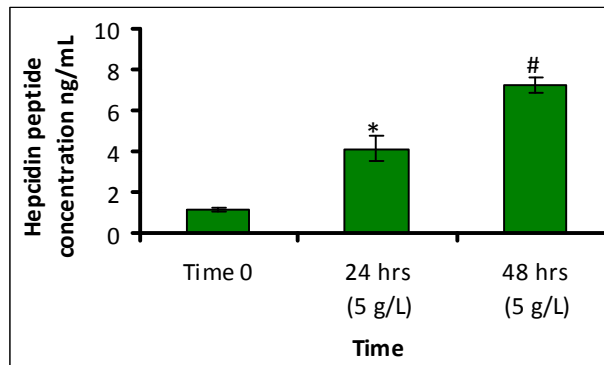


**Fig. 3.22 Holotransferrin overdose and hepcidin peptide production by CHO TRVb1 cells**

CHO TRVb1 cells were treated with holotransferrin overdose and hepcidin peptides secreted into the medium after treatment were measured as described in methods section 2.2.22.

Time 0 represent cells under steady state conditions i.e. in maintenance medium. Data is presented as mean  $\pm$  SEM (n=3). \* p<0.01 compared to time 0, # p<0.01 compared to 24 h.

To further understand hepcidin peptide production by the CHO TRVb1 cells within a shorter time exposure to iron overdose, cells were treated with 5 g/L holotransferrin for up to 4 h. To ensure that the cells received the planned overdose, iron levels in the treatment media were determined (Fig. 3.23).

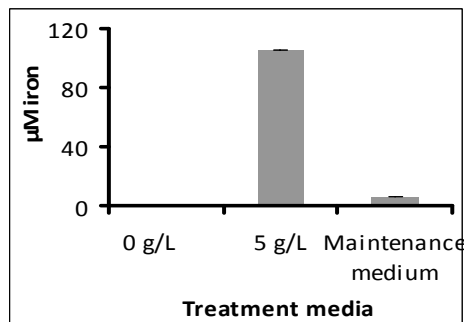


**Fig. 3.23 Iron content in CHO TRVb1 treatment media**

Iron levels in the media used to treat the CHO TRVb1 cells were measured by the ferrozine assay as described in methods section 2.2.17.1. 0 g/L represents serum-free and holotransferrin-free maintenance medium whereas 5 g/L represents serum-free maintenance medium supplemented with 5 g/L holotransferrin. Data is presented as mean  $\pm$  SEM (n=3).

The effect of holotransferrin treatment on cell viability was studied using the MTT assay. Results showed that iron overdose in the form of 5 g/L holotransferrin for a period of 4 h reduced cell viability by approximately 10-15 %, as compared to the untreated controls (Fig. 3.24). However, the data also showed that cell viability was approximately 30 % higher in a medium deprived of FCS and iron (0 g/L) than the maintenance medium (10%FCS).

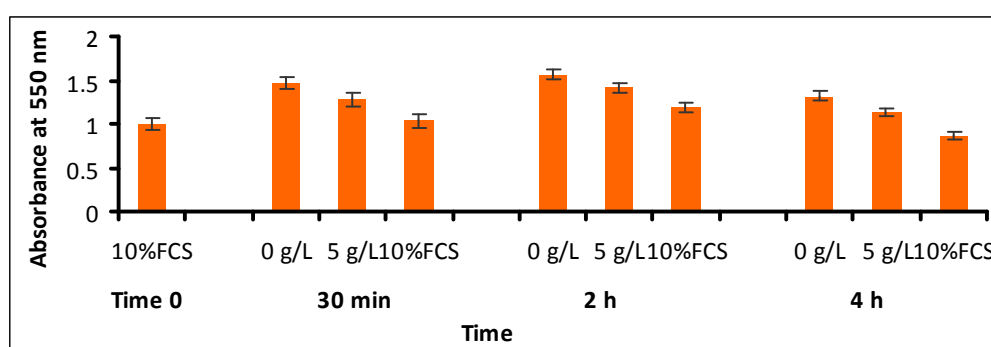


**Fig. 3.24 Viability studies in CHO TRVb1 cells**

CHO TRVb1 cells were treated with 5 g/L holotransferrin and the viability of the cells was studied by MTT assay as described in methods sections 2.2.15 and 2.2.16, respectively. 10%FCS represent cells in maintenance medium. Data is presented as mean  $\pm$ SEM (n=3).

Following holotransferrin treatments it was observed that there was no significant increase in intracellular iron content in the CHO TRVb1 cells; levels generally remained constant under serum deprivation and maintenance medium (Fig. 3.25).

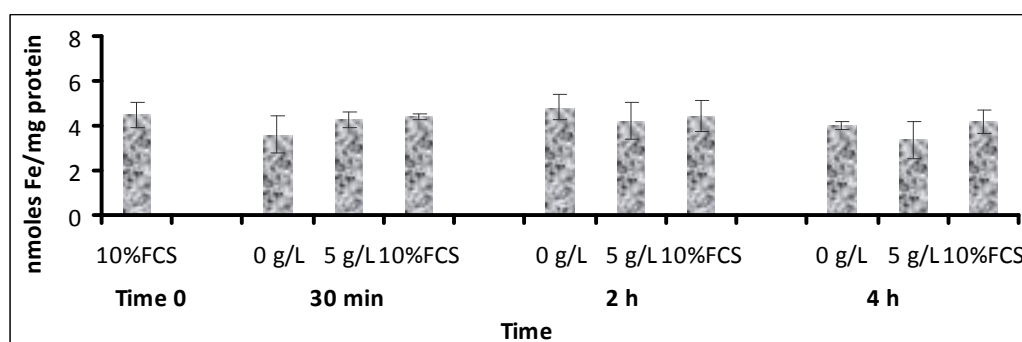


**Fig. 3.25 Intracellular iron levels in CHO TRVb1 cells upon iron supplementation**

CHO TRVb1 cells were treated with 5 g/L holotransferrin up to 4 h. Intracellular iron levels were determined by ferrozine assay as described in methods section 2.2.17 and shown in the figure. 10% FCS represent normal maintenance medium. Data is presented as mean  $\pm$ SEM (n=3).

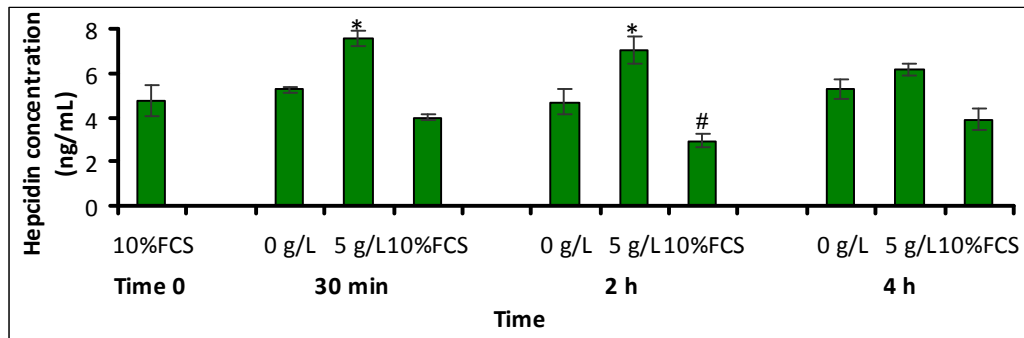


**Fig. 3.26 Hepcidin peptide secretion by CHO TRVb1 cells upon iron supplementation**  
 CHO TRVb1 cells were treated with 5 g/L holotransferrin up to 4 h. Hepcidin peptides released at various time points after treatment were measured as described in section 2.2.22 and shown in the figure. 10% FCS represent normal maintenance medium. Data is presented as mean  $\pm$  SEM (n=3). \*  $p < 0.03$  compared to the untreated controls at respective time points. #  $p < 0.03$  compared to hepcidin released at 30 min when in maintenance medium.

When in the maintenance medium, the CHO TRVb1 cells released constant levels of bioactive hepcidin up to 4 h (Fig. 3.26). A slight but significant decrease in hepcidin levels ( $p < 0.03$ ) was observed after 2 h, however, after 4 h hepcidin levels increased to those detected at time 0 and 30 min. Compared to the untreated control 0 g/L, hepcidin peptide production significantly increased upon holotransferrin overdose after 30 min and 2 h ( $p < 0.03$ ), although it appeared that the effect of holotransferrin gradually decreased with time. Serum and iron deprivation did not significantly decrease hepcidin production over the 4 h treatment period.

### 3.4 Discussion

Chinese hamster ovary cells have been used over the last 20 years in the biopharmaceutical industry for the production of therapeutic recombinant proteins for human use (reviewed in Bahr et al., 2009). Successful productions of such proteins include those offered for rheumatoid arthritis, colorectal cancer and

anaemia, as reviewed in Warner, (1999). The CHO TRVb1 cells are unique in that they are devoid of the endogenous hamster TfR1, and additionally over-express the human TfR1 (McGraw et al., 1987). Due to this characteristic these cells can be of immense use for iron-related studies and eventually can be valuable in the biopharmaceutical industry. In the present work, studies were conducted to understand iron-related responses exhibited by the CHO TRVb1 cells.

Previous studies relating to *hepcidin* gene expression following iron overdose to cell lines have given inconsistent results, primarily due to the lack of a suitable cell model for iron overdose experiments. This issue has been addressed in this study by using the CHO TRVb1 cells. Since the CHO TRVb1 cells over-express the human TfR1 (McGraw *et al.*, 1987), it was hypothesised that this characteristic should enable the cells to take up large amounts of iron via holotransferrin and the resultant effects on cells could be examined.

Accordingly, an objective of this project was to study the effect of iron overdose via holotransferrin on the expression of iron-related genes, particularly *hepcidin*. However, many iron-related genes in the hamster have not been characterised yet and this limits experimental work with this cell line. If the gene sequence information was known, then this would aid in expression analyses of genes via real time PCR. This, along with the fact that the CHO cells are easy to transfect and widely used, it would then be possible to establish the CHO TRVb1 cells as a model system to study iron regulation.

In order to characterise the unknown sequences of genes of interest, the concept of genome similarities between species was exploited. It was seen that the hamster, being a rodent, bore genomic similarities with the human, mouse and rat genomes (Table 3.1). Hence, primers were designed based on conserved nucleotides between the human, mouse and rat genomes. These were used to amplify the CHO DNA and the PCR products obtained were sequenced. The partially characterised CHO sequences of genes *ferroportin*, *Hfe* and *Irp2* showed high similarity with the corresponding pre-characterised gene sequences in the database (Table 3.2). This reconfirmed that indeed the hamster genome resembled the human, mouse and rat genomes. Also, the sizes of the CHO-gene products were very similar to gene products of the rat and mouse. For example, as seen in Fig. 3.4, in case of *Hfe*, *Irp2* and *ferroportin* genes, the size of the CHO-gene product was very similar to those of the rat liver DNA and mouse kidney cDNA. This suggests similarity in exon sizes and a probable similarity in exon-intron boundaries between the three species.

Since the objective behind sequencing iron-related genes in CHO cells was to perform gene expression studies through real time PCR, ideally the cDNA would have been a better choice to perform the preliminary PCRs. However the cDNA was not chosen because the basal mRNA levels of some genes may be low and hence it would be difficult to observe a product on the gel using the cDNA. In contrast, performing a PCR with DNA and visualising the product on the gel would at least confirm the presence of the gene and also indicate its probable size in the previously uncharacterised CHO cells. Secondly, PCR optimisations with cDNA

would be more expensive than using the DNA. An additional factor is the labile nature of RNA. Since RNA has a higher rate of degradation than the DNA, it is more difficult to optimise conditions with cDNA than with DNA.

In order to optimise PCR conditions, temperature gradient PCRs were performed with all the designed primers (appendix XIII). This helped to identify the most appropriate annealing temperature which would give unique products and following this, all subsequent PCRs for sequencing were performed at the chosen temperature. Generally, lower temperatures produced more products than higher temperatures. This is due to the non-specific binding of the primers to the template. Also, high temperatures such as 60 °C - 61 °C resulted in fraying of DNA or even complete loss of product, as seen in Fig. 3.3D. This suggests that although the specificity of primer binding increased with increasing annealing temperature, there was a certain optimum functional range for a particular primer pair which led to maximum product formation. Since all the primer pairs were designed to possess similar properties (described in methods section 2.2.17), most primer pairs yielded a single specific product around an annealing temperature 58 °C.

#### **3.4.1 Summary of *ferroportin*, *Hfe* and *Irp2* gene sequencing in CHO cells**

- Partial characterisation of *Hfe*, *ferroportin* and *Irp2* genes in CHO cells has been achieved, as represented by Fig. 3.4. The characterised gene sequences matched closely the corresponding gene sequences in other species (Table 3.2)

- Not only the gene sequences but also the translated protein sequences bear high resemblance to the corresponding proteins of other species, as seen in figures 3.5 - 3.7. These multiple sequence alignments of proteins showed conservation of many functionally significant motifs within the CHO proteome.
- CHO-specific primers were designed based on the characterised CHO gene sequences and real time PCR was optimised with the CHO-specific primers for the genes *ferroportin*, *Hfe* and *beta actin* (Fig. 3.8 and Fig. 3.9).

#### **3.4.2 *Hepcidin* gene sequencing in CHO cells**

In order to enable studies related to *hepcidin* gene expression in the CHO TRVb1 cells, here, attempts were made to acquire the previously unknown *hepcidin* gene sequence in CHO cells.

Since the *ferroportin*, *Hfe* and *Irp2* genes in CHO cells were successfully characterised, the same approach was used to acquire the CHO-*hepcidin* gene sequence. Accordingly, primers were designed based on conserved nucleotides between rat and mouse *hepcidin* transcripts. However, sequencing attempts using these primers could not yield the *hepcidin* gene sequence. Following this, several approaches were used to resolve the issue. These included redesigning primers (Fig. 3.10), using magnesium chloride to increase primer specificity (Fig. 3.11), increasing product yield to facilitate sequencing (Fig. 3.12), cloning of the DNA fragment (Fig. 3.13) and the cDNA fragment (Fig. 3.18) in order to separate and

then sequence closely sized products. None of these approaches yielded the desired sequence. Since the hamster showed high genomic and proteomic similarities to other species (Tables 3.1 and 3.2; Figures 3.5 - 3.7), published hepcidin primers used for these species were used to amplify the CHO DNA (Fig. 3.15). This was to check if one of the primer pairs could yield a unique product which could be *hepcidin*. However, no specific product was obtained. The lack of product formation could be either due to the specificity of the *hepcidin* gene in CHO cells or primer specificity.

The concept of the *hepcidin* gene in CHO cells being species-specific is related to genomic differences between these species. The existence of such differences is supported by the result that rat hepcidin primers could not amplify the mouse genome (Fig. 3.15B, lane 2). Also, using only the forward primer for amplification resulted in a product with hamster DNA but not with rat and mouse liver DNA (Fig. 3.14A, lanes 4 and 5). Together, these results point at the overall genomic differences between the hamster and other rodents. However, the reason for the lack of product formation in these examples may also be due to intronic variation between hamster and other rodents as opposed to overall genomic differences. Indeed, there are mRNA similarities between these species but introns in different species may vary considerably. The concept of primer specificity mentioned earlier reflects on the specificity of PCR reactions. Along this line, it has been reported that when primers specific for *hepcidin-1* and *hepcidin-2* for mice were probed with the mouse hepcidin cDNA, there was no amplification after 25 cycles, eventually implying high specificity of this particular PCR reaction (Ilyin et al., 2003).

Whether the hamster is genetically close to other rodents or humans can be examined. As seen in Fig. 3.15B, the rat hepcidin primers yielded multiple products with CHO DNA (Fig. 3.15B, lanes 3, 4) but not with the mouse DNA. This suggests that the hamster genome bears more resemblance to the rat genome than the mouse genome. As seen in Fig. 3.15C, lanes 3 and 4, on using human hepcidin primers to amplify CHO DNA, two prominent products were obtained. These were of sizes approximately 700 bp and 250 bp. The 700 bp product matched closely in size to rat and mouse products (lanes 1 and 2) whereas the 250 bp product matched in size to the human DNA product (lane H). Together, this suggests that the hamster genome bears resemblance to humans and rodents but this is only at specific locations, again pointing at the specificity of the *hepcidin* gene.

One major reason for the difficulties encountered in obtaining the sequence of the *hepcidin* gene arose from the fact that preprohepcidin is a small peptide of 84 amino acids in human and rat (Park *et al.*, 2001) and 83 amino acids in mouse (Pigeon *et al.*, 2001). Thus the transcripts' sizes are very small which offers fewer sections of conserved nucleotides to design primers. This was one of the constraints which led to designing degenerate primers. Such degenerate primers would be less specific and may bind to multiple regions in the genome to give multiple products, one of which could be a part of the *hepcidin* gene sequence.

It is interesting to note that amplification of hamster DNA and cDNA with similar but different primer pairs resulted in two closely-sized products. This suggests that, there may be two *hepcidin* genes in hamster, like the mouse (Pigeon *et al.*, 2001)

and the fish (Kim et al., 2005). These genes could be very similar in size and sequence. Since the designed hepcidin primers are degenerate, they may bind to both these genes giving two different products, barely separated on a gel.

The natural ligand for hepcidin is ferroportin (Nemeth et al., 2004). Conservation of the hepcidin binding domain in the CHO cells accompanied by conservation of C326 which is implicated in binding to hepcidin (De Domenico et al., 2008) strongly suggested that the *hepcidin* gene should exist in the CHO cells, but it is probably highly specific. Thus further work needs to be done to obtain the *hepcidin* gene sequence in CHO cells so that the CHO TRVb1 cells which over-express human TfR1 can be proven to be a valuable model for iron-related studies.

### **3.4.3 Effect of iron supplementation on CHO TRVb1 cells**

This study confirmed the presence of human TfR1 at mRNA and protein levels in the CHO TRVb1 cells (Fig. 3.19 and 3.20). Here, it was shown for the first time that regardless of iron overdose the CHO TRVb1 cells expressed stable levels of cell-surface TfR1 up to a period of 48 h (Fig. 3.21E). Since the TfR1 in these cells is not devoid of its iron-sensitive IRE, the constant levels of TfR1 reflect the inherent characteristic of TfR1 over-expression in these cells. This led to a large number of receptors being present on the cell surface at a particular time point. Notably, the CHO TRVb1 cells express approximately 150,000 receptors on their cell surface whereas its Wt counterpart displays only 65,000 receptors (McGraw et al., 1987). Conversely, the Wt HepG2 cells showed not only lower levels of surface TfR1 than the CHO TRVb1 cells, but also showed a decrease in expression over

time upon iron overdose as seen in figures 3.21 (D) and (E). This response implied a regulated mechanism of iron uptake by the TfR1 which was sensitive to intracellular iron levels and decreased TfR1 levels on surface on reaching cellular iron sufficiency. The Wt HepG2 cells were surrounded by an iron-rich environment and thus demonstrated an iron-regulated TfR1 response.

In the CHO TRVb1 cells, unlike the TfR1 levels which remained constant, iron overdose caused a significant rise in hepcidin peptide production over the period of 48 h ( $p < 0.01$ ). As seen in Fig. 3.22, this increase in bioactive hepcidin on increasing extracellular holotransferrin levels was demonstrated in this study for the first time and correlates with the normal physiological response exhibited by humans under the influence of increased circulating iron levels.

To further understand if such a response could be observed within a short time of exposure to iron, the CHO TRVb1 cells were exposed to holotransferrin overdose up to 4 h. Data showed that despite the over-expression of TfR1 protein on the cell surface, intracellular iron concentrations in these cells were not significantly raised upon increasing extracellular iron levels (Fig. 3.25). Essentially, iron overdose to cells did not result in intracellular iron overload in the CHO TRVb1 cells. Hence it was concluded that the abundance of TfR1 on cell surface does not necessarily lead to intracellular iron overload, primarily because the *TfR1* mRNA in these cells is regulated at transcription level by its IRE region (Casey et al., 1988) and this controls the uptake of iron by the cells.

Regardless of the overall stability in intracellular iron levels, holotransferrin treatments led to a significant 1.4- and 1.5-fold increases in hepcidin peptide secretion at 30 min and 2 h, respectively (Fig. 3.26), compared to the untreated controls. Within the 4 h treatment period, cells were the most responsive to extracellular iron levels at the 2 h time point. Together, the data suggested that a significant intracellular iron overload was not a prerequisite for an increase in hepcidin peptide levels by the CHO TRVb1 cells and that the levels of bioactive hepcidin could be raised by increasing extracellular iron levels which may have caused minor variation in intracellular iron levels.

As shown in Fig. 3.23, iron levels in the maintenance medium and 5 g/L holotransferrin medium were determined. Correlating the iron levels in treatment media with hepcidin peptide production, it was seen that approximately 7  $\mu\text{M}$  of iron present in the maintenance medium led to approximately 3.7 ng/mL of hepcidin whereas 105  $\mu\text{M}$  of iron in 5 g/L of holotransferrin induced approximately 6.9 ng/mL of hepcidin. This meant that 16-fold higher iron levels in 5 g/L holotransferrin could only lead to a 1.9-fold increase in bioactive hepcidin. FCS thus showed a better potential to induce hepcidin production than high iron levels in the holotransferrin treatment medium. This is not surprising as FCS may contain an array of growth factors, proteins, cytokines and interferons and these cytokines, particularly IL-6, IL1 alpha and IL1 beta are known to induce hepcidin synthesis (Nemeth et al., 2003, Darshan and Anderson, 2009). Also, interferon gamma has been shown to induce hepcidin expression (Frazier et al., 2011).

As seen earlier, the *hepcidin* gene sequence in the CHO TRVb1 cells could not be characterised despite assuming its similarity with the human *hepcidin* gene sequence. However, the hepcidin peptide in CHO TRVb1 cells was detectable by the rabbit anti-human hepcidin antibody (figures 3.22 and 3.26) which has successfully detected bioactive hepcidin in human serum (Busbridge et al., 2009). This suggests that although the gene sequence of *hepcidin* in the CHO cells may be unique and may have dissimilarity with the human *hepcidin* gene sequence, the peptide sequence of hepcidin in the two species is probably similar. This is supported by the fact that the hepcidin peptide sequence is highly conserved amongst different species, as discussed in chapter 1 and shown in the below alignment.

```

Human           1 DTHFPICIFCCGCHRSKCGMCKT 25
Mouse hepcidin-1 1 DTNFPICIFCCKCCNNSQCGICCKT 25
Mouse hepcidin-2 1 DINFPICRFCCQCCNKPSGICCEE 25
Rat              1 DTNFPICLFCCCKCCKNSSGGLCCIT 25
Dog              1 DTHFPICIFCCGCKTPKCGLCCKT 25
Pig              1 DTHFPICIFCCGCCRKAICGMCKT 25
Zebrafish        1 QSHLSLCRFCCCKCRNKGGCYCKF 25
:  ::.:* *** *.  ** **

```

Since in the CHO TRVb1 cells intracellular iron overload upon iron overdose was not achieved, whether intracellular iron levels influenced *hepcidin* transcription and peptide production remained a question. Another question was whether the increase in hepcidin peptide production, as observed here, was restricted only to the CHO cells under these specific cell culture conditions; particularly in the scene of variability in *hepcidin* transcription observed by other groups. Some of these issues were addressed via experiments conducted in the following chapter.

## Chapter 4

### Effect of iron overload on TfR1-recombinant HepG2 cells

#### 4.1 Introduction

An objective of this research was to understand the effect of iron overload on *hepcidin* gene expression, for which initially the CHO TRVb1 cells were chosen. However, characterisation of the *hepcidin* gene sequence in these cells could not be achieved which prevented gene expression studies from being carried out. Hence, experiments investigating hepcidin peptide production were conducted. Results showed that the CHO TRVb1 cells increased hepcidin peptide production upon overdose of extracellular holotransferrin (chapter 3). However, the lack of intracellular iron overload in these cells restricted the understanding of whether excess iron within the cells would make an impact on *hepcidin* expression. In order to study the effect of iron overload on *hepcidin* gene and peptide expression, a cell line was required which could facilitate intracellular iron overload and also possessed a characterised *hepcidin* gene sequence to enable mRNA expression studies.

To achieve this, the human liver carcinoma cell line, HepG2 was utilised. This was principally because the gene sequences of *hepcidin* and other iron-related genes have been pre-characterised which can enable gene expression analysis through real time PCR. Also, since it is a mammalian cell line it would provide a better understanding of cellular processes occurring in humans, as compared to the hamster ovarian cell line. For instance the HepG2 cells demonstrate many features

of hepatocytes including the ability to produce liver-specific proteins like albumin and transferrin (Bokhari et al., 2007). Another major advantage of these cells is that they are of hepatic origin and the liver acts as a main site for iron storage as well as hepcidin production (Kohgo et al., 2008). Considering these advantages, HepG2 cells were chosen for further studies and were cloned such that these would express an *IRE*-independent *TfR1* mRNA (methods section 2.2.3.2) which therefore would be insensitive to an increase in intracellular iron levels.

#### **4.1.1 Aims and objectives**

**Aim:** To study the effect of iron overload on gene expression of *hepcidin* and other iron-related genes using the TfR1-recombinant HepG2 cells (rec-TfR1 HepG2) which constitutively express human TfR1 on the cell surface. It was hypothesised that upon iron supplementation the rec-TfR1 HepG2 cells would continuously uptake iron through holotransferrin causing intracellular iron overload. This would lead to increased *hepcidin* gene expression and peptide production. The resultant effect on gene expression of *hepcidin* and other iron-related genes in the rec-TfR1 HepG2 cells was compared to the wild type HepG2 and the HepG2 (p) cells (HepG2 cells transfected with empty plasmid), both of which express unmodified iron-regulated *TfR1* mRNA.

#### **Objectives:**

1. To ascertain the cell-surface expression of TfR1.
2. Confirmation of the presence of iron-related genes in HepG2 cells.
3. Upon iron supplementation, to perform:

- a. Viability studies
- b. Confirmation of iron uptake by cells
- c. Gene expression analysis through real time PCR
- d. Determination of the levels of secreted bioactive hepcidin

## **4.2 Results**

### **4.2.1 Cell-surface expression of TfR1 in HepG2 cells**

The requirement of the rec-TfR1 HepG2 cells was that these cells expressed a greater amount of TfR1 on the cell surface as compared to the Wt HepG2 cells and also continuously uptake iron regardless of excess intracellular iron levels. To ascertain this, Wt and rec-TfR1 HepG2 cells were treated with holotransferrin (5 g/L) for 48 h and cell-surface TfR1 was analysed. Each treatment undergone by the rec-TfR1 HepG2 cells is shown in figures 4.1 (A), (B) and (C). Here, fluorescence is depicted in R2 and the resultant effect on expression of cell-surface TfR1 is depicted in figures 4.1 (D), (E) and (F).

Data showed that the rec-TfR1 HepG2 cells displayed significantly higher basal levels of TfR1 on the cell surface than the Wt HepG2 cells (Fig. 4.1D). When subjected to iron overdose, Wt HepG2 cells showed a slight but significant up-regulation of TfR1 expression after 24 h ( $p < 0.02$ ) and a plateau at 48 h (Fig. 4.1E). In contrast, the rec-TfR1 HepG2 cells showed constant levels of cell-surface TfR1 irrespective of holotransferrin overdose over time (Fig. 4.1F).

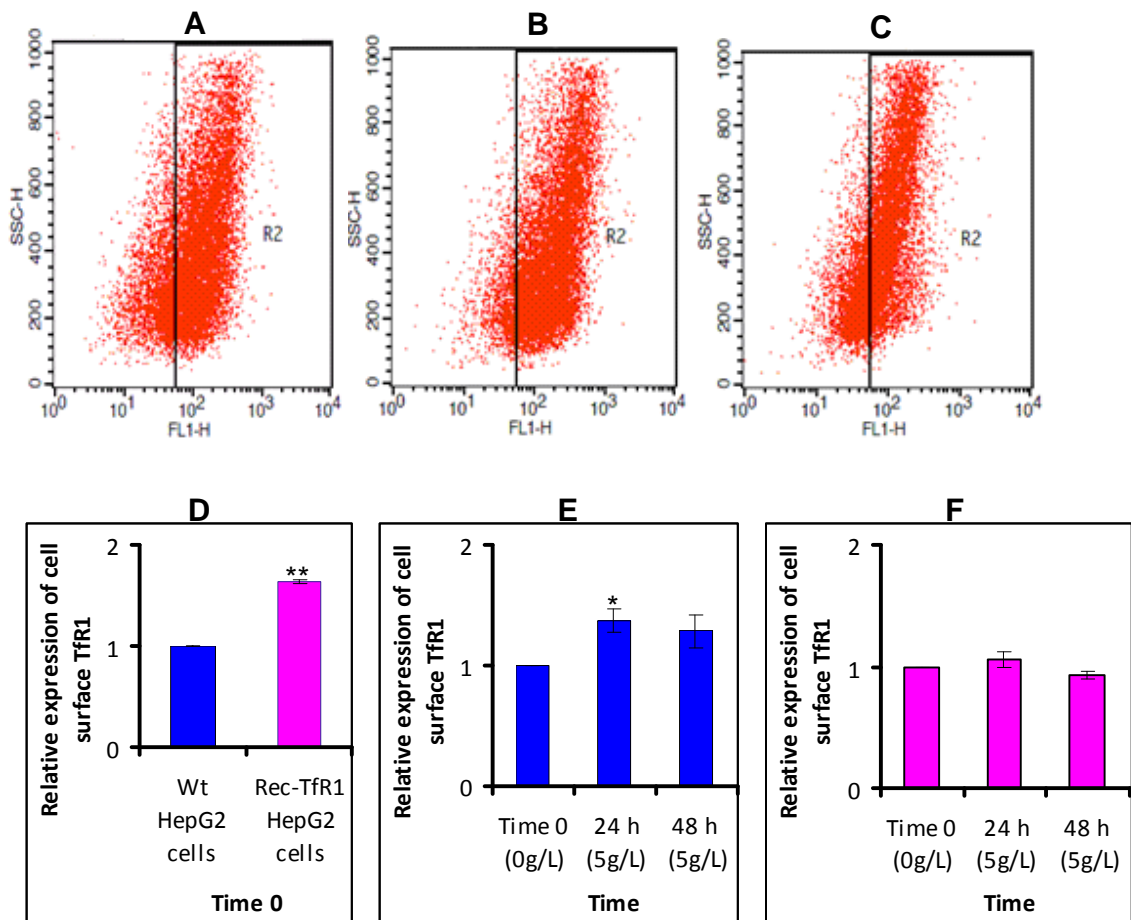


**Fig. 4.1 Effect of holotransferrin overdose on cell-surface expression of TfR1**

Wt and rec-TfR1 HepG2 cells were serum starved for 24 h (time 0) followed by treatment with 5 g/L holotransferrin for 48 h, as described in methods section 2.2.15. Cell-surface expression of TfR1 was studied at various time points after treatment as described in methods section 2.2.20. Flow cytometry images of serum starved rec-TfR1 HepG2 cells before treatment i.e. time 0 (**A**) and after holotransferrin treatment for 24 h (**B**) and 48 h (**C**) are shown.

**D:** Cell-surface TfR1 in rec-TfR1 HepG2 cells relative to Wt HepG2 cells before treatment (time 0). **E** and **F:** Cell-surface TfR1 in Wt HepG2 cells and rec-TfR1 HepG2 cells upon iron overdose, respectively, relative to time 0. Data is presented as mean  $\pm$  SEM (n=3). \*  $p < 0.02$ , \*\*  $p < 0.01$  compared to Wt HepG2 cells.

To further understand the TfR1 response, cells growing in the maintenance medium were treated with holotransferrin (5 g/L) without any period of serum starvation before the treatment. A representative cell response of each treatment undergone by the rec-TfR1 HepG2 cells is shown in Fig. 4.2 (A), (B) and (C) overleaf and the effect of the treatments is summarised in Fig. 4.2 (D) and (E).

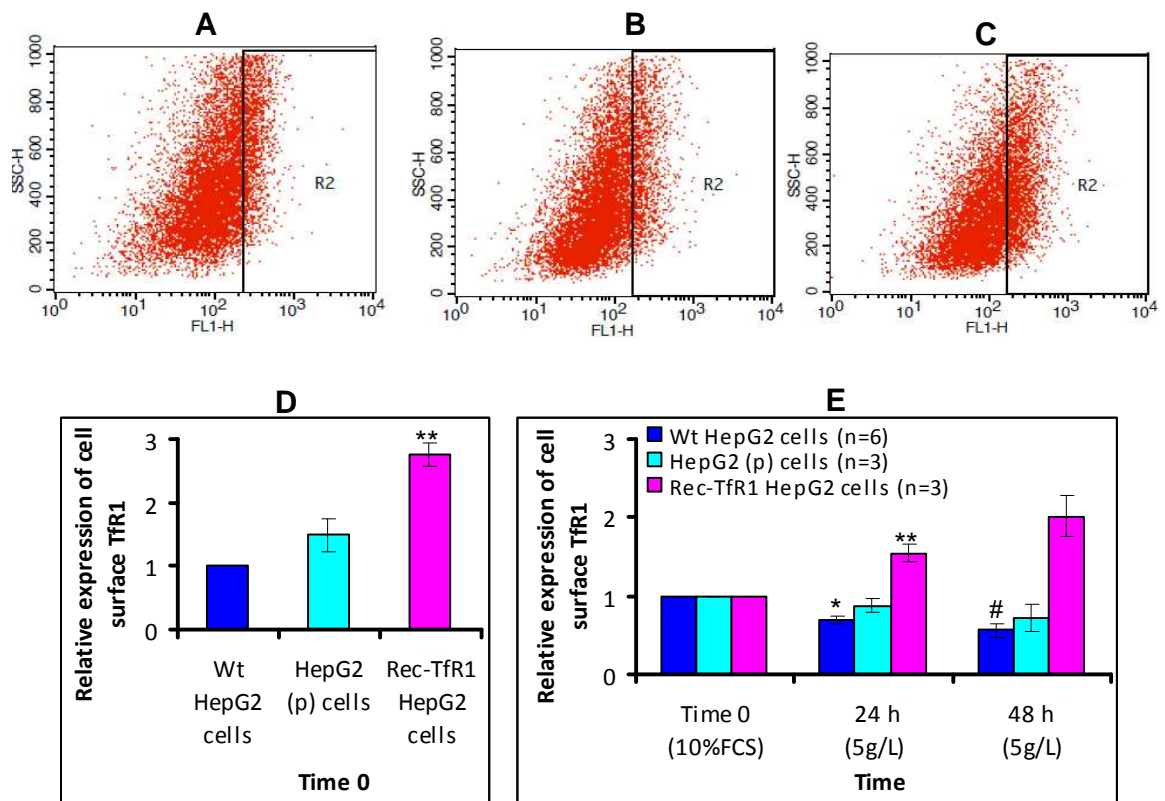


**Fig. 4.2 Effect of iron overdose on TfR1 cell-surface expression in HepG2 cells**

Wt and rec-TfR1 HepG2 cells were treated with 5 g/L holotransferrin up to 48 h and cell-surface expression of TfR1 before (time 0) and after treatment was studied, as described in methods section 2.2.20. Flow cytometry images of rec-TfR1 HepG2 cells before treatment i.e. time 0 (**A**) and after holotransferrin treatment for 24 h (**B**) and 48 h (**C**) are shown.

**D:** Cell-surface TfR1 of HepG2 (p) and rec-TfR1 HepG2 cells, relative to Wt HepG2 cells (n=3).

**E:** HepG2 TfR1 responses upon iron overdose, relative to time 0.

Data is presented as mean  $\pm$  SEM. \*  $p < 0.02$  compared to time 0 and \*\*  $p < 0.01$ , #  $p < 0.05$  compared to 24 h.

Under steady state conditions i.e. in the maintenance medium, there was no significant difference between the cell-surface expression of TfR1 in Wt HepG2 and HepG2 (p) cells (Fig. 4.2D). On the other hand, rec-TfR1 HepG2 cells expressed approximately 2-fold higher levels of TfR1 on the cell surface than Wt HepG2 and HepG2 (p) cells ( $p < 0.01$ ). On treating the Wt HepG2 and the HepG2 (p) cells with 5 g/L holotransferrin, TfR1 expression in these cells decreased with time whereas in the rec-TfR1 HepG2 cells, a significant increase in expression of cell-surface TfR1 was observed (Fig. 4.2E).

#### 4.2.2 Iron-related genes in rec-TfR1 HepG2 cells

Prior to gene expression analysis via real time PCR, the expression of genes of interest at the mRNA level in the rec-TfR1 HepG2 cells was confirmed by amplifying the cDNA with the designed primers and those published by other research groups (appendix V). Each amplicon observed in Fig. 4.3 was sent for sequencing to confirm its identity before proceeding with expression analysis (appendix V). As observed by other groups (Fein et al., 2007, Kulaksiz et al., 2004), here through Fig .4.3, it was shown that HepG2 cells express *hepcidin*.

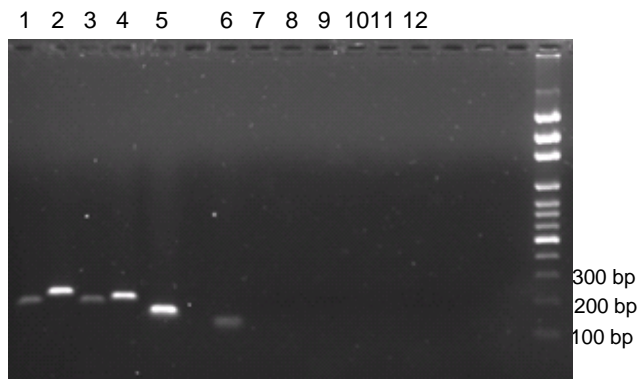


**Fig. 4.3 Amplicons of transcripts of iron-related genes in rec-TfR1 HepG2 cells**

cDNA from rec-TfR1 HepG2 cells was synthesised as explained in methods section 2.2.18 and amplified by PCR as described in methods section 2.2.8. Primers (Table 2.3) used to amplify the rec-TfR1 cDNA as seen in each lane, were as below:

- Lane 1= TfR1 (F) and (R); expected product size= 179 bp
- Lane 2= TFR1-IRE (F lb) and (R l); expected product size= 210 bp
- Lane 3= Hpcidin (F l) and (R l); expected product size= 189 bp
- Lane 4= Ferroportin (F l) and (R l); expected product size= 260 bp
- Lane 5= GAPDH (F) and (R); expected product size= 131 bp
- Lane 6 = HFE (F l) and R (l); expected product size=77 bp
- Lanes 7-12 = negative controls with respective primers

#### 4.2.3 HepG2 cells under steady state conditions: 48 h study

The viability of Wt and rec-TfR1 HepG2 cells under steady state conditions (i.e. in the maintenance medium) increased with time (figures 4.4 A and B). This indicated growth of cells and increase in cell numbers, although the increase in cell numbers

in rec-TfR1 HepG2 cells was at a slower rate than Wt HepG2 cells from 24 to 48 h. This slow growth rate could be due to the presence of plasmid in the rec-TfR1 HepG2 cells. Such plasmid-possessing recombinant cells may utilise a significant amount of the cell's resources to maintain the plasmid; the plasmid being a metabolic burden on the cells (Glick, 1995). Intracellular iron content was determined which showed that basal levels of iron in the rec-TfR1 HepG2 cells were higher than those in the Wt HepG2 cells (figures 4.4 C and D).

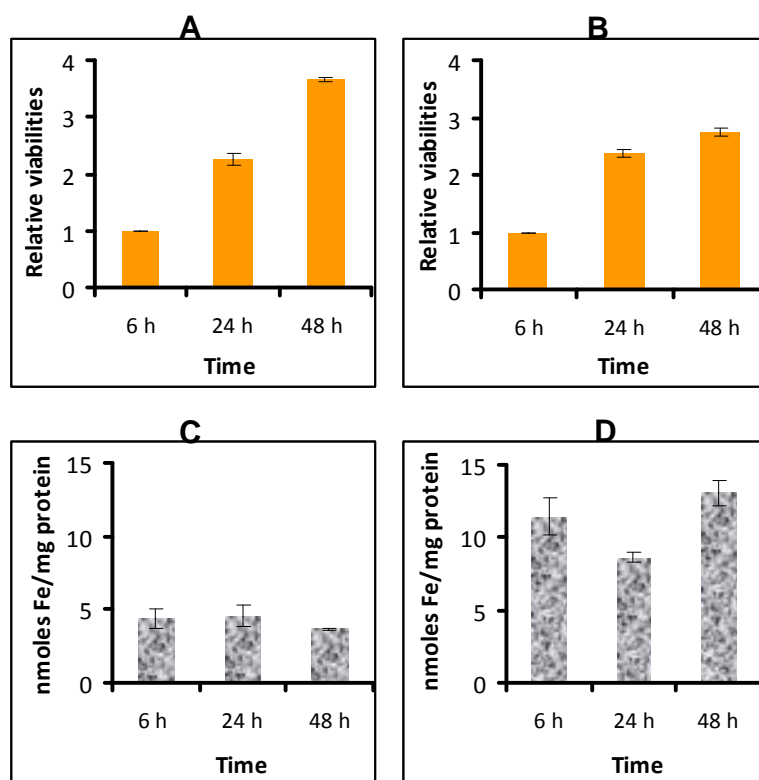


**Fig. 4.4 Viability studies and iron content in HepG2 cells under steady state conditions**

Wt and rec-TfR1 HepG2 cells growing in maintenance medium were assessed for viability and intracellular iron content at various time points, as described in methods section 2.2.16 and 2.2.17, respectively. Viabilities were expressed relative to the 6 h time point.

**A and B** : Cell viabilities of Wt HepG2 cells (n=2) and rec-TfR1 HepG2 cells (n=2), respectively.

**C and D** : Intracellular iron levels in Wt HepG2 cells (n=2) and rec-TfR1 HepG2 cells (n=3), respectively.

Data is presented as mean  $\pm$  SEM

In the preliminary RNA expression analysis of iron-related genes via real time PCR, three reference genes *actin*, *GAPDH* and *18s* were chosen. The  $C_T$  values of the genes showed that *GAPDH* was the most suitable under varying experimental conditions as it was the most stable (appendix XVI). Hence *GAPDH* was chosen as a reference gene to normalise expression of all the iron-related genes under study.

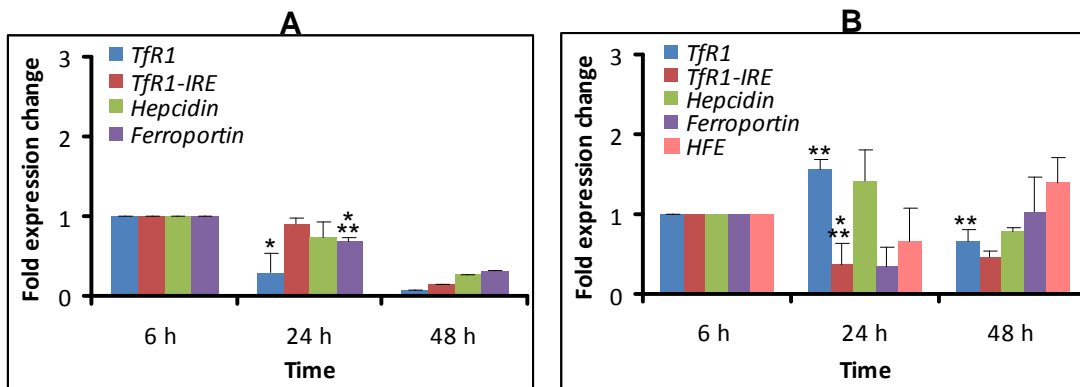


**Fig. 4.5 Basal mRNA expression of iron-related genes in HepG2 cells**

Wt and rec-TfR1 HepG2 cells growing in the maintenance medium were analysed for basal mRNA expression of iron-related genes of interest. RNA expression analysis was carried out as described in methods sections 2.2.18 and 2.2.19, and was expressed relative to the 6 h.

**A and B** : Expression of iron-related genes in Wt HepG2 cells and in rec-TfR1 HepG2, respectively. Data is presented as mean  $\pm$  SEM (n=1-3). \*  $p < 0.05$ , \*\*  $p < 0.02$  and \*\*\*  $p < 0.01$  compared to the previous time point.

Gene expression analysis showed that in Wt HepG2 cells *TfR1* levels significantly decreased after 24 h (Fig. 4.5A). Although no significant change in *hepcidin* mRNA was observed after 24 h, *ferroportin* expression showed a significant decrease, the cells aiming to retain intracellular iron levels. On the other hand, the rec-TfR1 HepG2 cells showed a significant increase in *TfR1* mRNA expression at 24 h and then a reduction after 48 h (Fig. 4.5B). However, the level at 48 h was higher than Wt HepG2 cells, despite the higher intracellular iron content than Wt HepG2 cells, as seen in Fig. 4.4D. This showed that the *TfR1* in the rec-TfR1 HepG2 cells were insensitive to high intracellular iron concentration, as expected, due to the absence

of the iron-regulated IRE element in the modified TfR1 in these cells. Also, in the rec-TFR1 HepG2 cells the mRNA of *TfR1-IRE*, which is a reflection of the endogenous iron regulated-*TfR1*, decreased at 24 h and 48 h (Fig. 4.5B) reflecting the cells' high intracellular iron status. In this situation the endogenous *TfR1* mRNA is expected to be down-regulated to prevent any further iron uptake.

The high intracellular iron status of rec-TfR1 Hep2 cells was reflected in the increased levels of *ferroportin* mRNA at 6 h followed by a drop at 24 h and then again a rise at 48 h, mirroring the pattern of intracellular iron levels seen in Fig. 4.4D. A similar pattern of *HFE* gene expression was observed. Although *hepcidin* mRNA levels were generally maintained, hepcidin expression appeared to be at a higher level than in the Wt HepG2 cells at the same time points.

#### **4.2.4 Iron overdose and Wt HepG2 cells : 48 h study**

On treating the Wt HepG2 cells with 1 g/L and 5 g/L holotransferrin, both the concentrations decreased cell viability by ~ 20 % at 6 h, remained stable at 24 h and increased by 50 % at 48 h with respect to the untreated control at each time point (Fig. 4.6A). A 24 h period of serum and iron deprivation did not have a major impact on cell viability but viability decreased by 40 % when deprivation was for 48 h (Fig. 4.6B). Intracellular iron levels were generally maintained regardless of the high circulating holotransferrin concentration (Fig. 4.6C), implying the regulatory effect of *TfR1-IRE*, which controlled iron uptake by the cells under high extracellular iron environment.

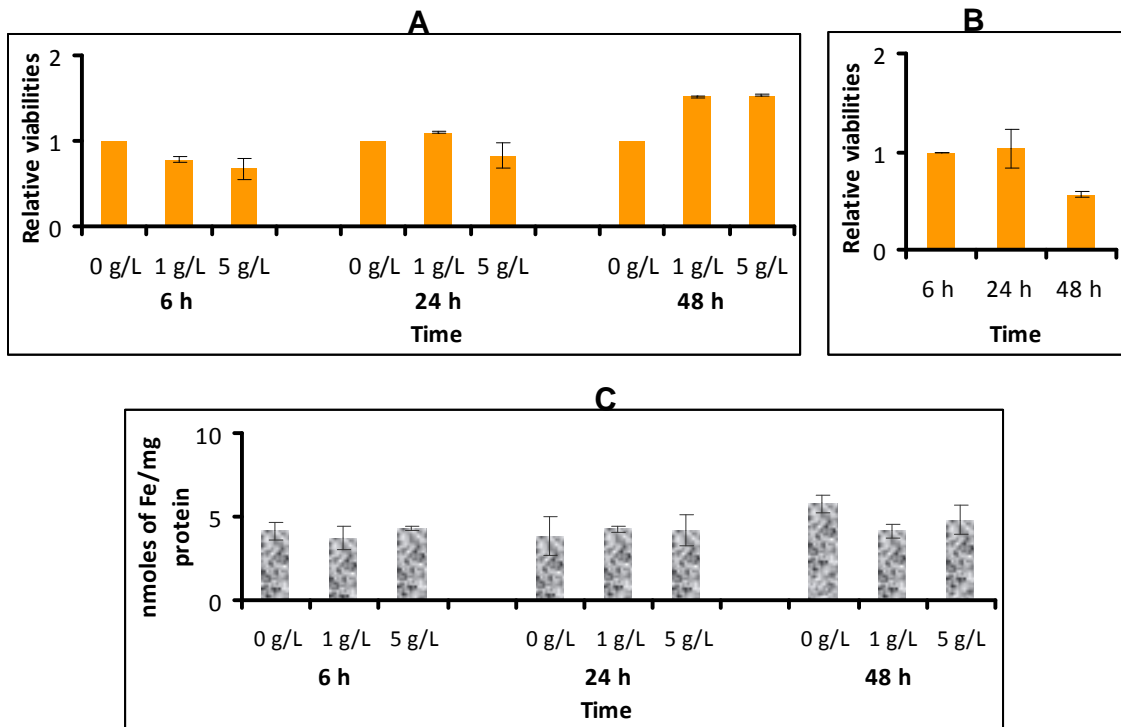


**Fig. 4.6 Viability studies and intracellular iron levels in Wt HepG2 cells under holotransferrin treatments**

Wt HepG2 cells were treated with different concentrations of holotransferrin for 48 h as described in methods section 2.2.15. Cell viability and intracellular iron levels after treatments were determined as mentioned in legend of Fig. 4.4. Viability of treated cells (1 g/L and 5 g/L holotransferrin) was expressed relative to viability of untreated cells (0 g/L) at each time point.

**A and B:** Effect of holotransferrin overdose and iron deprivation (0 g/L) on cell viability, respectively (6 h and 24 h: n=2; 48 h: n=1).

**C:** Effect of holotransferrin overdose on intracellular iron levels (n=2). Data is presented as mean  $\pm$  SEM.

Fig. 4.7 shows the effect of holotransferrin treatments on mRNA expression of various iron-related genes in the Wt HepG2 cells. It was observed that *TfR1* mRNA levels generally decreased upon holotransferrin treatment and increased by approximately 3-fold under serum and iron deprivation (Fig. 4.7A and B). Unlike *TfR1*, *hepcidin* mRNA levels increased upon iron exposure at 6 and 24 h, whereas 24 h-holotransferrin treatment (1 g/L) resulted in an approximately 2.9-fold increase in *hepcidin* mRNA levels (Fig. 4.7C).

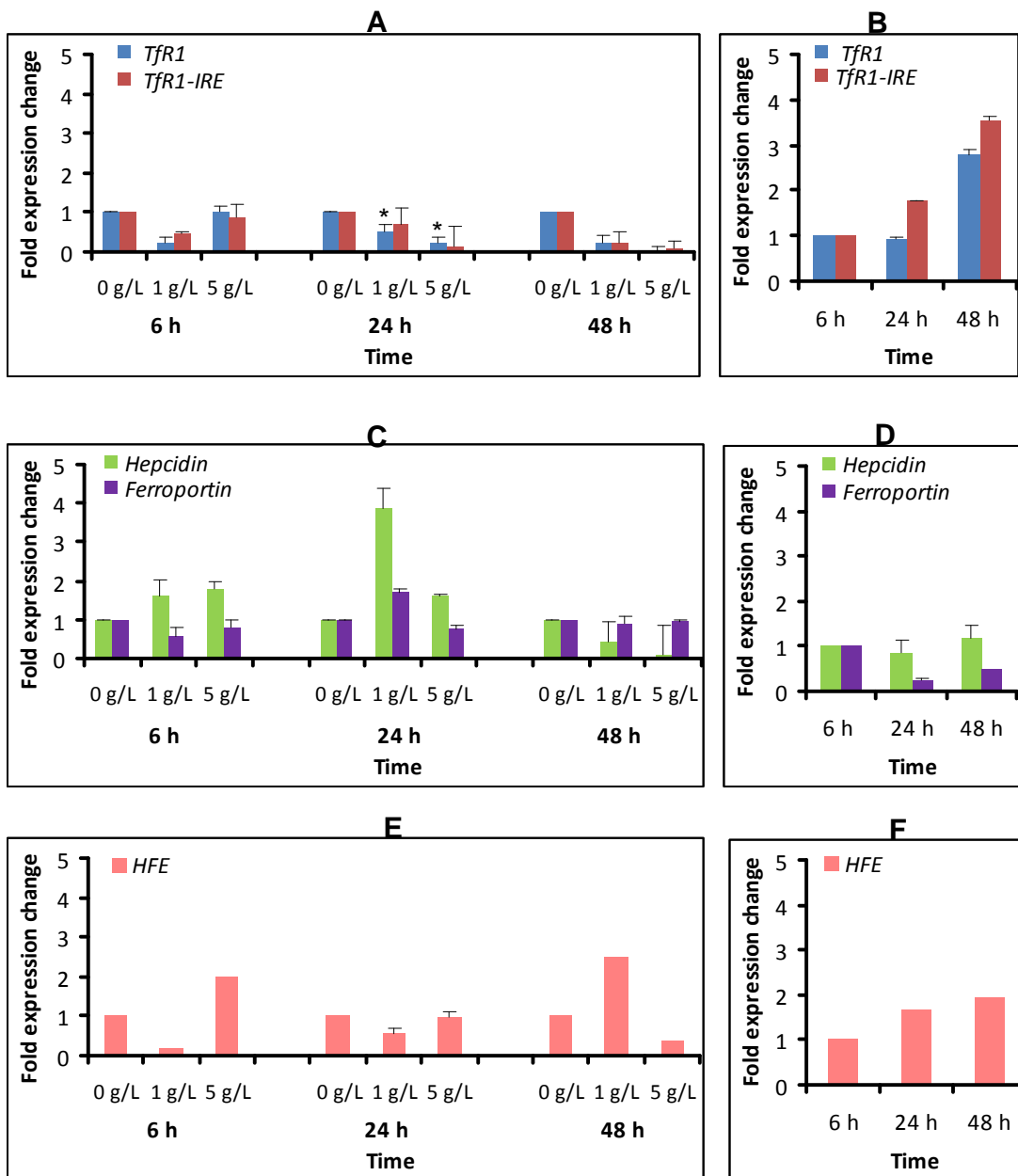


**Fig. 4.7 mRNA expression of iron-related genes in Wt HepG2 cells upon holotransferrin treatments**

Wt HepG2 cells were treated with different concentration of holotransferrin for 48 h as described in methods section 2.2.15. RNA expression analysis was per legend of Fig. 4.5. mRNA expression of treated cells (1 g/L and 5 g/L holotransferrin) was expressed relative to untreated cells (0 g/L) at each time point.

**A and B:** *Tfr1* and *Tfr1-IRE* expression upon holotransferrin treatment and under serum and holotransferrin deprivation (0 g/L), respectively; (6 h and 48 h: n=2; 24 h: n=3).

**C and D:** *Hepcidin* and *ferroportin* expression upon holotransferrin treatment and under serum and holotransferrin deprivation (0 g/L), respectively; (6 h and 24 h: n=2; 48 h: n=1).

**E and F:** *HFE* expression upon holotransferrin treatment and under serum and holotransferrin deprivation (0 g/L), respectively; (n=1)

Data is presented as mean  $\pm$  SEM. \* p<0.02 compared to untreated control.

*Ferroportin* mRNA levels were generally maintained at constant levels throughout the treatment (Fig. 4.7C), similar to the intracellular iron levels seen in Fig. 4.6C. This implied that there was no excess iron within the cells and hence the cells retained iron. The increase in *ferroportin* expression by approximately 70 % after 24 h of 1 g/L treatment may be to remove excess iron the cells have taken up. The down-regulation of *ferroportin* mRNA by approximately 20 % after 24 h in 5 g/L holotransferrin (compared to 0 g/L) was similar to that observed by Jacolot et al. (2008) on treatment of Wt HepG2 cells with 4.5 g/L of holotransferrin.

Preliminary studies of *HFE* transcription showed that its level steadily increased upon increasing iron dosage but remained stable as compared to the untreated control after 24 h (Fig. 4.7 E). This is unlike the response reported by Jacolot et al. (2008) where *HFE* gene expression was slightly down-regulated on treatment with 4.5 g/L of holotransferrin for 24 to 48 h.

#### **4.2.5 Iron overdose and rec-TfR1 HepG2 cells : 48 h study**

The viability of rec-TfR1 HepG2 cells generally remained steady over the period of 48 h when under holotransferrin treatment and serum and iron deprivation (Fig 4.8 A and B). Intracellular iron levels were determined which showed that in contrast to Wt HepG2 cells, the rec-TfR1 HepG2 cells showed a significant increase in iron uptake ( $p < 0.01$ ) with increasing holotransferrin concentration at 24 h (Fig. 4.8C).

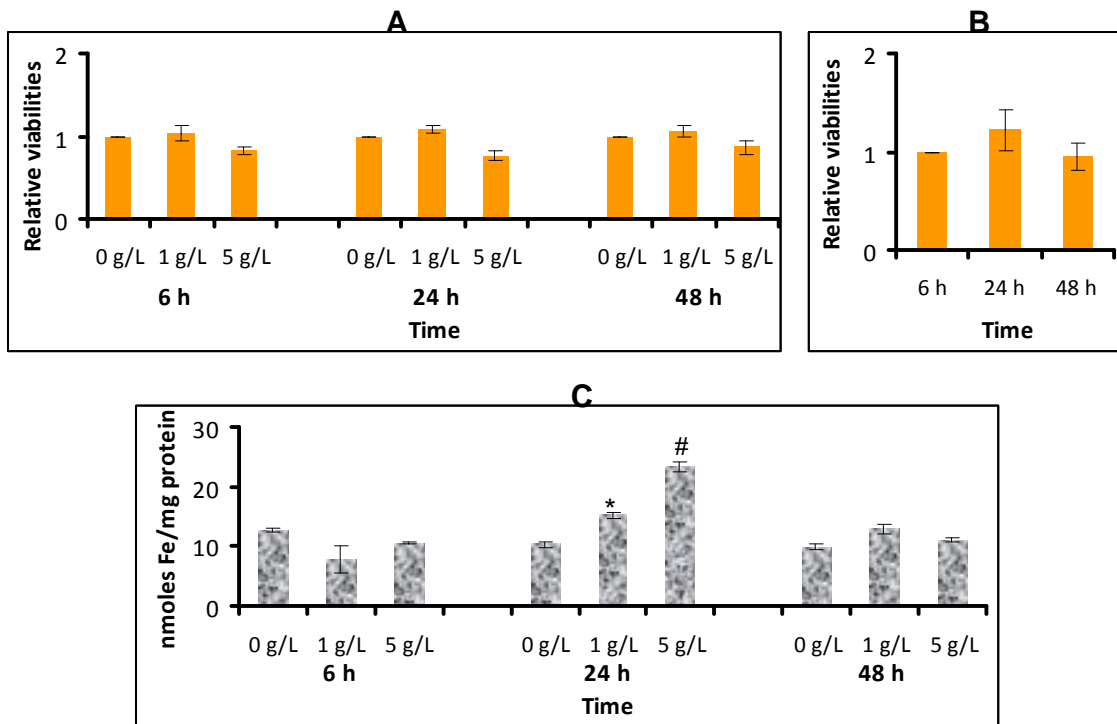


**Fig. 4.8 Viability studies and intracellular iron levels in rec-TfR1 HepG2 cells under holotransferrin treatments**

Rec-TfR1 HepG2 cells were treated with increasing concentrations of holotransferrin up to 48 h followed by measurement of cell viability and intracellular iron levels as described in legend of Fig. 4.6. Viability of treated cells (1 g/L and 5 g/L holotransferrin) was expressed relative to the viability of untreated cells (0 g/L) at each time point.

**A and B:** Effect of holotransferrin overdose and serum and iron deprivation (0 g/L) on cell viability, respectively (n=3).

**C:** Effect of holotransferrin overdose on intracellular iron levels (0g/L: n=6; 1 g/L and 5 g/L: n=3). Data is presented as mean  $\pm$  SEM. \* p<0.01 compared to untreated control, # p<0.01 compared to 1 g/L treatment.

Matching the pattern of iron uptake, *TfR1* mRNA levels were up-regulated in rec-TfR1 HepG2 cells upon increasing holotransferrin concentrations at 6 and 24 h (Fig. 4.9A). Following 2 g/L (data not shown) and 5 g/L holotransferrin treatment for 24 h, these cells showed a 2-fold and ~3-fold rise in *TfR1* mRNA ( $p < 0.04$ ) (Fig. 4.9A). Thus, unlike the Wt HepG2 cells, the rec-TfR1 HepG2 cells showed insensitivity to high intracellular iron levels by preventing *TfR1* mRNA down-regulation (Fig. 4.8 C).

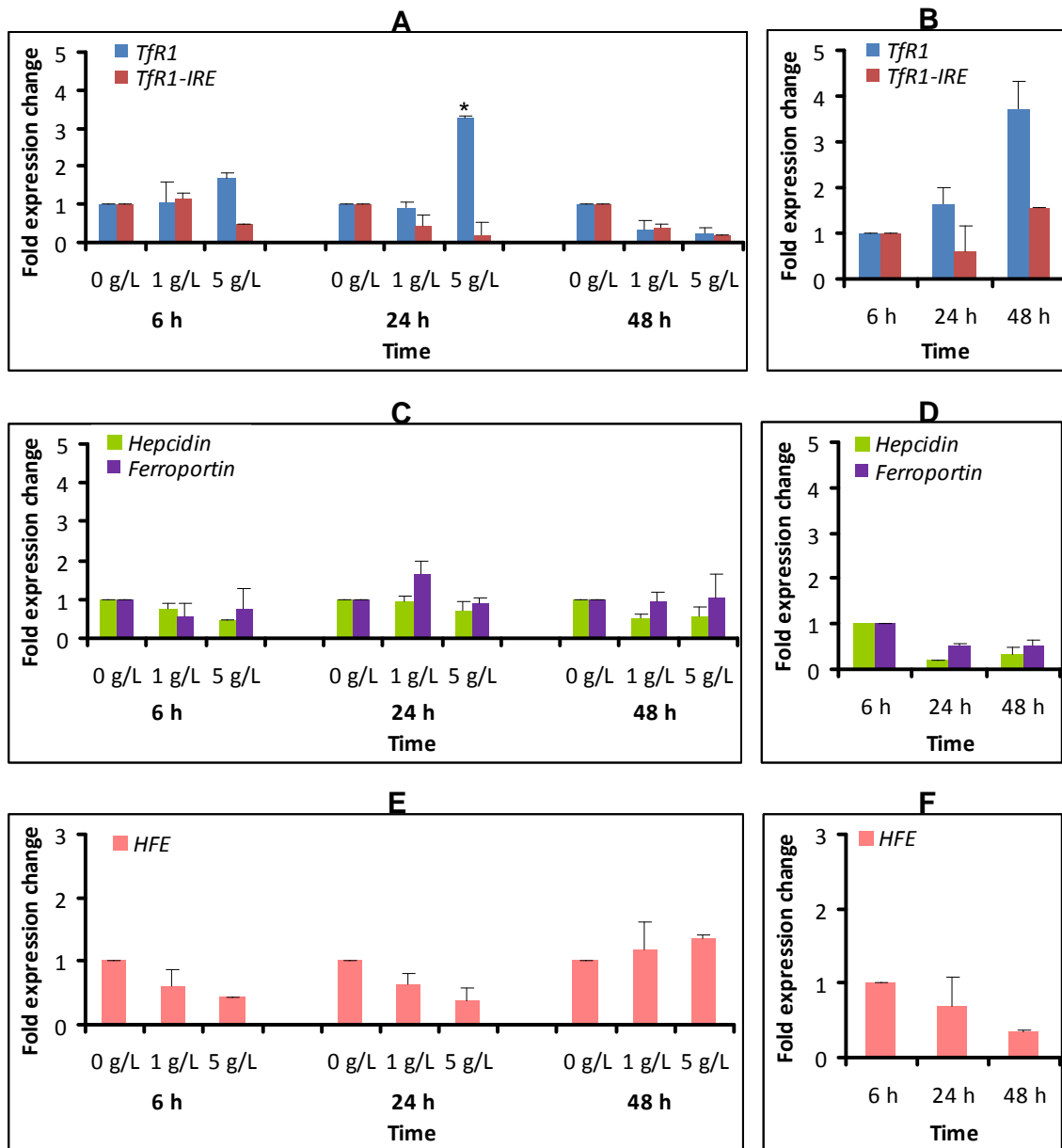


**Fig. 4.9 mRNA expression of iron-related genes in rec-TfR1 HepG2 cells upon holotransferrin treatment**

Rec-TfR1 HepG2 cells were treated with increasing concentrations of holotransferrin and mRNA expression was analysed as mentioned in legend of Fig. 4.7. mRNA expression of treated cells (1 g/L and 5 g/L holotransferrin) was expressed relative to untreated cells (0 g/L) at each time point.

**A and B:** *TfR1* and *TfR1-IRE* expression upon holotransferrin treatments and under serum and holotransferrin deprivation (0 g/L), respectively; (6 h and 48 h: n=2; 24 h: n=3)

**C and D:** *Hepcidin* and *ferroportin* expression upon holotransferrin treatments and under serum and holotransferrin deprivation, respectively (n=2).

**E and F:** *HFE* expression upon holotransferrin treatments and under serum and holotransferrin deprivation, respectively (n=2).

Data is presented as mean  $\pm$  SEM. \* p<0.01 compared to untreated control.

Under serum and iron deprivation, like the Wt HepG2 cells, the rec-TfR1 HepG2 cells increased *TfR1* mRNA levels, but unlike the Wt HepG2 cells the *TfR1-IRE* was either down-regulated or remained stable (Fig.4.9B), displaying a feature of regulated iron uptake. Also, unlike the Wt HepG2 cells, *hepcidin* and *ferroportin* mRNA expression did not show any significant change upon holotransferrin treatments at any time points (Fig. 4.9C). *HFE* expression levels decreased with increasing iron overdose after 6 h and 24 h (Fig. 4.9E), completely opposite to the pattern of iron uptake in these cells as seen in Fig. 4.8C.

In conclusion, the results showed that the 48 h period of iron overdose to the rec-TfR1 HepG2 cells, caused an intracellular iron overload but did not lead to a rise in *hepcidin* mRNA expression, as was hypothesised. Hence to determine if the expected increase in *hepcidin* mRNA expression occurred earlier than 6 h, the “time window” of measurements was changed in the subsequent experiments. Since previous results showed that the Wt and the rec-TfR1 HepG2 cells differed strikingly in their responses when treated with 5 g/L holotransferrin (figures 4.7A and 4.9A, 4.6C and 4.8C), the effect of iron supplementation on cell responses was studied within 4 h of 5 g/L holotransferrin treatment. Responses exhibited by rec-TfR1 HepG2 cells were compared to those of Wt HepG2 cells and HepG2 (p) cells i.e. Wt HepG2 cells with empty plasmid, in which the endogenous *TfR1* was unchanged and hence were expected to demonstrate regulated iron uptake like the Wt HepG2 cells.

#### 4.2.6 HepG2 cells under steady state condition : 4 h study

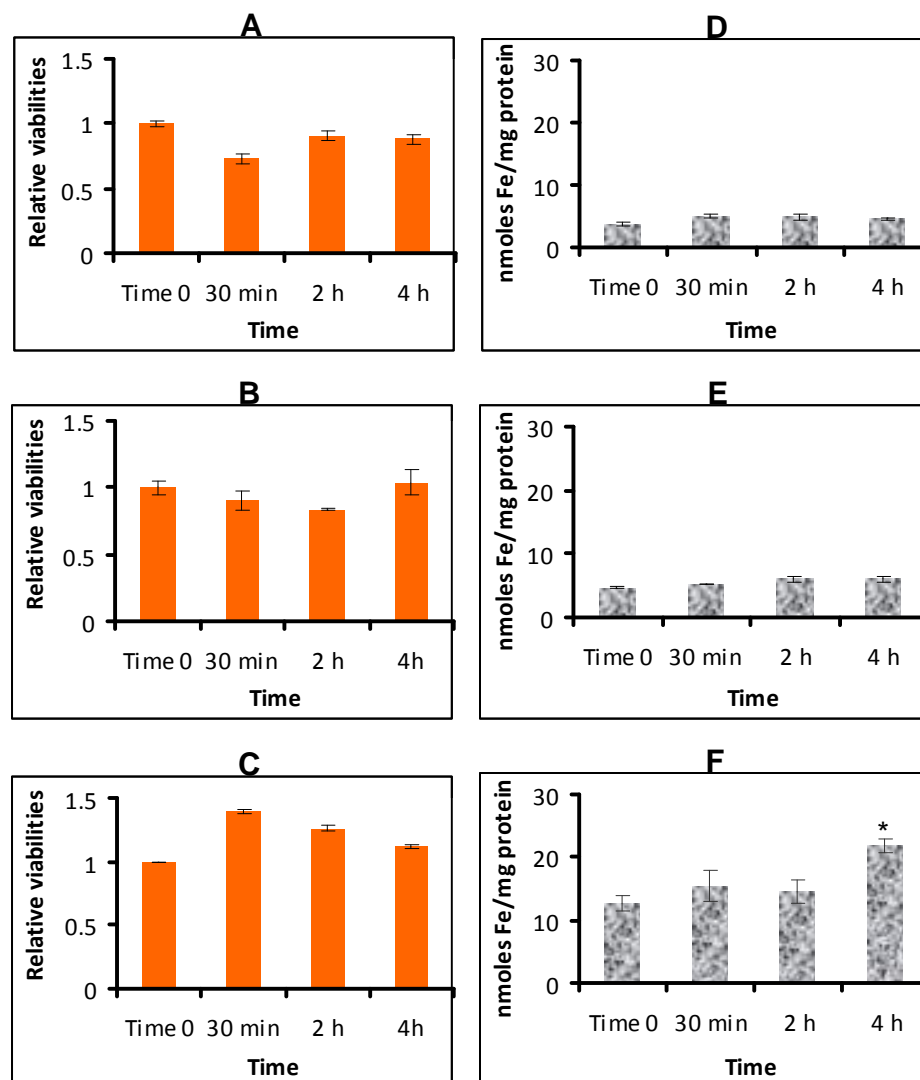


**Fig. 4.11 Viability and iron uptake in HepG2 cells under steady state conditions : 4 h study**

Wt HepG2, HepG2 (p) and rec-TfR1 HepG2 cells growing in maintenance medium were assessed for viability and intracellular iron content at various time points, as mentioned in legend of Fig. 4.4. Viabilities were expressed relative to the 1<sup>st</sup> time point of the assay (time 0).

**A, B, and C:** cell viabilities of Wt HepG2, HepG2 (p) and rec-TfR1 HepG2 cells, respectively.

**D, E and F:** Intracellular iron levels in Wt HepG2, HepG2 (p) and rec-TfR1 HepG2 cells, respectively.

Data is presented as mean  $\pm$  SEM (n=3). \* p<0.01 compared to time 0.

In the maintenance medium the viability of all cells generally remained stable within the 4 h period. Intracellular iron levels were also maintained at constant levels by the Wt HepG2 and HepG2 (p) cells, whereas rec-TfR1HepG2 cells showed a pattern of increasing iron uptake which significantly increased by 70 % after 4 h ( $p < 0.01$ ) (Fig. 4.11F). Iron levels in the Wt HepG2 cells measured in this study (3-4 nmoles/mg protein) are similar to those measured by Gu et al.,(2008).

The mRNA expression levels of various iron-related genes in the HepG2 cells in maintenance medium (i.e. under steady state) were analysed as shown in Fig.4.12.

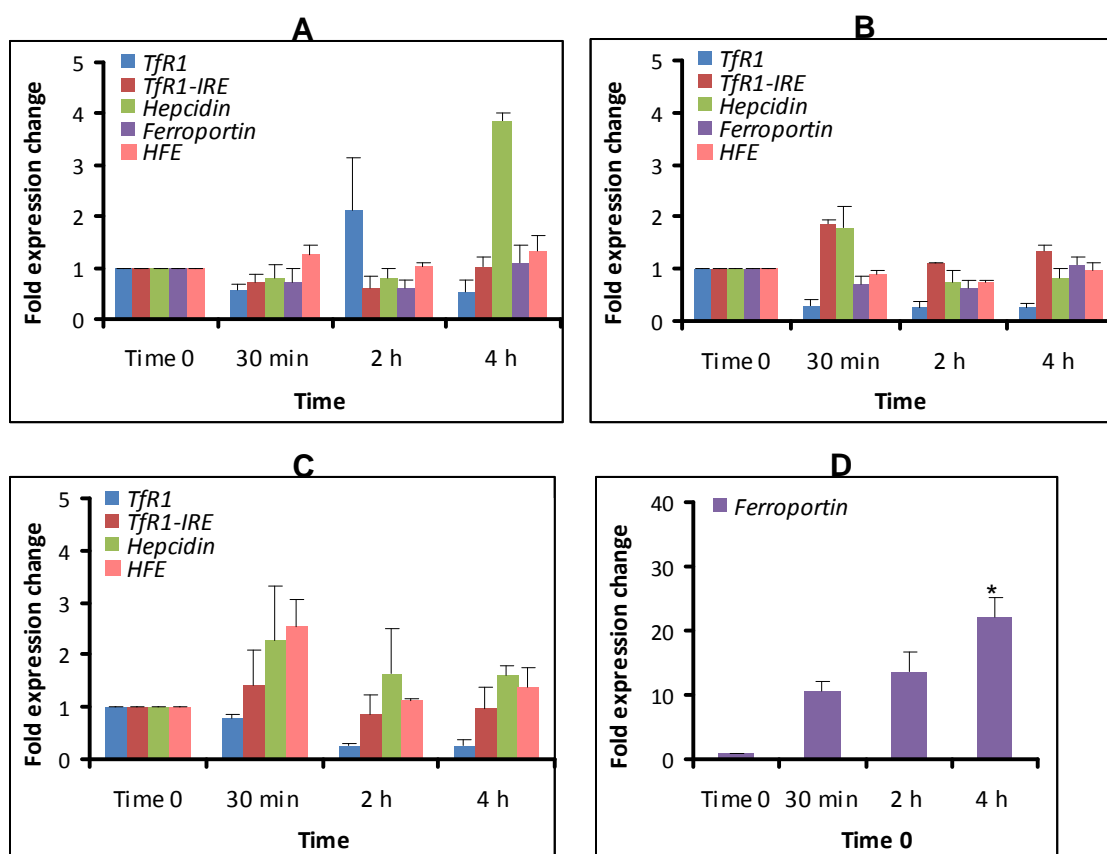


**Fig. 4.12 Basal mRNA expression of iron-related genes in HepG2 cells : 4 h study**  
Wt HepG2, HepG2 (p) and rec-TfR1 HepG2 cells growing in the maintenance medium were analysed for basal mRNA expression of iron-related genes of interest. RNA expression analysis was carried out as mentioned in legend of Fig. 4.5 and expressed relative to time 0. mRNA expression studies of iron-related genes in **A**: Wt HepG2 cells; **B**: HepG2 (p) cells; **C** and **D** : Rec-TfR1 HepG2 cells. Data is presented as mean  $\pm$  SEM (n=3).  
\*  $p < 0.01$  compared to time 0.

In the Wt HepG2 cells there was no significant change in gene expression over the 4 h period, except the rise in *hepcidin* mRNA expression after 4 h (Fig. 4.12A). In the HepG2 (p) cells the increase in *TfR1* and *hepcidin* mRNA within the first 30 min followed a gradual stabilisation after 2 h and 4 h (Fig. 4.12B). The rec-TfR1 HepG2 cells showed a notably different pattern of gene expression than the cells of Wt origin i.e. Wt HepG2 cells and HepG2 (p) cells. While the expression of *HFE* and *hepcidin* mirrored each other, these cells showed significantly high *ferroportin* mRNA levels ( $p < 0.01$ ) as seen in figures. 4.12 C and D.

#### 4.2.7 Effect of iron overdose on HepG2 cells : 4 h study

In order to ensure that the cells had received a high dosage of iron via holotransferrin, iron levels in the treatment media were measured. The results showed that iron levels in 5 g/L holotransferrin treatment media were 15-20 fold higher than those in the maintenance medium (Fig. 4.13).

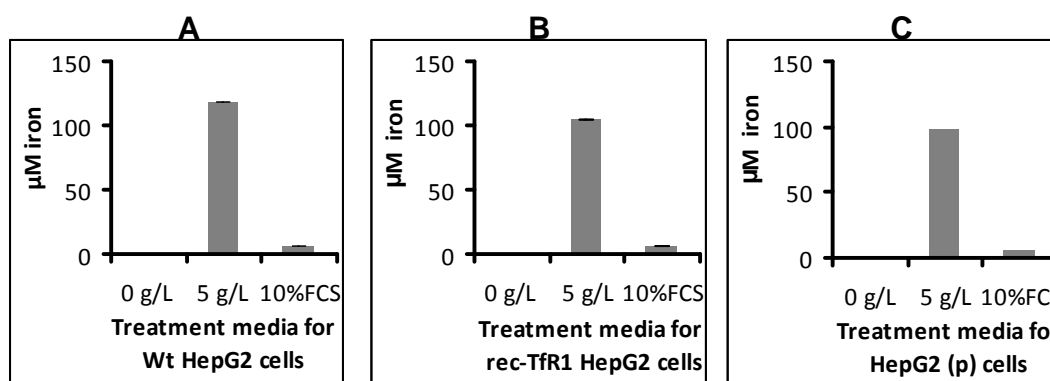


**Fig. 4.13 Iron levels in treatment media for HepG2 cells**

Iron levels in the treatment media used to treat HepG2 cells were detected as per methods section 2.2.17.1.

**A:** Wt HepG2 cells; **B:** HepG2 (p) cells; **C:** Rec-TfR1 HepG2 cells

10%FCS represent maintenance medium. Data is presented as mean  $\pm$  SEM (n=3)

Viability studies revealed that holotransferrin treatment of 5 g/L up to 4 h did not have a major impact on the viabilities of any of the cell lines (figures 4.14, A, B and C).

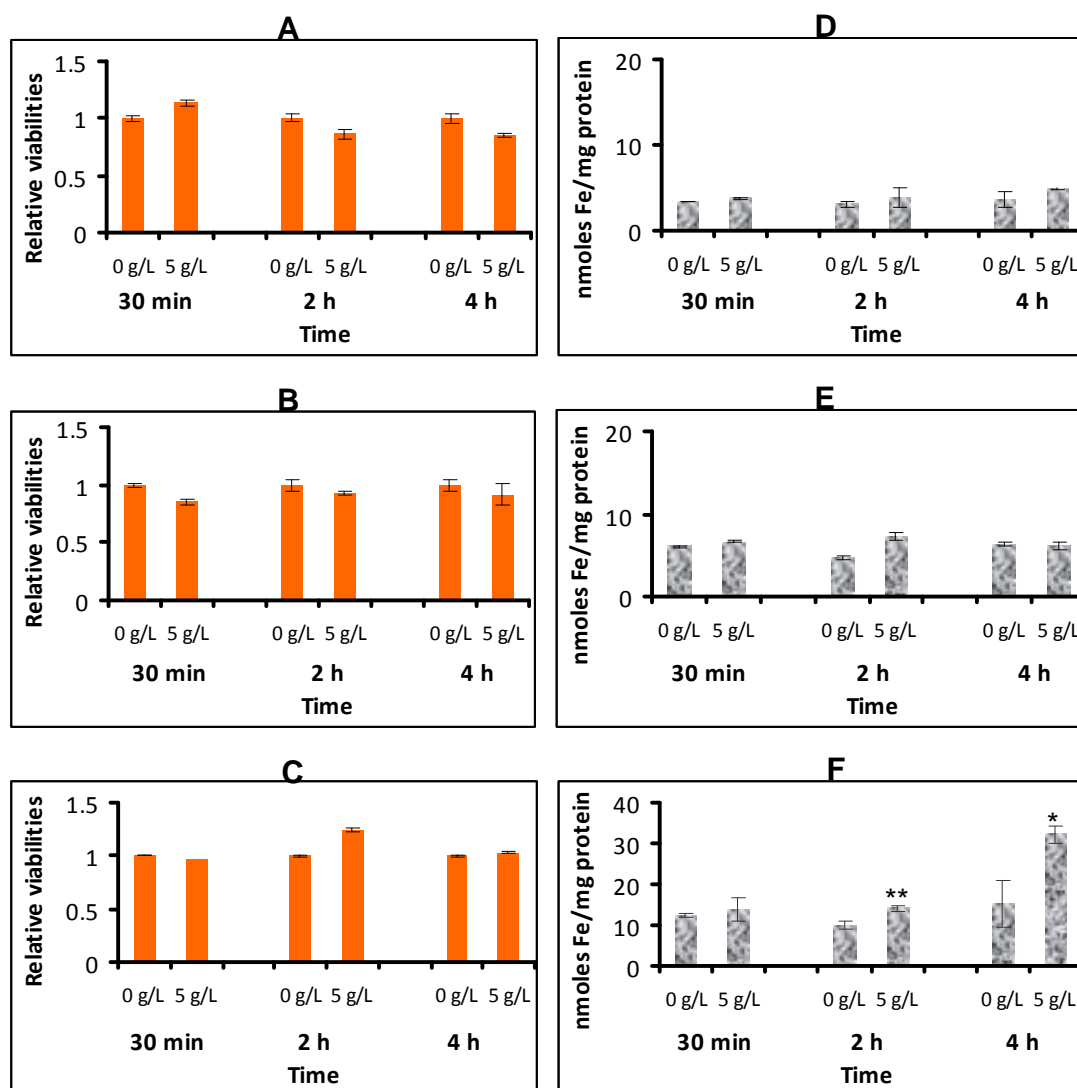


**Fig. 4.14 Viability studies and iron uptake in HepG2 cells under holotransferrin treatment : 4 h study**

HepG2 cells were treated with 5 g/L holotransferrin for 4 h as described in methods section 2.2.15. Cell viability and intracellular iron levels after treatments were determined as described in legend of Fig. 4.4. Viability of treated cells (5 g/L holotransferrin) was expressed relative to viability of untreated cells (0 g/L) at each time point.

**A, B and C :** Effect of holotransferrin treatment on viability of Wt HepG2, HepG2 (p) and rec-TfR1 HepG2 cells, respectively.

**D, E and F :** Effect of holotransferrin treatment on intracellular iron levels in Wt HepG2, HepG2 (p) and rec-TfR1 HepG2 cells, respectively.

Data is presented as mean  $\pm$  SEM (n=3). \*  $p < 0.05$ , \*\*  $p < 0.01$  compared to untreated control at respective time points.

Likewise, the Wt HepG2 and HepG2 (p) cells generally showed constant levels of intracellular iron regardless of high extracellular iron highlighting that the iron uptake regulatory mechanisms in these cells were functional (figures 4.14, D and E). In comparison, the rec-TfR1 HepG2 cells not only showed considerably higher basal levels of iron but also significantly increased iron uptake upon holotransferrin treatment for 2 and 4 h by approximately 1.4- and 2.1-fold, respectively (Fig. 4.14F), a feature of these cells as observed earlier (Fig. 4.8C).

Gene expression analysis under holotransferrin treatments in the three HepG2 cell lines under study has been captured in figures 4.15-4.17. In the Wt HepG2 cells (Fig. 4.15), holotransferrin treatment did not significantly affect the mRNA expression of *TfR1*, *ferroportin* and *HFE* genes in the first 30 min. When the duration of treatment increased to 2 h and 4 h, the expression of *TfR1* significantly decreased ( $p < 0.02$  and  $p < 0.01$ , respectively) compared to the untreated control at each time point. This was expected as the Wt HepG2 cells express IRE-regulated *TfR1* mRNA which made the cells sensitive to intracellular iron levels and prevented any further iron uptake on reaching cellular iron sufficiency by down-regulation of *TfR1*. While the other genes were stably expressed, *hepcidin* mRNA levels were up-regulated by 0.7-, 0.4- and 0.6-fold after 30 min, 2 h and 4 h of holotransferrin overdose, respectively, compared to the untreated control at each time point.

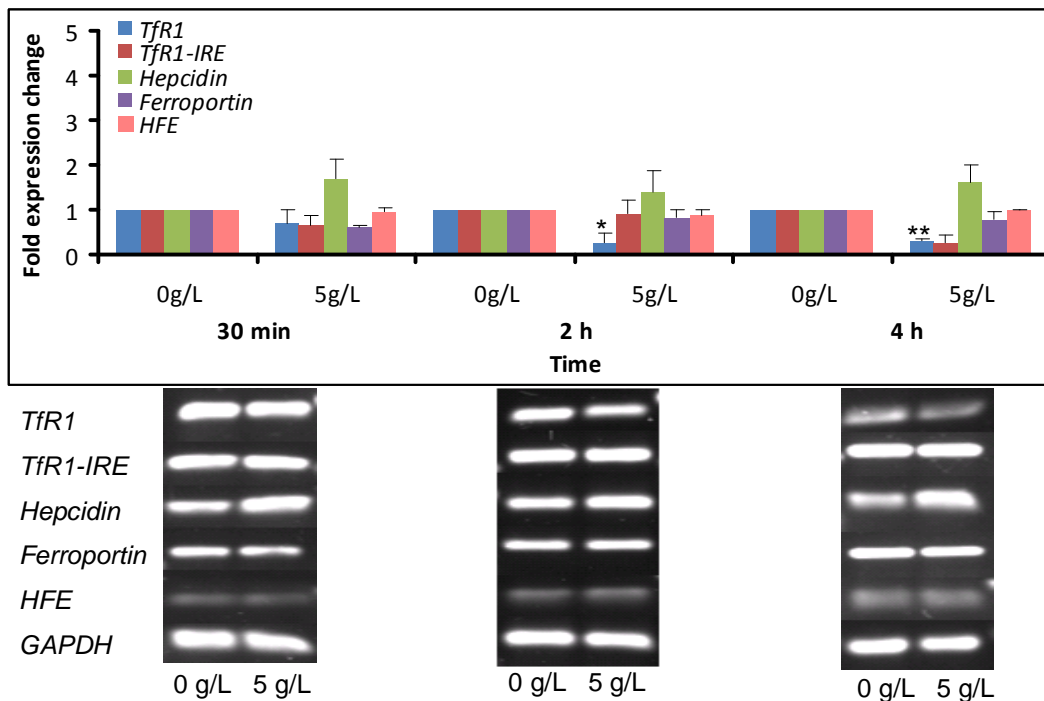


**Fig. 4.15 Effect of holotransferrin treatment on gene expression in Wt HepG2 cells**  
Wt HepG2 cells were treated with 5 g/L holotransferrin up to 4 h and their mRNA expression analysis was per legend of Fig. 4.7. mRNA expression of treated cells (5 g/L holotransferrin) was expressed relative to untreated cells (0 g/L) at each time point. 18  $\mu$ L of RT PCR products were electrophoresed on 1-1.5 % agarose gel. Data is presented as mean  $\pm$  SEM (n=3). \* p<0.02, \*\* p<0.01 compared to untreated control at respective time points.

The HepG2 (p) cells generally showed a similar pattern of gene expression to the Wt HepG2 cells (Fig. 4.16). Although these cells appeared to show increased *hepcidin* and *ferroportin* expression upon iron overdose, it was observed that these increases resulted from the changes in expression of the reference gene in these cells rather than changes in expression of *hepcidin* and *ferroportin* (appendix XVI). This conclusion was based on the  $C_T$  values of *hepcidin* and *ferroportin* as well as the products observed on the gel, which remained unchanged under untreated and treated conditions at all time points.

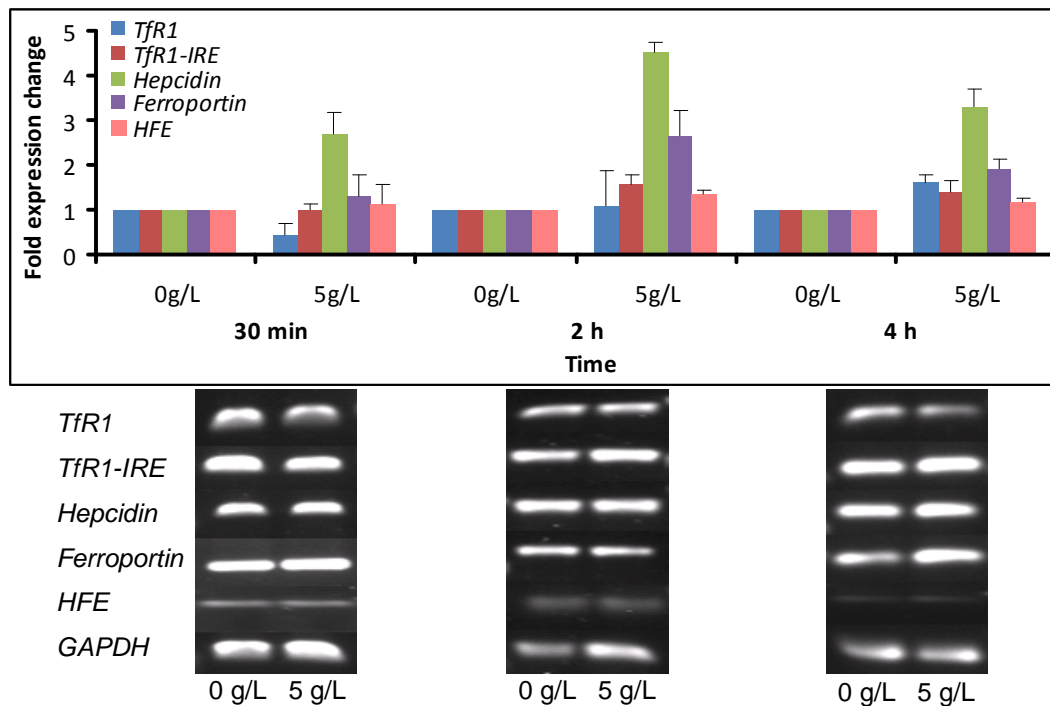


**Fig. 4.16 Effect of holotransferrin treatment on gene expression in HepG2 (p) cells**  
HepG2 (p) cells were treated with 5 g/L holotransferrin up to 4 h and their mRNA expression analysis was per legend of Fig. 4.7. mRNA expression of treated cells (5 g/L holotransferrin) was expressed relative to untreated cells (0 g/L) at each time point. 18  $\mu$ L of RT PCR products were electrophoresed on 1.5 % agarose gel. Data is presented as mean  $\pm$  SEM (n=3).

The rec-TfR1 HepG2 cells displayed their typical characteristic of up-regulation of *TfR1* mRNA under holotransferrin treatment (Fig. 4.17) as previously observed in Fig. 4.9A. Although *hepcidin* and *HFE* expression did not significantly change, *ferroportin* expression showed a pattern of increasing expression as the duration of treatment increased, similar to the pattern of iron uptake by these cells as seen in Fig. 4.14F.

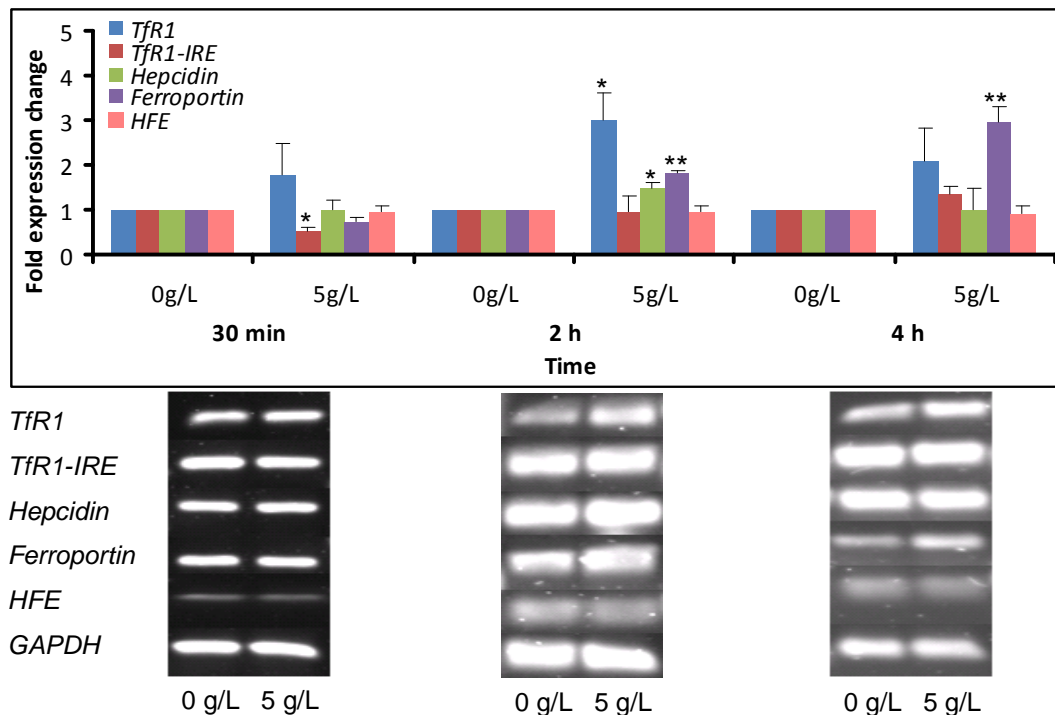


**Fig. 4.17 Effect of holotransferrin treatment on gene expression in rec-TfR1 HepG2 cells**  
 Rec-TfR1 HepG2 (p) cells were treated with 5 g/L holotransferrin up to 4 h and their mRNA expression analysis was per legend of Fig. 4.7. mRNA expression of treated cells (5 g/L holotransferrin) was expressed relative to untreated cells (0 g/L) at each time point. 18  $\mu$ L of RT PCR products were electrophoresed on 1-1.5 % agarose gel. Data is presented as mean  $\pm$  SEM (n=3). \*  $p < 0.02$ , \*\*  $p < 0.01$  compared to untreated control at respective time points.

Although Wt HepG2 and HepG2 (p) cells showed similar patterns of gene expression with holotransferrin overdose over time, some differences surfaced with respect to *hepcidin* and *ferroportin* gene expression (figures 4.18 A and B). In Wt HepG2 cells, where *hepcidin* expression was down-regulated, the HepG2 (p) cells showed an elevated response after 30 min which gradually subsided after 4 h to a level similar to that in Wt HepG2 cells. Likewise, *ferroportin* mRNA levels were found to be generally up-regulated compared to the Wt HepG2 cells. The rec-TfR1 HepG2 cells exhibited a different response (figures 4.18 C and D). Notably, after 30 min, the cells showed increased *TfR1-IRE*, *hepcidin*, *HFE* and *ferroportin* expression. It was observed again that *HFE* and *hepcidin* expression mirrored

each other. At 2 h and 4 h, the rec-TfR1 HepG2 cells expressed *HFE* and *ferroportin* genes at higher levels than the Wt HepG2 cells at the same time points.

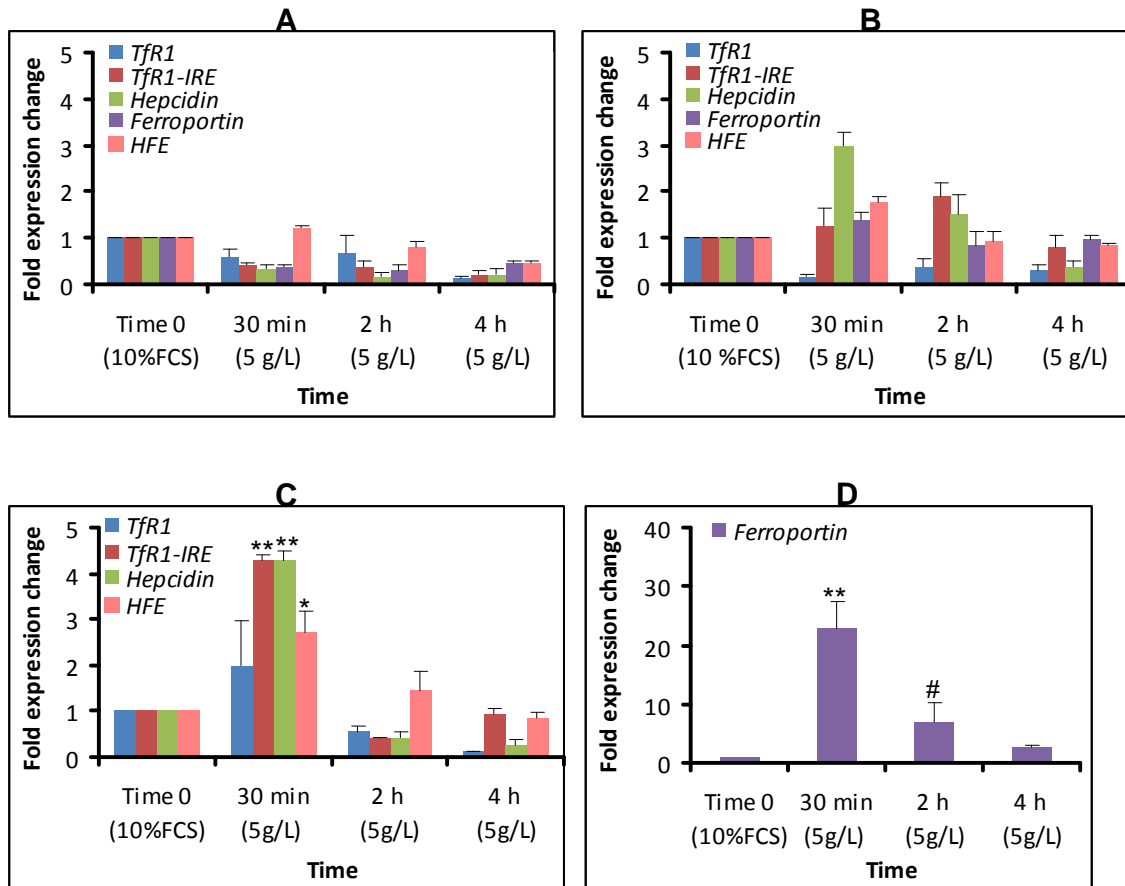


**Fig. 4.18 Gene expression in HepG2 cells under holotransferrin overdose over time**  
 The figure shows changes in gene expression over time in  
**A:** Wt HepG2 cells; **B :** HepG2 (p) cells ; **C and D :** Rec-TfR1 HepG2 cells  
 Data is presented as mean± SEM (n=3). \* p<0.05, \*\* p<0.01, compared to time 0,  
 # p<0.05 compared to 30 min.

#### 4.2.8 Iron overdose and hepcidin secretion by HepG2 cells

Holotransferrin overdose to the HepG2 cells resulted in increased hepcidin peptide secretion (Fig. 4.19). As seen in the figure, Wt and rec-TfR1 HepG2 cells increased hepcidin peptide secretion regardless of a prior 24 h period of serum deprivation. Fig. 4.19B shows that the Wt HepG2 cells significantly

increased hepcidin secretion in the first 24 h exposure to holotransferrin overdose followed by a plateau in Wt HepG2 and HepG2 (p) cells. Unlike this, the rec-TfR1 HepG2 cells showed a significant steady increase in hepcidin peptide levels up to 48 h.

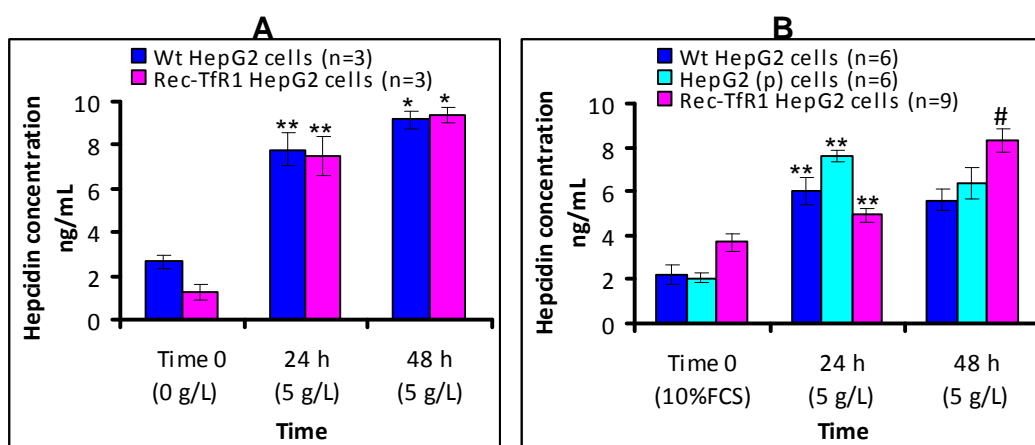


**Fig. 4.19 Effect of prolonged iron overdose on hepcidin peptide secretion by HepG2 cells**

Wt and rec-TfR1 HepG2 cells were serum starved for 24 h (time 0) and treated with 5 g/L holotransferrin for 48 h, as described in methods section 2.2.15. Cell-surface expression of TfR1 was studied at various time points after treatment as described in methods section 2.2.20. Determination of the level of hepcidin excreted in the treatment medium was as explained in methods section 2.2.22.

**A and B:** Hepcidin peptide levels in HepG2 cells after a prior period of serum deprivation and without any period of serum deprivation, respectively.

10% FCS represent maintenance medium. Data is presented as mean  $\pm$  SEM.

\*  $p < 0.05$  compared to 24 h, \*\*  $p < 0.01$  compared to time 0, #  $p < 0.01$  compared to 24 h.

Similarly, holotransferrin overdose for a short period of 4 h resulted in increased hepcidin peptide secretion (~2-fold) by all the HepG2 cell lines (Fig. 4.20). In the case of rec-TfR1 HepG2 cells, the released levels of hepcidin were significantly higher than the untreated cells as well as cells in the maintenance medium. In the maintenance medium, the Wt and rec-TfR1 HepG2 cells secreted constant levels of hepcidin, although the secretion was decreased in rec-TfR1 HepG2 cells at 4 h

( $p < 0.01$ ). Serum and iron deprivation (0 g/L) up to 4 h resulted in a significant 1.7-fold decrease in hepcidin peptide levels by the Wt HepG2 cells compared to 0 g/L treatment for 2 h.

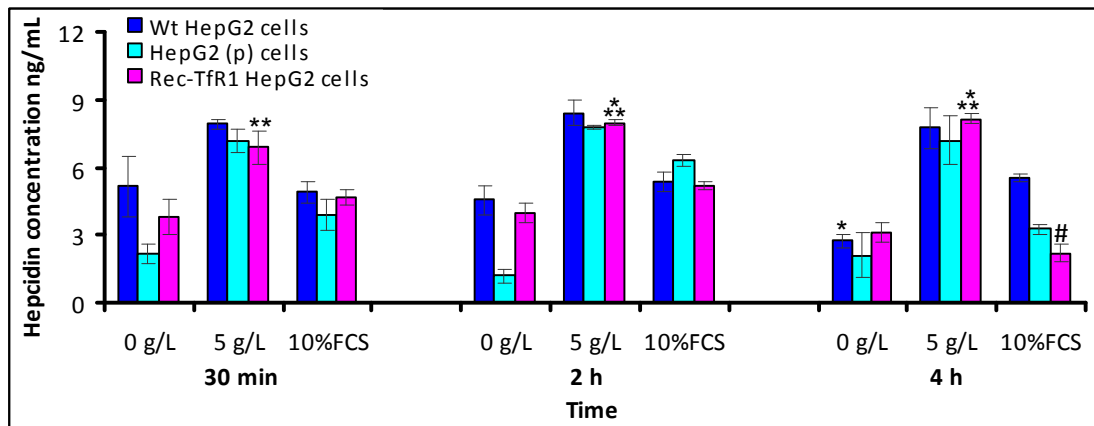


**Fig. 4.20 Effect of iron overdose on hepcidin peptide secretion by HepG2 cells**  
HepG2 cells were treated with holotransferrin overdose for 4 h and the hepcidin peptide levels were measured as described in legend of Fig. 4.17. 10%FCS represent maintenance medium. Data is presented as mean  $\pm$  SEM (n=3). \*  $p < 0.058$  compared to 2 h 0 g/L, \*\*  $p < 0.05$  and \*\*\*  $p < 0.02$  compared to 0 g/L at respective time points. #  $p < 0.01$  compared to 2 h in maintenance medium (10%FCS).

### 4.3 Discussion

To date, experiments conducted by different groups showed that *hepcidin* mRNA expression varied on exposure to iron overdose (Gehrke et al., 2003, Jacolot et al., 2008, Nemeth et al., 2003, Rapisarda et al., 2010). The observed variability in results was primarily due to the lack of an appropriate model system that would mimic human physiological conditions. In the present study, while trying to establish a suitable cell model for iron-related studies, iron overdose experiments were designed with the intention of observing the same effect on hepcidin expression as observed in human and animal models (Lin et al., 2007, Nemeth et al., 2003, Pigeon et al., 2001).

Hepcidin-25 has been shown to bind iron and it was proposed that iron may play an important role in regulating hepcidin expression (Farnaud et al., 2008). Based on this information, in the present study it was hypothesised that intracellular iron overload would cause a rise in *hepcidin* mRNA expression and that such an increase in HepG2 cells would not require the presence of other cell types. To check this hypothesis, mRNA expression of *hepcidin* and other iron-related genes were analysed upon iron exposure. Through this, the intention was to study how iron regulates *hepcidin* gene expression, which has not been previously understood.

Before proceeding with iron supplementations, the proportion of holotransferrin in the transferrin treatment medium was determined by using a 6 M urea gel assay (section 2.2.13). Results showed that the transferrin preparation used for iron supplementation experiments possessed a high proportion (approximately 80%) of holotransferrin (Fig. 2.4). This confirmed that the cells would be surrounded by an iron-rich environment to enable intracellular iron overload. Holotransferrin concentrations ranging from 1g/L to 5 g/L were initially chosen for iron supplementations to cover the normal human physiological range of transferrin (2-4 g/L) (Sternberg, 1986) and to create an iron-rich environment to facilitate intracellular iron overload.

As seen in chapter 3 (Fig. 3.25) holotransferrin overdose to CHO TRVb1 cells did not lead to intracellular iron overload but increased the secretion of hepcidin peptide levels (Fig. 3.26). To investigate whether intracellular iron overload could

affect *hepcidin* gene expression, rec-TfR1 HepG2 cells were created such that they expressed an IRE-independent *TfR1* mRNA to maximise iron uptake. Using these cells, *hepcidin* expression and several other genes and iron-related aspects were studied.

#### **4.3.1 Regulation of iron uptake by TfR1**

In order to confirm the expression of recombinant TfR1 on the cell membrane of rec-TfR1 HepG2 cells, the level of total TfR1 proteins on the cell-surfaces of Wt HepG2 and rec-TfR1 HepG2 cells were compared. As expected, the rec-TfR1 HepG2 cells displayed higher basal levels of cell-surface TfR1 than Wt HepG2 cells (figures. 4.1D and 4.2D).

In the Wt HepG2 cells, serum deprivation followed by holotransferrin overdose resulted in an increased expression of TfR1 on the cell surface (Fig. 4.1E). Such a response reflected the cells' necessity for increased iron uptake for survival and growth, particularly after a period of serum starvation. After 24 to 48 h the cells may have reached intracellular iron sufficiency and hence the plateau or a slight down-regulation of TfR1, as seen at the 48 h time point (Fig. 4.1E). The mechanism is supported by the results obtained when the Wt HepG2 cells were treated with holotransferrin overdose without any prior period of serum starvation; in this instance cell-surface TfR1 was found to be down-regulated (Fig. 4.2E). This was an expected response in which cellular iron sufficiency would lead to down-regulation of TfR1 to prevent any further iron uptake. Both responses (i.e. up-regulation of TfR1 following serum and iron deprivation and down regulation under

holotransferrin overdose), are expected and characteristic of the well characterised regulated mechanism in which iron uptake is regulated by the functional *TfR1*-IRE.

In contrast, the rec-TfR1 HepG2 cells showed either constitutive or up-regulated levels of cell-surface TfR1 upon holotransferrin overdose (figures 4.1E and 4.2E). This was expected since the recombinant *TfR1* construct in these cells was devoid of the IRE region. The result of such constitutive and high TfR1 expression on cell surface was that these cells showed higher basal levels of intracellular iron than the Wt HepG2 cells (figures. 4.4C and D). In addition, holotransferrin overdose led to increased iron uptake by the rec-TfR1 HepG2 cells, unlike the Wt HepG2 cells (figures 4.6C and 4.8C; 4.11D and F; 4.14D and F). Together, the results indicated that *TfR1* in the rec-TfR1 HepG2 cells was insensitive to the increase in intracellular iron levels and therefore independent of the regulatory mechanisms exhibited by the IRE region.

Correlating the TfR1 responses observed at protein levels to transcript levels, it was observed that the rec-TfR1 HepG2 cells showed higher basal levels of *TfR1* mRNA and increased *TfR1* mRNA expression upon holotransferrin overdose, unlike the Wt HepG2 cells (figures. 4.5, 4.7A, 4.9A). Decreased *TfR1* mRNA in the Wt HepG2 cells under holotransferrin treatments observed in this study is similar to that observed by Gehrke *et al.* (2003). The most striking difference between the Wt HepG2 and rec-TfR1 HepG2 cells was that 5 g/L holotransferrin treatment for 6 and 24 h led to a down-regulation of *TfR1* mRNA in Wt HepG2 cells (Fig.4.7A) and an up-regulation in the rec-TfR1 HepG2 cells (Fig. 4.9A).

Another observation was that, as expected, serum and iron deprivation increased *TfR1* mRNA levels in both the Wt HepG2 (similar to that reported by Jacolot et al. (2008)) and the rec-TfR1 cells. However, the *TfR1-IRE*, which is a reflection of the endogenous *TfR1*, was up-regulated in Wt HepG2 cells but not to the same extent in rec-TfR1 HepG2 cells (figures. 4.7B and 4.9B). This could be explained as follows. Along with the IRE-independent *TfR1* mRNA, the rec-TfR1 HepG2 cells possess the endogenous *TfR1* with its regulatory IRE region. High cell-surface TfR1 (Fig. 4.2D) along with high basal intracellular iron levels in these cells prevented any major increase in the endogenous *TfR1*, i.e. *TfR1-IRE* mRNA. Hence it could be concluded that the up-regulation of *TfR1* mRNA by the rec-TfR1 HepG2 cells, under holotransferrin-free conditions (0 g/L) was more due to *TfR1*-insensitivity towards the high intracellular iron levels rather than cellular necessity to uptake iron.

Together these results highlighted the difference in iron uptake mechanisms between the Wt and rec-TfR1 HepG2 cells, eventually highlighting the significance of TfR1 in regulating iron uptake.

#### **4.3.2 Effect of intracellular iron overload on hepcidin expression**

Although intracellular iron levels in the Wt HepG2 cells were lower than rec-TfR1 HepG2 cells and upon holotransferrin treatments did not show a significant increase in iron uptake (figures 4.4C and 4.6C), *hepcidin* mRNA was up-regulated at 6 h and 24 h in the Wt HepG2 cells (Fig. 4.7C). The approximately 2.9-fold increase in *hepcidin* mRNA upon 1 g/L holotransferrin treatment (24 h) by the Wt

HepG2 cells is similar to that reported by Lin et. al (2007) where 1 g/L holotransferrin treatment to mouse hepatocytes for 18-24 h led to a  $2.5 \pm 0.6$  fold increase in *hepcidin* mRNA compared to iron-free medium. Also, the 0.6-fold increase (24 h) and 0.8-fold decrease (48 h) in *hepcidin* mRNA upon 5 g/L holotransferrin treatment observed in this study is similar to that observed by Jacolot et al. (2008), where 24-48 h treatment with 4.5 g/L holotransferrin resulted in a 0.82-fold decrease in *hepcidin* mRNA. Likewise, an average 0.6-fold increase in *hepcidin* mRNA following 5 g/L holotransferrin treatment for 30 min, 2 and 4 h, was also observed in the Wt HepG2 cells (Fig.4.15).

In comparison, although the rec-TfR1 HepG2 cells showed high basal intracellular iron levels and increased intracellular iron uptake upon holotransferrin treatments, the expected increase in *hepcidin* mRNA levels was not observed (Fig. 4.9C and 4.17). Interestingly, 2 h of 5 g/L holotransferrin treatment caused a significant 0.5-fold increase in *hepcidin* mRNA followed by significant increase in *ferroportin* mRNA expression after 2 h and 4 h (Fig. 4.17). This scenario proposes a two-stage response under intracellular iron overload. In the first stage *hepcidin* mRNA expression shows a subtle physiological increase (here 0.5-fold) in an attempt to regulate high extracellular iron levels. However, prolonged high extracellular iron exposure along with increased intracellular iron levels leads to an increase in *ferroportin* expression to remove the excess iron, rather than further increasing *hepcidin* mRNA levels in an attempt to regulate extracellular iron levels.

Thus, data suggests that under these experimental conditions a minor increase in intracellular iron levels led to an increase in *hepcidin* mRNA, as expected, but a major and further increase in intracellular iron levels did not lead to a further increase in *hepcidin* mRNA levels. The observed increase in *hepcidin* mRNA in the Wt HepG2 cells, where there was no significant increase in intracellular iron levels, suggests that *hepcidin* mRNA levels subtly increase only under physiologically relevant conditions (i.e. optimal intracellular iron levels along with minor increases in extracellular iron levels).

To complement the *hepcidin* mRNA studies, hepcidin peptide levels secreted into the medium were measured. Unlike the mRNA levels, hepcidin peptides exhibited a different response to extracellular holotransferrin overdose. For the first time, through this study it was shown that hepcidin peptide levels significantly increased upon holotransferrin overdose (figures 4.19 and 4.20) and decreased upon iron deprivation in a cell culture system (Fig. 4.21), as observed in human and animal models (Lin et al., 2007, Nemeth et al., 2003, Pigeon et al., 2001).

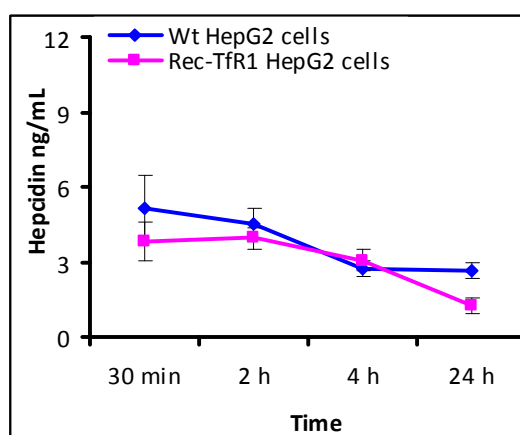


**Fig. 4.21 Hepcidin secretion by HepG2 cells under iron deprivation**

Effect of serum and iron deprivation (0 g/L) on hepcidin peptide secretion over time is shown. Data is presented as mean  $\pm$  SEM (n=3)

Although holotransferrin overdose triggered hepcidin peptide production, it was observed that FCS had a better capacity to induce hepcidin peptide secretion than holotransferrin overdose. As shown in Fig. 4.22, compared to the maintenance medium, 17-fold higher iron levels could only lead to a 1.6-fold increase in hepcidin peptide production. Results reported by other groups showed that serum factors in the FCS played a significant role in triggering *hepcidin* transcription (Dzikaite et al., 2006). In the present study, the influence of FCS was observed at peptide levels as well. This suggests that hepcidin peptide secretion is not only influenced by intracellular or extracellular iron status, but also by a combination of various factors.

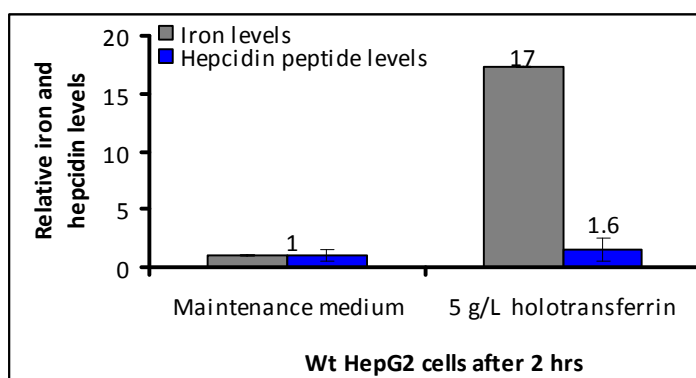


**Fig. 4.22 Hepcidin induction by holotransferrin and maintenance medium**

#### 4.3.3 Influence of holotransferrin concentration and exposure-time on hepcidin

In this study it was observed that an increase in *hepcidin* transcription in Wt HepG2 cells was not directly proportional to an increase in extracellular holotransferrin concentration (Fig. 4.23). A similar response has been reported where low dosage of Fe-NTA (1- 3  $\mu$ M) induced *hepcidin* transcription and high dosage of 65  $\mu$ M Fe-NTA resulted in its down-regulation below basal levels (Fein et al., 2007). Since the purpose of hepcidin is to regulate circulating iron levels, such a response is an

attempt by the cell to regulate high extracellular iron levels. Thus, Fig. 4.23 shows the influence of increasing holotransferrin concentration on *hepcidin* mRNA levels.

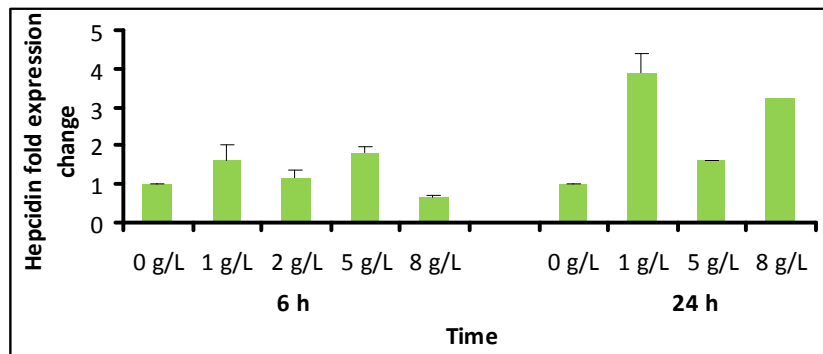


**Fig. 4.23 *Hepcidin* mRNA response towards increasing holotransferrin concentrations**

Pattern of hepcidin mRNA levels exhibited by Wt HepG2 cells is shown. Data is presented as mean  $\pm$  SEM (n=2)

Where previous studies showed that recombinant hepcidin is secreted in the medium within 1 h of its synthesis (Wallace et al., 2006), in this study, hepcidin peptides showed an immediate response to holotransferrin overdose. Both, the HepG2 and the CHO TRVb1 cell lines secreted hepcidin into the medium within 30 minutes of increased iron exposure (figures 3.15 and 4.20). This fast response is not surprising as hepcidin is a hormone and its secretion in the extracellular environment should be a rapid process to be able to exhibit a quick response. There could be two possible scenarios mediating this quick response. Firstly, transcription of *hepcidin* gene could occur even earlier than 30 min. A quicker generation of preprohepcidin at the mRNA level is possible because it is only 430 bases long. Secondly, hepcidin could be quickly secreted from the proposed prohepcidin pools stored within the cells (Farnaud, personal communication). Since the Wt and rec-TfR1 HepG2 cells showed similar increases in hepcidin peptide secretion on iron overdose, both at shorter and longer exposure time to

holotransferrin overdose (figures 4.19 and 4.20), where their *hepcidin* mRNA levels were variable (figures 4.7C and 4.9C), secretion of hepcidin from prohepcidin pools is probable.

The response of hepcidin was also seen to be influenced by exposure time to holotransferrin. Fig. 4.24 shows the effect of holotransferrin overdose on hepcidin secretion over time.

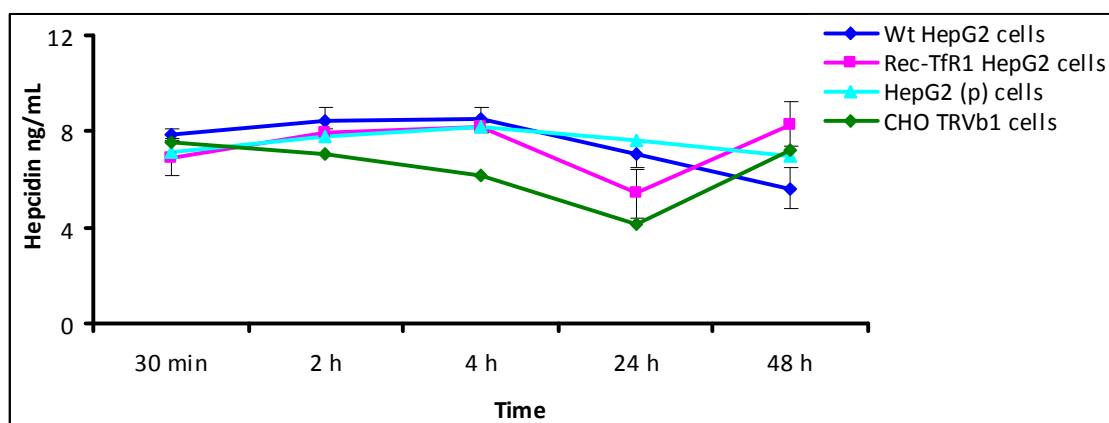


**Fig. 4.24 Hepcidin peptide release under holotransferrin overdose over time**  
Effect of 5 g/L holotransferrin on hepcidin peptide secretion over time is shown. Data is presented as mean  $\pm$  SEM (n=3)

Both the recombinant cell types i.e., the CHO TRVb1 cells and the rec-TfR1 HepG2 cells showed comparatively low hepcidin secretion at 24 h and an increase again at 48 h. This drop followed by an increase predicts the same pattern of hepcidin response by the Wt HepG2 cells. Accordingly, the drop in hepcidin levels in the cells of Wt origin as seen at 48 h may be followed by an increase at 72 h. Although the cells of Wt origin (i.e. Wt HepG2 and HepG2 (p) cells) showed similar pattern of hepcidin secretion, it was different from that of the recombinant cells (i.e. rec-TfR1 HepG2 and CHO TRVb1 cells). The reason for these differences in

hepcidin responses could be attributed to TfR1 in these cells; the CHO TRVb1 possess over-expressed human TfR1 and the rec-TfR1 HepG2 cells possess over-expressed *TfR1* which is devoid of the *IRE*-region, unlike the Wt and HepG2 (p) cells. These results highlight the role of TfR1 in hepcidin induction, probably via the proposed HFE-TfR1 dissociation mechanism (Schmidt et al., 2008).

#### **4.3.4 Relationship between HFE and hepcidin**

The effect of TfR1-regulated iron uptake on hepcidin expression suggests a probable link between HFE and hepcidin expression. It has been shown that HFE influences hepcidin expression. The absence of HFE abolishes *hepcidin* mRNA up-regulation in the HepG2 cells (Gao et al., 2009). Similarly in the case of HFE-related haemochromatosis, the absence of HFE on the cell surface is linked to reduced *hepcidin* mRNA (Bridle et al., 2003). Since both hepcidin and HFE are predominantly expressed in hepatocytes (Holmstrom et al., 2003, Zhang et al., 2004) an inter-dependence between an up-regulated hepcidin response and the level of HFE expression can be envisaged.

In the present study the rec-TfR1 HepG2 system can be described as being “haemochromatotic” since it is characterised by high intracellular iron content which is the case in haemochromatosis, however, with a major difference. Haemochromatosis is characterised by low levels of circulating hepcidin which is suggested to be linked with a mutated HFE which does not reach the cell surface (Feder et al., 1996, Bridle et al., 2003) and therefore cannot induce hepcidin

synthesis. In contrast the rec-TfR1 HepG2 cells showed increased hepcidin peptide production on iron treatment (figures. 4.19 and 4.20), possibly due to the presence of functional HFE on its cell-surface.

Additionally, in this study, the expression of *hepcidin* and *HFE* genes mirrored each other at the mRNA level. *Hepcidin* mRNA expression increased only in the presence of stable or increased *HFE* mRNA expression (figures. 4.12C and 4.18C). Since hepcidin regulates systemic iron levels and HFE is necessary to exhibit a hepcidin response, it could be concluded that HFE contributes to the regulation of extracellular iron levels via hepcidin. Since a relation between *hepcidin* and *HFE* expression at mRNA and protein level is shown to exist, it is important to fully understand which one of the two, HFE and hepcidin, regulated the other. This issue has been addressed in the following chapter.

Like hepcidin, the expression of *HFE* was also observed to be dependent on the duration of exposure to holotransferrin. Cell exposure to high holotransferrin levels for a shorter time span did not lead to any significant changes in *HFE* expression (figures 4.15-4.17). However, notable changes were observed at longer exposure times (figures. 4.7E and F; 4.9E and F). Correlating this to hepcidin peptide levels, hepcidin was induced regardless of the differences in *HFE* gene expression (figures. 4.19 and 4.20). Based on the proposed mechanism of hepcidin induction by Schmidt et al. (2008), it could be explained that high dosage of iron for a shorter time span (i.e. up to 4 h) led to hepcidin induction due to cell-surface dissociation of TfR1 from the HFE allowing free HFE to then bind to TfR2 to induce hepcidin

expression. However, when the cells were exposed for a long time (e.g. 6 to 24 h), the mechanism of cell-surface dissociation of HFE from TfR1 may not be sufficient to deal with increased extracellular iron. Hence notable changes in *HFE* mRNA expression were observed at the later time points. Thus, it could be concluded that the response of HFE to induce hepcidin was dependent on the time of iron-exposure.

#### 4.3.5 Effect of intracellular and extracellular iron levels on *HFE*

It has been shown that in mouse hepatocytes the function of HFE is to bind to TfR1 and regulate iron uptake by the cells (Chua et al., 2008). In the present study it was observed that increasing iron overdose to Wt HepG2 cells led to increased *HFE* mRNA expression, particularly at 6 h (Fig. 4.25A).

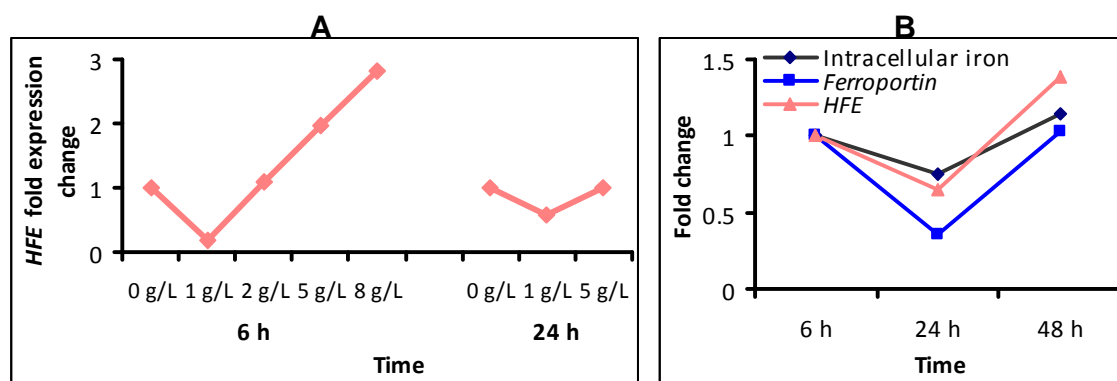


**Fig. 4.25 *HFE* sense iron levels**

**A:** *HFE* in Wt HepG2 cells sense extracellular iron levels

**B:** *HFE* in rec-TfR1 HepG2 cells sense intracellular iron levels under basal conditions.

This is an expected response when extracellular iron levels are high and the cells' attempt to control iron uptake via the HFE-TfR1 association, as proposed (Fleming and Britton, 2006). Since the Wt HepG2 cells did not show intracellular iron overload, the increase in *HFE* mRNA could be attributed exclusively to the

increasing extracellular holotransferrin concentrations, suggesting that the *HFE* is sensitive to extracellular iron levels. On the other hand, the similarity in patterns of intracellular iron content, *ferroportin* and *HFE* gene expressions in rec-TfR1 HepG2 cells when in maintenance medium possibly suggests that the HFE participated in sensing intracellular iron levels (Fig. 4.25B).

However, the existence of high intracellular iron levels in the rec-TfR1 HepG2 cells implies that the expected regulatory function of HFE via HFE-TfR1 association could not be executed due to the over-expression of TfR1 on the cell surface of these cells. Probably a certain ratio of HFE and TfR1 on the cell surface is required for the physiological regulation of iron uptake by the cells, which would suggest that in the rec-TfR1 HepG2 cells the expression of HFE was not sufficient to interact with the high number of TfR1 receptors on the cell surface and perform its suggested function of limiting iron uptake. The disturbance in this normal ratio in rec-TfR1 HepG2 cells led to uncontrolled iron uptake by these cells.

Unlike the Wt HepG2 cells, the *HFE* expression in rec-TfR1 HepG2 cells decreased with increasing holotransferrin concentration at the 24 h time point (Fig. 4.26). This decrease in HFE expression was similar to the decrease in *TfR1*-IRE which sensed the increase in intracellular iron levels and therefore decreased its mRNA expression, as expected. Since no IREs have been identified on *HFE* as yet, it is likely that *HFE* sensed iron status via *TfR1*. This confirms a correlation between the HFE and TfR1 as previously shown where HFE expression in HepG2

cells which were devoid of HFE led to an increase in *TfR1* mRNA (Gao et al., 2008).

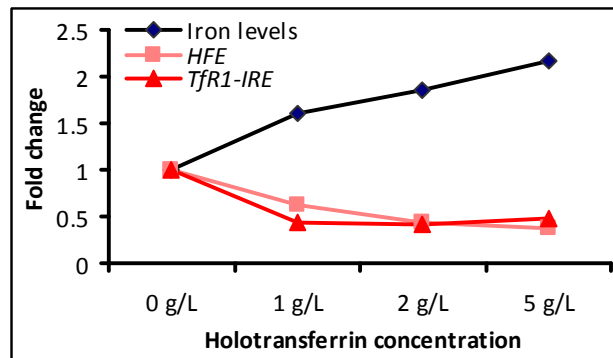


**Fig. 4.26 Iron sensing by *HFE* in rec-TfR1 HepG2 cells under increasing holotransferrin concentrations**

If the proposition of iron sensing via *HFE* is correct, then the presence of an 'iron insensitive' *TfR1* in the rec-TfR1 HepG2 cells may have informed the *HFE* incorrectly of the intracellular iron status. Consequently, instead of increasing *HFE* expression to control iron uptake, the cells decreased *HFE* levels upon holotransferrin overdose despite the high intracellular iron content. This resulted in an uncontrolled iron uptake by the recombinant TfR1 on the cell surface. Thus this suggests that *HFE* controls and is controlled by intracellular iron levels via the TfR1. Essentially, when HFE is absent on the cell surface as in case of haemochromatosis, or present in lesser amounts compared to TfR1 as in the rec-TfR1 HepG2 cells, regulated iron uptake by cells is abolished resulting in intracellular iron overload and prevention of increased hepcidin induction.

#### 4.3.6 HepG2 cells have an iron holding threshold

HepG2 cells belong to the cell lineage of hepatocytes which are known for their iron storing function. Hence these cells should be capable of accommodating large amounts of iron. However, increased *ferroportin* expression in the rec-TfR1 HepG2 cells (figures. 4.12D, 4.17, 4.18D) showed that the cells were losing intracellular iron. Such up-regulation in hepatic *ferroportin* mRNA expression was also observed in haemochromatotic patients where intracellular iron levels were high (Bridle et al., 2003). This implies that the iron-storing cells can hold a large amount of iron but only up to a certain threshold and perhaps only under a normal physiological environment where the levels of iron are 'manageable' by the cells. Once the cells reach a certain iron-holding threshold, *ferroportin* expression would be raised to remove the excess intracellular iron to mediate intracellular iron homeostasis.

In conclusion, it is certain that the homeostasis of extracellular/circulating iron levels is a complex process and it would be incorrect to state that hepcidin alone is the iron homeostasis regulator. As seen in this study, it involves an interaction between the key iron-related genes studied here and possibly may involve many more iron-related genes. Hepcidin would be synthesised, secreted and execute its function of maintaining iron homeostasis only if all interactions between genes and proteins function optimally.

## Chapter 5

### Significance of preprohepcidin derivatives

#### 5.1 Introduction

HFE-associated haemochromatotic patients as well as iron overloaded *HFE*<sup>-/-</sup> mice showed decreased levels of *hepcidin* mRNA (Bridle *et al.*, 2003). Thus it has been observed that HFE influences hepcidin synthesis. Parallel to this, in the current study the transcription of *hepcidin* and *HFE* genes mirrored each other where increased *hepcidin* mRNA levels accompanied increased *HFE* mRNA levels (chapter 4). Whether the HFE informed hepcidin synthesis or vice versa and whether this information was signalled by a direct physical interaction between HFE and derivatives of preprohepcidin remain to be elucidated.

There are several aspects which support this putative interaction. Firstly, although HFE it is a pseudo major histocompatibility complex (MHC), it has been proposed that the binding groove of HFE is too narrow to accommodate a peptide for typical antigen presentation like the MHC class I molecule (Lebron *et al.*, 1998).

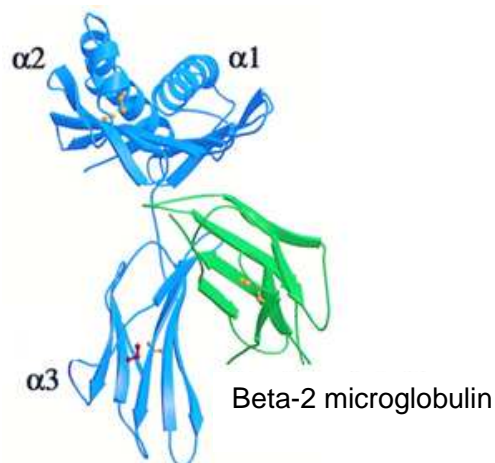


**Fig. 5.1 Crystal structure of cytoplasmic region of HFE protein**  
Alpha 1 and alpha 2 regions of the HFE protein as well as the alpha 3 region which binds to beta-2 microglobulin protein are displayed. Structure adapted from Lebron *et al.* (1998).

However, unpublished results (Moss, personal communication) suggest that the groove is large enough to accommodate a peptide. Additionally, the structural similarity between the HFE and MHC class I molecule (Lebron et al., 1998) support this proposed peptide binding. Secondly, the *HFE* and *MHC I* genes are located on the same chromosome (6p21.3 in humans) quite proximal to each other. Genes located on the same chromosome may belong to the same multigene family which by definition, are “a set of genes descended by duplication and variation from some ancestral gene” (King and Stansfield., 1990). This implies that the genes on the same chromosome, here the *HFE* and *MHC I*, may have a similar or the same function (i.e. peptide binding and its presentation on cell-surface). On the other hand, the fate of the 35-mer pro-region generated as a result of furin cleavage of prohepcidin is unknown.

### **5.1.1 Aims and objectives**

**Aim:** The aim was to understand the significance of preprohepcidin derivatives.

The pro-region of preprohepcidin may bear functional significance. Like the MHC class I molecule, binding of a peptide, possibly a part of the pro-region, may stimulate the HFE to traverse across the endoplasmic reticulum and present the peptide to the cell surface. The presence of a nuclear localisation signal within the pro-region suggests a functional role in the nucleus.

#### **Objectives:**

1. To understand the interaction between preprohepcidin derivatives and HFE *in silico*.
2. To perform localisation studies with the preprohepcidin derivative in Wt HepG2 cells.

## 5.2 Results

### 5.2.1 Identification of hydrophilic regions in preprohepcidin

The hydrophilic regions in a protein are usually exposed on the surface of the protein to enable interactions with surrounding proteins whereas the hydrophobic amino acids are usually buried into the interior of a protein. In order to identify the region of hydrophilicity within the preprohepcidin peptide sequence, a Hopp-Woods hydrophathy plot was created. As per the scaling pattern of the plot, for every amino acid, any value higher than 0 is considered as hydrophilic. In this case the C-terminus of the pro-region was identified as the most hydrophilic (Fig. 5.2). Hence, this region is most likely to be exposed on the outer surface of the peptide and is thus the most potential protein-binding region within preprohepcidin.

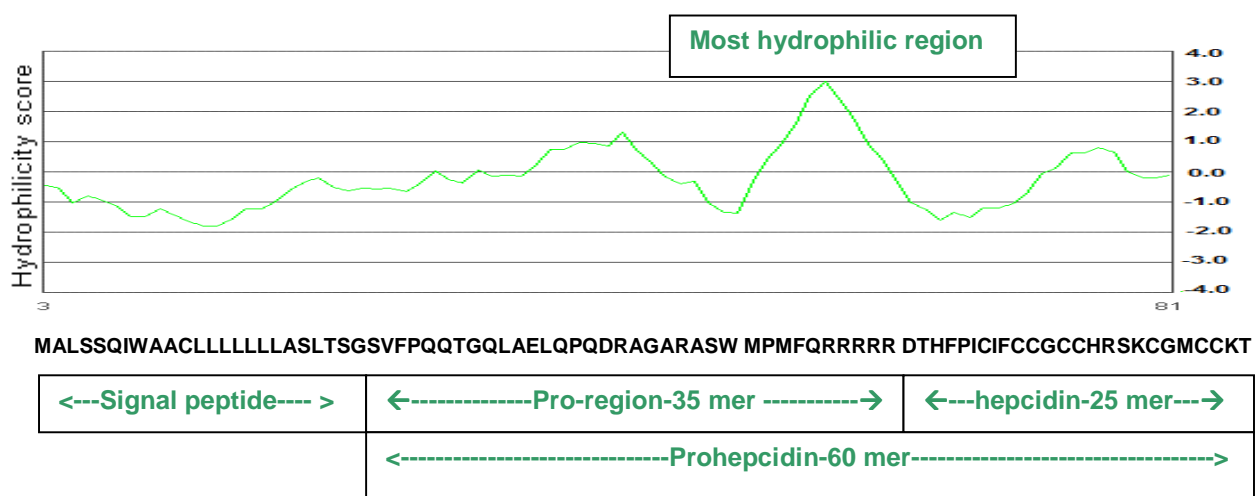


**Fig. 5.2 Hydrophilicity scale for human preprohepcidin**

A Hopp-Woods scale identifies the most hydrophilic regions in preprohepcidin; created at 'Molecular toolkit' (available at <http://www.vivo.colostate.edu/molkit/hydrophathy/index.html>).

### 5.2.2 Putative binding of preprohepcidin derivatives to HFE

Since the HFE bears structural similarity to MHC I molecule (referred as human leucocyte antigen, HLA in humans) (Feder *et al.*, 1996), it was hypothesised that peptide binding to the HLA molecule should be similar to peptide binding to the

HFE molecule. Hence, binding affinities of different serotypes of HLA molecules to different combinations of nonamers from preprohepcidin was assessed through bioinformatics software *HLA\_BIND* at ExPASy. Only those interactions with scores of 100 or above 100 were plotted in the graph (Fig. 5.3). The figure shows the regions within preprohepcidin which may interact with an HLA and hence the HFE. Along with the test interactions, a positive control (i.e. a concatenated amino acid sequence suggested by the software), was also used which gave the highest binding score of 30,000 (data not shown for brevity).

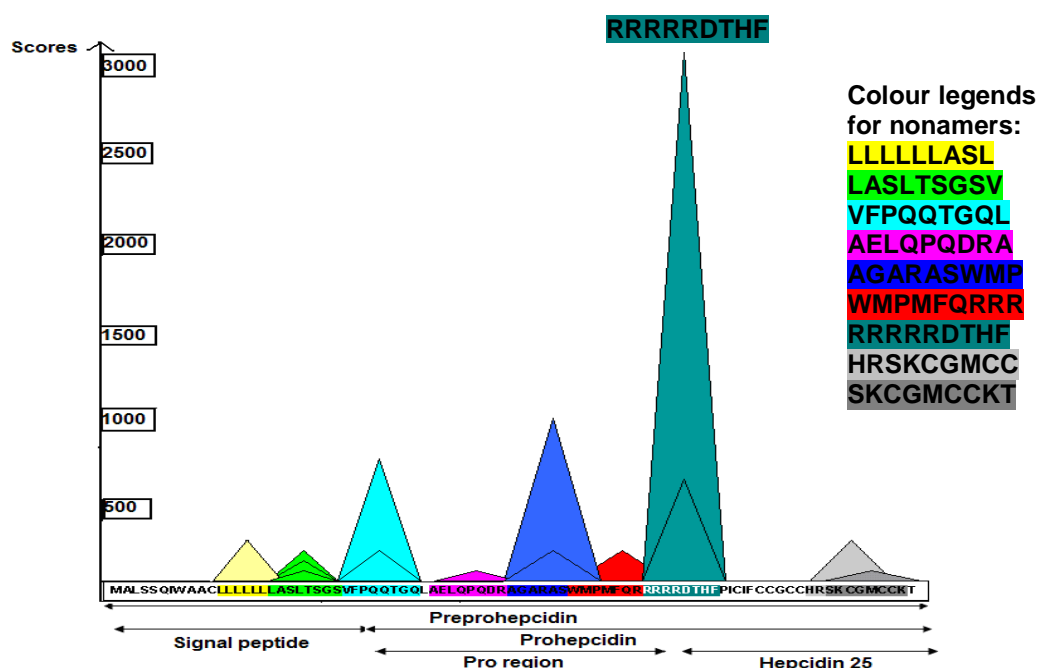


**Fig. 5.3 Graphical representation of binding scores of HLA to different combinations of preprohepcidin nonamers**

Bioinformatics' software *HLA\_BIND* at ExPASy (available at [http://bimas.dcrn.nih.gov/molbio/hla\\_bind](http://bimas.dcrn.nih.gov/molbio/hla_bind)) was used for prediction of MHC class I (HLA) binding to preprohepcidin protein derivatives. All triangles represent scores achieved by a particular nonamer of preprohepcidin with a particular HLA serotype.

The data shows that the nonamer **RRRRRDTHF** scored the highest binding score of 3,000 with the HLA molecule B\_2705. This nonamer is located at the C-terminal region of pro-hepcidin and N-terminal region of bioactive hepcidin-25.

This is a part of the most hydrophilic region within preprohepcidin, as identified previously in Fig. 5.2. Other scores (represented by dark blue triangle) also suggest that the pro-region has a high possibility of interacting with the HLA and hence the HFE. In comparison to the pro-region, the regions in the signal peptide and bioactive hepcidin show the least likelihood of binding to HLA, as per the data extrapolated from the *HLA\_BIND* software.

### 5.2.3 Conservation of regions of potential interaction

Since the  $\alpha$ -1 and  $\alpha$ -2 regions in the HFE molecule form a groove within which the proposed putative peptide binding may occur, conservation of these regions in different species was checked (Fig. 5.4). As seen in the alignment, the  $\alpha$ -1 and  $\alpha$ -2 regions are highly conserved amongst species, which strengthens the possibility of these regions being functionally significant and involved in peptide binding.



**Fig. 5.4 Conservation of alpha regions in the HFE protein in various species**  
 This protein multiple sequence alignment was created using the tool ClustalW2 (available at <http://www.ebi.ac.uk/Tools/msa/clustalw2/>). The alignment highlights regions of conservation in the HFE protein sequence amongst different species.

Key to Fig :

- $\alpha$ -1 and  $\alpha$ -2 regions in the HFE protein
- ---- represents amino acids and \* represents conserved amino acid between species.

Likewise, a clustalx protein multiple sequence alignment of preprohepcidin which involved a variety of species showed high conservation of the leucines and arginines (Fig. 5.5). The leucines are a part of the signal peptide of preprohepcidin and the arginines are a part of the pro-region (boxed). This is the region most hydrophilic and possibly antigenic as shown previously in Fig. 5.2 and Fig. 5.3. Together, it could be concluded that there is conservation of the proposed regions of interaction between the HFE and pro-region of preprohepcidin (Fig. 5.4 and Fig. 5.5).

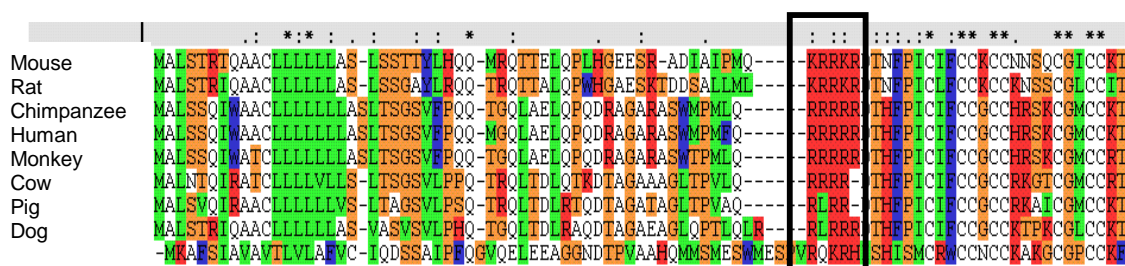


**Fig. 5.5 Conservation of amino acids within the pro-region of preprohepcidin**  
 The alignment was created by using clustalx, a windows interface for ClustalW multiple sequence alignments. It highlights the conservation of arginine residues within the preprohepcidin protein sequence in different species. \* represents conserved amino acid between species.

### 5.2.4 Nuclear localisation signals in preprohepcidin

As seen in Fig. 5.5, the C-terminal region of prohepcidin encompasses repeats of arginines residues, typical to a nuclear localisation signal (Dingwall and Laskey, 1986). The conservation of this region in different species suggested that it may be biologically significant. To ascertain this, the software programme cNLS mapper (Kosugi et al., 2008, Kosugi et al., 2009a) was used to assess the presence of nuclear localisation within the preprohepcidin sequence (Fig. 5.6). As per the programme, a score of 1-2 indicates localisation of the protein in the cytoplasm, a score of 4-5 indicates location of the protein in both the cytoplasm and the nucleus



gi 2598167	8	[11].EE.[4].LDSAQRKLY.[1].DVMLNFRN.[3].VG.[2].SFK.[1].DMISQL.[5].LWM	68		
gi 2623622	5	[11].FE.[4].LDPAQNDLY.[1].DVMLNFSH.[3].LG.[1].AVA.[2].YLVTFI.[5].SSG	65		
gi 12643384	8	[11].EE.[4].LHPAQRKLY.[1].DVMLNFTN.[3].VG.[2].PFH	PFHFLR.[3].FWM	65	
gi 14848338	14	[11].KE.[4].LDLAQRITLY.[1].EVMLNCGI.[3].LG.[1].PVP.[2].ELIHL.	[5].PWT	74	
gi 2342506	217	[11].QE.[4].QDPSKRALS.[1].DTVQESYEN.[3].LE.[1].HIP.[3].VPGTQV.	[5].LWD	278	
gi 2789430	245	[11].ED.[4].LDEWQKELY.[1].NLVKENYKT.[3].LD.[2].GSV.[3].DAPVQA.	[5].PCV	307	
gi 6094362	23	[11].KK.[4].MKSSSEKIVY	VYMKLNVEV.[3].LG.[1].KVT.[2].PFMRSK.	[5].HGN	82
gi 3043610	275	[11].RE.[4].LDRRQKELY.[1].DVMRNVEI.[3].LG.[1].AAA.[2].DLISKI.	[5].FVI	335	
gi 6647873	14	[11].RD.[4].LAPSRNLY.[1].DVMLNFRN.[3].LG.[1].PFT.[2].KVISLI.	[5].PWE	74	
gi 23396993	221	[11].PG.[3].LDSSQVNLV.[1].DEKQNHSS.[3].LG.[1].EIQ.[3].RDLPPV.	[5].KEH	281	
gi 3445131	149	[11].QQ	LHPAQRNFC.[1].NGIWNNSD.[3].AG.[1].CVA.[2].DLVSLI.	[5].FWM	205
gi 3445131	20	[11].QE.[4].LNPIQRNLY.[1].KVMLNFRN.[3].LG.[1].CVS.[2].DVISSL.	[5].PWT	80	
gi 12585544	4	[11].LE.[4].LDTAQRNLY.[1].DVMLNFRN.[3].LG.[1].VVS.[2].DLVTCL.	[5].PLI	64	
gi 20140946	1	[11].QE.[4].LDTAQRALY.[1].RVMLNDFAL.[3].LG.[1].STG.[2].RVVIQI.	[5].PWW	61	
gi 3417237	532	[11].FE.[4].LRPAQRALY.[1].DVMLNFRN.[3].LG.[1].PGP.[2].ALISWM.	[5].AWS	592	
gi 11136027	1	[9].DA.[4].LEPGQRNLY.[1].DTKLETCSN.[3].MG.[1].QDP.[2].GLVSKL.	[5].RWS	59	
gi 1531651	5	[11].FE.[4].LEPVQRNLY.[1].DVMLNFRN.[3].LG.[1].TFS.[2].FLVTFL.	[5].PWF	65	
gi 20141959	4	[11].LE.[4].LRPAQRNLY.[1].DVMLNFRN.[3].LG.[1].VVS.[2].DLITFL.	[5].PWN	64	
gi 6984170	8	[11].EE.[4].LDPVQRNLY.[1].DVMLNFRN.[3].VG.[2].PFK	HDVFLI.[5].LDI	67	
gi 487836	232	[11].QD.[4].LDSAQRNLY.[1].DVMLNFRN.[3].LV.[1].PFT.[2].ALISWL.	[4].FWG	291	
gi 11136100	220	[11].RE.[3].LDPSQRDLI.[1].DNRPENFRN.[3].LG.[1].ETR.[3].RELASK.	[4].TGI	279	
gi 456269	21	[11].QE.[4].LSAYERDLY.[1].DVMLNFRN.[3].LA.[2].SIS.[2].DVISSL.	[5].PWW	82	
gi 12644133	3	[11].AK.[4].LEPVQRDLY.[1].DTKLECSN.[3].MG.[1].QDP.[2].DIVSVL.	[4].PSS	62	
gi 431182	15	[11].QE.[4].LSTQRITLY.[1].KVMSETFRN.[3].VG.[2].KKP.[1].EPSSDL.	[5].EQK	75	
gi 758661	4	[11].KE.[4].LDSAQRITLY.[1].DVMLNFRN.[3].VE.[2].LFK	RDKPYL.[5].PQM	63	
gi 1389741	12	[11].QE.[4].LDPAQRALY.[1].DVMLNFRN.[3].VG.[1].HIT.[2].DMIRKL.	[5].LWT	72	
gi 478627	1	[2].LE.[4].LDTAQRNLY.[1].NVMLNFRN.[3].LG.[1].AVS.[2].DLITCL.	[5].PWN	52	
gi 3915027	23	[11].KK.[4].MKYSEKISY	VYMKRNYKA.[3].LG.[1].KVT.[2].PFMCNK.	[5].QGN	82
gi 3915036	23	[11].KE.[4].MKVSEKIVY	VYMKRNYEA.[3].LG.[1].KAT.[2].PFMRNK.	[5].QGN	82
gi 1731409	1	[11].QD.[4].LRPAQRITLY.[1].EVMLNFRN.[3].LG.[1].SFS.[2].ELITQL.	[5].TWR	61	
gi 2501717	4	[11].FE.[4].LDPDQRNLY.[1].DVMLNFRN.[3].LG.[1].AIS.[2].DLVTCL.	[5].PYN	64	
gi 1731419	27	[11].RQ.[4].LDPAQRITLY.[1].DVMLNFRN.[3].VG.[1].CVA.[2].EMIFKL.	[5].LWI	87	
gi 12643434	28	[11].QE.[4].LDPGQRDLF.[1].DVTLENYTH.[3].IG.[1].QVS.[2].DVISQL.	[5].FVI	88	
gi 6137308	14	[11].QE.[4].LDPAQRSLY.[1].DVMLNFRN.[3].LD.[2].NRD.[1].DEEPTV.	[5].EIE	74	
gi 3025319	4	[11].LE.[4].LDLAQRNLY.[1].DVMLNFRN.[3].VG.[1].TVC.[2].GLITCL.	[5].PWN	64	
gi 11140929	12	[11].QE.[4].LDPSQRALY.[1].DVMLNFRN.[3].VG.[1].CVH.[2].EVIKFL.	[5].FWK	72	
gi 2501714	14	[11].QE.[4].VGPQRSLY.[1].DVMLNFRN.[3].LG.[1].QVS.[2].EVIKFL.	[5].FVI	74	
gi 6137312	14	[11].KT.[4].LDLQRITLY.[1].QVMLNFRN.[3].VG.[1].AFS.[2].NLVSQL.	[5].FVI	74	
gi 141686	1	[3].QE.[4].LDPQRITLY.[1].DVMLNFRN.[3].IG.[1].ELP.[2].EVIKFL.	[5].LWV	53	
gi 549835	14	[11].RE.[4].LDTAQRIVY.[1].NVMLNFRN.[3].LG.[1].QLI.[2].DVIKFL.	[5].PWL	74	
gi 1731444	8	[11].QR.[4].LDPSQRNLY.[1].DVMLNFRN.[3].LG.[1].EVM.[2].DVIKFL.	[5].PWW	68	
gi 2501719	14	[11].QE.[4].LDPAQRNLY.[1].DVMLNFRN.[3].VG.[1].QLC.[2].SLISKV.	[4].LKT	73	
gi 11136151	1	[9].AA.[4].LDPAQRNLY.[1].DVMLNFRN.[3].MG.[1].QAP.[2].DMISKI.	[5].PWL	59	
gi 141685	4	[11].RE.[4].LDPQRALY.[1].EVMLNFRN.[3].LA.[2].LVP.[2].ELISRL.	[5].PWW	65	
gi 1731416	6	[11].QE.[4].LQPAQRDLY.[1].CVMLNFRN.[3].LG.[1].SIS.[2].DVISSL.	[5].PWL	66	
ProHepc.	18	[11].QT [5].LQPQRAGA.[1].ASWMPQR	[4]		

Human ZFP-1 [9].AA.[4].LDPAQRNLY.[1].DVMLNFRN.[3].MG.[1].QAP.[2].DMISKI.[5].PWL 59  
Human ZFP-4 [11].RE.[4].LDPQRALY.[1].EVMLNFRN.[3].LA.[2].LVP.[2].ELISRL.[5].PWW 65  
Human ZFP-6 [11].QE.[4].LQPAQRDLY.[1].CVMLNFRN.[3].LG.[1].SIS.[2].DVISSL.[5].PWL 66  
Pro-region 18 [11].QT [5].LQPQRAGA.[1].ASWMPQR [4]

### Fig. 5.7 Similarity between KRAB and pro-region of preprohepcidin

An alignment of some human zinc-finger proteins was created using the NCBI protein *blastp* followed by conserved domain search. A section of the pro-region showed similarity with the KRAB of ZFP. NCBI accessions of human ZFP 37,7 and 140 are gi1136151, gi141685 and gi1731416, respectively.

## 5.2.5 Localisation studies of pro-peptide of preprohepcidin

In order to assess whether the nuclear localisation signal in prohepcidin identified *in silico* (Fig. 5.6) performed a biological role *in vitro*, localisation studies were performed by transfecting Wt HepG2 cells with a recombinant pEGFPN1 plasmid containing the pre-pro region, as explained in the following sections.

### 5.2.5.1 Screening of plasmid constructs

Firstly, the four pEGFPN1 recombinant plasmid constructs (referred to as P1 to P4), each possessing a unique derivative of preprohepcidin with either a GFP or V5 tag, required identification of the derivative and the tag in each construct. To achieve this, the plasmid constructs were screened via restriction enzyme digestion, as shown in Fig. 5.8.

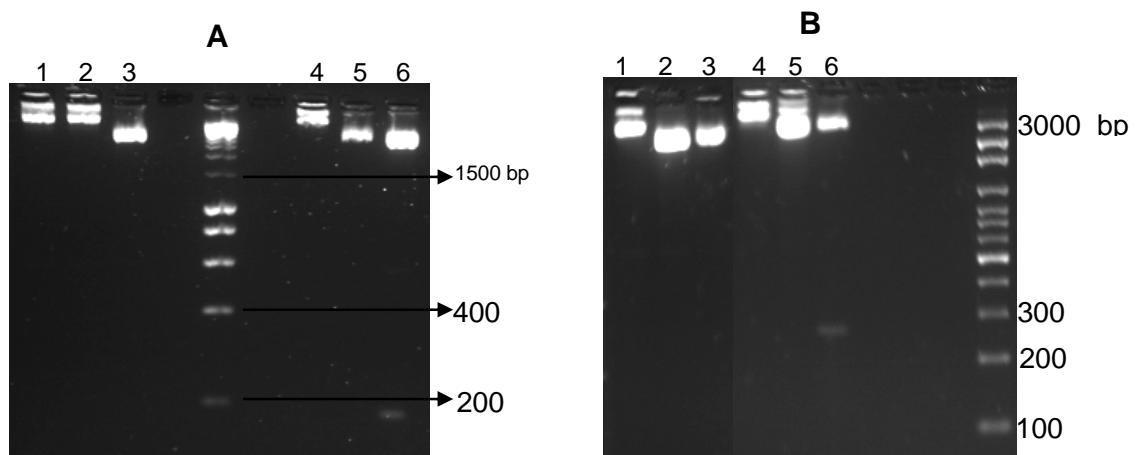


**Fig. 5.8 Restriction digests of pEGFPN1 plasmid constructs**

Recombinant plasmids P1, P2, P3 and P4 containing unknown preprohepcidin derivatives were transformed in *E. Coli XL-1* blue competent cells, extracted, purified, and subjected to digestion with restriction enzymes as explained in methods section 2.2.23. The digested products were electrophoresed on 2 % agarose gels.

**A:** Restriction digests of plasmids P2 (lanes 1-3) and P3 (lanes 4-6)

Lane 1= uncut plasmid; expected product size ~4956 bp

Lane 2= plasmid cut with BamHI; expected product size ~4956 bp

Lane 3= plasmid cut with BamHI and Hind III; expected product size~ 4704 bp and 252 bp

Lane 4= uncut plasmid; expected product size ~4956 bp

Lane 5= plasmid cut with BamHI; expected product size ~4956 bp

Lane 6= plasmid cut with BamHI and Hind III; expected product size ~ 4779 bp and 177 bp

**B:** Restriction digests of plasmids P1 (lanes 1-3) and P4 (lanes 4-6)

Lane 1= uncut plasmid; expected product size ~4956 bp

Lane 2= plasmid cut with BamHI; expected product size ~4956 bp

Lane 3= plasmid cut with BamHI and Hind III; expected product size ~ 4779 bp and 177 bp

Lane 4= uncut plasmid; expected product size ~4956 bp

Lane 5= plasmid cut with BamHI; expected product size ~4956 bp

Lane 6= plasmid cut with BamHI and Hind III; expected product size~ 4704 bp and 252 bp

As seen in the Fig. 5.8, the expected size products were observed for the plasmids

P3 and P4, but not for plasmids P1 and P2. Thus, to confirm the identity of the

constructs in all the plasmids via sequencing, vector primers (pEGFPN primers) were designed as shown below.

```

5'GGTGGGAGGTCTATATAAGCAGAG >>> 3'
pEGFPN1  ACGGTGGGAGGTCTATATAAGCAGAGCTGGTTTAGTGAACCGTCAGATCCGCTAGCGCTA 600
pEGFPN2  ACGGTGGGAGGTCTATATAAGCAGAGCTGGTTTAGTGAACCGTCAGATCCGCTAGCGCTA 600
*****

3' <<< TGTGGAGGGGACTTGA 5'
pEGFPN1  -----ACATTTGTAGAGGTTTTACTTGCTTTAAAAAACCTCCCACACCTCCCCCTGAACC 1488
pEGFPN2  -----ACATTTGTAGAGGTTTTACTTGCTTTAAAAAACCTCCCACACCTCCCCCTGAACC 2098
*****

```

Each purified plasmid construct was amplified with the designed pEGFPN primers and the amplicons were electrophoresed on a 1 % agarose gel, as shown in Fig. 5.9 and sent for sequencing to confirm its identity.

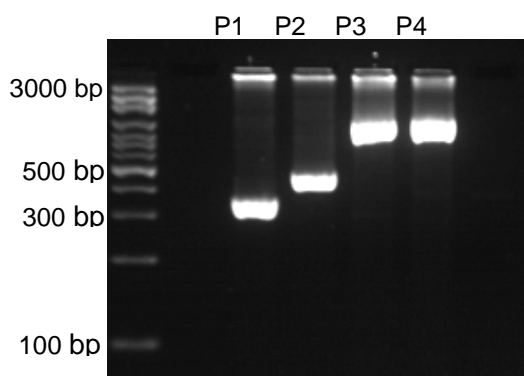


**Fig. 5.9 Amplicons of pEGFPN-preprohepcidin constructs with designed vector primers**

Each recombinant plasmid was amplified with the designed vector primers as described in methods section 2.2.8. Following this, each product was gel purified and sent for sequencing as described in methods section 2.2.12.

The characterised sequences of the recombinant plasmids were translated to protein sequences and the preprohepcidin derivative and the tag in each plasmid construct was identified as shown in Table. 5.1. Following identification, the aim was to perform localisation studies using all the constructs, commencing from the plasmid containing the pre-pro construct.

Plasmid construct	Partial section of translated nucleotide sequence	Conclusion
P1	5'3' Frame 3 S A S A T G L R S R A Q A S N S A V D G T A G P G S Met G K P I P N P L L G L D S T S V F P Q Q T G Q L A E L Q P Q D R A G A R A S W Met P Met F Q R R R R R D Stop S R S Stop S A I P H	Pro region of preprohepcidin with V5 tag at N-terminus.
P2	5'3' Frame 1 X X X X R X I R Stop R Y R T Q I S S S S S F E F K L Met A L S S Q I W A A C L L L L L L L A S L T S G S V F P Q Q T G Q L A E L Q P Q D R A G A R A S W Met P Met F Q R R R R R D T H F P I C I F C C G C C H R S K C G Met C C K T G K P I P N P L L G L D S T Stop S R S Stop S A I P H L Stop R F Y L L Stop K T S H X X X X E P	Preprohepcidin with V5 tag at C-terminus
P3	D V D R S A P D S D L E L K L M A L S S Q I W A A C L L L L L L L A S L T S G S V F P Q Q T G Q L A E L Q P Q D R A G A R A S W M P M F Q R R R R R R D P P V A T M V S K G E E L F T G V V P I L V E L E G D V N G H K F S V S G E G E G D A T Y G K L T L K F I C T T G K L P V P W P T	Prepro region with GFP tag at C-terminus
P4	5'3' Frame 2 L V C V D R S A P D S D L E L K L M A L S S Q I W A A C L L L L L L L A S L T S G S V F P Q Q T G Q L A E L Q P Q D R A G A R A S W M P M F Q R R R R R D T H F P I C I F C C G C C H R S K C G M C C K I D P P V A T M V S K G E E L F T G V V P I L V E L D G D V N G H K F S V S G E G E G D A T Y G K L T L K F I C T T G K	Preprohepcidin with GFP tag at C-terminus.

**Table 5.1 Identification of plasmid pEGFPN1-preprohepcidin constructs**

Proteomics tool 'Translate' at ExPASy (<http://web.expasy.org/translate/>) was used to translate the characterised plasmid sequences to amino acid sequences and the preprohepcidin derivative in each construct was identified. Sequence information on preprohepcidin was obtained from Protein Knowledgebase UniProtKB (P81172). Tags were identified using *blastn* at NCBI.

Key to table:

- Pre region of preprohepcidin
- Pro-hepcidin
- V5 tag
- GFP Tag

### 5.2.5.2 Localisation study of hepcidin pro-peptide in Wt HepG2 cells

Once the recombinant plasmid containing the pre-pro derivative was confirmed via sequencing, Wt HepG2 cells were transfected with this recombinant plasmid and the non-recombinant empty pEGFPN1 plasmid which acted as a control. The results of transfection are shown in Fig. 5.10.

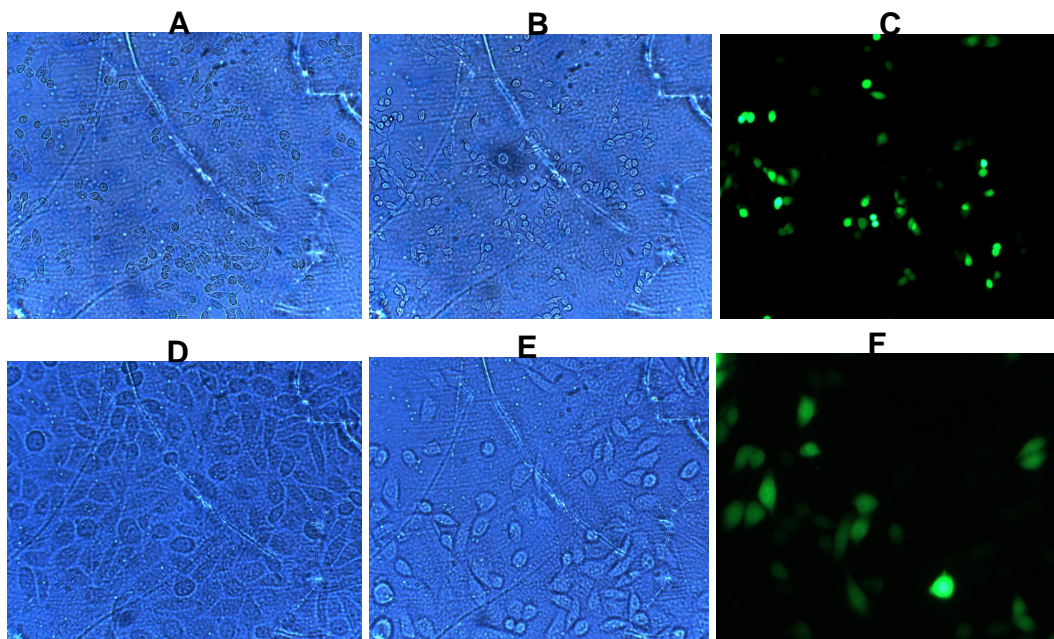


**Fig. 5.10 Transfection of HepG2 cells with pEGFPN1 plasmids**

Wt HepG2 cells were transfected with the plasmid containing the prepro-construct, as described in methods section 2.2.24, to identify the location of the construct in the cells.

**A, B and C** : Transfection with non-recombinant pEGFP N1 plasmid (20X)

**A** : Control; untransfected cells

**B** : Transfected cells under normal light

**C** : Transfected cells under fluorescent light

**D, E and F** : Transfection with prepro-pEGFP N1 construct (40X)

**D** : Control; untransfected cells

**E** : Transfected cells under normal light

**F** : Transfected cells under fluorescent light

Following this, the images were observed under a confocal microscope, as shown in Fig. 5.11. In the case of transfection with the non-recombinant host plasmid (control), the fluorescence from the GFP tag was seen all over the cell, including the nucleus (Fig. 5.11 B and C). However, transfection of cells with the recombinant plasmid containing the pre-pro construct resulted in fluorescence being found exclusively in the nucleus (Fig. 5.11 D, E and F).

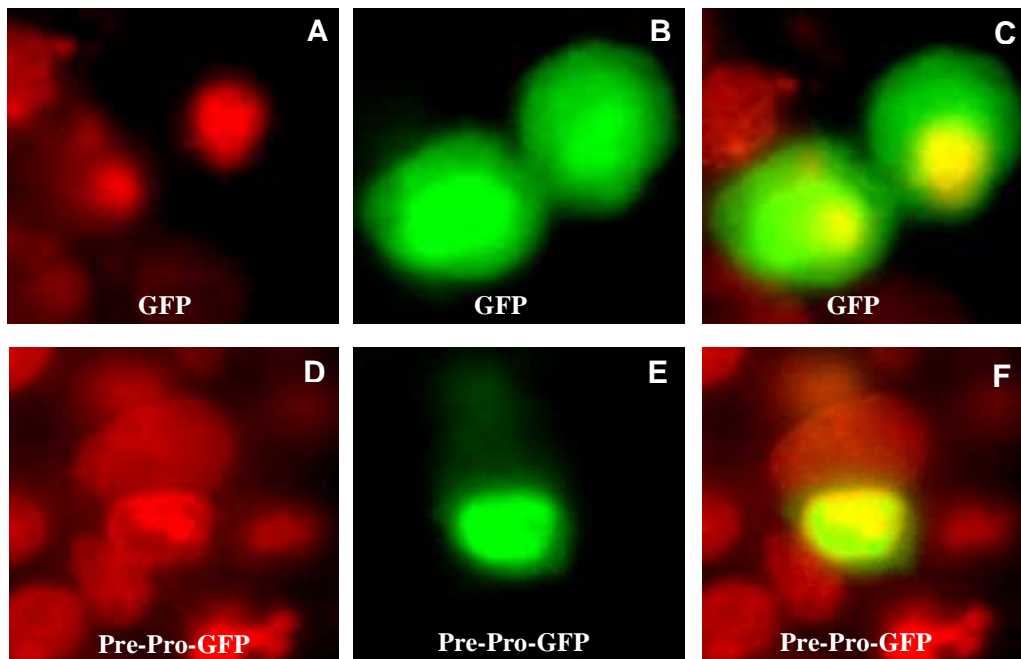


**Fig. 5.11 Localisation of prepro-region in HepG2 cells**

Wt HepG2 cells were transfected with the plasmid containing the 'prepro' construct, as described in methods section 2.2.24, to identify the location of the construct in the cells.

**A, B, C** : Transfection with non-recombinant pEGFP N1 plasmid

**A**: Location of nucleus in the cells.

**B**: Localisation of GFP in the cells.

**C**: Superimposition of the images A and B.

**D, E, F**: Transfection with prepro-pEGFP N1 construct

**D**: Location of nucleus in the cells

**E**: Location of GFP tag within the cell.

**F**: Superimposition of images D and E.

### 5.3 Discussion

The 84-mer preprohepcidin in humans is cleaved to yield a 25-mer bioactive hepcidin and a 35-mer pro-region (Park *et al.*, 2001) which has an unknown function. Based on the similarities in structures between the HFE protein and MHC class I molecules, it was hypothesised that HFE may be involved in peptide binding and presentation like the MHC class I molecule and that this peptide could be a part of the pro-region. Hence to explore this hypothesis, bioinformatics was used to investigate the putative interaction between the pro-region of preprohepcidin and

the HFE. The study showed that the C-terminal part of the prohepcidin sequence was the most hydrophilic and hence would be the most antigenic region (Fig. 5.2). Since the HFE is regarded as a pseudo MHC (HLA) (Feder *et al.*, 1996), the binding affinity between nonamers of preprohepcidin and different serotypes of HLAs was investigated (Fig. 5.3). Data suggested that the C-terminal region of the pro-region showed the highest possibility of interaction with the HLA. Additionally, this region matched the most hydrophilic region in preprohepcidin as seen in Fig. 5.2. Together this suggests that the C-terminus of the pro-region had the most potential for binding to a HLA and hence the HFE protein.

Conservation of  $\alpha$ -1 and  $\alpha$ -2 regions of HFE in different species (Fig. 5.4) suggests that these regions might be functionally significant. Although it has been established that the HFE protein, through its  $\alpha$  -1 and  $\alpha$  - 2 regions, interacts with TfR1 and regulates iron uptake by cells (Fleming, 2009), it should not be excluded that that these  $\alpha$ -regions may also be involved in peptide binding, particularly in the scenario when the HFE has been proposed to exhibit multiple roles. The bound peptide could be a section of the pro-region which by binding to the HFE in the endoplasmic reticulum (ER) would allow its maturation and may activate the HFE to traverse across the ER to be expressed on the cell surface where it would fulfil its role of limiting iron import inside the cell. Another role of the section of the pro-peptide could be where its presentation on the cell surface may be a part of a signal to regulate hepcidin levels via a feedback mechanism. The C-terminal part of the pro-region, RRRRRDTHF, which was found to be the most hydrophilic and antigenic (figures 5.2 and 5.3), also contains a motif typical of a nuclear localisation

signal (figures 5.5 and 5.6). This motif indicates functional significance of the pro-region as found in many proteins with arginine-rich domains that function as a nuclear localisation signal, for example as found in the HIV type 1, Tat and Rev proteins (Truant and Cullen, 1999). Further bioinformatics analysis indicated that the pro-region bore a similarity to the KRAB domain of some of the members of the Zinc-finger protein (ZFP) family (Fig. 5.7). The KRAB is a domain of around 75 amino acids located at the N-terminal part of about one third of eukaryotic ZFP and some of the functions of the KRAB-containing protein family include transcriptional repression of RNA polymerase I, II, and III promoters, binding and splicing of RNA (Hirasawa and Feil, 2008, Pengue and Lania, 1996). Since the KRAB-zinc fingers constitute the largest class of transcription factors within the human genome (Mark et al., 1999), here it was hypothesised that the pro-region or part of the pro-region with the amino acids RRRRRDTHF may localise into the nucleus.

Localisation studies of prohepcidin have been conducted by other research groups. Pigeon et.al. (2001) used a GFP-construct in which the GFP tag was inserted at the N-terminus of the prohepcidin sequence. When the recombinant peptide was expressed in HepG2 cells, it was found to be located in the nucleus. This showed the presence of GFP-tagged prohepcidin in the nucleus. However, this construct did not include the 'pre' region and therefore probably may not have been expressed through the ER but directly in the cytoplasm. Although the primary sequence of prohepcidin does not suggest posttranslational modifications, the presence of an ER targeting sequence in the first 24 amino acids in the preprohepcidin suggests that it is important for the recombinant peptide to traverse

across the ER for the original maturation process. Since the pro-region is proposed to be cleaved by a furin-like convertase to release the mature peptide it could be that in the study by Pigeon et.al. (2001) the GFP-pro region may have entered the nucleus. However, GFP is a much larger protein (238 mer, 26.9 kD)(Tsien, 1998) than the small pro-region (35 mer) and whether the size and placement of the GFP tag during the creation of the chimera influenced the localisation process, needs to be fully understood.

Another study which used antibodies raised against human prohepcidin showed that in the HepG2 cells prohepcidin was localised in intracellular vesicular structures (Kulaksiz et al., 2004). Also, when human preprohepcidin was transfected in human embryonic kidney cells, the C-terminal part (i.e. tagged hepcidin-25) or prohepcidin was localised to the golgi complex (Wallace et al., 2006). Detection of hepcidin or pro-hepcidin in vesicular structures or the golgi complex is not surprising as these may have been captured when prohepcidin was about to mature into hepcidin-25, ready to be cleaved by furin which is found to be localised in the transgolgi network (Nakayama, 1997) or when hepcidin-25 was about to exit the cell.

Hence, to further investigate the potential role of the pro-region as a NLS, recombinant plasmid pEGFPN1 with the pre-pro-GFP was transfected into Wt HepG2 cells. In this construct the GFP tag was placed after the pre-pro region to allow normal process through the ER and to alleviate any interference in localisation from the huge GFP tag, unlike the previous studies. Here, localisation

studies showed that the construct entered the nucleus (Fig. 5.11 E and F). Since the pre-region of preprohepcidin is cleaved by the signal peptidase (Nemeth and Ganz, 2006), it is probably only the pro-GFP protein that is localised in the nucleus. The role of the pro-peptide in the nucleus remains to be identified. Its similarity with the KRAB motif suggests that it may act as a transcription factor to regulate gene expression of *hepcidin* or other iron-regulated genes. Further localisation studies using all the other characterised preprohepcidin constructs will be necessary to better understand the cellular trafficking of hepcidin and any role of the pro-region.

## Chapter 6

### Overall summary and future work

#### 6.1 Overall summary

The aim of this project was to understand how iron regulates *hepcidin* gene expression. To achieve this, in the first instance CHO TRVb1 cells were chosen for iron overdose studies. It was hypothesised that due to the over-expression of human TfR1, these cells would be able to uptake excess amounts of iron via holotransferrin and the resultant effect on gene expression of *hepcidin* and other iron-related genes could be investigated. Since the sequences of iron-related genes of interest in the CHO cells were not known, their characterisation was carried out to enable gene expression studies through real time PCR.

Subsequently, in this study (chapter 3), CHO gene sequences of *Hfe*, *ferroportin* and *Irf2* were partially characterised.

However, the gene sequence of *hepcidin* in these cells could not be characterised which prevented the evaluation of *hepcidin* mRNA expression. Hence, studies focusing on hepcidin peptide secretion were carried out. For the first time it was shown that the CHO TRVb1 cells secreted significantly increased hepcidin peptide levels after 30 min, 2, 4, 24 and 48 hours following holotransferrin overdose (figures 3.22 and 3.26), as observed in human and animal models (Lin et al., 2007, Nemeth et al., 2003, Pigeon et al., 2001). Despite over-expressing TfR1 on the cell surface, the CHO TRVb1 cells did not uptake increased amounts of iron (Fig. 3.25) implying that over-expressed TfR1 along with holotransferrin overdose may not

necessitate intracellular iron overload, primarily because the *TfR1* mRNA in these cell was *IRE*-regulated which limited the amount of iron intake via TfR1. Since the increase in hepcidin peptide levels by the CHO TRVb1 cells was achieved without intracellular iron overload, it was important to understand the effect of intracellular iron overload on *hepcidin* mRNA and peptide expression. Hence, rec-TfR1 HepG2 cells were created such that they expressed an *IRE*-independent *TfR1* so that the *TfR1* mRNA would be insensitive to increase in intracellular iron content and this would maximise iron uptake (chapter 4). Consequently, the cells showed higher basal levels of iron than Wt HepG2 cells (figures 4.4C and 4.11F) and significantly increased iron uptake with increased holotransferrin concentrations at 2, 4 and 24 hours after treatment (figures 4.8C and 4.14F).

Holotransferrin dosage of 1 g/L and 5 g/L to the control Wt HepG2 cells for 30 min, 2, 4, 6 and 24 h resulted in a physiological increase in *hepcidin* mRNA levels (figures 4.7C and 4.15). Despite increased intracellular iron levels, the rec-TfR1 HepG2 cells did not demonstrate an expected increase in *hepcidin* mRNA levels, although after 2 h of 5 g/L holotransferrin treatment, a 0.5-fold increase was observed ( $p < 0.02$ ) (Fig. 4.17). This suggested that *hepcidin* mRNA expression was not directly proportional to intracellular iron levels. Interestingly, it was also observed that *ferroportin* mRNA levels in the rec-TfR1HepG2 cells were considerably higher compared to the Wt HepG2 cells and also significantly increased upon 5 g/L holotransferrin treatment indicating that the rec-TfR1 HepG2 cells were excreting intracellular iron (figures 4.5B, 4.12D, 4.17).

Additionally, in this study, it was shown for the first time that HepG2 cells secreted significantly increased levels of hepcidin peptide upon holotransferrin overdose (Fig. 4.19 and 4.20) as observed in humans and animal models (Lin et al., 2007, Nemeth et al., 2003, Pigeon et al., 2001). Similarity in the levels of hepcidin peptide secretion by both the Wt and rec-TfR1 HepG2 cells, despite having different intracellular iron contents, suggested that both intracellular and extracellular iron concentrations affected hepcidin synthesis and secretion.

Gene expression studies demonstrated the impact of HFE on hepcidin. The *HFE* and *hepcidin* gene expressions mirrored each other (figures 4.12C and 4.18C) which suggested that in the human body HFE may participate in regulating circulating iron levels via hepcidin. HFE is crucial for hepcidin expression, as is evident by comparing hepatocytes from haemochromatotic patients where the absence of HFE on the cell-surface is linked to reduced hepcidin production (Feder et al., 1996) and rec-TfR1 HepG2 cells where hepcidin is secreted with the help of functional HFE on the cell-surface. This study also suggested a probable role of HFE in sensing intracellular iron levels, either independently (Carlson et al., 2005) or via TfR1, and also in sensing extracellular iron levels (Fig. 4.25). Thus it appeared that HFE played multiple roles depending on the extracellular and intracellular iron environment.

Gene expression studies showed evidence of opposing functionalities of *TfR1* and *ferroportin* transcripts in regulating intracellular iron levels. For example, in the Wt HepG2 cells, basal intracellular iron levels along with increased extracellular iron

levels reduced *TfR1* mRNA expression to prevent any further iron uptake (figures 4.7A and 4.15). On the other hand, in the rec-TfR1 HepG2 cells, high basal intracellular iron content along with increased extracellular iron levels led to increased *ferroportin* mRNA expression to excrete the excess iron (Fig. 4.17). The process of down-regulation of the *TfR1* transcript and up-regulation of the *ferroportin* transcript had the same purpose which was to maintain intracellular iron homeostasis.

Simultaneously, this study attempted to understand the significance of the pro-region of preprohepcidin. As a result of the *in silico* studies demonstrated in chapter 5, a potential binding between the HFE and a section of the pro-region of preprohepcidin has been proposed. The first proposed role of the pro-region is to aid in the maturation process of HFE to be expressed on the cell surface.

Localisation of the pro-region within the cell was investigated which revealed that transfection of HepG2 cells with the pre-pro-GFP construct resulted in localisation of the pro-GFP in the nucleus (Fig. 5.11). This, along with the similarity of the pro-region with the KRAB domain of ZFP family (Fig. 5.7) together propose a second role of the pro-region which is to act as a transcription factor in regulating gene expression.

## **6.2 Future work**

Although hepcidin is regarded as a key iron homeostatic regulator, its expression is linked with the expression of other iron-related proteins. Hence, to obtain a complete picture of iron regulation it would be more beneficial to study hepcidin

expression along with and in relation to other iron-related proteins such as HFE, TfR2 and ferritin. Such a study is supported by the fact that liver cells express HFE in higher amounts than other cells, hepcidin is produced predominantly by the liver and TfR2 is present only on hepatocytes (Zhang et al., 2004, Park et al., 2001, Pigeon et al., 2001, Schmidt et al., 2008, Rapisarda et al., 2010). The three proteins influence each other and hence the interrelationship between the expressions of their genes would help in the overall understanding of iron regulation.

The rec-TfR1 HepG2 cells possess an *IRE*-independent *TfR1* and were able to demonstrate intracellular iron overload (figures 4.8C and 4.14F). However, increased *ferroportin* mRNA expression in the rec-TfR1 HepG2 cells implies that the cells may have only partially retained the iron content. Hence the question whether high intracellular iron levels influence *hepcidin* mRNA and protein expression and if so to what extent, still remains to be fully answered. This involves the influence of other genes like *ferroportin* and *HFE*. The loss of intracellular iron occurring in the rec-TfR1 HepG2 cells could be prevented by deletion of the 5' *IREs* in the *ferroportin* gene. This will ensure that both the entry and the exit points of iron via TfR1 and ferroportin, respectively, are modified to maximise iron uptake and then retain the attained high intracellular iron. The effect on hepcidin expression could then be investigated. In addition, since HFE has been shown to limit intracellular iron uptake (Chua et al., 2008), iron supplementation experiments could be performed on HFE-deficient HepG2 cells and HFE- over-expressing cells

and the effects could be compared to Wt HepG2 and rec-TfR1 HepG2 cells used in this study.

Also, the potential binding between the HFE and preprohepcidin derivative suggested by *in silico* studies performed in chapter 5 could be fully elucidated by *in vitro* peptide binding studies. Synthetic nonamers of HFE and the pro-region could be synthesised and their binding could be checked by probing the HFE nonamers to the pro-sections and vice-versa. This will not only help to understand the relationship between HFE and hepcidin but also aid in elucidating the proposed multiple roles of HFE, which have not yet been fully understood.

Furin cleavage of prohepcidin into bioactive hepcidin is affected by the amino acids positioned C-terminal to the cleavage site (Lee, 2008). In the pre-pro-GFP construct used here, the furin cleavage site (RRRRR) as well as the first amino acid after the cleavage site i.e. aspartic acid (D) are preserved. Hence, it would be important to know if the substitution of hepcidin with GFP tag in the construct has affected the furin-cleavage process. This could be shown by performing an SDS-PAGE with the extracted plasmids from transfected cells and comparing the sizes of the furin-cleaved and uncleaved products. Also, further studies should be performed with the other preprohepcidin GFP-construct characterised in this study.

In the case of preprohepcidin constructs with GFP, a large GFP tag is attached to a small peptide whose movement within the cell is required to be traced. In order to ease the process, various combinations of preprohepcidin constructs could be

created with V5 tags at the C and N termini, two of which are already characterised in this study. These could be probed with V5 antibodies which will provide finer information than studies with the larger GFP-tagged preprohepcidin constructs. The tag will identify the location of the construct whereas the coherent view of all the constructs will show the pathway of secretion of bioactive hepcidin. Thus, such localisation studies will help to better understand the cell trafficking of hepcidin and may provide a new insight into the secretion process. It has been proposed by Farnaud et al. (2008) that iron may play a role in processing of prohepcidin. In order to verify this proposition, a combination of iron supplementation and localisation studies in HepG2 cells should be carried out. This may provide a better insight into the bio-processing of hepcidin as well as the destination of the pro-region within the cell.

It is clear that hepcidin regulation and secretion to regulate circulating iron levels is a complex mechanism, involving various genes/proteins and their responses under different extracellular and intracellular environments. The responses of cells are also governed by the concentration and exposure-time of iron. Since gene expressions are affected by the extracellular environment and vice-versa, the challenge is to elucidate what acts as the first trigger.

## References

- AISEN, P. (2004) Transferrin receptor 1. *Int J Biochem Cell Biol*, 36, 2137-43.
- ANDREWS, N. C. & SCHMIDT, P. J. (2007) Iron Homeostasis. *Ann Rev of Physiol*, 69, 69-85.
- ANDREWS, P. A. (2000) Disorders of iron metabolism. *N Engl J Med*, 342, 1293.
- ASHBY, D. R., GALE, D. P., BUSBRIDGE, M., MURPHY, K. G., DUNCAN, N. D., CAIRNS, T. D., TAUBE, D. H., BLOOM, S. R., TAM, F. W., CHAPMAN, R. S., MAXWELL, P. H. & CHOI, P. (2009) Plasma hepcidin levels are elevated but responsive to erythropoietin therapy in renal disease. *Kidney Int*, 75, 976-81.
- BABITT, J. L., HUANG, F. W., WRIGHTING, D. M., XIA, Y., SIDIS, Y., SAMAD, T. A., CAMPAGNA, J. A., CHUNG, R. T., SCHNEYER, A. L., WOOLF, C. J., ANDREWS, N. C. & LIN, H. Y. (2006) Bone morphogenetic protein signaling by hemojuvelin regulates hepcidin expression. *Nat Genet*, 38, 531-9.
- BAHR, S. M., BORGSCHULTE, T., KAYSER, K. J. & LIN, N. (2009) Using microarray technology to select housekeeping genes in Chinese hamster ovary cells. *Biotechnol Bioeng*, 104, 1041-6.
- BEKRI, S., GUAL, P., ANTY, R., LUCIANI, N., DAHMAN, M., RAMESH, B., IANNELLI, A., STACCINI-MYX, A., CASANOVA, D., BEN AMOR, I., SAINT-PAUL, M. C., HUET, P. M., SADOUL, J. L., GUGENHEIM, J., SRAI, S. K., TRAN, A. & LE MARCHAND-BRUSTEL, Y. (2006) Increased adipose tissue expression of hepcidin in severe obesity is independent from diabetes and NASH. *Gastroenterology*, 131, 788-96.
- BINDER, R., HOROWITZ, J. A., BASILION, J. P., KOELLER, D. M., KLAUSNER, R. D. & HARFORD, J. B. (1994) Evidence that the pathway of transferrin receptor mRNA degradation involves an endonucleolytic cleavage within the 3' UTR and does not involve poly(A) tail shortening. *Embo J*, 13, 1969-80.
- BOKHARI, M., CARNACHAN, R. J., CAMERON, N. R. & PRZYBORSKI, S. A. (2007) Culture of HepG2 liver cells on three dimensional polystyrene scaffolds enhances cell structure and function during toxicological challenge. *J Anat*, 211, 567-76.

BORRIONE, P., SPACCAMIGLIO, A., RIZZO, M., TERMINE, A., CHIERTO, E., CAMPOSTRINI, N., QUARANTA, F., DI GIANFRANCESCO, A. & PIGOZZI, F. (2011) Urinary hepcidin identifies a serum ferritin cut-off for iron supplementation in young athletes: a pilot study. *J Biol Regul Homeost Agents*, 25, 427-34.

BRIDLE, K. R., FRAZER, D. M., WILKINS, S. J., DIXON, J. L., PURDIE, D. M., CRAWFORD, D. H., SUBRAMANIAM, V. N., POWELL, L. W., ANDERSON, G. J. & RAMM, G. A. (2003) Disrupted hepcidin regulation in HFE-associated haemochromatosis and the liver as a regulator of body iron homeostasis. *Lancet*, 361, 669-73.

BUSBRIDGE, M., GRIFFITHS, C., ASHBY, D., GALE, D., JAYANTHA, A., SANWAIYA, A. & CHAPMAN, R. S. (2009) Development of a novel immunoassay for the iron regulatory peptide hepcidin. *Br J Biomed Sci*, 66, 150-7.

CARLSON, H., ZHANG, A. S., FLEMING, W. H. & ENNS, C. A. (2005) The hereditary hemochromatosis protein, HFE, lowers intracellular iron levels independently of transferrin receptor 1 in TRVb cells. *Blood*, 105, 2564-70.

CASEY, J. L., HENTZE, M. W., KOELLER, D. M., CAUGHMAN, S. W., ROUAULT, T. A., KLAUSNER, R. D. & HARFORD, J. B. (1988) Iron-responsive elements: regulatory RNA sequences that control mRNA levels and translation. *Science*, 240, 924-8.

CHUA, A. C., HERBISON, C. E., DRAKE, S. F., GRAHAM, R. M., OLYNYK, J. K. & TRINDER, D. (2008) The role of Hfe in transferrin-bound iron uptake by hepatocytes. *Hepatology*, 47, 1737-44.

CRICHTON, R. R., WILMET, S., LEGSSYER, R. & WARD, R. J. (2002) Molecular and cellular mechanisms of iron homeostasis and toxicity in mammalian cells. *J Inorg Biochem*, 91, 9-18.

DARSHAN, D. & ANDERSON, G. (2009) Interacting signals in the control of hepcidin expression. *BioMetals*, 22, 77-87.

DE DOMENICO, I., NEMETH, E., NELSON, J. M., PHILLIPS, J. D., AJIOKA, R. S., KAY, M. S., KUSHNER, J. P., GANZ, T., WARD, D. M. & KAPLAN, J. (2008) The hepcidin-binding site on ferroportin is evolutionarily conserved. *Cell Metab*, 8, 146-56.

DE DOMENICO, I., WARD, D. M., LANGELIER, C., VAUGHN, M. B., NEMETH, E., SUNDQUIST, W. I., GANZ, T., MUSCI, G. & KAPLAN, J. (2007) The Molecular Mechanism of Hepcidin-mediated Ferroportin Down-Regulation. *Mol. Biol. Cell*, 18, 2569-2578.

DE DOMENICO, I., WARD, D. M., MUSCI, G. & KAPLAN, J. (2006) Iron overload due to mutations in ferroportin. *Haematologica*, 91, 92-5.

DINGWALL, C. & LASKEY, R. A. (1986) Protein import into the cell nucleus. *Annu Rev Cell Biol*, 2, 367-90.

DZIKAITE, V., HOLMSTROM, P., STAL, P., ECKES, K., HAGEN, K., EGGERTSEN, G., GAFVELS, M., MELEFORS, O. & HULTCRANTZ, R. (2006) Regulatory effects of tumor necrosis factor-alpha and interleukin-6 on HAMP expression in iron loaded rat hepatocytes. *J Hepatol*, 44, 544-51.

FARNAUD, S., RAPISARDA, C., BUI, T., DRAKE, A., CAMMACK, R. & EVANS, R. W. (2008) Identification of an iron-hepcidin complex. *Biochem J*, 413, 553-7.

FARNAUD, S. Personal communication, University of Westminster.

FEDER, J. N., GNIRKE, A., THOMAS, W., TSUCHIHASHI, Z., RUDDY, D. A., BASAVA, A., DORMISHIAN, F., DOMINGO, R., ELLIS, M. C., FULLAN, A., HINTON, L. M., JONES, N. L., KIMMEL, B. E., KRONMAL, G. S., LAUER, P., LEE, V. K., LOEB, D. B., MAPA, F. A., MCCLELLAND, E., MEYER, N. C., MINTIER, G. A., MOELLER, N., MOORE, T., MORIKANG, E., PRASS, C. E., QUINTANA, L., STARNES, S. M., SCHATZMAN, R. C., BRUNKE, K. J., DRAYNA, D. T., RISCH, N. J., BACON, B. R. & WOLFF, R. K. (1996) A novel MHC class I-like gene is mutated in patients with hereditary haemochromatosis. *Nature Genetics*, 13, 399-408.

FEIN, E., MERLE, U., EHEHALT, R., HERRMANN, T. & KULAKSIZ, H. (2007) Regulation of hepcidin in HepG2 and RINm5F cells. *Peptides*, 28, 951-7.

FERNANDEZ-REAL, J. M., LOPEZ-BERMEJO, A. & RICART, W. (2002) Cross-talk between iron metabolism and diabetes. *Diabetes*, 51, 2348-2354.

FINBERG, K. E., WHITTLESEY, R. L., FLEMING, M. D. & ANDREWS, N. C. (2010) Down-regulation of Bmp/Smad signaling by *Tmprss6* is required for maintenance of systemic iron homeostasis. *Blood*, 115, 3817-26.

FLEMING, R. E. & BRITTON, R. S. (2006) Iron Imports. VI. HFE and regulation of intestinal iron absorption. *Am J Physiol Gastrointest Liver Physiol*, 290, G590-4.

FLEMING, R. E. (2009) Iron sensing as a partnership: HFE and transferrin receptor 2. *Cell Metab*, 9, 211-2.

FRAZIER, M. D., MAMO, L. B., GHIO, A. J. & TURI, J. L. (2011) Heparin expression in human airway epithelial cells is regulated by interferon-gamma. *Respir Res*, 12, 100.

GANZ, T. (2011) Heparin and iron regulation, 10 years later. *Blood*, 117, 4425-33.

GAO, J., CHEN, J., KRAMER, M., TSUKAMOTO, H., ZHANG, A. S. & ENNS, C. A. (2009) Interaction of the hereditary hemochromatosis protein HFE with transferrin receptor 2 is required for transferrin-induced heparin expression. *Cell Metab*, 9, 217-27.

GAO, J., ZHAO, N., KNUTSON, M. D. & ENNS, C. A. (2008) The hereditary hemochromatosis protein, HFE, inhibits iron uptake via down-regulation of Zip14 in HepG2 cells. *J Biol Chem*, 283, 21462-8.

GEHRKE, S. G., KULAKSIZ, H., HERRMANN, T., RIEDEL, H. D., BENTS, K., VELTKAMP, C. & STREMMEL, W. (2003) Expression of heparin in hereditary hemochromatosis: evidence for a regulation in response to the serum transferrin saturation and to non-transferrin-bound iron. *Blood*, 102, 371-6.

GLICK, B. R. (1995) Metabolic load and heterologous gene expression. *Biotechnol Adv*, 13, 247-61.

GREENWELL, P. Personal communication, University of Westminster.

HIRASAWA, R. & FEIL, R. (2008) A KRAB domain zinc finger protein in imprinting and disease. *Dev Cell*, 15, 487-8.

HOLMSTROM, P., DZIKAITIS, V., HULTCRANTZ, R., MELEFORS, O., ECKES, K., STAL, P., KINNMAN, N., SMEDSRÖD, B., GAFVELS, M. & EGGERTSEN, G. (2003) Structure and liver cell expression pattern of the HFE gene in the rat. *J Hepatol*, 39, 308-14.

HUEBERS, H. A. & FINCH, C. A. (1987) The physiology of transferrin and transferrin receptors. *Physiol Rev*, 67, 520-82.

HUNTER, H. N., FULTON, D. B., GANZ, T. & VOGEL, H. J. (2002) The solution structure of human heparin, a peptide hormone with antimicrobial activity that is involved in iron uptake and hereditary hemochromatosis. *J Biol Chem*, 277, 37597-603.

ILYIN, G., COURSELAUD, B., TROADEC, M. B., PIGEON, C., ALIZADEH, M., LEROYER, P., BRISSOT, P. & LOREAL, O. (2003) Comparative analysis of mouse heparin 1 and 2 genes:

evidence for different patterns of expression and co-inducibility during iron overload. *FEBS Lett*, 542, 22-6.

JACOLOT, S., FEREC, C. & MURA, C. (2008) Iron responses in hepatic, intestinal and macrophage/monocyte cell lines under different culture conditions. *Blood Cells Mol Dis*, 41, 100-8.

JORDAN, J. B., POPPE, L., HANIU, M., ARVEDSON, T., SYED, R., LI, V., KOHNO, H., KIM, H., SCHNIER, P. D., HARVEY, T. S., MIRANDA, L. P., CHEETHAM, J. & SASU, B. J. (2009) Hepsidin revisited, disulfide connectivity, dynamics, and structure. *J Biol Chem*, 284, 24155-67.

KANG, D. K., JEONG, J., DRAKE, S. K., WEHR, N. B., ROUAULT, T. A. & LEVINE, R. L. (2003) Iron regulatory protein 2 as iron sensor - Iron-dependent oxidative modification of cysteine. *J Biol Chem*, 278, 14857-14864.

KIM, Y. O., HONG, S., NAM, B. H., LEE, J. H., KIM, K. K. & LEE, S. J. (2005) Molecular cloning and expression analysis of two hepcidin genes from olive flounder *Paralichthys olivaceus*. *Biosci Biotechnol Biochem*, 69, 1411-4.

KING, R., STANSFIELD, W. (1990) *Dictionary of genetics*, 3<sup>rd</sup> edition, Oxford University Press.  
KOHGO, Y., IKUTA, K., OHTAKE, T., TORIMOTO, Y. & KATO, J. (2008) Body iron metabolism and pathophysiology of iron overload. *Int J Hematol*, 88, 7-15.

KOSUGI, S., HASEBE, M., ENTANI, T., TAKAYAMA, S., TOMITA, M. & YANAGAWA, H. (2008) Design of peptide inhibitors for the importin alpha/beta nuclear import pathway by activity-based profiling. *Chem Biol*, 15, 940-9.

KOSUGI, S., HASEBE, M., MATSUMURA, N., TAKASHIMA, H., MIYAMOTO-SATO, E., TOMITA, M. & YANAGAWA, H. (2009a) Six classes of nuclear localization signals specific to different binding grooves of importin alpha. *J Biol Chem*, 284, 478-85.

KOSUGI, S., HASEBE, M., TOMITA, M. & YANAGAWA, H. (2009b) Systematic identification of cell cycle-dependent yeast nucleocytoplasmic shuttling proteins by prediction of composite motifs. *Proc Natl Acad Sci U S A*, 106, 10171-6.

KRAUSE, A., NEITZ, S., MAGERT, H. J., SCHULZ, A., FORSSMANN, W. G., SCHULZ-KNAPPE, P. & ADERMANN, K. (2000) LEAP-1, a novel highly disulfide-bonded human peptide, exhibits antimicrobial activity. *FEBS Lett*, 480, 147-50.

KROOT, J. J., TJALSMA, H., FLEMING, R. E. & SWINKELS, D. W. (2011) Heparin in human iron disorders: diagnostic implications. *Clin Chem*, 57, 1650-69.

KULAKSIZ, H., GEHRKE, S. G., JANETZKO, A., ROST, D., BRUCKNER, T., KALLINOWSKI, B. & STREMMEL, W. (2004) Pro-hepcidin: expression and cell specific localisation in the liver and its regulation in hereditary haemochromatosis, chronic renal insufficiency, and renal anaemia. *Gut*, 53, 735-743.

LEBRON, J. A., BENNETT, M. J., VAUGHN, D. E., CHIRINO, A. J., SNOW, P. M., MINTIER, G. A., FEDER, J. N. & BJORKMAN, P. J. (1998) Crystal structure of the hemochromatosis protein HFE and characterization of its interaction with transferrin receptor. *Cell*, 93, 111-23.

LEE, P. (2008) Commentary to: "Post-translational processing of hepcidin in human hepatocytes is mediated by the prohormone convertase furin," by Erika Valore and Tomas Ganz. *Blood Cells Mol Dis*, 40, 139-40.

LEE, P. L. & BEUTLER, E. (2009) Regulation of hepcidin and iron-overload disease. *Annu Rev Pathol*, 4, 489-515.

LIN, L., VALORE, E. V., NEMETH, E., GOODNOUGH, J. B., GABAYAN, V. & GANZ, T. (2007) Iron transferrin regulates hepcidin synthesis in primary hepatocyte culture through hemojuvelin and BMP2/4. *Blood*, 110, 2182-9.

LOU, D. Q., NICOLAS, G., LESBORDES, J. C., VIATTE, L., GRIMBER, G., SZAJNERT, M. F., KAHN, A. & VAULONT, S. (2004) Functional differences between hepcidin 1 and 2 in transgenic mice. *Blood*, 103, 2816-21.

MAKEY, D. G. & SEAL, U. S. (1976) The detection of four molecular forms of human transferrin during the iron binding process. *Biochim Biophys Acta*, 453, 250-6.

MARK, C., ABRINK, M. & HELLMAN, L. (1999) Comparative analysis of KRAB zinc finger proteins in rodents and man: evidence for several evolutionarily distinct subfamilies of KRAB zinc finger genes. *DNA Cell Biol*, 18, 381-96.

MCGRAW, T. E., GREENFIELD, L. & MAXFIELD, F. R. (1987) Functional expression of the human transferrin receptor cDNA in Chinese hamster ovary cells deficient in endogenous transferrin receptor. *J. Cell Biol*, 105, 207-214.

MIRET, S., SIMPSON, R. J. & MCKIE, A. T. (2003) Physiology and molecular biology of dietary iron absorption. *Annu Rev Nutr*, 23, 283-301.

MONTOSI, G., CORRADINI, E., GARUTI, C., BARELLI, S., RECALCATI, S., CAIRO, G., VALLI, L., PIGNATTI, E., VECCHI, C., FERRARA, F. & PIETRANGELO, A. (2005) Kupffer cells and macrophages are not required for hepatic hepcidin activation during iron overload. *Hepatology*, 41, 545-52.

MOSMANN, T. (1983) Rapid colorimetric assay for cellular growth and survival: application to proliferation and cytotoxicity assays. *J Immunol Methods*, 65, 55-63.

MUCKENTHALER, M. U., GALY, B. & HENTZE, M. W. (2008) Systemic iron homeostasis and the iron-responsive element/iron-regulatory protein (IRE/IRP) regulatory network. *Annu Rev Nutr*, 28, 197-213.

MUCKENTHALER, M., ROY, C. N., CUSTODIO, A. O., MINANA, B., DEGRAAF, J., MONTROSS, L. K., ANDREWS, N. C. & HENTZE, M. W. (2003) Regulatory defects in liver and intestine implicate abnormal hepcidin and *Cybrd1* expression in mouse hemochromatosis. *Nature Genetics*, 34, 102-107.

MUNOZ, M., GARCIA-ERCE, J. A. & REMACHA, A. F. (2011) Disorders of iron metabolism. Part II: iron deficiency and iron overload. *J Clin Pathol*, 64, 287-96.

NAKAYAMA, K. (1997) Furin: a mammalian subtilisin/Kex2p-like endoprotease involved in processing of a wide variety of precursor proteins. *Biochem J*, 327 ( Pt 3), 625-35.

NEMETH, E. & GANZ, T. (2006) Regulation of iron metabolism by hepcidin. *Annu Rev Nutr*, 26, 323-42.

NEMETH, E., TUTTLE, M. S., POWELSON, J., VAUGHN, M. B., DONOVAN, A., WARD, D. M., GANZ, T. & KAPLAN, J. (2004) Hepcidin Regulates Cellular Iron Efflux by Binding to Ferroportin and Inducing Its Internalization. *Science*, 306, 2090-2093.

NEMETH, E., VALORE, E. V., TERRITO, M., SCHILLER, G., LICHTENSTEIN, A. & GANZ, T. (2003) Hepcidin, a putative mediator of anemia of inflammation, is a type II acute-phase protein. *Blood*, 101, 2461-3.

NICOLAS, G., BENNOUN, M., PORTEU, A., MATIVET, S., BEAUMONT, C., GRANDCHAMP, B., SIRITO, M., SAWADOGO, M., KAHN, A. & VAULONT, S. (2002) Severe iron deficiency anemia in transgenic mice expressing liver hepcidin. *Proc Natl Acad of Sci, USA* 99, 4596-4601.

NICOLAS, G., VIATTE, L., LOU, D. Q., BENNOUN, M., BEAUMONT, C., KAHN, A., ANDREWS, N. C. & VAULONT, S. (2003) Constitutive hepcidin expression prevents iron overload in a mouse model of haemochromatosis. *Nat Genet*, 34, 97-101.

PARK, C. H., VALORE, E. V., WARING, A. J. & GANZ, T. (2001) Hepcidin, a Urinary Antimicrobial Peptide Synthesized in the Liver. [J Biol Chem](#). 276, 7806-7810.

PENGUE, G. & LANIA, L. (1996) Kruppel-associated box-mediated repression of RNA polymerase II promoters is influenced by the arrangement of basal promoter elements. *Proc Natl Acad Sci U S A*, 93, 1015-20.

PIETRANGELO (2006) Hereditary haemochromatosis. *Biochim Biophys Acta.*, 7, 700-710.

PIGEON, C., ILYIN, G., COURSELAUD, B., LEROYER, P., TURLIN, B., BRISSOT, P. & LOREAL, O. (2001) A new mouse liver-specific gene, encoding a protein homologous to human antimicrobial peptide hepcidin, is overexpressed during iron overload. *J Biol Chem*, 276, 7811-9.

PROVENZANO, M. J., FITZGERALD, M. P., KRAGER, K. & DOMANN, F. E. (2007) Increased iodine uptake in thyroid carcinoma after treatment with sodium butyrate and decitabine (5-Aza-dC). *Otolaryngol Head Neck Surg*, 137, 722-8.

RAFFIN, S. B., WOO, C. H., ROOST, K. T., PRICE, D. C. & SCHMID, R. (1974) Intestinal absorption of hemoglobin iron-heme cleavage by mucosal heme oxygenase. *J Clin Invest*, 54, 1344-52.

RAPISARDA, C., PUPPI, J., HUGHES, R. D., DHAWAN, A., FARNAUD, S., EVANS, R. W. & SHARP, P. A. (2010) Transferrin receptor 2 is crucial for iron sensing in human hepatocytes. *Am J Physiol Gastrointest Liver Physiol*, 299, G778-83.

RECALCATI, S., LOCATI, M., MARINI, A., SANTAMBROGIO, P., ZANINOTTO, F., DE PIZZOL, M., ZAMMATARO, L., GIRELLI, D. & CAIRO, G. (2010) Differential regulation of iron homeostasis during human macrophage polarized activation. *Eur J Immunol*, 40, 824-35.

- RIEMER, J., HOEPKEN, H. H., CZERWINSKA, H., ROBINSON, S. R. & DRINGEN, R. (2004) Colorimetric ferrozine-based assay for the quantitation of iron in cultured cells. *Anal Biochem*, 331, 370-5.
- SCHMIDT, P. J., TORAN, P. T., GIANNETTI, A. M., BJORKMAN, P. J. & ANDREWS, N. C. (2008) The transferrin receptor modulates Hfe-dependent regulation of hepcidin expression. *Cell Metab*, 7, 205-14.
- SEVIER, C. S. & KAISER, C. A. (2002) Formation and transfer of disulphide bonds in living cells. *Nat Rev Mol Cell Biol*, 3, 836-47.
- SHARP P., SRAI. S.K. (2007) Molecular mechanisms involved in intestinal iron absorption. *World J Gastroenterol*, 13, 4716-4724.
- SHAYEGHI, M., LATUNDE-DADA, G. O., OAKHILL, J. S., LAFTAH, A. H., TAKEUCHI, K., HALLIDAY, N., KHAN, Y., WARLEY, A., MCCANN, F. E., HIDER, R. C., FRAZER, D. M., ANDERSON, G. J., VULPE, C. D., SIMPSON, R. J. & MCKIE, A. T. (2005) Identification of an intestinal heme transporter. *Cell*, 122, 789-801.
- SILVA, A. M. & HIDER, R. C. (2009) Influence of non-enzymatic post-translation modifications on the ability of human serum albumin to bind iron. Implications for non-transferrin-bound iron speciation. *Biochim Biophys Acta*, 1794, 1449-58.
- SMITH, G. C., ALPENDURADA, F., CARPENTER, J. P., ALAM, M. H., BERDOUKAS, V., KARAGIORGA, M., LADIS, V., PIGA, A., AESSOPOS, A., GOTSIS, E. D., TANNER, M. A., WESTWOOD, M. A., GALANELLO, R., ROUGHTON, M. & PENNELL, D. J. (2011) Effect of deferiprone or deferoxamine on right ventricular function in thalassemia major patients with myocardial iron overload. *J Cardiovasc Magn Reson*, 13, 34.
- SOW, F. B., FLORENCE, W. C., SATOSKAR, A. R., SCHLESINGER, L. S., ZWILLING, B. S. & LAFUSE, W. P. (2007) Expression and localization of hepcidin in macrophages: a role in host defense against tuberculosis. *J Leukoc Biol*, 82, 934-45.
- STERNBERG JC. (1986) Rate nephrometry In Rose NR Frideman H, Fahey JL eds manual of clinical laboratory immunology 3rd edition, Washington DC, American Society for Microbiology 33-7.

- TRUANT, R. & CULLEN, B. R. (1999) The arginine-rich domains present in human immunodeficiency virus type 1 Tat and Rev function as direct importin beta-dependent nuclear localization signals. *Mol Cell Biol*, 19, 1210-7.
- TRUKSA, J., LEE, P., PENG, H., FLANAGAN, J. & BEUTLER, E. (2007) The distal location of the iron responsive region of the hepcidin promoter. *Blood*, 110, 3436-7.
- TSIEN, R. Y. (1998) The green fluorescent protein. *Annu Rev Biochem*, 67, 509-44.
- TURKEWITZ, A. P., AMATRUDA, J. F., BORHANI, D., HARRISON, S. C. & SCHWARTZ, A. L. (1988) A high yield purification of the human transferrin receptor and properties of its major extracellular fragment. *J Biol Chem*, 263, 8318-25.
- WALLACE, D. F., HARRIS, J. M. & SUBRAMANIAM, V. N. (2009) Functional analysis and theoretical modeling of ferroportin reveals clustering of mutations according to phenotype. *Am J Physiol Cell Physiol*, 298, C75-84.
- WALLACE, D. F., JONES, M. D., PEDERSEN, P., RIVAS, L., SLY, L. I. & SUBRAMANIAM, V. N. (2006) Purification and partial characterisation of recombinant human hepcidin. *Biochimie*, 88, 31-7.
- WANG, R. H., LI, C., XU, X., ZHENG, Y., XIAO, C., ZERFAS, P., COOPERMAN, S., ECKHAUS, M., ROUAULT, T., MISHRA, L. & DENG, C. X. (2005) A role of SMAD4 in iron metabolism through the positive regulation of hepcidin expression. *Cell Metab*, 2, 399-409.
- WARNER, T. G. (1999) Enhancing therapeutic glycoprotein production in Chinese hamster ovary cells by metabolic engineering endogenous gene control with antisense DNA and gene targeting. *Glycobiology*, 9, 841-50.
- WRIGHTING, D. M. & ANDREWS, N. C. (2006) Interleukin-6 induces hepcidin expression through STAT3. *Blood*, 108, 3204-9.
- YAMASHIRO, D. J., TYCKO, B., FLUSS, S. R. & MAXFIELD, F. R. (1984) Segregation of transferrin to a mildly acidic (pH 6.5) para-Golgi compartment in the recycling pathway. *Cell*, 37, 789-800.
- ZHANG, A. S., XIONG, S., TSUKAMOTO, H. & ENNS, C. A. (2004) Localization of iron metabolism-related mRNAs in rat liver indicate that HFE is expressed predominantly in hepatocytes. *Blood*, 103, 1509-14.